Design and synthesis of novel pH-responsive fatty acid-based lipids for the development of nano-delivery systems to enhance vancomycin activity against Methicillin-resistant *Staphylococcus aureus* (MRSA)

by

Sifiso S. Makhathini

(MSc Health Science – University of KwaZulu-Natal)

Submitted as a fulfillment of the requirements for the degree of Doctor of Philosophy in Pharmaceutics at the Discipline of Pharmaceutical Sciences of the School of Health Sciences at the University of KwaZulu-Natal Health Sciences at the University of KwaZulu-Natal

UNIVERSITY OF KWAZULU-NATAL ™

INYUVESI YAKWAZULU-NATALI

Supervisor: Professor Thirumala Govender

(PhD, University of Nottingham, United Kingdom)

Date submitted: **29 / 07 / 2020**

Quote

"Our work is the presentation of our capabilities."

--Edward Gibbon--

Dedication

This work is dedicated to my family especially my parents, for their unceasing support, encouragement, patience and understanding during my studies since the day they put me into school.

Declaration 1 – Plagiarism

I, Mr. Sifiso Makhathini, declare that

1. The research data reported in this thesis, except where otherwise indicated, are my original work.
2. This thesis has not been submitted for any degree or examination at any other university.
3. This thesis does not contain data, pictures, graphs, or other information belonging to other people unless specifically acknowledged as being sourced from other people.
4. This thesis does not contain any other persons' writing unless specifically acknowledged as being sourced from other researchers. Where other written sources have been quoted, then:
   a. Their words have been rephrased, but the general information attributed to them has been referenced.
   b. Where their exact words have been used, their writing has been placed inside quotation marks and referenced.
5 Where I have reproduced a publication of which I am an author, co-author, or editor, I have indicated in detail which part of the publication was written by myself alone and have fully referenced such publications.
6 This dissertation does not contain any graphics, text or tables copied from the internet unless specifically acknowledged and the source being detailed in the reference sections of the dissertation.

Signed: Date:**29 / 07 /2020**

I, Professor Thirumala Govender as supervisor of the Ph.D. studies herby consent to the submission of this Ph.D. thesis.

Signed: Date:**29/ 07/ 2020**

Declaration 2 –Publications

Mr. Sifiso S. Makhathini performed the literature search that leads to the conceptualization, design and execution of these projects. He contributed to the synthesis and structural elucidation of novel lipids using different techniques. These techniques include Fourier-transform infrared (FT-IR) spectroscopy, proton and carbon nuclear magnetic resonance spectroscopy (^{1}H NMR and ^{13}C NMR), high-resolution mass spectrometry (HRMS) analysis bio-safety assessment and *in vitro* antibacterial potential. He also contributed to the formulation and characterization of pH-responsive lipid-based nano-drug delivery systems, optimization of methods, modification and interpretation of data. The nanosystems were characterized in terms of particle size, polydispersity index, zeta potential, entrapment efficiency, surface morphology, *in vitro* drug release and both *in vitro and in vivo* antimicrobial activity. Mr. Sifiso Makhathini was responsible for the collection and analysis of data and wrote entire draft versions of all first-authored articles and revised them according to co-author's comments. Dr. R.S. Kalhapure, Dr. A. Y. Waddad and Dr. R Gannimani assisted with the inception, conceptualization, overall design of the projects, solving any technical problems and supervision of the studies. Dr. Sanjeev Rambharose assisted in performing *in vitro* cytotoxicity studies of the synthesized novel materials and in the *in vivo* antibacterial studies. Dr. Chunderika Mocktar supervised the *in vitro* and *in vivo* antibacterial studies. Prof. Thirumala Govender served as supervisor and was responsible for project conceptualization, problem-solving, manuscript editing and general supervision of the study.

Research output from the dissertation

1. First authored Publications

The following research papers were published as results generated from specific objectives from this study and they include:

- **Makhathini SS**, Kalhapure RS, Jadhav M, Waddad AY, Gannimani R, Omolo CA, Rambharose S, Mocktar C, Govender T. Novel two-chain fatty acid-based lipids for development of vancomycin pH-responsive liposomes against *Staphylococcus aureus* and methicillin-resistant *Staphylococcus aureus* (MRSA). Journal of Drug Targeting. 2019 Nov 26;27(10):1094-107. (Impact factor: 3.277). DOI: 10.1080/1061186X.2019.1599380.
- **Makhathini SS**, Omolo CA, Gannimani R, Mocktar C, Govender T. pH-Responsive Micelles from an Oleic Acid Tail and Propionic Acid Heads Dendritic Amphiphile for the Delivery of Antibiotics. Journal of Pharmaceutical Sciences. 2020 May 27, In Press. (Impact factor: 3.197). DOI: 10.1016/j.xphs.2020.05.011.

2. Conference Presentations

The following conference presentations were produced from the data generated during the doctoral study:

- **Sifiso S. Makhathini,** Rahul S. Kalhapure, Mahantesh Jadhav, Ayman Y. Waddad, Ramesh Gannimani, Calvin A. Omolo, Sanjeev Rambharose, Chunderika Mocktar &Thirumala Govender, Novel two-chain fatty acid-based lipids for development of vancomycin pH-responsive liposomes against *Staphylococcus aureus* and methicillin-resistant *Staphylococcus aureus* (MRSA). Presented at :
    - ICONAN 2017, 25-27 September 2017, Barcelona, Spain (Poster presentation).
    - 38th Annual Conference of the Academy of Pharmaceutical Sciences of South Africa, 06-08 July 2017, Johannesburg, South Africa (Poster presentation).
    - College of Health Sciences Annual Research Symposium, University of KwaZulu Natal, 05-06 October 2017 Durban, South Africa. (Oral presentation).
    - College of Health Sciences Annual Research Symposium, University of KwaZulu Natal, 11-12 October 2018 Durban, South Africa. (Oral presentation).

3. Co-authored publications

The following study was also undertaken during the Ph.D. study. This article highlights the synthesis of novel HA-OLA conjugates, *in vitro* toxicity evaluation of synthesized compounds, formulation of VCM loaded polymersomes and characterization of its physical and *in vitro* antibacterial properties.

- Walvekar, P., Gannimani, R., Salih, M., **Makhathini, S**., Mocktar, C., and Govender, T. (2019). Self-assembled oleylamine grafted hyaluronic acid polymersomes for delivery of vancomycin against methicillin resistant *Staphylococcus aureus* (MRSA). Colloids and Surfaces B: Biointerfaces, 182:110388. (doi: 10.1016/j.colsurfb.2019.110388) (Impact factor 3.997).

The following review was also written during the PhD study. This invited review provides an extensive and critical overview of pH-, enzyme-, redox- and ionic microenvironment-responsive nanocarriers that have been reported in the literature to date, with an emphasis on the mechanisms of drug release, the nanomaterials used, the nanosystems constructed and the antibacterial efficacy of the nanocarriers. The review also highlights further avenues of research for optimizing their potential and commercialization and confirms the potential of intrinsic stimuli-responsive nanocarriers for enhanced drug delivery and antibacterial killing.

- Devnarain, N., Osman, N., Fasiku, V., **Makhathini, S**., Salih, M., Ibrahim, U., and Govender, T. (2020). Intrinsic Stimuli-Responsive Nanocarriers for Smart Drug Delivery of Antibacterial Agents – An In-Depth Review of the Last Two Decades. WIREs Nanomedicine and Nanobiotechnology – Accepted, Manuscript ID NANOMED-651.R1 (IF: 7.689)

Abstract

The ability of antimicrobials to prevent and treat infections caused by a range of microorganisms, including bacteria, is threatened by the emergence of drug-resistant microorganisms that is associated with high mortality rates globally. Novel nano-drug delivery systems, including lipid-based drug delivery systems, represent an alternative therapeutic approach to combat antimicrobial resistance resulting from conventional dosage forms. Since bacteria are associated with an acidic environment and the bacterial envelope is made up of lipid bilayer, the application of pH-responsive lipid-based nanomaterials for targeted antibiotic delivery is recognized as an active area of research. The aim of this study was to design and synthesize fatty acid-based pH-responsive lipids (FAL, OLA-SPDA and DMGSAD-lipid) and explore their potential for the preparation of pH-responsive nano-based vancomycin (VCM) delivery systems to treat infectious diseases caused by methicillin-resistant *Staphylococcus aureus* (MRSA) infections. All the lipids were synthesized, and its structures were confirmed by FTIR, ^{1}H NMR, ^{13}C NMR and HR-MS. The nontoxic nature of the synthesized lipids was demonstrated by cell viability results above 75% on all tested mammalian cell lines using the MTT assay. After the synthesis and characterization, the novel fatty acid-based lipids were employed to formulate three pH-responsive lipid-based nano-drug delivery systems (liposomes, micelles and lipid polymer hybrid nanoparticles) for efficient and targeted delivery of VCM for the treatment *S. aureus* and MRSA infections. These systems were characterised for their physicochemical properties (Zetasizer), *in vitro* drug release (dialysis bag), morphology (HR-TEM), *in vitro* cell viability studies (flow cytometry), *in vitro* cytotoxicity (MTT assay), *in vitro* antibacterial activity (broth dilution method) and *in vivo* antibacterial activity (mice skin infection model).

The four formulated pH-responsive liposomes had a mean size ranging from 86.28 ± 11.76 to 282 ± 31.58 nm, with their respective PDI's ranging from 0.151 ± 0.016 to 0.204 ± 0.014 at pH 7.4 and 6.0 respectively. The ZP values were negative at physiological pH (7.4) and shifted towards positivity with a decrease in pH (6.0). The encapsulation efficiency (%EE) and loading capacity were in the range of 29.86 ± 4.5% and 44.27 ± 9.2%, The drug release profiles of all formulations at both pH 7.4 and 6.0 were sustained throughout the studied period of 72 h. Enhanced *in vitro* antibacterial activity at pH 6.0 was observed for the DOAPA-VAN-Liposome and DLAPA-VAN-Liposome formulations. Flow cytometry studies indicated a high killing rate of MRSA cells using DOAPA-VAN-Lipo (71.98%) and DLAPA-VAN-Lipo (73.32%) using the MIC of 1.59 µg/ml. *In*

vivo studies showed reduced MRSA recovery from mice treated with liposome formulations (DOAPA-VAN-Lipo and DLAPA-VAN-Lipo) by 4- and 2-folds compared to bare VCM-treated mice respectively.

The pH-responsive oleic acid-based dendritic lipid amphiphile self-assembled into stable micelles with particle size, PDI, ZP and %EE of 84.16 ± 0.184 nm, 0.199 ± 0.011 and -42.6 ± 1.98 mV and 78.80 ± 3.26%, respectively. The micelles demonstrated pH-responsiveness with an increase in particle size to 141.1 ± 0.070 nm at pH 6.0. The drug release profiles of formulations at both pH 7.4 and 6.0 were sustained throughout the studied period of 72 h. The *in vitro* antibacterial efficacy of VCM-OLA-SPDA-micelle against MRSA was 8-fold better when compared to bare VCM, and the formulation was 4-fold better at pH 6.0 when compared to the formulation's MIC at pH 7.4. The MRSA viability assay showed that the micelles had a high percentage killing of 93.39% when compared to bare VCM (58.21%) at the same MIC (0.98 µg/ml). The *in vivo* mice skin infection model also demonstrated an enhanced antibacterial effect, showing 8-fold reduction in MRSA burden on skin treated with VCM-OLA-SPDA-micelles when compared with the skin sample treated with bare VCM.

The optimized pH responsive lipid polymer hybrid nanoparticles (LPHNPs) formulations, RH40_VCM_LPHNPs had a particle size, PDI and ZP of 64.05 ± 0.64 nm, 0.277 ± 0.057 and 0.55 ± 0.14Vm, respectively, whereas SH15_VCM_LPHNPs displayed a size of 73.41 ± 0.468 nm, PDI of 0.487 ± 0.001 and ZP of -1.55 ± 0.184 Vm at pH 7.4. There was a significant change in particle size and ZP to 113.6 ± 0.20 nm and 9.44 ± 0.33 Vm for RH40_VCM_LPHNPs, respectively, whereas for SH15_VCM_LPHNPs, there was no change in is size but a significant change in surface charge switch to 9.83 ± 0.52 Vm at pH 6.0. The drug release profiles of formulations at both pH 7.4 and 6.0 were sustained throughout the studied period of 72 h. The VCM release profile, together with release kinetic study on LPHNPs, demonstrated the influence of pH on the high rate of VCM release at pH 6.0 as compared to pH 7.4. The LPHNPs a had better antibacterial activity against *S. aureus* and MRSA at both pH conditions when compared to bare VCM. Furthermore, the MIC of LPHNPs against MRSA was better by 8-fold at pH 6.0 than at 7.4.

In summary, synthesized novel lipid materials showed superior biosafety profiles and potential in the development of lipid-based pH-responsive nanoantibiotic delivery systems against bacterial infections and other disease types characterized by low pH. The data from this study has resulted

in three first-authored research publications, one co-authored research publication and one co-authored review article.

Acknowledgments

I want to extend my gratitude and sincere appreciation to my family for their support, encouragement and guidance throughout the course of my PhD. My sincere appreciation also goes to my supervisor, Professor Thirumala Govender for your guidance and motivation throughout my PhD. Your best interest has always been at seeing everyone of us strive for greatness and without your valuable criticism and expertise, this project would not have been possible. For that I thank you, and for allowing me to be part of your team. You have granted me the opportunity to learn many skills and equipped me with valuable tools I will need as a young researcher.

My thanks also go to Dr Chunderika Mocktar for her encouragement, support, advice and her teaching/training that has allowed me to learn valuable lab techniques.

Special thanks goes to my mentors and colleagues , Dr. Rahul Kalhapure, Dr. Ayman Waddad, Dr. Ramesh Ganimani, Dr Calvin A. Omolo, Dr Nikita Devnarain, Dr. Sanjeev Rambharose, Dr. Ruma Maji, Dr. Andile Mbuso Faya, Dr Pavan Walvekar, Abdeen Mohamed, Nawras Abdelmoniem, Victoria Fasiku, Danford Mhule, Melissa Ramtahal and Leslie Murugan for all their support, technical assistance in the laboratory and life-long friendship. I would also like to acknowledge all the organisations that gave me indispensable generous resources, including the National Research Foundation (NRF), UKZN Nanotechnology Platform and the College of Health Sciences at UKZN. Without their support and financial help, it would not have been possible for me to pursue and to complete my studies. My appreciation goes to Ms Carrin Martin for editorial assistance, the Electron Microscope Unit (MMU), and Biomedical Resource Unit (BRU) at UKZN for their technical support. Lastly, I would like to express my appreciations towards my friends Malusi Ninela and Nqobile Makhanya who believed that it is possible when the darkness clouded my light.

Table of Contents

List of Abbreviations

CDC	Center for Disease Control and Prevention	MIC	Minimum Inhibitory Concentration
A549	Adenocarcinoma Human Alveolar Epithelial	Mpeg	Monomethoxy Polyethylene Glycol
AMR	Antimicrobial Resistance	MRSA	Methicillin-Resistant *Staphylococcus Aureus*
BCS	Biopharmaceutical Classification System	MSSA	Methicillin-Susceptible *Staphylococcus Aureus*
CFU	Colony Forming Unit	MST	Microscale Thermophoresis
DCM	Dichloromethane	MTT	3-(4, 5-Dimethylthiazolyl-2)-2,5-Diphenyltetrazolium Bromide
DLS	Dynamic Light Scattering	NCE	New Chemical Entity
DMSO	Dimethyl Sulfoxide	NMR	Nuclear Magnetic Resonance Spectroscopy
DSC	Differential Scanning Calorimetry	OA	Oleic Acid
EE	Encapsulation Efficiency	CA	Community-acquired
HA	Hospital-acquired	P188	Poloxamer 188
VISA	Vancomycin-intermediate Resistant *Staphylococcus aureus*	PI	Propidium Iodide
DDS	Drug delivery systems	PDI	Polydispersity Index
PNPs	Polymeric nanoparticle	PVP	Polyvinylpyrrolidone
FT-IR	Fourier-Transform Infrared	QL	Quaternary Lipid
CMC	Critical micelle concentration	RMSE	Root-Mean-Square Error
H&E	Hematoxylin and Eosin	*S. aureus*	*Staphylococcus aureus*
HEK 293	Human Embryonic Kidney 293 Cells	SCVS	Small Colony Variants in Persistent Infections

SLNs	Solid lipid nanoparticles	LPHNPs	Lipid polymer hybrid nanoparticles
NEs	Nanoemulsions	TEM	Transmission Electron Microscopy
LBDDs	Lipid-based drug delivery system	THF	Tetrahydrofuran
DSAPE	Di -Stearoyl Amino Propionic acid tert-butyl Ester	UKZN	University of Kwazulu-Natal
DOAPE	Di - Oleoyl Amino Propionic acid tert-butyl Ester	FAL	Fatty acid-based lipids
DLAPE	Di- Linoleoyl Amino Propionic acid tert-butyl Ester	VCM/VAN	Vancomycin
DLLAPE	Di- LinoLenoyl Amino Propionic acid tert-butyl Ester	CHEMS	Cholesteryl hemisuccinate
MHA	Mueller Hinton Agar	EPR	Enhanced permeability retention time
MHB	Mueller Hinton Broth	WHO	World Health Organization
VRSA	Vancomycin-Resistant *Staphylococcus aureus*	RBCs	Red blood cells
BRU	Biomedical Resource Unit	DCC	*N*,*N'*-dicyclohexyl carbodiimide
DMAP	*p-dimethylamino pyridine*	PE	Phosphatidylethanolamine
		PN	Polymeric nanoparticles
RT	Room temperature	SA	Stearic acid
LA	Linoleic acid	SD	Standard deviation
LLA	Linolenic acid	EDC.HCl	1-Ethyl-3- (3-dimethylaminopropyl)carbodiimide hydrochloride

List of Figures and Tables

CHAPTER 1

INTRODUCTION

1.1 Introduction

This chapter provides a brief background to the study and highlights the status of infectious diseases, limitations associated with antibiotic therapy and the emergence of antimicrobial resistance. Furthermore, it provides details on alternative strategic solutions to enhance antibiotic therapy, which resulted in the proposed aims and objectives of the study. It also highlights the novelty and significance of the study.

1.2 Background to the study

For several decades in the history of infectious diseases, antimicrobial resistance (AMR) caused by pathogenic microorganisms such as bacteria, viruses, fungi and parasites has been the greatest threat to human health globally[1]. Since the late 1960s, infectious diseases were thought to be under control and some were almost completely eradicated[2]. Unfortunately, resistance to various antimicrobials gave rise to new threats, which continue to endanger the existence of the human population[3]. Antimicrobial resistance is a consequence of the evolutionary response of microbes and this process attenuates the impact of various treatment options such as antibacterial, antiparasitic, antiviral and antifungal drugs against the array of infections, thus, rendering them ineffective[4]. Therefore, AMR has been responsible for uncontainable infections and costly treatment associated with prolonged illnesses in infected patients and a subsequent increase in mortality rate[1]. Despite the scientific advancement and availability of new antimicrobial agents, the global rate of infection occurrence and the high number of deaths per year have been highlighted as the major threat on world economies and to the public healthcare system[5, 6].

Compared to any cause of death throughout human history, infectious diseases have been and continue to be the leading cause of death in both developing and developed countries as we continue to fight the known and unknown pathogens[6]. The severity of infectious diseases has been exacerbated by the emergence of new infections and the re-emergence of known infections[7]. The discovery of salvarsan in 1910 and penicillin in 1928 by Ehrlich and Fleming, respectively, were the earliest successful attempts to control infectious diseases[8, 9]. After this period, the development and introduction of more new antibiotics gave more hope into believing that the infectious disease

era will soon be phased out and the golden era of antibiotics, which existed between the 1930s to 1960s, will rise above all infections[10]. Unfortunately, the extensive overuse of antibiotics resulted in the emergence of multidrug-resistant bacteria which made treatment less effective and completely inefficient[10]. In this regard, antibiotic resistance reduces the ability of current medicines to treat common infections[11]. For instance, antibiotics, which have played a significant role in preventing and treating infection in the clinical setting on patients who are receiving chemotherapy treatment, with chronic diseases such as diabetes and rheumatoid arthritis, are now rendered ineffective[11, 12]. The World Health Organization (WHO) projections on AMR, as shown in **Figure 1**, suggest that if no viable solutions are adopted by 2050, morbidity rates are estimated to be at 10 million and 28 million and people will experience severe poverty. Additionally, the global economy may also experience a possible loss of more than $100 trillion annually due to AMR[13, 14].

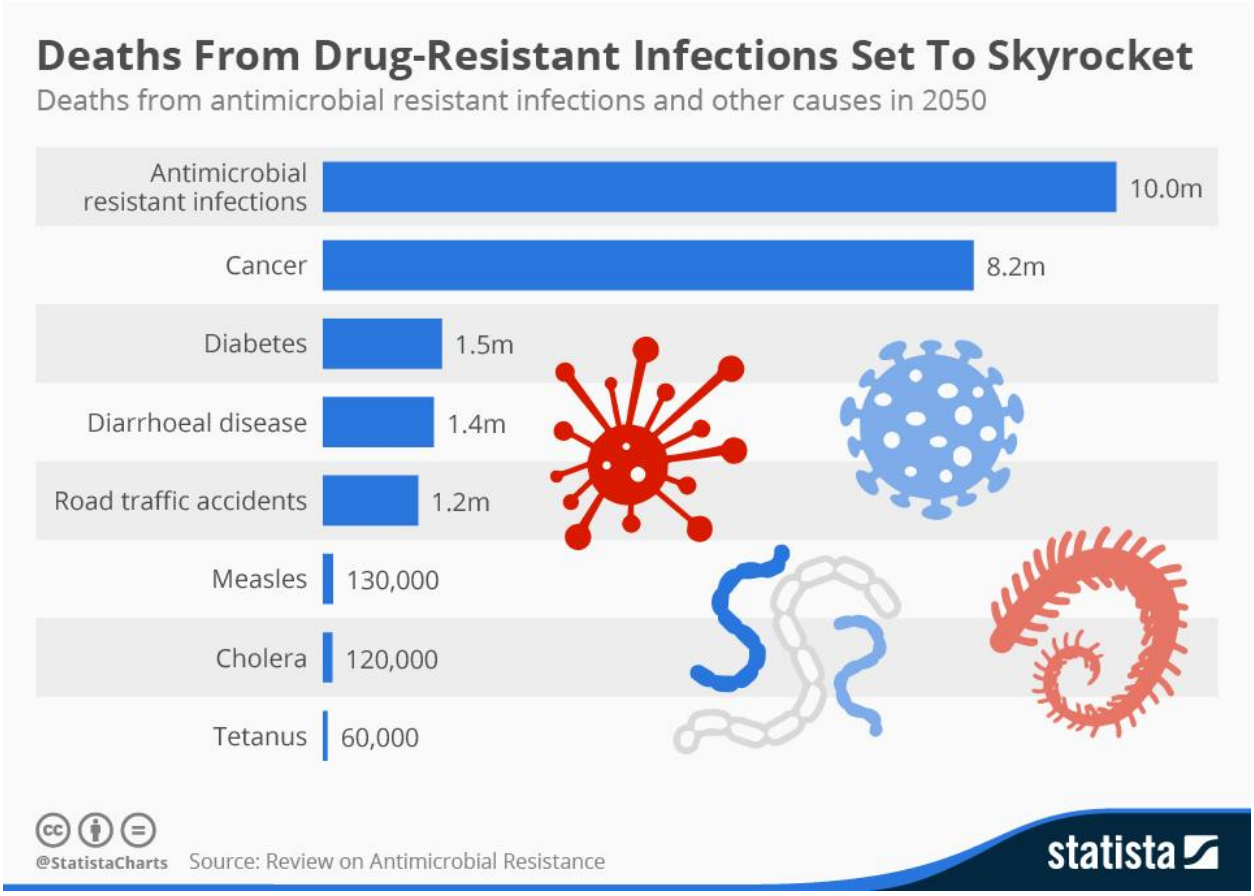

Figure 1. The number of deaths attributable to antimicrobial-resistant infections and other causes in 2050[15].

Pathogenic microorganisms have always evolved to resist the impact of new medicines applied against them. Among infectious diseases, bacterial infections are recognized as the major cause of death and with the emergence of AMR, they have become increasingly difficult to manage[16]. According to WHO and the Center for Disease Control and Prevention (CDC), over 2 million cases of infections are caused by antibiotic-resistant bacteria resulting to about 23 000 deaths, with over $20 billion excess healthcare cost and $35 billion societal costs annually in US alone[17, 18]. Methicillin-resistant *Staphylococcus aureus* is one of the most difficult bacterial pathogens to treat among the ESKAPE pathogens (*Enterococcus faecium, Staphylococcus aureus, Klebsiella pneumonia, Acinetobacter baumannii, Pseudomonas aeruginosa and* Enterobacter spp.), which are responsible for nosocomial infections and deaths globally[19]. MRSA is one of the leading causes of nosocomial infections since their first report in the 1960s in the United Kingdom (UK) shortly after the introduction of methicillin[20, 21]. The virulence of MRSA strains has been associated with a rapid increase of life-threatening pneumonia, necrotizing fasciitis, endocarditis, osteomyelitis, severe sepsis, and toxinoses such as toxic shock syndrome, occurring in both healthcare and community settings[20, 22].

It was further reported that 13 to 74% of *S. aureus* infections reported are MRSA and the source of *S. aureus* infections around the world from both community-acquired (CA) and hospital-acquired (HA) infection reported cases is changing [23, 24]. Additionally, in all WHO regions, the prevalence of MRSA has been recorded to exceed 20% and above 80% in some regions[25]. For all the HA infections in Europe caused by the antibiotic-resistant bacterium, 44% were MRSA and contributed to over 20% excess mortality[23]. Whereas in the United States of America (USA) alone within the community setting, over 80,461 invasive MRSA infections and more than 11,285 related deaths were recorded in 2011[24, 26]. This resulted in the hospital/healthcare cost of about 1.4 to 13.8 billion in the USA and 380 million annual loss in Europe in the fight against MRSA infections[24]. According to WHO report in 2014, even though the impact of MRSA infections in western countries is well document, the magnitude of MRSA infections in other regions like Africa is not known[27]. For example, whilst South Africa has a reported decline from 34 to 28% in 2011, in some part of Africa, cases of reported MRSA infections were exceeding 82%[18, 28]. Therefore, countries of low-prevalence MRSA infections are still at risk due to changes in the global epidemiology[20].

The continuous growth and unmonitored spread of MRSA prevalence from the nosocomial environment to communities in countries with intensified international mobility and lacking healthcare facilities to control of the infection are significantly contributing to the global spread of MRSA[29]. Even though vancomycin (VCM) has been the mainstay for the treatment of MRSA infections since 1958[30, 31], the extensive use of VCM for over 50 years and the emergence of MRSA isolates with reduced susceptibility to VCM indicate the risk of running out of effective antibiotics to treat MRSA infections[32-35]. These MRSA isolates are termed vancomycin-intermediate resistant *Staphylococcus aureus* (VISA) and vancomycin-resistant *Staphylococcus aureus* (VRSA). Although the total number of cases reported related to these MRSA isolates is currently low, new infections of this nature are being identified[21, 36]. Since VCM is often regarded as the last resort for *S. aureus* infections, their treatment becomes a daunting challenge. This phenomenon poses a serious threat as the number of VISA and VRSA incidences continues to rise. Collectively, these challenges advocate for new effective therapeutic approaches to be introduced or adopted to prevent, treat, and control the spread of these infectious diseases. Hence, there is a need for the development of new antimicrobial drugs or even novel effective approaches to treating microbial infections[21, 35].

Despite the great successes in using a conventional antibiotic therapeutic approach to treat bacterial infections, which has saved millions of lives, this approach has been associated with several limitations. This has resulted in antibiotic therapeutic failure and subsequent development of antibiotic resistance over the years[37]. Antibiotics were designed to treat and prevent bacterial infections by killing and inhibiting their growth through conventional antibiotic therapies[38]. Unfortunately, limitations associated with traditional dosage forms have been reported. These include a fast bio/chemical degradation and reduced circulation time in the bloodstream, non-site-specific and non-target-oriented drug delivery, as well as inadequate drug uptake at the site of infection, which leads to sub-optimal therapeutic outcomes. In this case, the frequency of administration is increased to maintain a fixed/desirable plasma drug level, which may lead to the development of side effects and subsequent poor patient compliance[39]. These shortcomings became the major contributors to the development of resistance, which has reduced the antibiotic timeline between the antibiotic introduction and resistance development[40]. The decline of antibiotic therapy resulted in many pharmaceutical companies opting to discontinue their

investments towards the development of newer classes of antibiotics due to low profits, the short life span of the product and complicated regulatory approval procedures[41]. As shown in **Figure 2** below, since 1984, no new class of antibiotics has been discovered, which is being outpaced by the continuous spread of AMR[42]. Therefore, the innovative alternative approaches that can enhance therapeutic outcomes of the current antibiotics to combat drug resistance development are warranted.

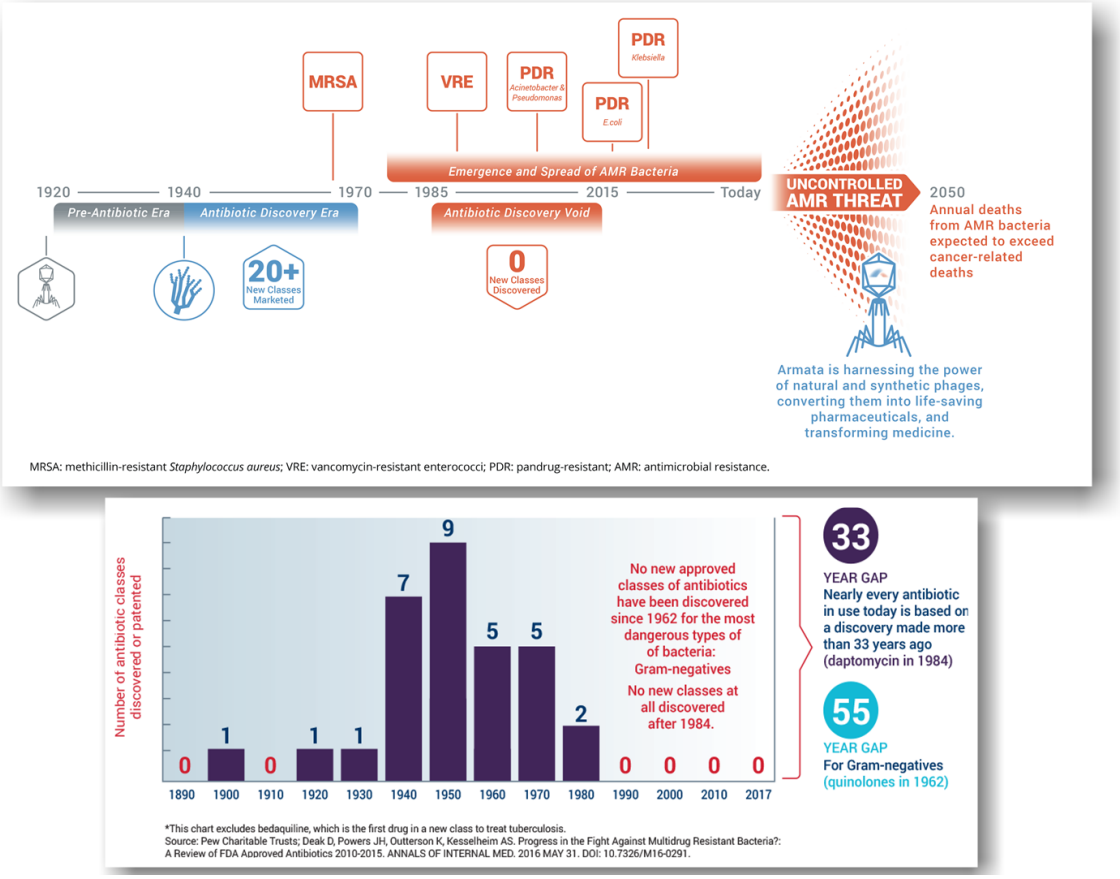

Figure 2. History of antibiotics and resistance[42, 43].

Over the past decades, the use of nanotechnology based-nanomedicine through integrated approaches in an attempt to enhance and restore the efficacy of the drugs has been widely reported in literature[44]. Nanomedicine involves the use of nanoscale structures for diagnosis, monitoring, control, prevention, treatment of diseases, and for better understanding the pathophysiology of diseases to improve the quality of life of patients[45, 46]. Since the discovery of nanoscale structures, they have become a promising tool to overcome the therapeutic failures associated with

conventional therapeutic treatments[46-48]. **Figure 3** below represents the first generation of nanotechnology-based drug delivery systems (DDSs) that were approved by the FDA for clinical use and several drug nanocarriers, including antibiotic nanocarriers, are in different stages of development[49-52]. Furthermore, DDSs have been identified as a promising strategy to addresses several problems associated with antibiotic therapy, including antibiotic resistance[53]. These nanomaterials for antibiotic delivery offers several major advantages such as: i) targeting drug delivery to a specific site of infection; ii) improving the delivery of poorly soluble drugs and prevent serum instability issues; iii) improving transportation of the drug across tight epithelial and endothelial barriers; iv) preventing non-specific binding of the drug to healthy cells; v) releasing drugs at a sustained rate and controlled manner; vi) enabling uniform distribution in the target tissue and vii) improving cellular internalization. These advantages restore and improve the pharmacokinetic properties of the drug with reduced frequency of administration, toxicity and related side effects, which may improve patient compliance[51, 53, 54]. A range of nanodelivery systems including liposomes, solid lipid nanoparticles (SLNs), polymeric nanoparticles (PNPs), dendrimers, nanoemulsions (NEs), lipid polymer hybrid nanoparticles (LPHNs) and micellar systems are among the nanodelivery systems used for antibiotic delivery[55]. Even though there has been a great advancement in nanotechnology-based medicine, the application of nanoantibiotic formulation is still a new concept as compared to cancer and cardiovascular diseases[56]. Therefore, this suggests a need to develop more novel nanoantibiotic delivery systems to explore their potential in overcoming antibiotic resistance.

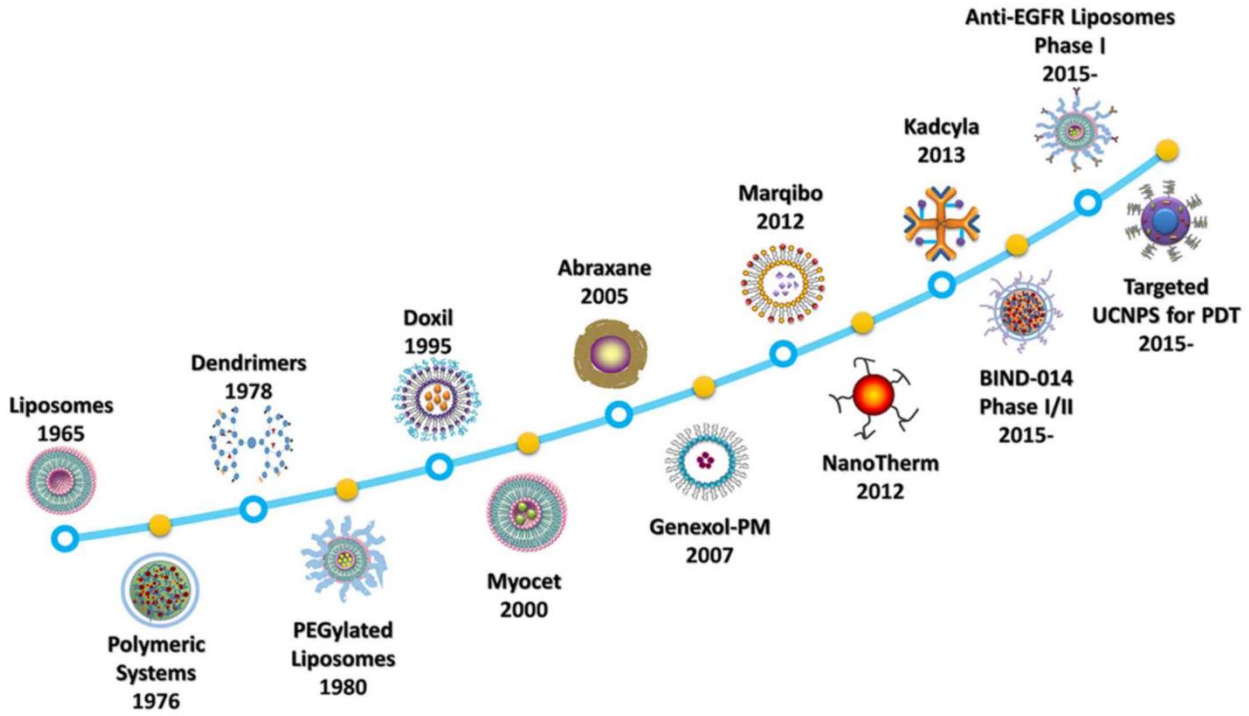

Figure 3. Timeline of nanotechnology-based drug delivery[57].

Nanodrug delivery systems have shown promising results in preclinical studies (animal models) through passive and receptor-mediated targeting, as well as enhanced permeability and retention (EPR) effect. However, they suffer from non-specific bio-distribution and uncontrollable drug release [58, 59]. To overcome these challenges, a significant progress has been made in developing stimuli-responsive nanocarriers that respond to the intrinsic physicochemical and pathological factors at the disease site to increase the specificity of drug delivery[58-60]. This could lower the dosage frequency while maintaining the required drug dose in the targeted organs/tissues for a much longer period at a very low toxicity range, thus improving therapeutic efficacy[59]. The common stimuli used for active targeting and drug release can be classified into physical (e.g., magnetic field, electric field, ultrasound, temperature, and osmotic pressure); chemical (e.g., pH, ionic strength and glucose); and biological (enzymes and endogenous receptors)[61, 62]. Among these stimuli-responsive nanodelivery systems reported for effective drug delivery, pH-responsive nanosystems have been investigated for delivery of the drug at disease sites characterized by low pH such as bacteria-infected tissue/organs.

Briefly, bacterially infected tissues are associated with lower pH conditions due to anaerobic fermentation and subsequent inflammation; therefore, pH factor becomes the prime lead in developing innovative approaches and alternative strategies to treat bacterial infections[58]. The pH variation that exists across the biological system (both cellular and systemic levels in the pathological state) has been exploited for targeted drug delivery and triggered release in response to subtle environmental changes associated with pathological conditions that are different from physiological pH 7.4[63]. Therefore, designing pH-responsive nanosystems requires a good understanding of the target site and the mechanism of release. In general, targeted drug delivery using stimuli-responsive nanomaterials is achieved through long-term stability in blood circulation as well as EPR, reduced premature drug release to the non-specific sites, as well as their ability to accumulate and enhance drug release once at the target site in response to a specific stimuli[64]. Additionally, there are two main mechanisms of targeted drug release in which pH-responsive nanosystems adapt in response to change in pH. These are i) the use of biomaterials with ionizable groups that undergo either or both conformational and solubility changes and ii) the use of biomaterials with acid-labile bond/linkers that hydrolyze under acidic conditions to facilitate drug release at the target site[58, 65]. The figure below (**Figure 4**) summarizes strategic ways in which a pH-responsive nanoparticle can be engineered to fit the required design[66].

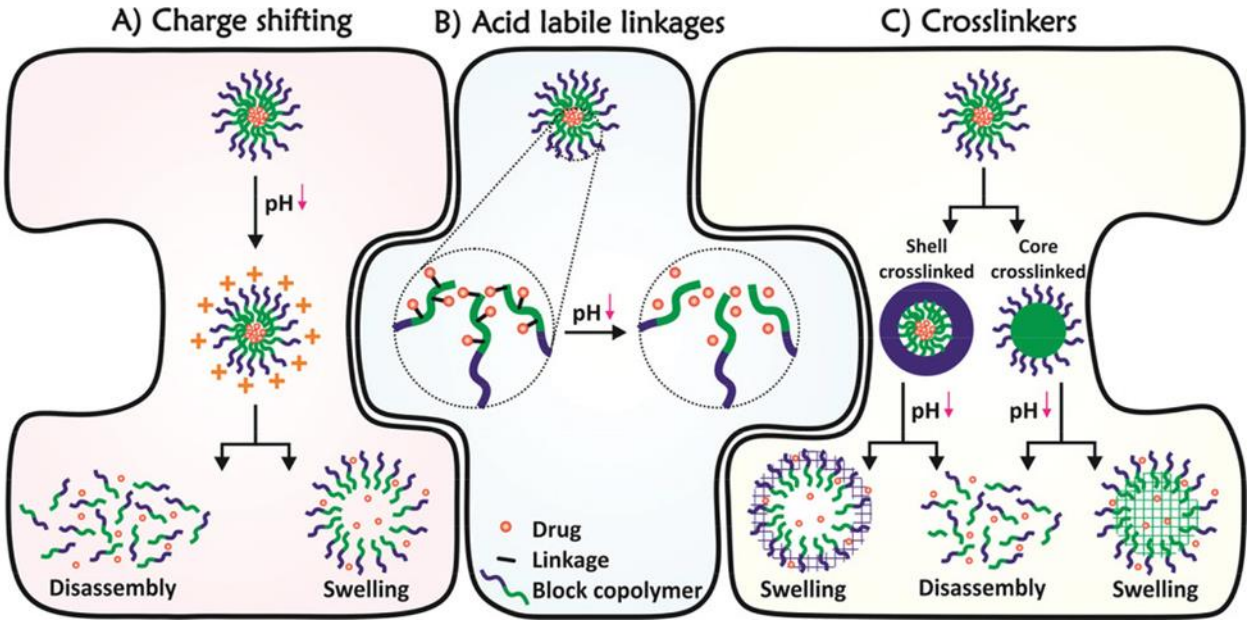

Figure 4. Approaches to design pH-responsive nanosystems. A) use of charge shifting polymers, B) Acid-labile linkages or C) Crosslinkers that can either combine charge shifting polymers with non-cleavable linkages to create swellable particles or acid-labile linkages, which lead to pH-responsive disassembly[66].

There is a range of biomaterials that have been incorporated in the formulation of nanodrug delivery systems such as lipids, polymers, and metals[67]. These biomaterials can be functionalized to impart stimuli-responsive properties of the nanocarrier to maximize targeted delivery. Most DDSs have been faced with the challenges associated with toxicity except for lipid-based drug delivery systems (LBDDSs), which have been considered as the safer DDS[68]. The significant benefits of LBDDSs include simplicity in modification for multiple applications, biocompatibility and biodegradability. They also possess membrane-like properties that facilitate its application as a nanocarrier for intracellular delivery[69]. LBDDSs have been studied and several lipid-based carriers, including liposomes, nanoemulsions, solid lipid nanoparticles, micelles, core-shell-type biomimetic vesicles, lipid-polymer hybrids, have been developed for mostly cancer therapy[70-73]. Additionally, extensive progress has been made in the development of pH-responsive LBDDSs for cancer therapy and have demonstrated promising results, but major progress is needed for antibiotic delivery. Additionally, the application of nanomedicines for bacterial infections is still a relatively new concept.[49]. Therefore, to address the challenges associated with conventional antibiotic dosage forms and the emergence of antibiotic-resistant bacteria, novel lipid-based nanoantibiotic approaches are warranted. Therefore, in this study, we explored three novel approaches, which employ the use of lipid materials to formulate lipid-based nanodelivery systems with stimuli-responsive properties: i) pH-responsive liposomes derived from novel two chain fatty acid-based lipids, ii) pH-responsive micelles from an oleic acid-lipid dendritic amphiphile and, iii) pH-responsive lipid-polymer hybrid nanoparticles (LPHNPs) from a stearic acid-based lipid amphiphile to efficiently deliver and enhance VCM activity against MRSA infections.

Liposomes are one of the first generations of LBDDSs that were FDA approved and commercialized [74-76]. They are phospholipid vesicles consisting of one or more lipid bilayers and can effectively encapsulate and deliver both hydrophilic and hydrophobic bioactive materials[40]. Since the discovery of liposomes, some changes have been made in their basic structure to facilitate

triggered release in response to environmental conditions and to enhance their *in vivo* liposome-mediated drug delivery[77]. For example, liposomes containing pH-sensitive lipid components are designed specifically to control the release of the drug in response to acidic pH of the endosomal system[78]. More studies have been conducted to investigate the therapeutic efficacy of pH-responsive liposomes and reports in the literature suggest that pH-responsive liposomes can target and accumulate the anti-cancer drugs in tumours more efficiently than the conventional liposomes[78, 79]. Even though more studies have confirmed the efficiency of pH-responsive liposomes as the best candidate for the delivery of drugs to the disease site characterized by acidic pH, very few studies have been reported on antibiotic delivery. pH-responsive liposomes for delivery of antibiotics reported so far include gentamycin[80], streptomycin[81] and VCM[82], amongst others. Cationic, anionic and zwitterionic lipids are commonly used to formulate of pH-responsive liposomes, which contribute towards the overall surface charge of liposomes[83]. However, cationic and anionic lipids are still faced with challenges that limit their *in vivo* application. For example, even though negatively charged, or neutral liposomes can avoid early opsonization, their cellular internalization is affected because of the repulsive force between the liposome and negatively charged cell membrane[84, 85]. On the other hand, cationic liposomes can maximize cellular internalization through electrostatic interaction/binding with the negatively charged cell membrane but also suffer from non-specific binding with serum proteins before reaching the site of infection[83]. This makes zwitterionic lipids the best candidate to impart fusogenic and pH-responsive properties, possessing positive attributes from both anionic and cationic lipids[86]. Zwitterionic lipids can be differentially ionized to promote surface charge switching in response to change in pH. For instance, at physiological pH, they remain neutral or negatively charged to avoid early opsonization and non-specific binding; and under acidic conditions they induce surface charge switching to positive, thus maximizing cellular internalization to enhance therapeutic outcome[87-89]. Limited studies have been conducted exploring the potential applicability of zwitterionic lipids in the formulation of pH-responsive liposome in the fight against disease infections characterized by acidic pH, such as bacterial infections. Since gram-positive bacteria, such MRSA, have negatively charged teichoic acids linked to thick peptidoglycan layers, using surface charge switching lipids such as zwitterionic lipids in the formulation of liposomes can facilitate electrostatic binding and enhance fusogenic properties of liposomes; which will further enhance cellular uptake[90]. Therefore, designing fusogenic liposomal systems with pH-responsive

properties can enhance targeting and remain to be explored for enhanced therapeutic outcomes in several diseases associated with acidic conditions at the disease site such as infections and cancer.

The self-assemblies of dendritic amphiphiles have become an attractive strategy in developing a new class of delivery systems, possessing positive attributes from both polymeric and small molecular self-assemblies[91]. Dendritic amphiphiles are highly branched architectures with multiple functional headgroups, which self-assemble into nanosystems that are highly stable polymeric assemblies and display membrane properties like in small molecular assemblies[92]. However, several reports have shown their lack of active targeting and active release of the drug carrier in response to a specific stimulus for an improved pharmacokinetics and pharmacodynamics for the drug with reduced undesired side effects[93]. Among the endogenous stimuli, pH has been widely used as a control parameter for targeted drug delivery and controlled drug release because of the pH difference that exists between the healthy and disease sites[94]. Given the acidic conditions of the bacterially infected site, using pH-responsive dendritic amphiphiles can lead to the development of a more stable, membrane penetrating nanosystem with controlled drug release properties for efficient drug delivery. This can ensure sufficient eradication of bacterial infection and reduced chances of antibiotic-resistance development. pH-responsive dendritic polymeric micelles are the one of the well-studied hyperbranched and multifunctional nanosystems for the efficient delivery of anticancer drugs[95]. To the best of to our knowledge, no pH-responsive lipid-dendritic micelles for antibiotic delivery have been reported in the literature. Therefore, this study highlights the need for the synthesis and delivery application of a lipid-based dendritic amphiphile to explore their potential in targeted delivery.

Since the discovery of liposomes and polymer-based nanosystems, extensive progress has been made in developing new and advance DDSs that address their challenges that limit their scope of application in the fight against different disease types[96]. Lipid polymer hybrid nanoparticles have emerged as one of the promising novel DDS, derived from both liposomes and polymeric based nanoparticles to overcome their shortcomings[96, 97]. This novel DDS has shown to enhance cell membrane permeability and long circulation time and display serum stability, differential targeting and biocompatibility. Using fatty acid-based zwitterionic pH-responsive lipids in the formulation of LPHNPs can facilitate their efficiency of targeted delivery at disease site characterized by acidic

pH, such bacterial infection. Even though LPHNPs have accumulated so much interest as the new generation of novel DDSs, they still remain under investigated[98]. To the best of our knowledge there is no report on fatty acid-based zwitterionic pH-responsive lipid for the development of LPHNPs for targeted delivery of any drug type. This highlights the importance of developing pH-responsive LPHNPs to enhance the therapeutic efficacy of antibiotics. Our group have reported pH-responsive hybrid nanosystems for targeted of delivery of VCM against MRSA infections with promising *in vivo* results[99, 100]. Therefore, using these pH-responsive nanosystems for VCM delivery to treat MRSA infections can help address the therapeutic limitations associated with traditional dosage forms of VCM.

Vancomycin is a tricyclic glycopeptide antibiotic, used to treat acute infections caused by gram-positive bacteria, especially with the emergence of MRSA in hospitals[101]. Vancomycin mechanism of action against gram-positive bacteria is through inhibiting cell wall synthesis in susceptible organisms. However, the extensive use of VCM to treat MRSA infections has led to the development of new MRSA isolates termed vancomycin-intermediate *Staphylococcus aureus* (VISA) with reduced susceptibility to VCM[102]. The common occurrence of these resistant isolates of MRSA, MSSA, and VISA, is the reduced potential ability of VCM to treat these infections, which can lead to life-threatening conditions, such as sepsis[103-105]. In this regard, alternative treatment approaches are warranted. Therefore, the proposed studies were aimed at enhancing the antibacterial activity and performance of VCM against MRSA using nano-drug delivery systems such as pH-responsive liposomes consisting of fatty acid-based lipids and pH-responsive micelles derived from oleic acid-based dendritic lipid amphiphiles, respectively. Chapters two, three and four highlight the strategies used in the development of new nanosystems to efficiently deliver VCM against MRSA.

1.3 Problem statement

Among infectious diseases, the resistance of bacterial pathogens to common antimicrobial therapies are increasing rapidly and it has been associated with high morbidity and mortality globally. Several limitations such as drug exposure to healthy tissue, insufficient drug concentration at infection/target sites due to low bioavailability, rapidly degradation and quick elimination, high frequency of administration, severe adverse effects and poor patient compliance have been encountered using conventional dosage forms. These limitations are the leading cause

of poor therapeutic outcomes and subsequent development of antimicrobial resistance crisis globally. Nano-drug delivery systems have become an attractive solution to overcome challenges associated with traditional dosage forms. The identification and application of novel nano-based approaches to enhance antibiotic therapy through targeting infection sites, can contribute to enhancing patient therapy and disease treatments. The design and synthesis of unconventional lipid materials for developing pH-responsive nano-formulations are essential to improve the antibacterial effect of the currently available antibiotics. Additionally, nano-drug delivery systems that are specifically responsive to unique conditions at disease sites are a current trend in nanotechnology aimed at enhancing drug therapy.

1.4 Aims and objectives of this study

The broad aim of this study was to design and synthesize fatty acid-based pH-responsive lipids and explore their potential for the preparation of pH-responsive nano-based drug delivery systems to treat infectious diseases caused by *S. aureus* and MRSA infections. The specific aims and objectives of this study are highlighted below.

Aim 1

The aim of the study was to synthesize four novel pH-sensitive two chain fatty acid-based lipid derivatives (stearic, oleic, linoleic and linolenic acid derivatives) and explore their potential in the formulation of pH-responsive liposomes for the targeted delivery of VCM against *S. aureus* and MRSA. To achieve this aim, the objectives of the study were to:

1. Use a six-step synthetic scheme to synthesize four novel pH-sensitive two chain fatty acid-based lipid derivatives (stearic, oleic, linoleic and linolenic acid derivatives):
    a. Di -Stearoyl Amino Propionic acid tert-butyl Ester (DSAPE)
    b. Di - Oleoyl Amino Propionic acid tert-butyl Ester (DOAPE)
    c. Di- Linoleoyl Amino Propionic acid tert-butyl Ester (DLAPE)
    d. Di- LinoLenoyl Amino Propionic acid tert-butyl Ester (DLLAPE)
2. Characterize the lipid derivatives using structural elucidation techniques such as FT-IR, ^{1}H NMR and ^{13}C NMR and HRMS.
3. Determine the *in vitro* cytotoxicity of the synthesized lipid derivatives to confirm its bio-safety profile.

4. Formulate VCM-loaded liposomes from lipids with pH-responsive properties and evaluate them in terms of size, PDI, ZP, morphology, entrapment efficiency, *in vitro* drug release, bacterial cell viability using flow cytometry, *in vitro* and *in vivo* antibacterial activity.

Aim 2

The aim of the study was to synthesis a novel oleic acid-derived lipid dendritic amphiphile (OLA-sodium propionate dendritic amphiphile (OLA-SPDA)) and explored its potential in the formulation of pH-responsive micelles for the targeted delivery of VCM against *S. aureus* and MRSA. To achieve this aim, the objectives of the study were to:

1. Use a seven-step synthetic scheme to synthesize a novel oleic acid-derived lipid dendritic amphiphile (OLA-sodium propionate dendritic amphiphile (OLA-SPDA)).
2. Characterize the lipid derivatives using structural elucidation techniques such as FT-IR, ^{1}H NMR and ^{13}C NMR and HRMS.
3. Determine the *in vitro* cytotoxicity of the synthesized lipid derivatives to confirm its bio-safety profile.
4. Formulate VCM-loaded micelles with pH-responsive properties and evaluate them in terms of critical micelle concentration (CMC), size, PDI, ZP, morphology, entrapment efficiency, *in vitro* drug release, bacterial cell viability using flow cytometry, *in vitro* and *in vivo* antibacterial activity.

Aim 3

The aim of the study was to synthesize a novel fatty acid-based bi-tailed zwitterionic lipid conjugated to dimethylglycine head groups (DMGSAD-lipid) and explore its potential in the formulation of pH-responsive LPHNPs for the targeted delivery of VCM against *S. aureus* and MRSA. To achieve this aim, the objectives of the study were to:

1. Use an eleven-step synthetic scheme to synthesize a novel fatty acid-based bi-tailed zwitterionic DMGSAD-lipid.
2. Characterize the DMGSAD-lipid using structural elucidation techniques such as FT-IR, ^{1}H NMR and ^{13}C NMR and HRMS.

3. Determine the *in vitro* cytotoxicity of the synthesized lipid derivative to confirm its bio-safety profile.
4. Formulate VCM-loaded LPHNPs with pH-responsive properties and evaluate them in terms of size, PDI, ZP, morphology, entrapment efficiency, *in vitro* drug release, bacterial cell viability using flow cytometry, *in vitro* and *in vivo* antibacterial activity.

1.5 The novelty of the study

The novelty of the research work presented in the two experimental chapters is as follows,

Aim 1

The research work performed in this study is novel for the following reasons:

- This study reports the synthesis and characterization of bi-tailed fatty acid-based pH-responsive zwitterionic lipids, which have not been reported in the literature previously.
- This study reports the use of bi-tailed fatty acid-based pH-responsive zwitterionic lipids to formulate liposomes, which have not been reported previously for intracellular delivery of any class of drugs.
- This work reports for the first time the surface charge switching liposomes comprising of novel bi-tailed fatty acid-based pH-responsive zwitterionic lipids for targeted delivery of VCM against *S. aureus* and MRSA.

Aim 2

- This study reports the design and synthesis of a novel oleic acid-derived lipid dendritic amphiphile (OLA-sodium propionate dendritic amphiphile (OLA-SPDA)), which has not been reported in the literature before.
- OLA-SPDA has not been reported in the literature for any application, including its use as a nano-based delivery system for any class of drugs.
- The study is the first to investigate the antibacterial potential of OLA-SPDA as an antibiotic delivery vehicle against *S. aureus* and MRSA.
- Whilst polymeric-based dendritic amphiphiles have been reported to deliver anti-cancer agents only, this is the first study that reports the encapsulation and delivery of an antibiotic (VCM) via self-assembly of lipid-based dendritic amphiphile.

Aim 3

- This study reports the synthesis and characterization of fatty acid-based bi-tailed pH-responsive zwitterionic DMGSAD-lipid, which has not been reported in the literature before.
- This study reports the use of novel fatty acid-based bi-tailed pH-responsive zwitterionic DMGSAD-lipid to formulate LPHNPs, which have not been reported before for intracellular delivery of any class of drug.
- This work report for the first time the surface charge switching LPHNPs comprising of novel fatty acid-based bi-tailed pH-responsive zwitterionic DMGSAD-lipid for targeted delivery of VCM against *S. aureus* and MRSA.

1.6 The significance of the study

The novel approach adopted in this study using the nano-based delivery system to enhance antibiotic efficacy can contribute to overcoming the current challenge of antibiotic resistance and avoid limitations associated with their conventional dosage forms. The significance of this study is highlighted below:

New pharmaceutical products: The proposed VCM-loaded pH-responsive liposomes and VCM-loaded pH-responsive micelles are new pharmaceutical products that have not been yet reported, which has the potential to stimulate the local pharmaceutical industries to manufacture cost-effective, superior medicines.

Improved patient therapy and disease treatment: The proposed formulations can improve patient therapy and treatment of various diseases associated with bacterial infections by enhancing antibacterial performance, minimizing doses, lowering side effects and improving patient compliance. It can, therefore, contribute to enhancing the quality of lives of patients and saving lives.

Creation of new knowledge to the scientific community: These proposed studies can lead to new knowledge being generated in pharmaceutical sciences. It can include the following:

- Synthesis schemes for new materials, preparation procedures for the novel drug delivery systems and their properties *in vitro* and *in vivo* can contribute to the creation of new scientific knowledge.

- The extensive *in vivo* testing of these novel systems can provide knowledge for *in vitro in vivo* correlations.

Stimulation of new research: The proposed pH-responsive VCM-loaded liposomes, micelles and LPHNPs systems hold great potential as nano-delivery systems in enhancing the antibacterial activity of VCM against MSSA and MRSA infections. It can stimulate further studies on their clinical evaluation, the potential for other applications and the design of new materials.

1.7 Overview of dissertation

The research work performed is presented in this thesis in a publication format, according to the guidelines of the University of Kwa-Zulu Natal, College of Health Sciences. It specifies the inclusion of a brief introductory chapter, published papers, and a final chapter on the conclusions. A PhD study requires at least three first-authored papers, two of which must be experimental.

CHAPTER 2: EXPERIMENTAL PAPER ONE: This chapter addresses Aim 1, Objectives 1 - 4 and is a first-authored experimental article published in an ISI International Journal: Journal of Drug Targeting (Impact Factor = 3.277). This article highlights the synthesis of novel two-tail fatty acid-based lipid derivatives and explores their potential in the formulation of pH-responsive liposomes. Also, the *in vitro* toxicity evaluation, formulation of the ultra-small vesicles (VCM-liposome) to deliver VCM, characterization of its physical properties and *in vitro* and *in vivo* antibacterial properties were also highlighted.

CHAPTER 3: EXPERIMENTAL PAPER 2: This chapter addresses Aim 2, Objectives 1 - 4 and is a first-authored experimental article published in the ISI international journal: Journal of Pharmaceutical Sciences (Impact Factor 3.197). This article highlights the synthesis of a novel OLA-SPDA lipid dendritic amphiphile. It also highlights the *in vitro* toxicity evaluation, hemolytic study, formulation of the pH-responsive micelles (VM-OLA-SPDA-micelles) for targeted delivery of VCM, characterization of its physical and antibacterial properties both in *vitro* and *in vivo* activity.

CHAPTER 4: EXPERIMENTAL PAPER 3: This chapter addresses Aim 3, Objectives 1–3 and is a first-authored experimental article in preparation for submission. This article highlights the synthesis of a novel fatty acid-based bi-tailed pH-responsive zwitterionic DMGSAD-lipid, the *in*

vitro toxicity evaluation, formulation development of LPHNPs, characterization of its physical properties, *in vitro* and *in vivo* antibacterial properties.

CHAPTER 5. CO-AUTHORED PAPER: In addition to the first authored experimental papers in Chapters 2, 3 and 4 focusing on aims 1, 2 and 3, I have also been involved in other papers within our group as a Ph.D. student. As these papers also focused on the broad aim of this PhD project to improve the treatment of bacterial infections, these papers have been included in the thesis. This chapter, therefore, includes one published experimental paper and one communicated review article in an ISI International Journals: Colloids and Surfaces B: Biointerfaces (Impact Factor = 4.389) and WIREs Nanomedicine & Nanobiotechnology (Impact Factor = 7.689).

CHAPTER 6: CONCLUSION: This chapter includes the overall conclusions from research findings in the study which, provides information on the potential significance of the findings and makes recommendations for future research work in the field of strategic solutions to combat bacterial resistance of antibiotics.

1.8 References

1. World Health Organization. (2014). Antimicrobial resistance: global report on surveillance. World Health Organization. Retrieved from https://apps.who.int/iris/handle/10665/112642.

2. Dan M. Infectious diseases--the progress is huge--a lot remains to be done. Harefuah. 2009; 148 (11):775-7..

3. Brownlie, J.; Peckham, C.; Waage, J.; Woolhouse, M.; Catherine Lyall, C.; Meagher, L.; Tait, J.; Baylis, M.; Nicoll, A., Infectious Diseases: Preparing for the Future: Future Threats. London: Office of Science and Innovation 2006.

4. Michael, C. A.; Dominey-Howes, D.; Labbate, M., The antimicrobial resistance crisis: causes, consequences, and management. Frontiers in public health. 2014, 2, 145.

5. Bloom, D. E.; Cadarette, D., Infectious Disease Threats in the 21st Century: Strengthening the Global Response. Frontiers in immunology. 2019, 10, 549.

6. Nelson, D. W.; Moore, J. E.; Rao, J. R., Antimicrobial resistance (AMR): significance to food quality and safety. Food quality and safety. 2019, 3 (1), 15-22.

7. Fenner, F.; Henderson, D. A.; Arita, I.; Jezek, Z.; Ladnyi, I. D., Smallpox and its eradication. World Health Organization Geneva: 1989, 4(2), 343-5.

8. Ligon BL. Penicillin: its discovery and early development. In Seminars in pediatric infectious diseases. 2004, 15 (1), 52-57.

9. Zaffiri, L.; Gardner, J.; Toledo-Pereyra, L. H., History of antibiotics. From salvarsan to cephalosporins. Journal of Investigative Surgery. 2012, 25 (2), 67-77.

10. Vouga, M.; Greub, G., Emerging bacterial pathogens: the past and beyond. Clinical Microbiology and Infection. 2016, 22 (1), 12-21.

11. Ventola, C. L., The antibiotic resistance crisis: part 1: causes and threats. Pharmacy and therapeutics. 2015, 40 (4), 277.

12. Gould, I. M.; Bal, A. M., New antibiotic agents in the pipeline and how they can help overcome microbial resistance. Virulence. 2013, 4 (2), 185-191.

13. Bhatia, R., Universal health coverage framework to combat antimicrobial resistance. The Indian journal of medical research. 2018, 147 (3), 228.

14. World Health Organization. (2018). Antimicrobial resistance and primary health care: brief. World Health Organization. Retrieved from https://apps.who.int/iris/handle/10665/328084.

15. King DT, Wasney GA, Nosella M, Fong A, Strynadka NC. Structural insights into inhibition of Escherichia coli penicillin-binding protein 1B. Journal of Biological Chemistry. 2017; 292 (3): 979-93.

16. Kapoor, G.; Saigal, S.; Elongavan, A., Action and resistance mechanisms of antibiotics: A guide for clinicians. Journal of anaesthesiology, clinical pharmacology. 2017, 33 (3), 300.

17. Centers for Disease Control and Prevention. (2013). Antibiotic resistance threats in the United States. Retrieved from www.cdc.gov/drugresistance/threat-report-2013.

18. Gelband, H.; Molly Miller, P.; Pant, S.; Gandra, S.; Levinson, J.; Barter, D.; White, A.; Laxminarayan, R., The state of the world's antibiotics 2015. Wound healing southern Africa. 2015, 8 (2), 30-34.

19. Rodvold, K. A.; McConeghy, K. W., Methicillin-resistant Staphylococcus aureus therapy: past, present, and future. Clinical infectious diseases. 2014, 58 (1), 20-27.

20. Garoy, E. Y.; Gebreab, Y. B.; Achila, O. O.; Tekeste, D. G.; Kesete, R.; Ghirmay, R.; Kiflay, R.; Tesfu, T., Methicillin-resistant Staphylococcus aureus (MRSA): prevalence and antimicrobial sensitivity pattern among patients—a multicenter study in Asmara, Eritrea. Canadian Journal of Infectious Diseases and Medical Microbiology. 2019, 2019.

21. Ahmed M . Methicillin Resistant Staphylococcus Aureus (MRSA), A Challenge and an

Opportunity! . WebmedCentral PUBLIC HEALTH 2011;2(6):WMC001996.

22. Monecke S, Coombs G, Shore AC, Coleman DC, Akpaka P, Borg M, Chow H, Ip M, Jatzwauk L, Jonas D, Kadlec K. A field guide to pandemic, epidemic and sporadic clones of methicillin-resistant Staphylococcus aureus. PloS one. 2011; 6 (4), 17936.

23. Hassoun, A.; Linden, P. K.; Friedman, B., Incidence, prevalence, and management of MRSA bacteremia across patient populations—a review of recent developments in MRSA management and treatment. Critical care. 2017, 21 (1), 211.

24. Köck R, Becker K, Cookson B, van Gemert-Pijnen JE, Harbarth S, Kluytmans JA, Mielke M, Peters G, Skov RL, Struelens MJ, Tacconelli E. Methicillin-resistant Staphylococcus aureus (MRSA): burden of disease and control challenges in Europe. Eurosurveillance. 2010; 15 (41): 19688.

25. World Health Organization. (2014). Antimicrobial resistance: global report on surveillance. World Health Organization. Retrieve from https://apps.who.int/iris/handle/10665/112642.

26. Abdulgader, S. M.; Shittu, A. O.; Nicol, M. P.; Kaba, M., Molecular epidemiology of Methicillin-resistant Staphylococcus aureus in Africa: a systematic review. Frontiers in microbiology. 2015, 6, 348.

27. World Health Organization. (2014). WHO's first global report on antibiotic resistance reveals serious, worldwide threat to public health. Retrieved from https://www.who.int/news-room/detail.

28. Falagas ME, Karageorgopoulos DE, Leptidis J, Korbila IP. MRSA in Africa: filling the global map of antimicrobial resistance. PloS one. 2013; 8 (7): 68024.

29. Di Ruscio, F.; Guzzetta, G.; Bjørnholt, J. V.; Leegaard, T. M.; Moen, A. E. F.; Merler, S.; De Blasio, B. F., Quantifying the transmission dynamics of MRSA in the community and

healthcare settings in a low-prevalence country. Proceedings of the National Academy of Sciences. 2019, 116 (29), 14599-14605.

30. Holmes, N. E.; Tong, S. Y.; Davis, J. S.; Van Hal, S. J. In Treatment of methicillin-resistant Staphylococcus aureus: vancomycin and beyond, Seminars in respiratory and critical care medicine, Thieme Medical Publishers. 2015; 36 (1): 17-30.

31. Barna, J.; Williams, D., The structure and mode of action of glycopeptide antibiotics of the vancomycin group. Annual review of microbiology. 1984, 38 (1), 339-357.

32. Rasmussen, R. V.; Fowler Jr, V. G.; Skov, R.; Bruun, N. E., Future challenges and treatment of Staphylococcus aureus bacteremia with emphasis on MRSA. Future microbiology. 2011, 6 (1), 43-56.

33. Panlilio, A. L.; Culver, D. H.; Gaynes, R. P.; Banerjee, S.; Henderson, T. S.; Tolson, J. S.; Martone, W. J.; System, N. N. I. S., Methicillin-resistant Staphylococcus aureus in US hospitals, 1975–1991. Infection Control & Hospital Epidemiology. 1992, 13 (10), 582-586.

34. Drews, T. D.; Temte, J. L.; Fox, B. C., Community-associated methicillin-resistant Staphylococcus aureus: review of an emerging public health concern. Wisconsin Medical Journal-MADISON. 2006, 105 (1), 52.

35. Choo, E. J.; Chambers, H. F., Treatment of methicillin-resistant Staphylococcus aureus bacteremia. Infection & chemotherapy. 2016, 48 (4), 267-273.

36. Tang, J.; Hu, J.; Kang, L.; Deng, Z.; Wu, J.; Pan, J., The use of vancomycin in the treatment of adult patients with methicillin-resistant Staphylococcus aureus (MRSA) infection: a survey in a tertiary hospital in China. International journal of clinical and experimental medicine. 2015, 8 (10), 19436.

37. Davies, J.; Davies, D., Origins and evolution of antibiotic resistance. Microbiology and Molecular Biology Reviews. 2010, 74 (3), 417-433.

38. Walsh, C., Antibiotics: actions, origins, resistance. American Society for Microbiology. 2003, 13 (11): 3059–3060.

39. Gao, W.; Chen, Y.; Zhang, Y.; Zhang, Q.; Zhang, L., Nanoparticle-based local antimicrobial drug delivery. Advanced drug delivery reviews 2018, 127, 46-57.

40. Aminov, R. I., A brief history of the antibiotic era: lessons learned and challenges for the future. Frontiers in microbiology 2010, 1, 134.

41. Cheesman, M. J.; Ilanko, A.; Blonk, B.; Cock, I. E., Developing new antimicrobial therapies: are synergistic combinations of plant extracts/compounds with conventional antibiotics the solution? Pharmacognosy reviews 2017, 11 (22), 57.

42. Andrei, S.; Valeanu, L.; Chirvasuta, R.; Stefan, M.-G., New FDA approved antibacterial drugs: 2015-2017. Discoveries. 2018, 6 (1), 81.

43. Madhav, N.; Oppenheim, B.; Gallivan, M.; Mulembakani, P.; Rubin, E.; Wolfe, N., Pandemics: risks, impacts, and mitigation. In Disease Control Priorities: Improving Health and Reducing Poverty. 3rd edition, The International Bank for Reconstruction and Development/The World Bank. 2017, 9, 315 – 345.

44. Wang, R.; Billone, P. S.; Mullett, W. M., Nanomedicine in action: an overview of cancer nanomedicine on the market and in clinical trials. Journal of Nanomaterials. 2013, 2013, 12.

45. Tinkle, S.; McNeil, S. E.; Mühlebach, S.; Bawa, R.; Borchard, G.; Barenholz, Y.; Tamarkin, L.; Desai, N., Nanomedicines: addressing the scientific and regulatory gap. Annals of the New York Academy of Sciences. 2014, 1313 (1), 35-56.

46. Patra, J. K.; Das, G.; Fraceto, L. F.; Campos, E. V. R.; del Pilar Rodriguez-Torres, M.; Acosta-Torres, L. S.; Diaz-Torres, L. A.; Grillo, R.; Swamy, M. K.; Sharma, S., Nano based drug delivery systems: recent developments and future prospects. Journal of nanobiotechnology. 2018, 16 (1), 71.

47. Zazo, H.; Colino, C. I.; Lanao, J. M., Current applications of nanoparticles in infectious diseases. Journal of Controlled Release. 2016, 224, 86-102.

48. Saidi, T.; Fortuin, J.; Douglas, T. S., Nanomedicine for drug delivery in South Africa: a protocol for systematic review. Systematic reviews. 2018, 7 (1), 1-7.

49. Immordino, M. L.; Dosio, F.; Cattel, L., Stealth liposomes: review of the basic science, rationale, and clinical applications, existing and potential. International journal of nanomedicine. 2006, 1 (3), 297.

50. Wagner, V.; Dullaart, A.; Bock, A.-K.; Zweck, A., The emerging nanomedicine landscape. Nature biotechnology. 2006, 24 (10), 1211-1217.

51. Zhang, L.; Gu, F.; Chan, J.; Wang, A.; Langer, R.; Farokhzad, O., Nanoparticles in medicine: therapeutic applications and developments. Clinical pharmacology & therapeutics. 2008, 83 (5), 761-769.

52. Davis, M. E., Zhuo (Georgia) Chen and Dong M. Shin. Nanoparticle therapeutics: an emerging treatment modality for cancer Nature. Nature Reviews Drug Discovery. 2008, 7 (9):771-82.

53. McNeil, S. E., Nanoparticle therapeutics: a personal perspective. Wiley Interdisciplinary Reviews: Nanomedicine and Nanobiotechnology. 2009, 1 (3), 264-271.

54. Soares, S.; Sousa, J.; Pais, A.; Vitorino, C., Nanomedicine: principles, properties, and regulatory issues. Frontiers in chemistry, 2018, 6, 360.

55. Kalhapure, R. S.; Suleman, N.; Mocktar, C.; Seedat, N.; Govender, T., Nanoengineered drug delivery systems for enhancing antibiotic therapy. Journal of pharmaceutical sciences. 2015, 104 (3), 872-905.

56. Huh, A. J.; Kwon, Y. J., "Nanoantibiotics": a new paradigm for treating infectious diseases using nanomaterials in the antibiotics resistant era. Journal of controlled release. 2011, 156 (2), 128-145.

57. Shi, J.; Votruba, A. R.; Farokhzad, O. C.; Langer, R., Nanotechnology in drug delivery and tissue engineering: from discovery to applications. Nano letters. 2010, 10 (9), 3223-3230.

58. Mura, S.; Nicolas, J.; Couvreur, P., Stimuli-responsive nanocarriers for drug delivery. Nature materials. 2013, 12 (11), 991-1003.

59. Rao, N. V.; Ko, H.; Lee, J.; Park, J. H., Recent progress and advances in stimuli-responsive polymers for cancer therapy. Frontiers in bioengineering and biotechnology. 2018, 6, 110.

60. Mi, P., Stimuli-responsive nanocarriers for drug delivery, tumor imaging, therapy and theranostics. Theranostics. 2020, 10 (10), 4557.

61. Zhao, Y.; Guo, Y.; Tang, L., Engineering cancer vaccines using stimuli-responsive biomaterials. Nano Research. 2018, 11 (10), 5355-5371.

62. Lopes, J. R.; Santos, G.; Barata, P.; Oliveira, R.; Lopes, C. M., Physical and chemical stimuli-responsive drug delivery systems: targeted delivery and main routes of administration. Current pharmaceutical design. 2013, 19 (41), 7169-7184.

63. Liu, J.; Huang, Y.; Kumar, A.; Tan, A.; Jin, S.; Mozhi, A.; Liang, X.-J., pH-sensitive nano-systems for drug delivery in cancer therapy. Biotechnology advances. 2014, 32 (4), 693-710.

64. Su, C.; Liu, Y.; Li, R.; Wu, W.; Fawcett, J. P.; Gu, J., Absorption, distribution, metabolism and excretion of the biomaterials used in Nanocarrier drug delivery systems. Advanced drug delivery reviews. 2019, 143, 97-114.

65. Luo, M.; Jia, Y.-Y.; Jing, Z.-W.; Li, C.; Zhou, S.-Y.; Mei, Q.-B.; Zhang, B.-L., Construction and optimization of pH-sensitive nanoparticle delivery system containing PLGA and UCCs-2 for targeted treatment of Helicobacter pylori. Colloids and Surfaces B: Biointerfaces. 2018, 164, 11-19.

66. Deirram, N.; Zhang, C.; Kermaniyan, S. S.; Johnston, A. P.; Such, G. K., pH-Responsive Polymer Nanoparticles for Drug Delivery. Macromolecular rapid communications. 2019, 40 (10), 1800917.

67. Xie, J.; Fan, Z.; Li, Y.; Zhang, Y.; Yu, F.; Su, G.; Xie, L.; Hou, Z., Design of pH-sensitive methotrexate prodrug-targeted curcumin nanoparticles for efficient dual-drug delivery and combination cancer therapy. International journal of nanomedicine. 2018, 13, 1381.

68. Kaur, I. P.; Kakkar, V.; Deol, P. K.; Yadav, M.; Singh, M.; Sharma, I., Issues and concerns in nanotech product development and its commercialization. Journal of Controlled Release. 2014, 193, 51-62.

69. Čerpnjak, K.; Zvonar, A.; Gašperlin, M.; Vrečer, F., Lipid-based systems as promising approach for enhancing the bioavailability of poorly water-soluble drugs. Acta pharmaceutica. 2013, 63 (4), 427-445.

70. Li, R.; He, Y.; Zhang, S.; Qin, J.; Wang, J., Cell membrane-based nanoparticles: a new biomimetic platform for tumor diagnosis and treatment. Acta Pharmaceutica Sinica B. 2018, 8 (1), 14-22.

71. Zhang, R. X.; Ahmed, T.; Li, L. Y.; Li, J.; Abbasi, A. Z.; Wu, X. Y., Design of nanocarriers for nanoscale drug delivery to enhance cancer treatment using hybrid polymer and lipid building blocks. Nanoscale. 2017, 9 (4), 1334-1355.

72. Stella, B.; Peira, E.; Dianzani, C.; Gallarate, M.; Battaglia, L.; Gigliotti, C. L.; Boggio, E.; Dianzani, U.; Dosio, F., Development and characterization of solid lipid nanoparticles loaded with a highly active doxorubicin derivative. Nanomaterials. 2018, 8 (2), 110.

73. Jaiswal, M.; Dudhe, R.; Sharma, P., Nanoemulsion: an advanced mode of drug delivery system. 3 Biotech. 2015, 5 (2), 123-127.

74. Sercombe, L.; Veerati, T.; Moheimani, F.; Wu, S. Y.; Sood, A. K.; Hua, S., Advances and challenges of liposome assisted drug delivery. Frontiers in pharmacology. 2015, 6, 286.

75. Gabizon, A.; Dagan, A.; Goren, D.; Barenholz, Y.; Fuks, Z., Liposomes as in vivo carriers of adriamycin: reduced cardiac uptake and preserved antitumor activity in mice. Cancer research. 1982, 42 (11), 4734-4739.

76. Zylberberg, C.; Matosevic, S., Pharmaceutical liposomal drug delivery: a review of new delivery systems and a look at the regulatory landscape. Drug Delivery. 2016, 23 (9), 3319-3329.

77. Ferreira, D. d. S.; Lopes, S. C. d. A.; Franco, M. S.; Oliveira, M. C., pH-sensitive liposomes for drug delivery in cancer treatment. Therapeutic delivery. 2013, 4 (9), 1099-1123.

78. Paliwal, S. R.; Paliwal, R.; Vyas, S. P., A review of mechanistic insight and application of pH-sensitive liposomes in drug delivery. Drug delivery. 2015, 22 (3), 231-242.

79. Karanth, H.; Murthy, R., pH-Sensitive liposomes-principle and application in cancer therapy. Journal of pharmacy and pharmacology. 2007, 59 (4), 469-483.

80. Lutwyche, P.; Cordeiro, C.; Wiseman, D. J.; St-Louis, M.; Uh, M.; Hope, M. J.; Webb, M. S.; Finlay, B. B., Intracellular delivery and antibacterial activity of gentamicin encapsulated in pH-sensitive liposomes. Antimicrobial agents and chemotherapy. 1998, 42 (10), 2511-2520.

81. Su, F.-Y.; Chen, J.; Son, H.-N.; Kelly, A. M.; Convertine, A. J.; West, T. E.; Skerrett, S. J.; Ratner, D. M.; Stayton, P. S., Polymer-augmented liposomes enhancing antibiotic delivery against intracellular infections. Biomaterials science. 2018, 6 (7), 1976-1985.

82. Omolo, C. A.; Megrab, N. A.; Kalhapure, R. S.; Agrawal, N.; Jadhav, M.; Mocktar, C.; Rambharose, S.; Maduray, K.; Nkambule, B.; Govender, T., Liposomes with pH responsive 'on

and off'switches for targeted and intracellular delivery of antibiotics. Journal of liposome research 2019, 1-19.

83. Sudimack, J. J.; Guo, W.; Tjarks, W.; Lee, R. J., A novel pH-sensitive liposome formulation containing oleyl alcohol. Biochimica et Biophysica Acta (BBA)-Biomembranes. 2002, 1564 (1), 31-37.

84. Bernkop-Schnürch, A., Strategies to overcome the polycation dilemma in drug delivery. Advanced drug delivery reviews. 2018, 136, 62-72.

85. Foteini, P.; Pippa, N.; Naziris, N.; Demetzos, C., Physicochemical study of the protein–liposome interactions: Influence of liposome composition and concentration on protein binding. Journal of liposome research. 2019, 29 (4), 313-321.

86. Kim, M. W.; Kwon, S.-H.; Choi, J. H.; Lee, A., A promising biocompatible platform: lipid-based and bio-inspired smart drug delivery systems for cancer therapy. International journal of molecular sciences. 2018, 19 (12), 3859.

87. Sabín, J.; Vázquez-Vázquez, C.; Prieto, G.; Bordi, F.; Sarmiento, F. l., Double charge inversion in polyethylenimine-decorated liposomes. Langmuir. 2012, 28 (28), 10534-10542.

88. Obata, Y.; Tajima, S.; Takeoka, S., Evaluation of pH-responsive liposomes containing amino acid-based zwitterionic lipids for improving intracellular drug delivery in vitro and in vivo. Journal of Controlled Release. 2010, 142 (2), 267-276.

89. Kim, M. W.; Jeong, H. Y.; Kang, S. J.; Choi, M. J.; You, Y. M.; Im, C. S.; Lee, T. S.; Song, I. H.; Lee, C. G.; Rhee, K.-J., Cancer-targeted nucleic acid delivery and quantum dot imaging using EGF receptor aptamer-conjugated lipid nanoparticles. Scientific reports. 2017, 7 (1), 1-11.

90. Makhathini, S. S.; Kalhapure, R. S.; Jadhav, M.; Waddad, A. Y.; Gannimani, R.; Omolo, C. A.; Rambharose, S.; Mocktar, C.; Govender, T., Novel two-chain fatty acid-based lipids for development of vancomycin pH-responsive liposomes against Staphylococcus aureus and methicillin-resistant Staphylococcus aureus (MRSA). Journal of drug targeting. 2019, 27 (10), 1094-1107.

91. Thota, B. N.; Berlepsch, H. v.; Böttcher, C.; Haag, R., Towards engineering of self-assembled nanostructures using non-ionic dendritic amphiphiles. Chemical Communications. 2015, 51 (41), 8648-8651.

92. Thota, B. N.; Urner, L. H.; Haag, R., Supramolecular architectures of dendritic amphiphiles in water. Chemical reviews. 2016, 116 (4), 2079-2102.

93. Ramireddy, R. R.; Raghupathi, K. R.; Torres, D. A.; Thayumanavan, S., Stimuli sensitive amphiphilic dendrimers. New Journal of Chemistry. 2012, 36 (2), 340-349.

94. Xu, S.; Krämer, M.; Haag, R., pH-Responsive dendritic core-shell architectures as amphiphilic nanocarriers for polar drugs. Journal of drug targeting. 2006, 14 (6), 367-374.

95. Fleige, E.; Achazi, K.; Schaletzki, K.; Triemer, T.; Haag, R., pH-responsive dendritic core–multishell nanocarriers. Journal of Controlled Release. 2014, 185, 99-108.

96. Zhang, L.; ZHANG, L., Lipid–polymer hybrid nanoparticles: synthesis, characterization and applications. Nano Life. 2010, 1 (01n02), 163-173.

97. Wakaskar, R. R., General overview of lipid–polymer hybrid nanoparticles, dendrimers, micelles, liposomes, spongosomes and cubosomes. Journal of drug targeting. 2018, 26 (4), 311-318.

98. Mukherjee, A.; Waters, A. K.; Kalyan, P.; Achrol, A. S.; Kesari, S.; Yenugonda, V. M., Lipid–polymer hybrid nanoparticles as a next-generation drug delivery platform: state of the art, emerging technologies, and perspectives. International journal of nanomedicine. 2019, 14, 1937.

99. Maji, R.; Omolo, C. A.; Agrawal, N.; Maduray, K.; Hassan, D.; Mokhtar, C.; Mackhraj, I.; Govender, T., pH-Responsive Lipid–Dendrimer Hybrid Nanoparticles: An Approach To Target and Eliminate Intracellular Pathogens. Molecular pharmaceutics. 2019, 16 (11), 4594-4609.

100. Hassan D, Omolo CA, Fasiku VO, Mocktar C, Govender T. Novel chitosan-based pH-responsive lipid-polymer hybrid nanovesicles (OLA-LPHVs) for delivery of vancomycin against methicillin-resistant Staphylococcus aureus infections. International Journal of Biological Macromolecules. 2020; 147, 385-98.

101. Bruniera, F.; Ferreira, F.; Saviolli, L.; Bacci, M.; Feder, D.; da Luz Goncalves Pedreira, M.; Sorgini Peterlini, M.; Azzalis, L.; Campos Junqueira, V.; Fonseca, F., The use of vancomycin with its therapeutic and adverse effects: a review. European review for medical and pharmacological sciences. 2015, 19 (4), 694-700.

102. Vazquez-Guillamet, C.; Kollef, M. H., Treatment of gram-positive infections in critically ill patients. BMC infectious diseases. 2014, 14 (1), 92.

103. Hasan, R.; Acharjee, M.; Noor, R., Prevalence of vancomycin resistant Staphylococcus aureus (VRSA) in methicillin resistant S. aureus (MRSA) strains isolated from burn wound infections. Tzu Chi Medical Journal. 2016, 28 (2), 49-53.

104. McGuinness, W. A.; Malachowa, N.; DeLeo, F. R., Focus: infectious diseases: vancomycin resistance in Staphylococcus aureus. The Yale journal of biology and medicine. 2017, 90 (2), 269.

105. Kullar, R.; Sakoulas, G.; Deresinski, S.; van Hal, S. J., When sepsis persists: a review of MRSA bacteraemia salvage therapy. Journal of Antimicrobial Chemotherapy. 2016, 71 (3), 576-586.

CHAPTER 2: EXPERIMENTAL PAPER 1

2.1 Introduction

This chapter addresses Aim 1 and Objectives 1 – 3 and it is a first authored published experimental article. This chapter highlights the formulation and characterization of VCM-loaded liposomes (VCM-Lipo) from synthesized novel pH-responsive fatty acid-based lipids. The lipids were evaluated for *in vitro* toxicity and the formulated liposomes were evaluated for their physicochemical properties, *in vitro* and *in vivo* antibacterial properties.

2.2 Graphical abstract

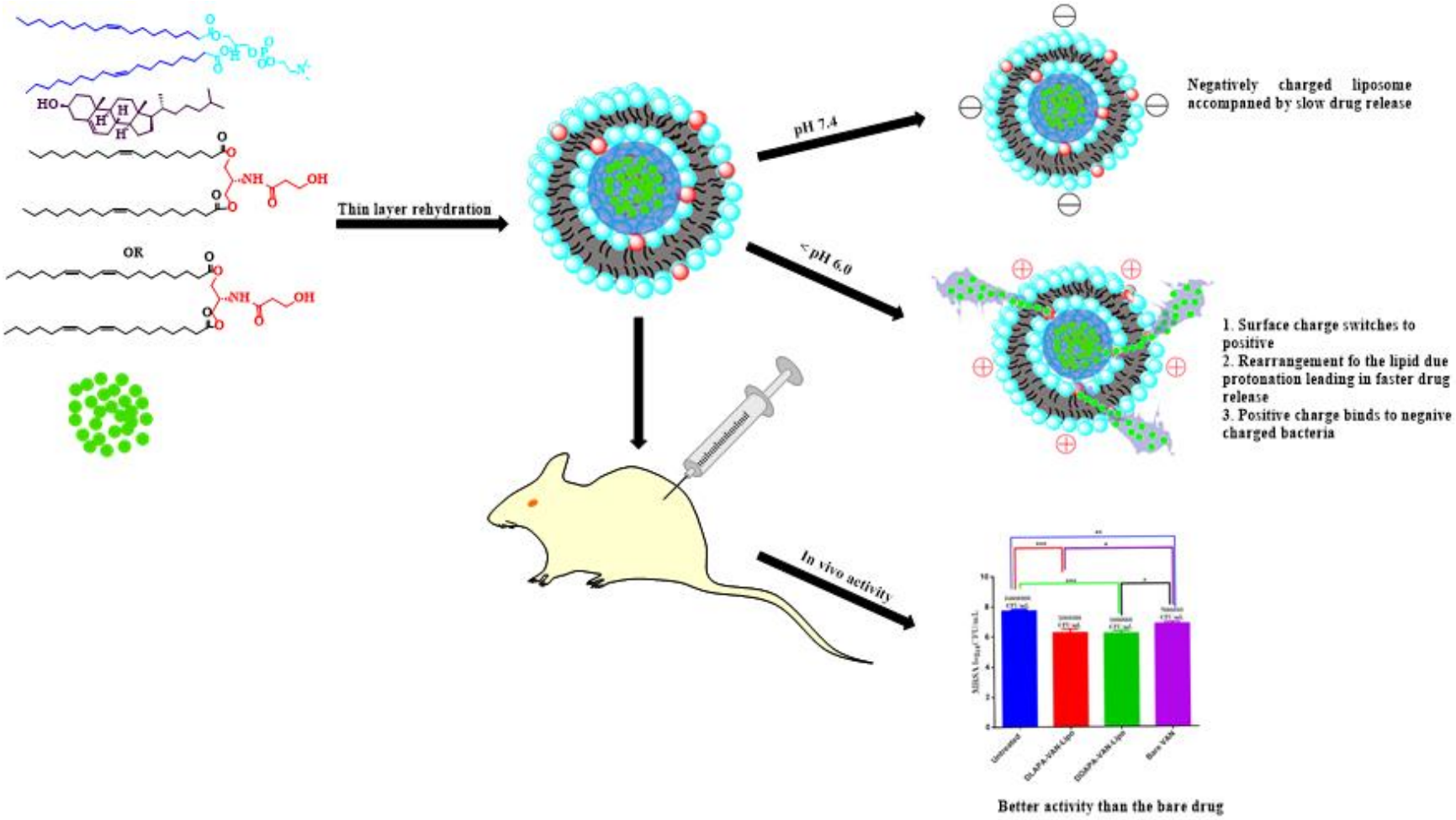

2.3 Published manuscript

Novel two chain fatty acid based-lipids for development of vancomycin pH-responsive liposomes against *Staphylococcus aureus* and Methicillin-resistant *Staphylococcus aureus* (MRSA)

Sifiso S. Makhathini[1], Rahul S. Kalhapure[1,3]*, Mahantesh Jadhav, Ayman Y. Waddad[1], Ramesh Gannimani[1], Calvin A. Omolo[1], Sanjeev Rambharose[1,2], Chunderika Mocktar[1], Thirumala Govender[1,*].

[1]Discipline of Pharmaceutical Sciences, College of Health Sciences, University of KwaZulu-Natal, Private Bag X54001, Durban, South Africa

[2]Division of Emergency Medicine, Department of Surgery, University of Cape Town, Cape Town, South Africa

[3]School of Pharmacy, The University of Texas at El Paso, 500 W University Ave, El Paso, TX 79968, USA.

*Corresponding author.

Email address: govenderth@ukzn.ac.za; rahul.kalhapure@rediffmail.com, rkalhapure@utep.edu

2.4 Abstract

The development of bacterial resistance against antibiotics is attributed to poor localization of lethal antibiotic dose at the infection site. This study reports on the synthesis and use of novel two chain fatty acid-based lipids (FAL) containing amino acid head groups in the formulation of pH-responsive liposomes for the targeted delivery of vancomycin (VAN). The formulated liposomes were characterized for their size, polydispersity index (PDI), surface charge and morphology. The drug loading capacity, drug release, cell viability, and *in vitro* and *in vivo* efficacy of the formulations were investigated. A sustained VAN release profile was observed and *in vitro* antibacterial studies against *S. aureus* and MRSA showed superior and prolonged activity over 72 hours at both pH 7.4 and 6.0. Enhanced antibacterial activity at pH 6.0 was observed for the DOAPA-VAN-Lipo and DLAPA-VAN-Lipo formulations. Flow cytometry studies indicated a high killing rate of MRSA cells using DOAPA-VN-Lipo (71.98%) and DLAPA-VN-Lipo (73.32%). *In vivo* studies showed reduced MRSA recovered from mice treated with formulations by 4 and 2 folds lower than bare VN treated mice respectively. The targeted delivery of VAN can be improved by novel pH-responsive liposomes from the two-chain (FAL) designed in this study

Keywords

Vancomycin; pH-responsive liposome; fatty acid-based lipids; MRSA; targeted drug delivery

2.5 Introduction

Bacterial infections remain a major public health concern worldwide [1], with the emergence of antimicrobial resistance increasingly compromising the effectiveness of first-line antibiotics. Methicillin-resistant *Staphylococcus aureus* (MRSA) is one such example, having developed resistance against the drug Vancomycin (VAN), which is one of the last options for treating this superbug [2, 3, 4]. There are reports on the increasing numbers of MRSA infections in different settings such as health care and community-associated MRSA across the globe and the development of resistance against VAN indicate an urgent need for alternative therapeutic methods to mitigate MRSA infections [5]. Unless there is an intervention, recent reports have indicated that resistant pathogens such as MRSA could increase mortality rate up to 10 million yearly by 2050 worldwide [6].

One of the strategies to fight antimicrobial resistance has been through nano-drug delivery systems that target infection sites. This can lead to efficient cellular uptake, improved antibiotic activity, reduced side effects, improved patient compliance and decreased resistance development [7, 8]. Liposomes are lipid-based vesicular nano-drug delivery systems with an aqueous core that can be employed to deliver both hydrophilic and hydrophobic drugs. Due to the versatility in formulating liposomes, materials responsive to specific stimuli, such as enzymes [9], temperature [10], Redox-sensitive [11], pH and others, can be incorporated in the bilayer or on the surface. This can potentiate a selective delivery of their payloads to the targeted infection site [12].

The acidic environment associated with some pathological conditions, compared with healthy states, can be exploited to potentiate targeted delivery by using pH-responsive delivery systems [13, 14]. Bacteria can thrive under acidic conditions, where antibiotics are prone to losing their activity [15]. Therefore, incorporating bio-safe pH-responsive biomaterials in the liposome formulation facilitates targeting and triggered drug release in response to change in pH at the site of infection [12]. pH-responsive liposomes have been extensively studied as a potential intracellular delivery system for various drug classes to treat infectious diseases [13, 16], however there is limited literature available on pH-responsive liposomes for delivery of antibiotics [17, 18, 19, 20, 21] Several approaches such as using dioleoylphospatidylethanolamine (DOPE) and ionizable acid lipids such as cholesteryl hemisuccinate lipid (CHEMS) [20, 22] have been employed to impact pH-sensitivity, fusogenic ability, stability in biological fluids and cellular internalization of the liposomes with great success [23, 24].

Several reports suggest that zwitterionic lipids, which can be differentially ionized and have better response in various pH conditions and are particularly useful in imparting a surface charge switching mechanism onto the liposomal surface [25]. Furthermore, these lipids undergo conformational changes that lead to disturbance in the membrane bilayer of the liposome thereby increasing the leakage of the drug at acidic conditions [15]. The surface switching of these lipids contributes to the overall cationic charge of the liposomes, promoting electrostatic targeting with the negatively charged bacterial cellular membrane, and enhancing fusogenicity and cellular uptake efficiency [26]. It is also reported that fusogenic properties of liposomes can be enhanced by incorporating fusogenic lipids bearing a long unsaturated/saturated acyl chain [27].

By designing lipids with above-mentioned properties and combining with a zwitterionic head group, both pH-responsive and fusogenic limitations can be addressed to enhance targeting. In this study, we devised and explored the potential of novel fatty acid based zwitterionic lipids to construct pH-responsive liposomes. These lipids typically contained a β-alanine amino acid head (ionizable head groups) that is connected to two long fatty acid tails by ester linkages. The pH-sensitivity of the lipids is achieved through protonation and deprotonation mechanisms of secondary amine and free carboxylic group with a change in pH [14, 15]. The limited literature on pH-responsive liposomes derived from novel synthetic pH-responsive fatty acid-based lipids highlights the need to explore novel pH-responsive lipids for targeted delivery of antibiotics, such as vancomycin (VAN). A recent study on pH-responsive liposome formulated from fatty acid based lipids with similar architecture to the one we are proposing demonstrated that pH-responsive liposome can restore the VAN activity and reduce antibiotic resistance development [18].

In this study, four novel pH-responsive two chain fatty acid-based lipid derivatives (stearic, oleic, linoleic and linolenic acid derivatives) were synthesized, characterized and employed to develop pH-responsive liposomes for the targeted delivery of vancomycin against *S. aureus* and MRSA. We envisage these lipids to be biocompatible for formulation into stable pH-responsive liposomes with good drug entrapment, sustained drug release, and most importantly, improved pH sensitivity and fusogenic properties to enhance drug localization and cellular uptake.

2.6 Materials and methods

2.6.1 Materials

Analytical grade 2-amino-1, 3-propanediol, Triisopropylsilane (TIPS) and tert-butyl acrylate were obtained from Sigma-Aldrich Co. Ltd., (UK). Stearic acid (SA), linoleic acid (LA), Oleic acid (OA), Linolenic acid (LLA), p-dimethylamino pyridine (DMAP), Cholesterol (Chol) and Vancomycin HCl (VAN) were purchased from Sigma-Aldrich Co. Ltd. (USA). Phosphatidylcholine from soybean (PC) was purchased from Lipoid (USA) and 3-(4,5-dimethylthiazol-2-yl)-2,5-diphenyltetrazolium bromide (MTT), Trifluoroacetic acid (TFA) and N, N'-dicyclohexylcarbodiimide (DCC) were purchased from Merck Co. Ltd., (Germany). Nutrient Broth, Nutrient Agar and Mueller Hinton Agar (MHA) were obtained from Biolab Inc. (South Africa) whilst Mueller- Hinton broth 2 (MHB) was obtained from Sigma-Aldrich (USA). Purified water was obtained using Elix® system from Millipore Corp. (USA). Bacterial strains used were *S. aureus* Rosenbach (ATCC®BAA-1683TM) (MRSA) and *S. aureus* (ATCC 25923).

2.6.2 Instrumentation

^{1}H NMR and ^{13}C NMR of all the lipid derivatives were recorded using Bruker 400 and 600 Ultrashield™ (United Kingdom) NMR spectrometer. FT-IR analysis was performed on a Bruker Alpha-p spectrometer with diamond ATR (Germany) whilst HRMS was performed on a Waters Micromass LCT Premier TOF-MS (United Kingdom) for all lipid derivatives. Purified water used in this study was obtained from the Milli-Q purification system (Millipore corp., USA). Optical density (OD) measurements were taken using a spectrophotometer (Spectrostar nano, Germany). Zetasizer Nano ZS90 (Malvern Instruments Ltd., UK) was used to measure and record particle size, polydispersity index and zeta potential whilst Jeol, JEM-1010 (Japan) at 200 kV was used to take Transmission Electron Microscopy (TEM) Images. Cell viability study was performed on The BD FACSCANTO II (Becton Dickinson, CA, USA).

2.7 Methods

2.7.1 *Synthesis and characterization of the lipids*

Scheme 1: Synthesis of mono-substituted two chain pH-responsive lipids (PRL)

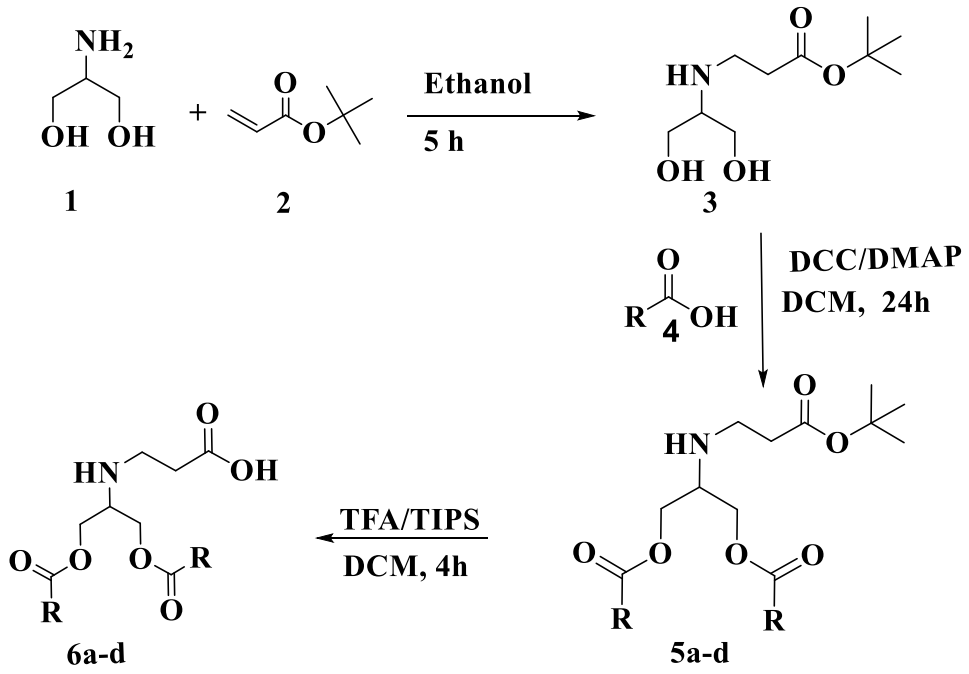

R = a) stearic acid (SAD), b) oleic acid (OAD), c) linoleic acid (LAD), d) linolenic acid (LLAD)

2.7.2 Synthesis of tert-butyl 3-((1,3-dihydroxypropan-2-yl) amino)propanoate (3)

Compound **3** was synthesized by adding 2-amino-1,3-propanediol **1** (1.0 mmol) dropwise at room temperature to a mixture of tert-butyl acrylate **2** (1.10 mmol) in ethanol and stirred for 5 hours. The crude product was obtained by removing the remaining ethanol and excess tert-butyl acrylate under vacuum. This crude was then recrystallized using a mixture of hexane and ethyl acetate (3:1) yielding a final product **3** as a white solid (92%). Characterization was as follows: ^{1}H NMR (400 MHz, $(CD_3)_2SO$) δ(ppm): 1.22 (bs, 9H), 2.13 (t, 2H, J=6.65 Hz), 2.27-2.33 (m, 2H), 2.57 (t, 2H, J=6.65 Hz), 3.08-3.20 (m, 6H); ^{13}C NMR (400 MHz, $(CD3)_2SO$) δ(ppm): 27.7, 36.1, 42.9, 60.7, 61.3, 63.3, 79.4, 171.4. HRMS (ES-TOF) $[M + H]^+$ calculated for $C_{10}H_{21}NO_4+H^+$: 242.1367 found 242.1368.

2.7.3 General procedure for esterification for compound 5a-d

To make a series of compounds (5a- d), the fatty acid (2.02 mmol) was added to a stirring solution of compound **3** (1 mmol) with DCC (2.025 mmol) and DMAP (0.1 mmol) in dry DCM. The reaction mixture was further stirred at room temperature (rt) for 24 hours under inert conditions

(nitrogen atmosphere). The dicyclohexylurea formed (precipitate) was filtered off and the filtrate (organic solvent) was removed under reduced pressure (*vacuum*), and the resulting crude material was purified by column chromatography on silica gel using an illusion system composed of ethyl acetate in hexane (10-15% v/v) to yield an ester derivative. For all the derivatives, yields of above 85% were obtained.

The synthesized ester derivatives were named with the following acronyms:

Di -**S**tearoyl **A**mino **P**ropionic acid *tert*-butyl **E**ster (DSAPE)

Di - **O**leoyl **A**mino **P**ropionic acid *tert*-butyl **E**ster (DOAPE)

Di- **L**inoleoyl **A**mino **P**ropionic acid *tert*-butyl **E**ster (DLAPE)

Di- **L**ino**L**enoyl **A**mino **P**ropionic acid *tert*-butyl **E**ster (DLLAPE)

2.7.3.1 ***Synthesis of DSAPE* (*5a*).** Stearic acid (5.2 g, 18.28 mmol) was added to a stirring solution of compound **3** (2.01 g, 9.12 mmol), DCC (3.763 g, 18.24 mmol) and DMAP (0.112 g, 0.92 mmol) in dry DCM (40 ml) under nitrogen at room temperature and the resulting mixture was stirred for 24 hours. The resulting product was separated into a white solid using the general procedure section (**2.2.2**) with a high yield of above 87%. Characterization was as follows; ^{1}H NMR (400 MHz, $CDCl_3$) δ(ppm): 0.810 (t, 6H, J=7.07 Hz), 1.18 (m, 56H),1.38 (s, 9H),1.56-1.51(m, 4H), 2.29 (t, 4H, J =7.53 Hz), 2.50(t, 2H, J =7.40 Hz), 2.63(t, 2H, J =6.83 Hz), 3.30-3.23(m, 1H), 4.23(d, 4H, J =4.52 Hz); ^{13}C NMR (400 MHz, $CDCl_3$) δ(ppm): 14.10, 22.68, 24.70, 28.0, 29.10, 29.4, 29.6, 31.9, 34.0, 42.4, 55.57, 79.5, 171.4, 173.3. HRMS (ES-TOF) $[M + H]^+$ calculated for $C_{46}H_{89}NO_6+H^+$: 774.6588, found 774.6595.

2.7.3.2 ***Synthesis of DOAPE (5b).*** Oleic acid (5.15 g, 18.24 mmol) was added to a stirring solution of compound **3** (2.0 g, 9.12 mmol), DCC (3.763 g, 18.24 mmol) and DMAP (0.111 g, 0.912 mmol) in dry DCM (40 ml) under nitrogen at room temperature and the resulting mixture was stirred for 24 hours. The resulting product was isolated into a colourless oil using the general procedure section (**2.2.2**) with a high yield of above 92%. Characterization was as follows; ^{1}H NMR (400 MHz, $CDCl_3$) δ (ppm): 0.76 (t, 6H), 1.15-1.19 (m, 40H), 1.33(s, 9H), 1.58-1.50 (m, 4H),1.87-1.90 (m, 8H), 2.18-2.22 (m, 4H), 2.3 (t, 2H, J=7.67 Hz), 2.79 (t, 2H, J=6.34 Hz), 2.93(m, 1H), 3.9-4.0 (s, 4H), 5.21-5.26 (m, 4H); ^{13}C NMR (400 MHz, $CDCl_3$) δ(ppm): 14.0, 22.6, 24.80, 27.1, 28.0, 29.10, 31.8, 34.0, 34.0, 35.8, 42.9, 55.3, 80.4,129.6, 129.8, 171.7, 173.3. HRMS (ES-TOF) $[M + H]^+$ calculated $C_{46}H_{85}NO_6+H^+$: 770.6275, found 770.6281.

2.7.3.3 ***Synthesis of DLAPE (5c).*** Compound **5c** was synthesized by adding linoleic acid (4.47 g, 15.96 mmol) to a stirring mixture of compound **3** (3.5 g, 15.9 mmol), DCC (6.58 g, 31.92 mmol) and DMAP (0.194 g, 1.59 mmol) in dry DCM (40 ml) under nitrogen at room temperature and the resulting mixture was stirred for 24 hours. The resulting product was isolated as a pale-yellow oil using the general procedure section (**2.2.2**) with a high yield of above 89%. Characterization was as follows; ^{1}H NMR (400 MHz, $CDCl_3$) δ (ppm) : 0.80-0.84 (m, 6H), 1.19-1.27 (m, 32H), 1.39 (s, 9H), 1.58-1.51 (m, 4H), 1.91-2.0 (m, 8H), 2.24 (t, 4H, J=7.54 Hz), 2.34 (m, 2H), 2.69 (m, 4H), 2.83 (t, 2H, J=6.48 Hz), 2.99-2.93 (m, 1H), 4.03 (d, 4H, J=5.48 Hz), 5.34-5.21 (m, 8H); ^{13}C NMR (400 MHz, $CDCl_3$) δ (ppm): 14.07, 22.3, 24.7, 25.0, 26.8, 28.0, 28.0, 28.9, 28.9, 29.5, 29.6, 29.8, 31.2, 32.5, 35.14, 37.0, 42.7, 55.3, 60.14, 80.0, 127.8, 129.7, 172.1, 173.3. HRMS (ES-TOF) $[M + H]^+$ calculated for $C_{46}H_{81}NO_6+H^+$: 766.5962, found 766.5976.

2.7.3.4 ***Synthesis of DLLAPE (5d).*** Linolenic acid (7.62 g, 26.36 mmol) was added to a stirring mixture of compound **3** (3 g, 13.68 mmol), DCC (5.65 g, 27.36 mmol) and DMAP (0.167 g, 1.37 mmol) in dry DCM (40 ml) under nitrogen at room temperature and the resulting mixture was stirred for 24 hours. The resulting product was isolated as a pale brown oil using the general procedure section (**2.2.2**) with a high yield of above 85.6%. Characterization was as follows; ^{1}H NMR (400 MHz, $CDCl_3$) δ(ppm): 0.804 (t, 6H, J=7.35 Hz), 1.15-0.97 (m, 24H), 1.28 (s, 9H), 1.30-1.27 (m, 4H), 2.0-1.75 (m, 8H), 2.11 (t, 4H, J=7.25 Hz), 2.34 (t, 2H, J=6.46 Hz), 2.68-2.40 (m, 8H), 3.60-3.54 (m, 1H), 4.0 (d,4H, J=5.73 Hz), 5.30-5.22 (m, 12H); ^{13}C NMR (400 MHz, $CDCl_3$) δ(ppm): 13.9, 19.9, 24.1,25.0, 26.5, 28.4, 28.6, 28.9, 30.3, 30.8, 39.4, 41.3, 54.5, 59.7, 126.8, 127.6, 129.7, 131.3, 171.5, 172.2. HRMS (ES-TOF) $[M + H]^+$ calculated for $C_{46}H_{77}NO_6+H^+$: 762.5649, found 762.5663.

2.7.4 General procedure for hydrolysis

To a solution of tert-butyl ester derivative (**4a-d**) in dry dichloromethane (DCM), a solution of DCM, trifluoroacetic acid (TFA) and triisopropylsilane (TIPS) (5:4:1 v/v/v) were added slowly, and this was further stirred at rt for 6 hours. The solvent and excess TFA were vacua evaporated and the resulting residue was triturated several times with chloroform for complete removal of remaining traces of TFA. The product was isolated by column chromatography on silica gel using an elution system composed of methanol in chloroform (10% v/v). The purified product was dried under vacuum for 48 hours and was then characterized by FT-IR, NMR (^{1}H and ^{13}C) and mass analysis for structural confirmation.

The synthesized final lipids were named with the following acronyms:

Di-**S**tearoyl **A**mino **P**ropionic **A**cid (DSAPA)

Di-**O**leoyl **A**mino **P**ropionic **A**cid (DOAPA)

Di-**L**inoleoyl **A**mino **P**ropionic **A**cid (DLAPA)

Di-**L**ino**L**enoyl **A**mino **P**ropionic **A**cid (DLLAPA).

2.7.4.1 ***Synthesis of DSAPA (6a).*** TFA (5 ml) and TIPS (2 ml) were added to a 10 ml mixture of compound **5a** (2 g) in DCM, and the desired product was purified following the procedure described in section **2.2.3** as a white solid with a high yield above 85 %. Characterization was as follows; FTIR: 3465.46, 2914.88, 2848.83, 1729.88, 1678.02, 1196.56, 1161.23 cm^{-1}; ^{1}H NMR (400 MHz, $(CD_3)_2SO$)δ (ppm): 0.833 (t, 6H, J=6.69 Hz), 1.27 (m, 56H), 1.59-1.54 (m, 4H), 2.35 (t, 4H, J=7.56 Hz), 2.50 (t, 2H, J=7.41 Hz), 2.68 (t, 2H, J=6.81 Hz), 3.74-3.70 (m, 1H), 4.23 (d, 4H, J=4.62 Hz); ^{13}C NMR (400 MHz, $(CD_3)_2SO$) δ(ppm): 14.25, 22.4, 24.69, 29.42,31.36, 31.70, 33.78, 42.23, 55.38, 60.64, 172.7, 172.79; HRMS (ES-TOF) $[M + H]^+$ calculated for $C_{42}H_{81}NO_6+H^+$: 696.6142; found 696.6147.

2.7.4.2 ***Synthesis of DOAPA (6b).*** TFA (7.5 ml) and TIPS (3 ml) were added to a 15 ml mixture of compound **5b** (2.9 g) in DCM, and the desired product was purified following the procedure described in section **2.2.3** as a viscous pale-yellow oil with a high yield above 76%. Characterization was as follows; FTIR: 3462.99, 2923.28, 1730.73, 1671.76, 1190.76, 1134.66 cm^{-1}; ^{1}H NMR (400 MHz, $(CD_3)_2SO$)δ (ppm): 0.78-0.80 (m, 6H), 1.20 (m, 40H), 1.49 (m, 4H), 1.91-1.93 (m, 6H), 2.24-2.28 (m, 3H), 2.60-2.62 (m, 2H), 3.13-3.16 (m, 2H), 3.53-3.55 (m, 1H), 4.1-4.2 (m, 4H), 5.2 (m, 3H), 7.58 (m, 1H); ^{13}C NMR (400 MHz, $(CD_3)_2SO$) δ(ppm): 13.60, 22.0, 24.1, 26.57, 28.6, 29.10, 31.30, 33.14, 41.4, 54.4, 60.25, 129.27, 131.0, 166, 172; HRMS (ES-TOF) $[M + H]^+$ calculated for $C_{42}H_{77}NO_6+H^+$: 692.5829; found 692.5833

2.7.4.3 ***Synthesis of DLAPA (6c).*** TFA (5 ml) and TIPS (2 ml) were added to a 10 ml mixture of compound **5c** (2 g) in DCM, and the desired product was purified following the procedure described in section 2.2.3 as a viscous pale-brown oil with a high yield above 84.6%. Characterization was as follows; FTIR: 3467.60, 3007.76, 2923.46, 2864.76, 1739.38, 1666.55, 1142.42 cm^{-1} ; ^{1}H NMR (400 MHz, CDCl3) δ(ppm): 0.87 (m, 7H,), 1.16-1.3(m, 32H), 1.37 (m, 5H),1.9-2.0 (m, 7H), 2.33-2.36 (m, 4H), 2.74-2.77 (m, 2H), 2.8 (m, 2H), 3.4 (m, 2H), 3.6-3.7 (m,

1H) 4.4 (m, 4H), 5.28-5.36(m, 5H); ^{13}C NMR (400 MHz, $CDCl_3$): δ 14.0, 22.5, 24.85, 25.6, 27.2, 29.0, 29.3, 29.7, 31.5, 31.8, 33.6, 42.4, 56.5,59.7, 127.8, 129.9, 173.2, 174.3; HRMS (ES-TOF) $[M + H]^+$ calculated for $C_{42}H_{73}NO_6+H^+$: 688.5516; found 688.5524.

2.7.4.4 ***Synthesis of DLLAPA (6d)***. TFA (10 ml) and TIPS (4 ml) were added to a 20 ml mixture of compound **5d** (3.55 g) in DCM, and the desired product was purified following the procedure from section **2.2.3** as a thick brown oil with a high yield above 88.4 %. Characterization was as follows; FTIR: 3431.45, 3009.92, 2926.97, 2857.17, 1728.66, 1666.85, 1159.69 cm^{-1}; ^1H NMR (400 MHz, $(CD_3)_2SO$) δ(ppm): 0.91 (m, 4H,), 1.2507 (m, 24H), 1.50-1.52 (m, 6H), 1.98-2.05 (m, 8H), 2.32 (t,4H, J=7.33 Hz), 2.68-2.77 (m, 8H), 3.27(m,1H), 3.76 (m, 1H), 4.29-4.30(m, 4H), 5.24-5.36(m, 12H); ^{13}C NMR (400 MHz, $(CD_3)_2SO$) δ(ppm): 13.9, 19.9, 24.1,25.0, 26.5, 28.4, 28.9, 30.3, 30.8, 39.4, 41.3, 54.5, 59.7, 126.8, 127.6, 129.7, 131.3, 171.5, 172.2; HRMS (ES-TOF): $[M + H]^+$ calculated for $C_{42}H_{69}NO_6+H^+$: 684.5203; found 684.5213.

2.8 In vitro cytotoxicity

The cytotoxicity evaluation of the newly synthesized lipid derivatives (DSAPA, DOAPA, DLAPA, and DLLAPA) was performed using the MTT assay as previously reported in literature [28]. The cell lines used in this study were: human alveolar basal epithelial cells (A549), human breast adenocarcinoma (MCF7), and human liver hepatocellular carcinoma (HepG2). Negative controls (culture medium with cells only) and positive controls (culture medium without cells) were conducted for validation of our results. 2.5×10^3 cells/mL were seeded into 96-well plates and treated with lipid solutions of different concentrations (20, 40, 60, 80 and 100 µg/ml) that were prepared from 1% w/v stock solution after incubating for 24 hours. Plates were then incubated for 48 hours at 37 ºC in 5% CO_2 humidified incubator. Thereafter spent media was replaced with fresh culture medium and MTT solution (100 µl) and incubated for 4 hours at 37 ºC. Spent media was removed and dimethyl sulfoxide was added to the well to dissolve MTT formazan crystals. Absorbance measurements were recorded for each well using a microplate spectrophotometer (Spectrostar nano, Germany) at 540 nm. All the experiments were run in triplicate. The percentage of viable cells was quantified using the equation below:

% Cell viability = (A_{540nm} treated cells/A_{540nm} untreated cells) x 100%

2.9 Preparation of VAN encapsulated pH-responsive liposomes

pH-responsive liposomes were prepared using thin film hydration method [29]. This method involves dissolving a 100 mg (5 ml of chloroform) mixture of Chol, PC and pH-responsive lipid

derivative (PRL) at a ratio of 1:3:1 w/w by mass respectively in a round bottom flask (RBF). The solvent was evaporated using rotavapor under reduced pressure (*vacuum*) at 40 ºC to form a thin film on the inner side of the round bottom flask. The resulting film was purged with nitrogen and stored in a vacuum desiccator overnight to remove the remaining trace amounts of the solvent. The film was then hydrated with 10 ml of the VAN solution of 1 mg/ml concentration in distilled water over 2 hours at room temperature for complete conversion into liposomes. The formed liposomes were vortexed for 3 minutes and the probe sonicated for 15 minutes at 30% amplitude using an Omni sonic rupture 400 Ultrasonic Homogenizer (Kennesaw, GA 30144, USA).

2.10 Particle size (PS), polydispersity index (PDI), zeta potential (ZP) and morphology

The formulated liposomes were characterized for their PS, PDI, and ZP using dynamic light scattering technique. This was done by diluting the formulation to a suitable concentration with suitable phosphate buffer solutions. Measurements were recorded using a Zetasizer instrument fitted with a 633 nm laser at 173° detection optics at room temperature (25 ºC) in triplicate to ensure reliability. The liposomes were further characterized for their morphological features using TEM analysis. The samples were appropriately diluted, stained with 1% uranyl acetate solution for 30 seconds, dried on a copper grid and images were acquired using JEOL Microscopy (JEM 1010, Japan) at 100 kV.

2.11 Entrapment efficiency (EE)

Ultrafiltration method using Amicon® Ultra-4 centrifugal filter tubes (10 kDa molecular weight cut-off) was used to determine encapsulated VAN amount in the liposomes. To separate the free drug from the vesicles, samples were centrifuged at 2000 rpm, 25 °C for 45 minutes using a centrifugal filter tube. The amount of drug in the supernatant was analyzed by a UV-Visible spectrophotometer (Shimadzu UV-1650 PC) at 280 nm. The entrapment efficiency (EE) was quantified using the following equation [30].

$$\%EE = \frac{(W_{\mathrm{TD}} - \mathrm{W}_{\mathrm{FD}})}{W_{\mathrm{TD}}} \times 100$$

W_{TD} is the total drug in the liposome formulation and W_{FD} is the total free drug in the supernatant obtained by centrifugation.

2.12 In vitro drug release study

The diffusion technique using a dialysis bag was used to investigate the *in vitro* drug release behaviour and the amount of drug release from both the pH-responsive VAN-liposomes and the

bare VAN solution. The dialysis bag (MWCO 14,000 Da) was used to load VAN encapsulated formulation (2 ml) and their corresponding blanks, sealed and immersed in 40 ml phosphate buffer solutions (pH 7.4, and pH 6.0). Samples were incubated at 37 °C in a shaking incubator (100 rpm). The amount of VAN released was measured by withdrawing 3 ml of sample from the receiver to be analyzed using a spectrophotometric method (UV-1650PC, Shimadzu, Japan) at 280 nm in triplicate. In order to maintain the sink condition, the volume of the release medium was kept constant by replacing it with an equal amount of fresh PBS after each sampling. The drug release kinetics of the liposomes were computed using various mathematical models (Zero order, First order, Higuchi, Weibull, Hixson-Crowell and Korsmeyer–Peppas) to understand the VAN release profile with respect to a change in the pH and models were analyzed using DDSolver software. The best fit model, the correlation coefficient (R^2) and root mean square error (RMSE) were calculated, with all experiments being performed in triplicate. Moreover, the Korsmeyer–Peppas model release exponent (n) and the Weibull model β value were calculated to determine the release mechanism [31].

2.13 Antibacterial studies

2.13.1 In vitro antibacterial activity

The *in vitro* antibacterial studies of liposomes formulated from synthesized pH-responsive fatty acid-based lipid were performed against MRSA and *S. aureus*. The minimum inhibitory concentration (MIC) of bare VAN, VAN-loaded formulations (DSAPA-VAN-Lipo, DOAPA-VAN-Lipo, DLAPA-VAN-Lipo and DLLAPA-VAN-Lipo), each containing 1 mg/ml of VAN and VAN free formulations (DSAPA- Lipo, DOAPA-Lipo, DLAPA -Lipo and DLLAPA- Lipo), were evaluated using the broth dilution method [32]. The MICs for all lipid derivatives (DSAPA, DOAPA, DLAPA, and DLLAPA) were also determined using the same procedure. Nutrient Broth was used to culture *S. aureus* and MRSA for 18 hours in a shaking incubator at 37 °C (Labcon, USA) set at 100 rpm. The bacterial cultures were diluted with sterile distilled water using a DEN-1B McFarland densitometer (Latvia) to make 0.5 McFarland's Standard (i.e. 1.5 x 10^8 colony forming units (CFU)/ml). A concentration of 1.5 x 10^8 colony forming units (CFU)/ml was further diluted 1:150 with sterile distilled water to a concentration of 5×10^5 CFU/ml. The VAN, drug-free (blank) liposomes and vancomycin loaded liposomes were serially diluted in MHB at both pH 6.0 and 7.4. The prepared bacterial cultures were added, and this was incubated at 37 °C for 18 hours in a shaking incubator set at 100 rpm. The MIC was determined by inoculating each diluted

sample onto Mueller-Hinton Agar (MHA) plates. After incubation, 10 µl of each dilution was spotted on MHA and again incubated at 37 °C for 18 hours. The MIC was determined as the lowest concentration where there was no bacterial growth after 24 hours, this procedure was repeated at 48 and 72 hours. All experiments including VAN free liposomes (negative control), VAN-loaded liposomes and bare VAN (positive controls) were performed in triplicate (n = 3).

2.13.2 Bacterial cell viability assay

Bacterial cell viability studies were conducted using the flow cytometry assay method [33, 34, 35]. The MRSA suspension was prepared as previously described to achieve a final concentration of 5 × 10^5 CFU/ml. Bare VAN (7.8 µg/ml), DOAPA-VAN-Lipo (1.56 µg/ml) and DLAPA-VAN-Lipo (1.56 µg/ml) were prepared equivalent to their respective MICs. Bare VAN was also prepared at the concentration (1.56 µg/ml) equivalent to the MIC of the liposome formulation. The MRSA (15 µl) was added to a solution in a 96-well plate and incubated at 37 °C for 6 hours in a shaking incubator (100 rpm). Untreated MRSA cells were used as a negative control, with percentage cell viability determined after incubation [33]. The volume of 50 µl of bare VAN (at both concentration), DOAPA-VAN-Lipo and DLAPA-VAN-Lipo were mixed with 350 µl of the sheath fluid in a separate flow cytometry tubes for each sample, and vortexed for 5 minutes [36]. The mixture was incubated at 37 °C for 30 minutes with 5 µl of the non-cell wall permeant Propidium iodide (PI) dye. PI fluorescence was excited by a 455-nm laser and collected through a 636 nm bandpass filter [37, 38]. Flow cytometry study was conducted using the BD FACSCANTO II (Becton Dickinson, CA, USA) instrument with the flow rate settings set up to 16 ml/min and 0.1 ml/min for the sheath fluid and the sample respectively. Data with the fixed cells were collected using flow cytometer software (BD FACSDIVA V8.0.1 software [USA]). The voltage settings used for the fluorescence-activated cell sorting (FACS) analysis were: 731 for the forward scatter [FSC], 538 for the side scatter [SSC] and 444 for PI. The forward scatter was used for the initial gating of the bacteria, after which the appropriate size of the cells was gated and for each sample with at least 10,000 cells being collected in triplicate. The positions of the 'live' and 'dead' cells that were gated were therefore determined. The detection threshold was set to 1,000 in SSC analyses to reduce the background signal from particles smaller than the bacteria [35]. The captured data was further analyzed using the Kaluza-1.5.20 (Beckman Coulter USA) flow cytometer software.

2.13.3 In vivo antibacterial activity and Histological evaluation

All the animal experiments were performed in accordance with the protocol approved by the Animal Research Ethics Committee of the University of KwaZulu-Natal (Approval number AREC/104/015PD). The *in vivo* efficacy of the bare VAN, DOAPA-VAN-Lipo, and DLAPA-VAN-Lipo were investigated against MRSA [39], which was grown as previously described and diluted with a sterile saline solution to an appropriate concentration of 1.5 x 10^8 CFU/ml. Biomedical Research Unit (UKZN) provided male BALB/c mice (18 - 20 g) which were divided into three groups: negative control, positive control and treated group. A small section at the back of the mice was shaved and disinfected with 70% ethanol to eliminate skin contamination prior to treatment. A bacterial suspension of (50 µl) was injected intradermally into the three stated groups of mice (n = 4 per group). After 30 minutes of infection, saline, bare VAN and VAN-liposome formulations were injected at the infection sites, of the mice which represent the negative control, positive control and treatment groups respectively. After 48 hours, the infected skin from the euthanized mice was harvested and homogenized in 5 ml of phosphate buffer solution pH 7.4 (PBS). This was followed by serial dilutions of tissue homogenates using PBS. Thereafter, 20 µl of each dilution was plated on to Nutrient Agar plates and incubated at 37 °C for 18 hours. The number of CFU/ml was analyzed after incubation. The histological evaluation of the treated and untreated skin samples was done as per a previously reported procedure[40]. This procedure involved harvesting of the skin tissue from both controls and skin samples treated with formulations and stored in formalin for 7 days at room temperature. On day seven, ethanol was used to dehydrate the sample followed by fixation with paraffin wax. The infected skin sections were collected on slides, dried, and stained with hematoxylin and eosin (H&E). Sections were viewed via light microscopy using the Nikon 80i light microscope (Japan), and NIS Elements D software and Nikon U2 camera (Japan) was used to digitally capture the images.

2.14 Physical Stability

VAN-liposomes formulations were kept at different temperatures (4 °C and rt) for 90 days to determine their short-term physical stability. The physical stability of the formulations was assessed at different time intervals (30, 60 and 90 days) by measuring the particle size, PDI, ZP and observing their physical appearance, this analysis was performed in triplicate.

2.15 Statistical analysis

The experiments were performed in triplicate, and the collected data are expressed as the mean ±standard deviation. GraphPad Prism® software (Graph Pad Software Inc., Version 6, San Diego, CA) was used for statistical analysis. One-way analysis of variance (ANOVA), followed by Bonferroni's multiple comparison tests was used to determine statistical significance, with *P* values of less than 0.05 being considered statistically significant.

2.16 Results and discussion

2.16.1 Synthesis and characterization of pH-responsive lipids

Novel pH-responsive lipids consisting of a β-alanine amino acid head group that is connected to two long fatty acid tails (different C-18 fatty acids) by ester linkages (DSAPA, DOAPA, DLAPA, and DLLAPA) were synthesized in three steps. The first step involved the formation of a carbon-nitrogen bond via mono Aza-Michael addition reaction between tertiary butyl acrylate and serinol to form compound **3 (Scheme 1)**. A broad singlet peak at chemical shift δ 1.39 ppm integrating to 9 protons in ^{1}H NMR, and the appearance of peaks at δ 27.7, 36, 48, 79.4 and 171 ppm in ^{13}C NMR corresponding to $C(CH_3)_3$-COO-, -CH_2C=O-, -CH_2-NH-and C=O functional groups, confirmed the formation of compound **3**. The compounds belonging to the series **5a-d** were obtained by esterification of different fatty acids (Stearic, Oleic, Linoleic, and Linolenic acid), with compound **3** using DCC/DMAP coupling chemistry. The appearance of peaks at chemical shift δ 0.806 (triplet), δ 1.18 (multiplet), δ 1.54 (multiplet) and δ 2.27 ppm (triplet) in ^{1}H NMR confirmed the formation of the products. The tertiary butyl ester groups of compounds **5a-d** were hydrolyzed using TFA and TIPS (scavenger) combination to obtain the desired pH-responsive lipids **6a-d,** as shown in **scheme 1**. The disappearance of the t-boc peak at 1.38 ppm in ^{1}H NMR and at 28 ppm in ^{13}C NMR confirmed the formation of the final product. Furthermore, the HRMS analysis confirmed the molecular mass of newly synthesized compounds, indicating their successful synthesis.

2.16.2 In vitro cytotoxicity

A cytotoxicity study of newly synthesized materials (lipid derivatives) is of importance in evaluating its biosafety [41, 42, 43]. Cell viability was quantified using the MTT (tetrazolium) cytotoxicity assay by exposing the tested material to mammalian cells that have the capacity to

metabolically reduce tetrazolium to insoluble formazan crystals. The reduction of tetrazolium can be related to cell metabolic activity, thus, the amount of formazan crystals formed is equivalent to the number of viable cells. Human cell lines (A549, MCF 7 and Hep G2) were used to assess the biosafety of all four lipids (DSAPA, DOAPA, DLAPA, and DLLAPA) samples. The MTT results revealed that all synthesized novel lipids displayed a high percentage cell viability (> 75%) after 48-hour exposure across all concentration range studied. The percentage cell viability of lipids from the different cell lines ranged from 79 - 86% for the A549 cells, 84 - 86% for the MCF 7 cells, and 80 - 84% for the Hep G2 cells for all concentrations studied, as shown in **figure 1**. The cell viability of all lipids was greater than 75%, with no dose-dependent trends observed. The low toxicity level of these lipids can be attributed to the non-toxic nature of the parent fatty acids, these findings confirming that the derivatization maintains the non-toxic nature of these biomaterials, and hence are safe for biomedical applications [44].

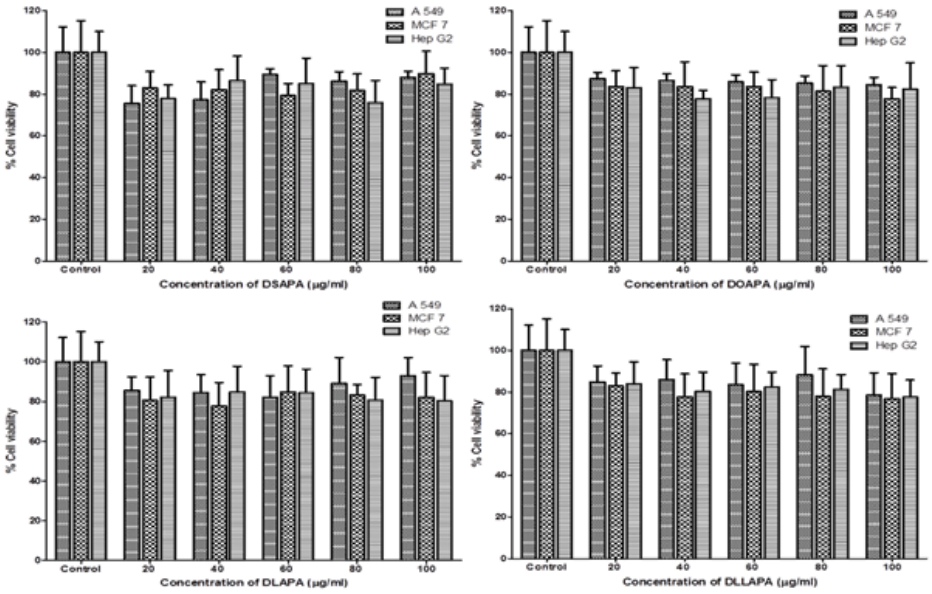

Figure 1. Cell viability study against A549, MCF 7 and Hep G2 cells exposed at various concentrations of DSAPA, DOAPA, DLAPA and DLLAPA for 48 h

2.16.3 Preparation and Characterization of VAN-loaded liposomes

2.16.3.1 Size, Surface charge, Entrapment efficiency, and Morphology

Having confirmed the biosafety of the two chain fatty acid based-lipids, the thin film hydration method was used in the subsequent preparation of the pH-responsive liposomes, with VAN as a model antibiotic drug [29]. The pH-responsive liposomes, composed of PC/Cholesterol/ pH-responsive lipid (PRL's) in a ratio of 1:3:1 w/w, were prepared in a stepwise process by thin film hydration, sonication and filtration [29, 45]. Stable pH-responsive liposomes were formed by varying the quantity of PRL's and Chol concentration. pH-responsive liposomes (VAN free and loaded) prepared using optimized formula were characterized for their size, PDI, surface charge switching (zeta potential), VAN entrapment efficiency and morphology.

The entrapment efficiency of VAN-Lipo, DSAPA-VAN-Lipo, DOAPA-VAN-Lipo, DLAPA-VAN-Lipo and DLLAPA-VAN-Lipo formulations was 37.83 ± 2.5%, 36.43 ± 0.64%, 44.27 ± 9.2%, 38.68 ± 4.7% and 29.86 ± 4.5% respectively **(table 1**), demonstrating similar results to previous reports of VAN-loaded liposomes prepared using this method [25]. The results, as shown in **table S1a and S1b**, indicate that all formulations presented a uniform liposome size ranging from 86.28 ± 11.76 to 282 ± 31.58 nm, with their respective PDI's ranging from 0.151 ± 0.016 to 0.204 ± 0.014 at different pHs. The TEM images revealed spherical shape with sizes that were in agreement with those obtained from DLS studies. The size range is in-line with the results obtained from our previously reported VAN loaded pH-responsive liposomes [18].

The effect of pH on the size and surface charge of all formulations was evaluated using DLS by exposing the liposome to different pH environments (pH 7.4, 6.0 and 5.5) (**table S1a and S1b)**. At pH 7.4, the liposome surface charge was found to be -11.8 ± 2.99 mV. However, as the pH decreased from the physiological pH to acidic pH, the surface charge switched to a positive value of 3.10 ± 0.583 mV at pH 5.5. This change in ZP was associated with an increase in the size of the liposomes (**table S1a and S1b)**. The change in physical properties of the liposomes can be attributed to their swelling and aggregation due to the protonation of the PRL within the bilayer membrane of liposomes. As the PRL gets protonated at acidic conditions, it induces a positive overall surface charge of the liposomes [46, 47]. The surface charge of the system switching is important for antibacterial activity, as it indicates possible binding of the positively charged liposomes to the negatively charged bacterial cell wall for enhancing the targeting and killing of

the bacteria.[15]. The two-chain fatty acid-based lipids designed in this study were therefore capable of successfully generating pH-responsive liposomes.

Table 1: Effect of the two-tailed fatty acid-based lipids on the entrapment efficiency of pH-responsive liposomes

Formulations	Entrapment efficiency (% EE)
VAN-Lipo	37.83 ± 2.5%
DSAPA-VAN-Lipo	36.43 ± 0.64%
DOAPA-VAN-Lipo	44.27 ± 9.2%
DLAPA-VAN-Lipo	38.68 ± 4.7%
DLLAPA-VAN-Lipo	29.86 ± 4.5%

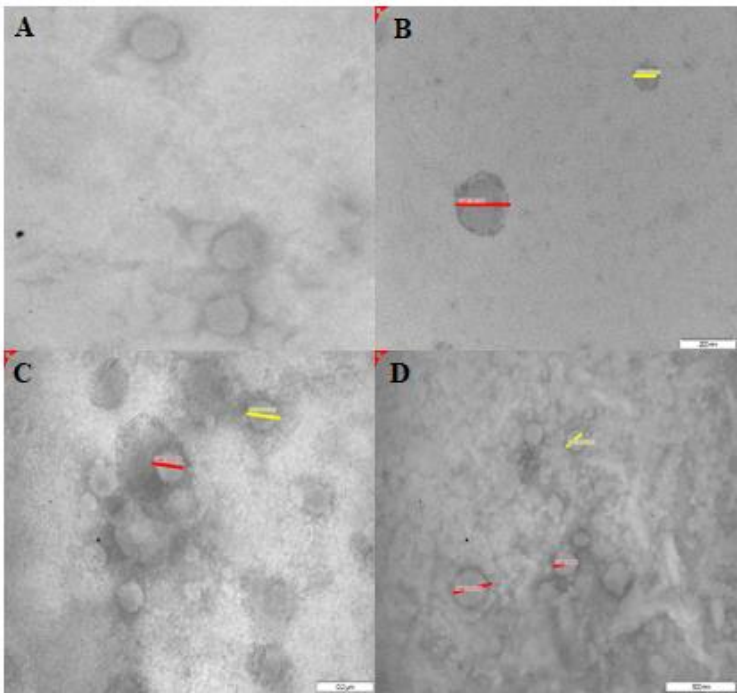

[**Figure 2**. TEM images of VAN loaded liposomes (A) DSAPA-VAN-Lipo, (B) DOAPA-VAN-Lipo, (C) DLAPA-VAN-Lipo and (D) DLLAPA-VAN-Lipo

2.16.4 In vitro drug release and release kinetics

In vitro drug release studies were performed to determine the release profiles of the VAN from both the liposomes and the bare drug solution at pH 7.4 and 6.0. F**igure**: **3A-B** represents the *in vitro* release profiles of the VAN loaded liposomes at both pH 7.4 and 6.0. During the first 3 hours, the cumulative VAN release from all the formulations was less than 30%, demonstrating a slow and sustained release profile, whilst the bare VAN solution released approximately 40% of VAN after 3 hours. Thus, the liposomal formulations displayed slower release across all pHs when compared to the bare VAN after the first 3 hours. The amounts of VAN released at both pH 7.4 and 6.0 were compared to determine whether there was a pH-dependent release of the VAN from the liposomal formulations.

The effect of a change in pH on the amount of VAN released between pH 7.4 and 6.0 was insignificant for all formulations at all-time intervals. It was observed that although the surface charge of the system switched from negative to positive, it did not induce a faster release at acidic pH as expected. However, after 5 hours, the DLLAPA-VAN-Lipo showed a higher release, with percentage cumulative VAN release of 31.75 ± 3.49 at pH 7.4 and 45.74 ± 0.77 at pH 6.0, whereas at the end of 24 hours, the VAN release was 39.33 ± 3.68% at pH 7.4 and 82.84 ± 3.86% at pH 6.0. More than one factor (acidic pH and degree of saturation) may have contributed towards the increase in the VAN release from the DLLAPA-VAN-Lipo after the fifth hour. The effect of acidic pH, structural conformation and the pecking order of the fatty acid chain within the bilayer can contribute towards the drug release mechanism of the liposomes formulated [48]. The effect of the acidic pH can lead to conformational changes of the PRL lipids within the bilayer, inducing swelling of the liposome vesicles, thus enhancing the VAN release via diffusion. The degree of unsaturation of the C_{18} fatty acid chain affects the pecking order of the lipids from forming bilayer into forming non-bilayer structures. It has been reported that the increase in the *cis* double bonds creates kink and bends at the position of the double bond, making it difficult to pack into a bilayer structure, which can contribute towards drug permeability, resulting in a high percentage cumulative release of the drug [48].

The release mechanism of the formulations was then analyzed with various mathematical models. The release kinetic analysis for all formulations at both pHs using mathematical models (Zero order, First order, Higuchi, Korsmeyer-Peppas, Hixon-Crowell, and Weibull) was performed to further understand the release behaviour of the VAN from the formulated liposomes. Among all

models tested for drug release behaviour from all the formulations at both pHs, the Weibull model was found to be the best fit, as it had the highest correlation coefficient (R^2) that was closer to 1 and the lowest root mean square error (RMSE) **(table S2a and 2b).** This model is mostly applicable when comparing the release profiles of the matrix type drug delivery by fitting parameters and is also useful in describing the release of pharmaceutical doses in terms of the fraction of drug accumulated in solution at a given time [49, 50]. In this manner, the model allows for direct assessment and quantification of proportionality and can predict the trajectory of the dissolution curve over time.

To further understand the VAN release mechanism for all formulations, the β value which describes the shape of the dissolution curve progression was calculated and found to fall within the range of $0.75 < \beta < 1$ (**table S3**) at both pHs, indicating that more than one release mechanism was involved. The diffusion controlled release in the normal Euclidean substrate and pH controlled release contributed to the release mechanism (combined release mechanism) and the shape of the dissolution profile of the formulation [50]. This suggested that the incorporation of pH-responsive lipids initiate release of the drug in response to change in pH. The release mechanism was also evaluated using the Korsmeyer-Peppas model exponent value (n), where n was found to be within the range of $0.43 < n < 0.85$ (**table S3**), confirming that the release mechanism from all formulations was non-Fickian at both pHs. The exponent values from the Korsmeyer-Peppas model and the beta value from the Weibull model gave an indication of the involvement of more than one drug release mechanism, a diffusion and pH-controlled release. Therefore, a high degree of unsaturation and reduced pH may contribute towards a high and fast VAN release which can enhance the antibacterial activity by improving the drug localization and bioavailability at the acidic infection site.

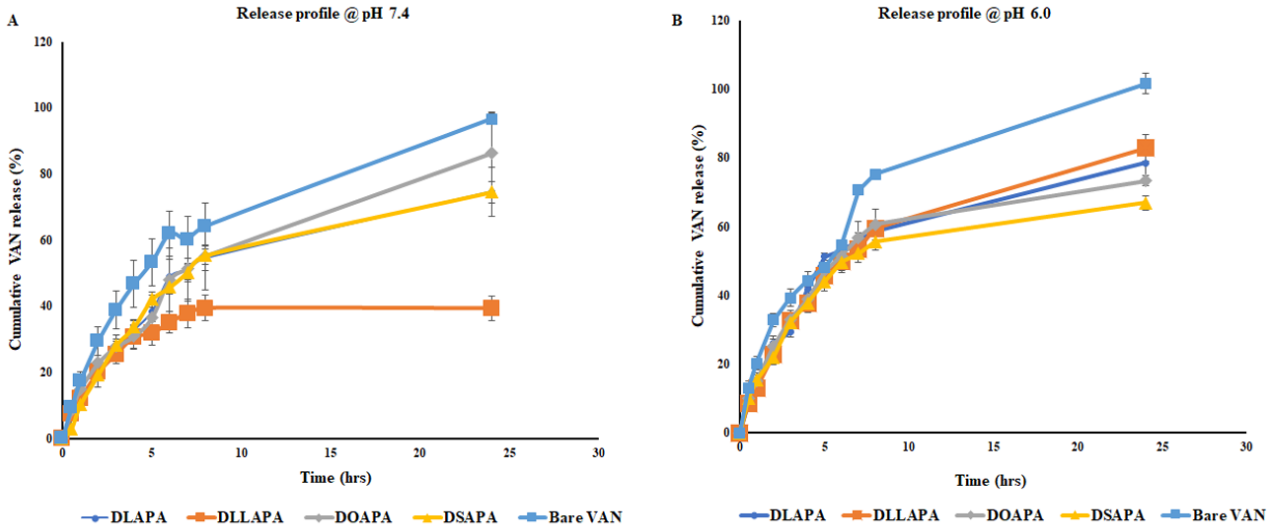

Figure 3: In vitro VAN release profile from (B) are VAN, DSAPA-VAN-Lipo, DOAPA-VAN-Lipo, DLAPA-VAN-Lipo and DLLAPA-VAN-Lipo formulations at both (A) pH 7.4 and (B) 6.0.

2.16.5 Antibacterial Efficacy

2.16.5.1 In vitro antibacterial activity

MRSA accounts for more than 64% of healthcare-associated *Staphylococcus aureus* infections and MRSA infections incidents, medical cost and mortality due to therapeutic failure were reported to be higher than those of methicillin-sensitive *Staphylococcus aureus*(MSSA) infections [51]. Infectious Diseases Society of America guidelines still suggest VAN as the drug of choice against pathogens belonging to gram-positive bacteria such as *S. aureus* and its resistant strain (MRSA) and have reported that vancomycin trough concentrations should be maintained at 15–20 mg/L for serious infections to avoid MRSA resistance to vancomycin [51, 52]. Reports suggest that unless alternative therapeutic methods are adopted, the extensive use of vancomycin reduces its effectiveness against MRSA infections [53]. Therefore, in this study VAN was used as a drug of choice for SA and MRSA, the latter was selected as a positive strain for the study and *S. aureus* was used as a control as it is a less lethal strain of the bacteria.

The MIC values of the parent lipid derivatives (DSAPA, DOAPA, DLAPA, and DLLAPA), bare VAN, VAN-liposomes (DSAPA-VAN-Lipo, DOAPA-VAN-Lipo, DLAPA-VAN-Lipo, and DLLAPA-VAN-Lipo) and their respective VAN free liposome formulations, are shown in **tables 2a** and **2b**. The parent lipid derivatives and VAN free liposome formulations showed no activity

at both pHs. Although the results from our previous study reported that the fatty acids used in the synthesis of these lipids have activity at higher concentration (> 625 µg/ml) [54], the lack of antibacterial activity could be attributed to the derivatization of the fatty acids into lipids and the low concentration of lipids used (< 100 µg/ml). Bare VAN at both pH 7.4 and 6.0 against *S. aureus* showed a loss of activity by 2-fold with a decrease in pH, which correlates with previously reported data **(table 2a and 2b)** [15, 55]. A concentration of 7.8 µg/ml of bare VAN was required against MRSA at both pHs to induce the antibacterial effect. VAN loaded liposomes from all lipid derivatives against both *S. aureus* and MRSA demonstrated a superior antibacterial activity when compared to the bare VAN at both pHs, confirming that the nano-formulations improved the activity of VAN.

The superiority of the formulation can be attributed to the encapsulation of VAN with surface charge switching liposomes which enhances the targeted delivery and provides protection against acidic conditions, which could extend the half-life and restore effectiveness at the site of infection, where bare VAN is known to lose its activity [56]. Surface charge switching liposomes can increase its association with the negatively charged bacterial membrane through increased electrostatic binding affinity under acid conditions creating a passage for the drug to the bacterial cells at a lethal dose. Therefore, enhanced cellular uptake of the drug using pH-responsive liposomes can significantly improve the therapeutic effect of antibiotics while minimizing the development of resistance. Additionally, MRSA membrane thickness and vancomycin affinity trapping prevent the diffusion of large molecules like vancomycin from reaching the cytoplasmic membrane where cell wall synthesis begins. This can be closely linked to vancomycin-resistance development requiring high levels of the drug to achieve membrane before reaching the site of action, thus the need for increased MIC in MRSA than SA [57]. However, through targeting via surface switching liposomes more drug can be delivered to the bacteria as the drug will only be released at the site of infection (bacterial vicinity). Also, the pH-responsive lipids are made of fatty acids which have been reported to transport the drug in the bacteria thus the reduction in MIC compared to the bare drug [58].

VAN loaded liposomes formulations were also compared at different pHs to assess their responsiveness in terms of antibacterial activity. The DSAPA-VAN-Lipo after 24 hours at both pHs against *S. aureus* had the MIC of 1.56 µg/ml, whereas against MRSA the activity was improved by 2.5-fold at pH 6.0 when compared to pH 7.4. DOAPA-VAN-Lipo, DLAPA-VAN-

Lipo and DLLAPA-VAN-Lipo enhanced the VAN activity by 2-fold at pH 6.0 against both *S. aureus* and MRSA strain as compared to pH 7.4. All the formulations had activity over a period of 72 hours at pH 6.0, however, DOAPA-VAN-Lipo and DLAPA-VAN-Lipo had the lowest MIC against both *S. aureus* and MRSA strain over a period of 72 hours at pH 6.0 when compared to pH 7.4.

These findings suggest that among all formulations, the DOAPA-VAN-Lipo and DLAPA-VAN-Lipo against both *S. aureus* and MRSA showed better activity at pH 6.0 when compared to pH 7.4, with the MIC values being 1.56 µg/ml for both formulations over a period of 72 hours. Particularly at pH 6.0, enhanced activity of the formulations can be associated with the protonation of the PRLs in the liposomes, contributing towards an overall positive surface charge of the liposomes. This can facilitate a fusion process by increasing the electrostatic binding affinity with the negatively charged bacterial membrane, which can improve targeting and enhance the exposure of the drug to the bacterial cells at a lethal dose [21]. The above-mentioned formulations also had sustained and extended activity, which can be correlated to their sustained drug release profile.

It is also widely reported from studies focusing on the structural relationship of long-chain unsaturated/saturated fatty acids, fatty acids derivatives and their antibacterial properties, that long-chain unsaturated fatty acids such as oleic acid and other unsaturated fatty acid are bactericidal against important pathogens including Methicillin-resistant *Staphylococcus aureus*, whereas stearic acid and other saturated long-chain fatty acids were found to be less active [59]. Therefore, zwitterion lipids derived from these fatty acids, possess antimicrobial activity which can help enhance the activity of the formulation [60]. These results suggest that pH-responsive lipids with a long unsaturated fatty-acid chain used in the formulation of liposomes can be a promising alternative for the targeted and enhanced delivery of antibiotics against *S. aureus* and MRSA at acidic infection sites. These results could be vital in lowering the dose required to treat infections with VAN without affecting the therapeutic outcomes and could go a long way towards improving patient compliance and lowering the dose-dependent toxicity of vancomycin, such as nephrotoxicity and Redman's syndrome

Table 2a. *In vitro* antibacterial activity of bare VAN and VAN loaded pH-responsive liposomes at pH 7.4.

MIC/ µg/ml	24 hours		48 hours		72 hours	
	S. aureus	MRSA	*S. aureus*	MRSA	*S. aureus*	MRSA
Bare VAN	1.95	7.8	NA	NA	NA	NA
DSAPA-VAN-Lipo	1.95	3.9	3.9	3.9	NA	NA
DOAPA-VAN-Lipo	**0.78**	**1.56**	**3.1**	**1.56**	**3.1**	**6.25**
DLAPA-VAN-Lipo	**0.78**	**1.56**	**1.56**	**1.56**	**3.1**	**1.56**
DLLAPA-VAN-Lipo	0.98	3.9	3.9	7.8	3.9	7.8

NA = No Activity

Table 2b. *In vitro* antibacterial activity of bare VAN and VAN loaded pH-responsive liposomes at pH 6.0.

MIC/ µg/ml	24 hours		48 hours		72 hours	
	S. aureus	MRSA	*S. aureus*	MRSA	*S. aureus*	MRSA
Bare VAN	3.9	7.8	NA	NA	NA	NA
DSAPA-VAN-Lipo	1.95	1.95	3.9	3.9	3.9	3.9
DOAPA-VAN-Lipo	**0.78**	**1.56**	**0.78**	**1.56**	**1.56**	**1.56**
DLAPA-VAN-Lipo	**0.78**	**1.56**	**1.56**	**1.56**	**1.56**	**1.56**
DLLAPA-VAN-Lipo	1.95	1.95	1.95	3.9	3.9	3.9

NA = No Activity

2.16.5.2 Bacterial cell viability assay

Cell (MRSA) viability was performed using a rapid flow cytometry method [61]. This study was performed on the DOAPA-VAN-Lipo and DLAPA-VAN-Lipo formulations, which were identified from the *in vitro* antibacterial activity study as the most promising formulations when compared to bare VAN and other formulations. Using a specialized dye (PI fluorescent), dead MRSA cell were detected after 6 hours incubation with bare VAN, DOAPA-VAN-Lipo and DLAPA-VAN-Lipo mediums separately by observing the morphological changes of the bacterial cell. PI fluorescent dye is a non-cell wall permeant that allows for the classification of cells into

dead cells in the population [62]. Histogram plots of the PI fluorescence versus cell count (PI uptake) of the incubated samples (**figure 4**) were generated using Kaluza-1.5.20 (Beckman Coulter USA) flow cytometer software. Figure **4A** represents live cells (negative events) with no PI uptake. Vancomycin has a well-known mode of action in inhibiting bacterial cell wall synthesis, thus upon treatment of the bacteria with VAN, the uptake of PI, which is a non-cell wall permeant dye it is expected. This results in a shift in fluorescence upon intercalation with the DNA of the bacteria, which can be quantified. The gates were created beyond the fluorescence of the viable cells for detecting the dead cells in the population. After treating the MRSA cells with bare VAN, DOAPA-VAN-Lipo, and DLAPA-VAN-Lipo, a PI fluorescence shift was observed (**figure 4B, C, and D**). VAN (**figure 4E**), DOAPA-VAN-Lipo (**figure 4C**), DLAPA-VAN-Lipo (**figure 4D**) at their respective MICs (7.8 µg/ml, 1.56 µg/ml and 1.56 µg/ml) displayed 63.40 ± 1.51%, 71.98 ± 1.3% and 73.32 ± 1.21% of MRSA dead cells in the population respectively. This indicates that at a lower concentration, the formulations showed higher killing percentages.

Incubating the MRSA cells with bare VAN at the same concentration as the MIC of the formulations (1.56 µg/ml), which is 5-folds lower than the MIC of bare VAN, displayed a killing percentage of only about 32.98 ± 1.49% dead cells. These results are in support with those from the previous section (*in vitro* antibacterial activity), thereby showing the superiority of encapsulating the VAN into the liposome, in terms of improving the antibacterial activity of VAN compared to conventional methods. This suggests that encapsulating the VAN in the pH-responsive liposomes enhances their efficacy and reduces the daily dose required to treat the infection, resulting in preventing the development of drug resistance.

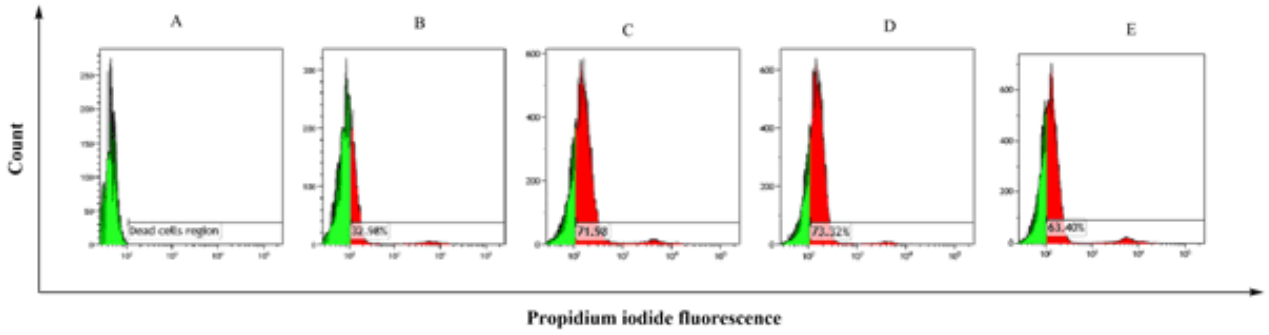

Figure 4: (A) untreated MRSA (live cells), B, C, D and E representing the percentage of dead cells after incubation with VAN, DOAPA-VAN-Lipo and DLAPA-VAN-Lipo at 1.59 mg/mL MIC and VAN at its MIC (7.8 mg/mL) respectively at pH 7.4.

2.16.5.3 In vivo antibacterial activity and Histological evaluation

DOAPA-VAN-Lipo and DLAPA-VAN-Lipo formulations when compared to the bare VAN and other formulation, demonstrated superior results from both the *in vitro* antibacterial activity and the bacterial cell viability studies. These formulations were further evaluated to confirm their *in vivo* efficacies in a biological system. This was performed using a BALB/c mice skin infection model, and the number of CFUs were being quantified for untreated, bare VAN, DOAPA-VAN-Lipo, and DLAPA-VAN-Lipo treated groups and represented as $\log_{10}$ CFU/ml. The one-way ANOVA tests demonstrated a significant reduction ($P < 0.0002$) in the bacterial load recovered from the treatment groups treated with the bare VAN, DOAPA-VAN-Lipo and, DLAPA-VAN-Lipo when compared to the untreated group.

The MRSA count was 7.7-fold significantly higher ($P = 0.0043$) for the untreated group when compared to the VAN treated mice skin. In all conditions, the DOAPA-VAN-Lipo and DLAPA-VAN-Lipo were the most effective in efficiently reducing the MRSA count of the treated skin. The MRSA count in the untreated mice, when compared to the DOAPA-VAN-Lipo and DLAPA-VAN-Lipo, was 32.4- fold ($P < 0.0002$) and 16- fold ($P < 0.0003$) folds. The DOAPA-VAN-Lipo and DLAPA-VAN-Lipo formulation reduced the MRSA count by 4.2-fold ($P = 0.023$) and 2.1-fold ($P = 0.035$) respectively when compared to the bare VAN. There was no significant difference in the CFU/mL reduction when comparing the groups treated with the DOAPA-VAN-Lipo and DLAPA-VAN-Lipo formulations ($P > 0.9$). These *in vivo* antibacterial activity results, together with the *in vitro* antibacterial activity and cell viability results of the formulations, show the effectiveness of the fatty acid-based lipid derivatives in formulations of pH-responsive liposomes as a practical alternative in the fight against MRSA compared to the bare VAN alone.

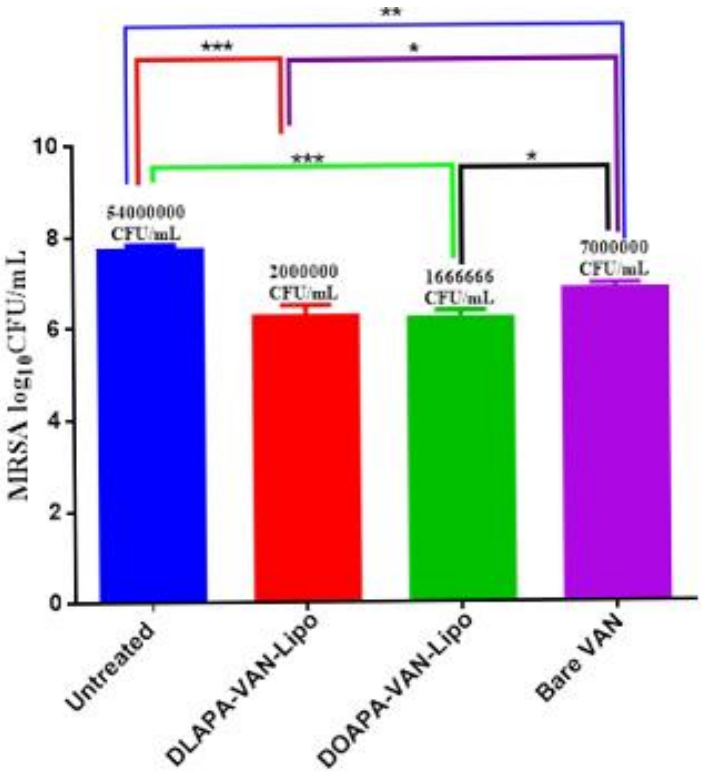

Figure 5: MRSA count post 48 h of treatment. Data represent the mean ± SD (n = 3). *denotes statistical significance for DOAPA-VAN-Lipo and DLAPA-VAN-Lipo versus the bare VM. **denotes significant difference between untreated versus bare VAN, and ***denotes the significant difference between the untreated and DOAPA-VAN-Lipo and DLAPA-VAN-Lipo.

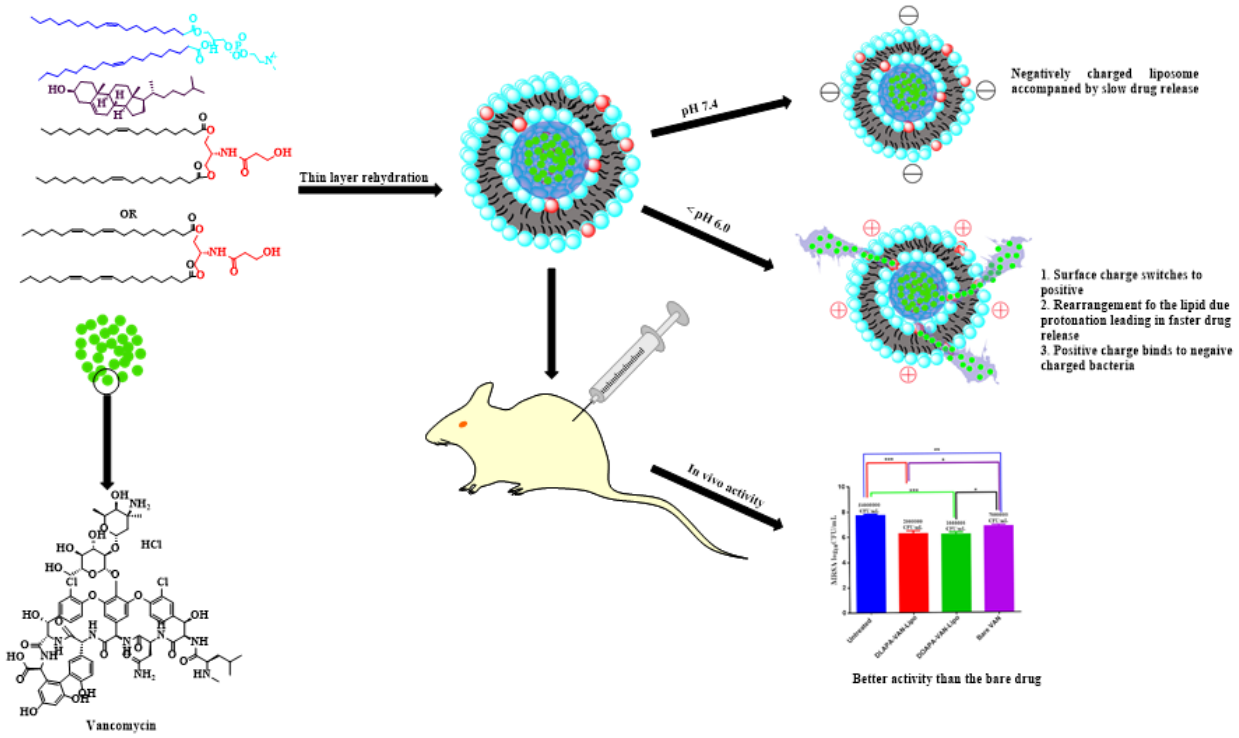

Figure 6: Schematic illustration of VAN-Lipo formulation and their in vivo efficacy

The morphological analysis was performed on all removed skin samples (untreated, bare VAN, DOAPA-VAN-Lipo and DLAPA-VAN-Lipo treated groups) to evaluate the histological changes and skin integrity at 48 hours after the MRSA infection. Using H&E stained slides, untreated skin samples showed signs of tissue inflammation and abscess formation (**figure 6A**). There was also signs of swelling and abscess formation on the bare VAN treated group, although the degree of inflammation was much less than that of the untreated group (**figure 6B**). A smaller region of abscess formation with a decreased inflammation, as represented by the decreased swelling, was observed from the DOAPA-VAN-Lipo treated group (**figure 6C**). This group (**figure 6D**) displayed no signs of abscess formation, with minimal signs of tissue inflammation being observed. The presence of white blood cells (WBCs) at the infection site is also an indication of the degree of inflammation. The untreated and bare VAN treated groups presented large quantities of WBCs, whereas the DLAPA-VAN-Lipo treated group presented a lower quantity of WBCs, which were minimal in the DLAPA-VAN-Lipo treated group.

There was a direct correlation between the histomorphological observations and the recovered bacterial loads from each study. A high count of bacteria loads at the infection site of the untreated

and VAN treated skin samples represented by high levels of inflammation, abscess formation and the presence of white blood cells as a result of the increased immune response. Whereas, infected skin samples treated with DOAPA-VAN-Lipo and DLAPA-VAN-Lipo showed a reduced immune response indicating the lowest count of isolated bacteria with minimal signs of inflammation and abscess formation. These findings of the histomorphological studies confirmed the antimicrobial advantage and superiority of the DOAPA-VAN-Lipo and DLAPA-VAN-Lipo compared to bare VAN.

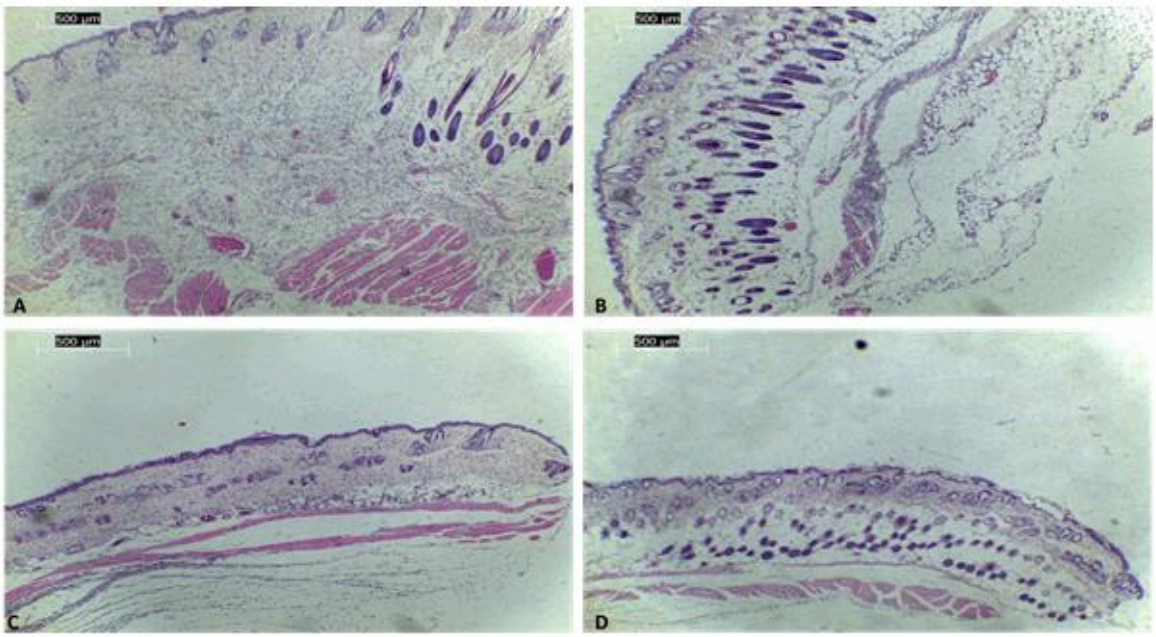

Figure 7: Light Microscopy (LM) micrographs of the control and the treated skin samples stained with H&E; (X40) (A) Untreated (MRSA and Saline), (B) Bare VM, (C) DOAPA-VAN-Lipo and (D) DLAPA-VAN-Lipo.

2.16.6 Physical stability studies

All formulations were investigated for short-term physical stability under different storage conditions (room temperature and at 4 ºC) for 3 months. The physical appearance, particle size, PDI and zeta potential were observed at 0, 30, 60 and 90 days. All formulations showed stability, with no significant differences ($P > 0.05$) in size, PDI and zeta values over a period of 90 days at 4 ºC. At room temperature, the DOAPA-VAN-Lipo and DLAPA-VAN-Lipo proved to be more stable than the DSAPA-VAN-Lipo and DLLAPA-VAN-Lipo formulations, which showed

instability in terms of physical appearance, indicating some precipitate after the second month, and a significant increase in particle size and PDI ($P < 0.05$) when compared to DOAPA-VAN-Lipo and DLAPA-VAN-Lipo

2.17 Conclusion

Bacterial resistance against one of the last-line antibiotics (e.g. VAN) has become a major concern to public health worldwide. Alternative therapeutic strategies, such as targeted delivery to address this problem, have been introduced. In this study, pH-responsive, VAN loaded liposomes were developed from novel pH-responsive two tail fatty acid-based lipid derivatives for targeted and sustained delivery of VAN at the site of infection. There were changes in size, PDI and zeta potential of the formulated liposome with respect to a change in pH from 7.4 to 6.0. The DOAPA-VAN-Lipo and DLAPA-VAN-Lipo were the most effective formulated liposomes, demonstrating enhanced *in vitro* antibacterial activity at acidic conditions. The *in vivo* studies also confirmed the superiority of these formulations over bare VAN against MRSA. The percentage killing of 71.98 ± 1.3% and 73.32 ± 1.21% for DOAPA-VAN-Lipo and DLAPA-VAN-Lipo, respectively suggested that these formulations are better than bare VAN at very low concentrations. This can help reduce effective doses required thereby preventing possible drug resistance. The biosafety of the lipids, together with their enhanced antibacterial activity, demonstrate the possible diverse use of these materials to develop pH-responsive delivery systems to deliver a range of drugs to treat various diseases that are characterized by acidic conditions.

Acknowledgements

The authors acknowledge the University of KwaZulu-Natal (UKZN), UKZN Nanotechnology Platform, Medical Research Council of South Africa and the National Research Foundation of South Africa for financial support (NRF Grant No. 87790 and 88453). The Microscopy and Microanalysis Unit and Biomedical Resource Unit at UKZN and Department of Human Physiology at UKZN are acknowledged for TEM, animal experiment facility and flow cytometry facility respectively. We thank Ms Carrin Martin and Charlotte Ramadhin for proofreading the manuscript.

Disclosure

The authors report no conflicts of interest in this work.

2.18 References

Gao W, Thamphiwatana S, Angsantikul P, et al. Nanoparticle approaches against bacterial infections. Wiley Interdisciplinary Review: Nanomedicine and Nanobiotechnology. 2014, 6 (6), 532-547.

2. Klevens RM, Edwards JR, Tenover FC, et al. Changes in the Epidemiology of Methicillin-resistant Staphylococcus aureus in Intensive Care Units in US Hospitals, 1992–2003. Clinical Infectious Diseases. 2006, 42 (3), 389-391.

3. Lodise TP, Miller CD, Graves J, et al. Predictors of high vancomycin MIC values among patients with Methicillin-resistant Staphylococcus aureus bacteraemia. Journal of Antimicrobial Chemotherapy. 2008, 62 (5), 1138-1141.

4. Sande L, Sanchez M, Montes J, et al. Liposomal encapsulation of vancomycin improves killing of Methicillin-resistant Staphylococcus aureus in a murine infection model. Journal of Antimicrobial Chemotherapy. 2012, 67 (9), 2191-2194.

5. Boucher HW, Corey GR. Epidemiology of Methicillin-resistant Staphylococcus aureus. Clinical Infectious Diseases. 2008, 46 (5), S344-S349.

6. de Kraker ME, Stewardson AJ, Harbarth S. Will 10 million people die a year due to antimicrobial resistance by 2050? PLoS medicine. 2016, 13 (11), 1002184.

7. Ravichandran R. Nanotechnology-Based Drug Delivery Systems. NanoBiotechnology. 2009, 5 (1), 17-33.

8. Suri SS, Fenniri H, Singh B. Nanotechnology-based drug delivery systems. Journal of occupational medicine and toxicology. 2007, 2 (1), 16.

9. Fouladi F, Steffen KJ, Mallik S. Enzyme-Responsive Liposomes for the Delivery of Anticancer Drugs. Bioconjugate Chemistry. 2017, 28 (4), 857-868.

10. Wang J, Ayano E, Maitani Y, et al. Tunable Surface Properties of Temperature-Responsive Polymer-Modified Liposomes Induce Faster Cellular Uptake. American Chemical Society Omega. 2017, 2(1), 316-325.

11. Bharti R, Dey G, Banerjee I, et al. Somatostatin receptor targeted liposomes with Diacerein inhibit IL-6 for breast cancer therapy. Cancer Letter. 2017, 388, 292-302.

12. Lee Y, Thompson D. Stimuli-responsive liposomes for drug delivery. Wiley Interdisciplinary Review: Nanomedicine and Nanobiotechnology. 2017, 9(5), 1450.

13. Jiayin Z, Xizi Liang T, Junjie Z. The Research Progress of Targeted Drug Delivery Systems. IOP Conference Series: Materials Science and Engineering. 2017, 207 (1), 012017.

14. Karanth H, Murthy R. pH-Sensitive liposomes-principle and application in cancer therapy. Journal of Pharmacy and Pharmacology. 2007,59 (4), 469-483.

15. Radovic-Moreno AF, Lu TK, Puscasu VA, et al. Surface charge-switching polymeric nanoparticles for bacterial cell wall-targeted delivery of antibiotics. American Chemical Society nano. 2012, 6 (5), 4279-4287.

16. Mura S, Nicolas J, Couvreur P. Stimuli-responsive nanocarriers for drug delivery. Nature Materials. 2013, 12 (11), 991-1003.

17. Cordeiro C, Wiseman DJ, Lutwyche P, et al. Antibacterial efficacy of gentamicin encapsulated in pH-sensitive liposomes against an in vivo Salmonella enterica serovar typhimurium intracellular infection model. Antimicrobial agents and Chemotherapy. 2000, 44(3), 533-539.

18. Jadhav M, Kalhapure RS, Rambharose S, et al. Novel lipids with three C18-fatty acid chains and an amino acid head group for pH-responsive and sustained antibiotic delivery. Chemistry and Physics of Lipids. 2018, 212, 12-25.

19. Liu K, Li H, Williams GR, et al. pH-responsive liposomes self-assembled from electrosprayed microparticles, and their drug release properties. Colloids and Surfaces A: Physicochemical and Engineering Aspects. 2018, 537, 20-27.

20. Paliwal SR, Paliwal R, Vyas SP. A review of mechanistic insight and application of pH-sensitive liposomes in drug delivery. Drug Delivery. 2015, 22 (3), 231-242.

21. Thamphiwatana S, Fu V, Zhu J, et al. Nanoparticle-stabilized liposomes for pH-responsive gastric drug delivery. Langmuir. 2013, 29 (39), 12228-12233.

22. Hafez IM, Ansell S, Cullis PR. Tunable pH-sensitive liposomes composed of mixtures of cationic and anionic lipids. Biophysical Journal. 2000,79 (3), 1438-1446.

23. Shi G, Guo W, Stephenson SM, et al. Efficient intracellular drug and gene delivery using folate receptor-targeted pH-sensitive liposomes composed of cationic/anionic lipid combinations. Journal of Control Release. 2002, 80 (1-3), 309-319.

24. Sugimoto T, Yamazaki N, Hayashi T, et al. Preparation of dual-stimuli-responsive liposomes using methacrylate-based copolymers with pH and temperature sensitivities for precisely controlled release. Colloids and Surfaces B: Biointerfaces. 2017, 155, 449-458.

25. Obata Y, Tajima S, Takeoka S. Evaluation of pH-responsive liposomes containing amino acid-based zwitterionic lipids for improving intracellular drug delivery in vitro and in vivo. Journal of Control Release. 2010, 142 (2), 267-276.

26. Mo R, Sun Q, Li N, et al. Intracellular delivery and antitumor effects of pH-sensitive liposomes based on zwitterionic oligopeptide lipids. Biomaterials. 2013, 34 (11), 2773-2786.

27. Bailey AL, Cullis PR. Membrane fusion with cationic liposomes: effects of target membrane lipid composition. Biochemistry. 1997, 36 (7), 1628-1634.

28. Omolo CA, Kalhapure RS, Jadhav M, et al. Pegylated oleic acid: A promising amphiphilic polymer for nano-antibiotic delivery. European Journal of Pharmaceutics and Biopharmaceutics. 2017, 112, 96-108.

29. Bangham A, Standish MM, Watkins J. Diffusion of univalent ions across the lamellae of swollen phospholipids. Journal of Molecular Biology. 1965, 13 (1), 238-IN27.

30. Yue P-F, Lu X-Y, Zhang Z-Z, et al. The study on the entrapment efficiency and in vitro release of puerarin submicron emulsion. American Association of Pharmaceutical Scientists. 2009, 10 (2), 376-383.

31. Dash S, Murthy PN, Nath L, et al. Kinetic modeling on drug release from controlled drug delivery systems. Acta poloniae pharmaceutica. 2010, 67 (3), 217-23.

32. Fayaz AM, Girilal M, Rahman M, et al. Biosynthesis of silver and gold nanoparticles using thermophilic bacterium Geobacillus stearothermophilus. Process biochemistry. 2011, 46 (10), 1958-1962.

33. Bexfield A, Bond AE, Roberts EC, et al. The antibacterial activity against MRSA strains and other bacteria of a <500Da fraction from maggot excretions/secretions of Lucilia sericata (Diptera: Calliphoridae). Microbes and Infection. 2008, 10 (4), 325-333.

34. Bexfield A, Nigam Y, Thomas S, et al. Detection and partial characterization of two antibacterial factors from the excretions/secretions of the medicinal maggot Lucilia sericata and their activity against methicillin-resistant Staphylococcus aureus (MRSA). Microbes and Infection. 2004, 6 (14), 1297-1304.

35. Renggli S, Keck W, Jenal U, et al. Role of autofluorescence in flow cytometric analysis of Escherichia coli treated with bactericidal antibiotics. Journal of Bacteriology. 2013, 195 (18), 4067-4073.

36. Bensch G, Rüger M, Wassermann M, et al. Flow cytometric viability assessment of lactic acid bacteria starter cultures produced by fluidized bed drying. Applied Microbiology and Biotechnology. 2014, 98 (11), 4897-4909.

37. Shrestha NK, Scalera NM, Wilson DA, et al. Rapid differentiation of Methicillin-resistant and Methicillin-susceptible Staphylococcus aureus by flow cytometry after brief antibiotic exposure. Journal of Clinical Microbiology. 2011, 49 (6), 2116-2120.

38. Stiefel P, Schmidt-Emrich S, Maniura-Weber K, et al. Critical aspects of using bacterial cell viability assays with the fluorophores SYTO9 and propidium iodide. BMC microbiology. 2015, 15 (1), 36.

39. Huang C-M, Chen C-H, Pornpattananangkul D, et al. Eradication of drug resistant Staphylococcus aureus by liposomal oleic acids. Biomaterials. 2011, 32 (1), 214-221.

40. Kalhapure RS, Jadhav M, Rambharose S, et al. pH-responsive chitosan nanoparticles from a novel twin-chain anionic amphiphile for controlled and targeted delivery of vancomycin. Colloids Surfaces B Biointerfaces. 2017, 158, 650-657.

41. Kong B, Seog JH, Graham LM, et al. Experimental considerations on the cytotoxicity of nanoparticles. Nanomedicine. 2011, 6 (5), 929-941.

42. Lewinski N, Colvin V, Drezek R. Cytotoxicity of nanoparticles. small. 2008, 4 (1), 26-49.

43. Sahu D, Kannan GM, Tailang M, et al. In Vitro Cytotoxicity of Nanoparticles: A Comparison between Particle Size and Cell Type. Journal of Nanoscience. 2016, 2016, 9.

44. Liu Z, Deng X, Wang M, et al. BSA-Modified Polyethersulfone Membrane: Preparation, Characterization and Biocompatibility. Journal of biomaterials science. Polymer edition. 2009, 20 (3), 377-397.

45. Muppidi K, Pumerantz AS, Wang J, et al. Development and stability studies of novel liposomal vancomycin formulations. International Scholarly Research Network Pharmaceutics. 2012, 2012, 636743.

46. De Oliveira MC, Fattal E, Couvreur P, et al. pH-sensitive liposomes as a carrier for oligonucleotides: a physico-chemical study of the interaction between DOPE and a 15-mer oligonucleotide in quasi-anhydrous samples. Biochimica et Biophysica Acta Biomembranes. 1998, 1372 (2), 301-310.

47. Gupta M, Agrawal U, Sharma V, et al. pH-sensitive liposomes. Advances and Challenges Volume. 2015, 1(1), 80-93

48. Kanicky JR, Shah DO. Effect of degree, type, and position of unsaturation on the pKa of long-chain fatty acids. Journal of Colloid and Interface Science. 2002, 256 (1), 201-207.

49. Cascone S. Modeling and comparison of release profiles: Effect of the dissolution method. European journal of pharmaceutical sciences. 2017, 106, 352-361.

50. Shaikh HK, Kshirsagar R, Patil S. Mathematical models for drug release characterization: a review. World journal of pharmacy and pharmaceutical sciences. 2015, 4, 324-338.

51. Tang J, Hu J, Kang L, et al. The use of vancomycin in the treatment of adult patients with methicillin-resistant Staphylococcus aureus (MRSA) infection: a survey in a tertiary hospital in China. International journal of clinical and experimental medicine. 2015, 8 (10), 19436.

52. Rodvold KA, McConeghy KW. Methicillin-resistant Staphylococcus aureus therapy: past, present, and future. Clinical infectious diseases. 2014, 58 (1): S20-S27.

53. Giuliano C, Haase KK, Hall R. Use of vancomycin pharmacokinetic–pharmacodynamic properties in the treatment of MRSA infections. Expert review of anti-infective therapy. 2010, 8(1), 95-106.

54. Kalhapure RS, Mocktar C, Sikwal DR, et al. Ion pairing with linoleic acid simultaneously enhances encapsulation efficiency and antibacterial activity of vancomycin in solid lipid nanoparticles. Colloids and Surfaces B Biointerfaces. 2014, 117, 303-311.

55. Mercier R-C, Stumpo C, Rybak MJ. Effect of growth phase and pH on the in vitro activity of a new glycopeptide, oritavancin (LY333328), against Staphylococcus aureus and Enterococcus faecium. Journal of Antimicrobial Chemotherapy. 2002, 50 (1), 19-24.

56. Suller M, Lloyd D. The antibacterial activity of vancomycin towards Staphylococcus aureus under aerobic and anaerobic conditions. Journal of Applied Microbiology. 2002, 92 (5), 866-872.

57. Cui L, Ma X, Sato K, et al. Cell wall thickening is a common feature of vancomycin resistance in Staphylococcus aureus. Journal of clinical microbiology. 2003;41(1):5-14.

58. Shrestha H, Bala R, Arora S. Lipid-based drug delivery systems. Journal of pharmaceutics. 2014, 2014, 10.

59. Zheng CJ, Yoo J-S, Lee T-G, et al. Fatty acid synthesis is a target for antibacterial activity of unsaturated fatty acids. Federation of European Biochemical Societies letters. 2005, 579 (23), 5157-5162.

60. Kabara JJ, Swieczkowski DM, Conley AJ, et al. Fatty acids and derivatives as antimicrobial agents. Antimicrobial agents and chemotherapy. 1972, 2 (1), 23-28.

61. O'Brien-Simpson NM, Pantarat N, Attard TJ, et al. A rapid and quantitative flow cytometry method for the analysis of membrane disruptive antimicrobial activity. PloS one. 2016, 11(3), 0151694.

62. Fittipaldi M, Nocker A, Codony F. Progress in understanding preferential detection of live cells using viability dyes in combination with DNA amplification. Journal of Microbiology Methods. 2012, 91 (2), 276-289.

Paper 1 Supporting information

Novel two chain fatty acid based-lipids for development of vancomycin pH-responsive liposomes against *Staphylococcus aureus* and Methicillin-resistant *Staphylococcus aureus* (MRSA)

Sifiso S. Makhathini[1], Rahul S. Kalhapure[1,3]*, Mahantesh Jadhav, Ayman Y. Waddad[1], Ramesh Gannimani[1], Calvin A. Omolo[1], Sanjeev Rambharose[1,2], Chunderika Mocktar[1], Thirumala Govender[1,*].

[1]Discipline of Pharmaceutical Sciences, College of Health Sciences, University of KwaZulu-Natal, Private Bag X54001, Durban, South Africa

[2]Division of Emergency Medicine, Department of Surgery, University of Cape Town, Cape Town, South Africa

[3]School of Pharmacy, The University of Texas at El Paso, 500 W University Ave, El Paso, TX 79968, USA.

*Corresponding author.

Email address: govenderth@ukzn.ac.za; rahul.kalhapure@rediffmail.com, rkalhapure@utep.edu

Supporting information

^{1}H NMR characterization of compound **3**

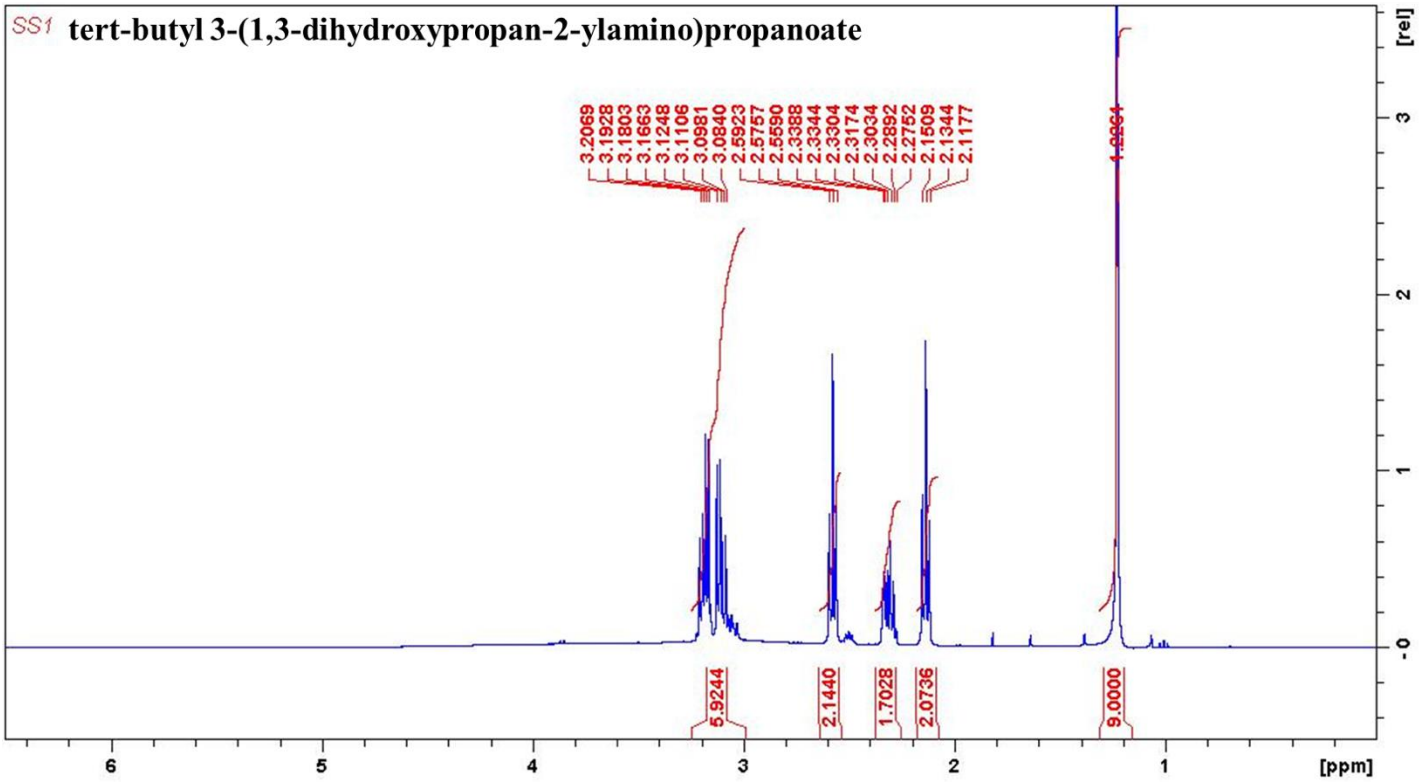

^{13}C NMR characterization of compound 3

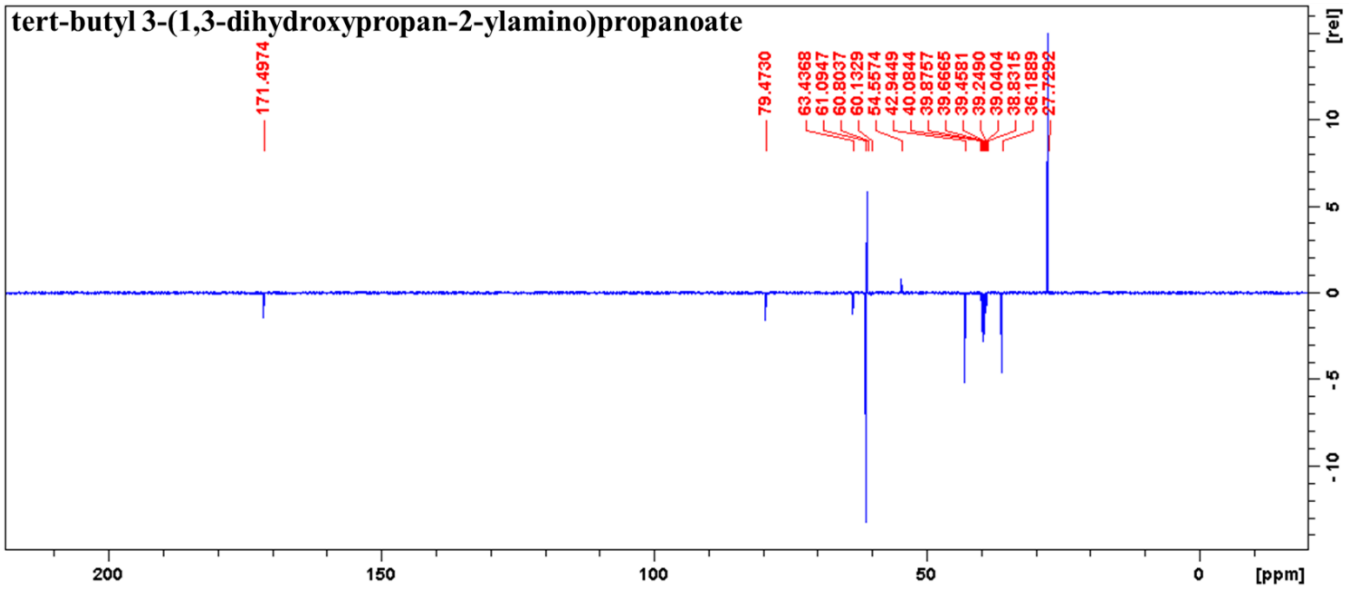

HRMS characterization of compound **3**

Elemental Composition Report **tert-butyl 3-(1,3-dihydroxypropan-2-ylamino)propanoate** **Page 1**

Single Mass Analysis
Tolerance = 5.0 PPM / DBE: min = -1.5, max = 100.0
Element prediction: Off
Number of isotope peaks used for i-FIT = 3

Monoisotopic Mass, Even Electron Ions
43 formula(e) evaluated with 1 results within limits (up to 20 closest results for each mass)
Elements Used:
C: 5-10 H: 20-25 N: 0-5 O: 0-5 Na: 0-1
DHAPE 58 (1.925) Cm (1:61)
TOF MS ES+

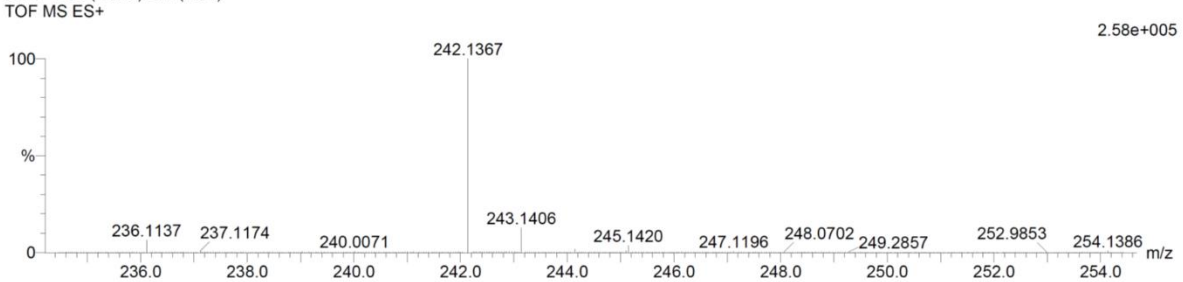

Minimum:				-1.5			
Maximum:		5.0	5.0	100.0			
Mass	Calc. Mass	mDa	PPM	DBE	i-FIT	i-FIT (Norm)	Formula
242.1367	242.1368	-0.1	-0.4	0.5	708.7	0.0	C10 H21 N O4 Na

^{1}H NMR characterization of compound 5a

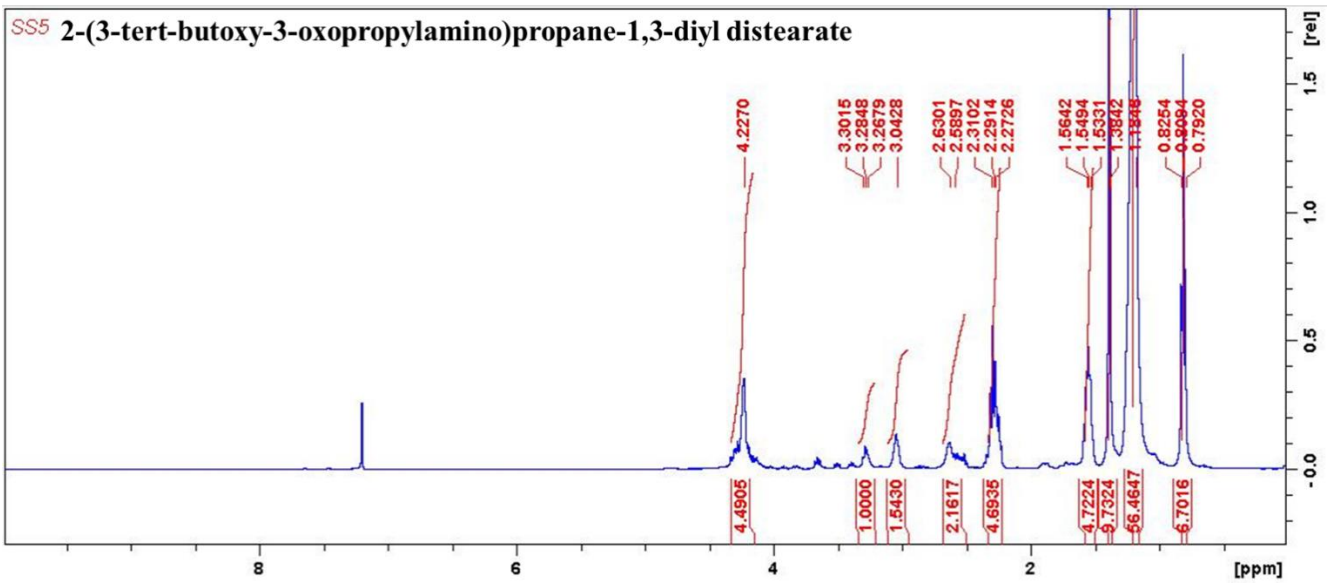

^{13}C NMR characterization of compound 5a

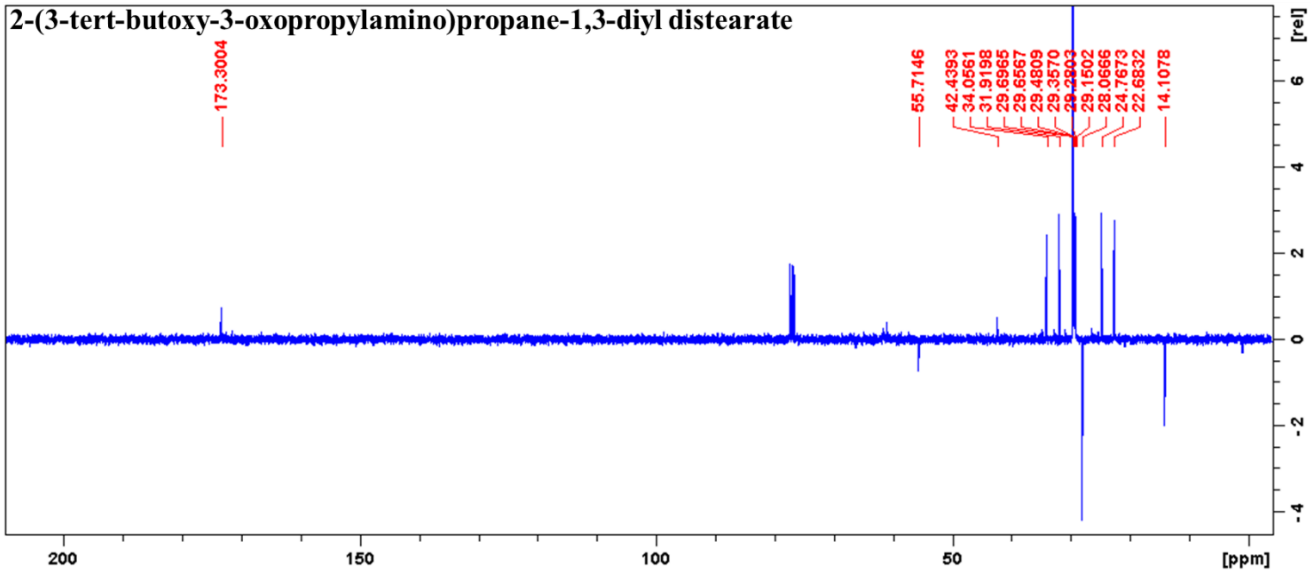

HRMS characterization of compound 5a

Elemental Composition Report **2-(3-tert-butoxy-3-oxopropylamino)propane-1,3-diyl distearate** **Page 1**

Single Mass Analysis
Tolerance = 5.0 PPM / DBE: min = -1.5, max = 100.0
Element prediction: Off
Number of isotope peaks used for i-FIT = 3

Monoisotopic Mass, Even Electron Ions
6 formula(e) evaluated with 1 results within limits (up to 20 closest results for each mass)
Elements Used:
C: 45-50 H: 85-90 N: 0-5 O: 5-10 Na: 1-1
DSAPE 21 (0.675) Cm (1:61)
TOF MS ES+

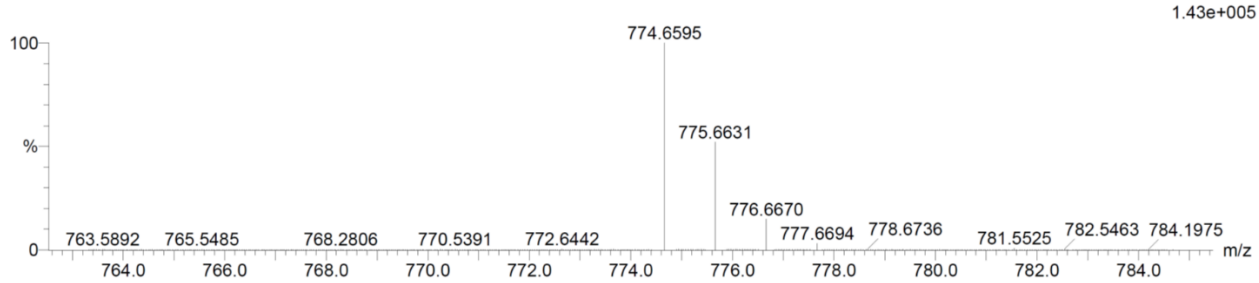

Minimum:				-1.5			
Maximum:		5.0	5.0	100.0			
Mass	Calc. Mass	mDa	PPM	DBE	i-FIT	i-FIT (Norm)	Formula

^{1}H NMR characterization of compound 5b

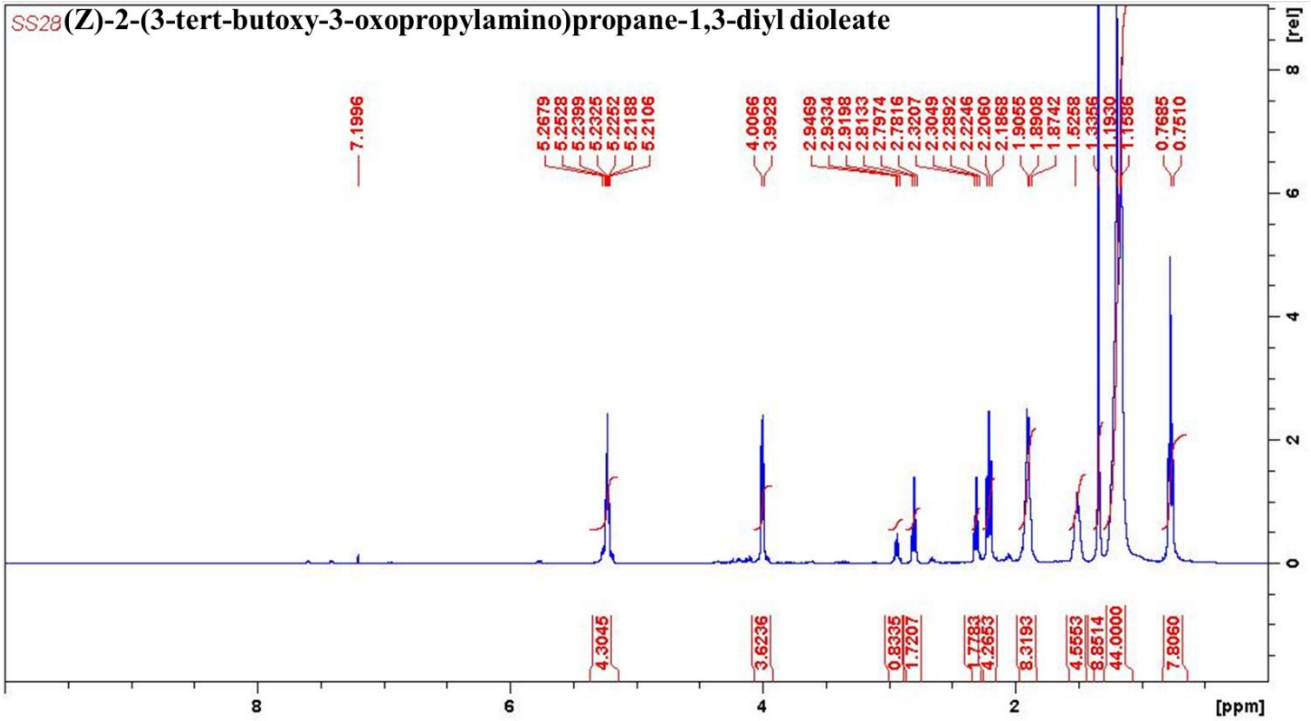

^{13}C NMR characterization of compound 5b

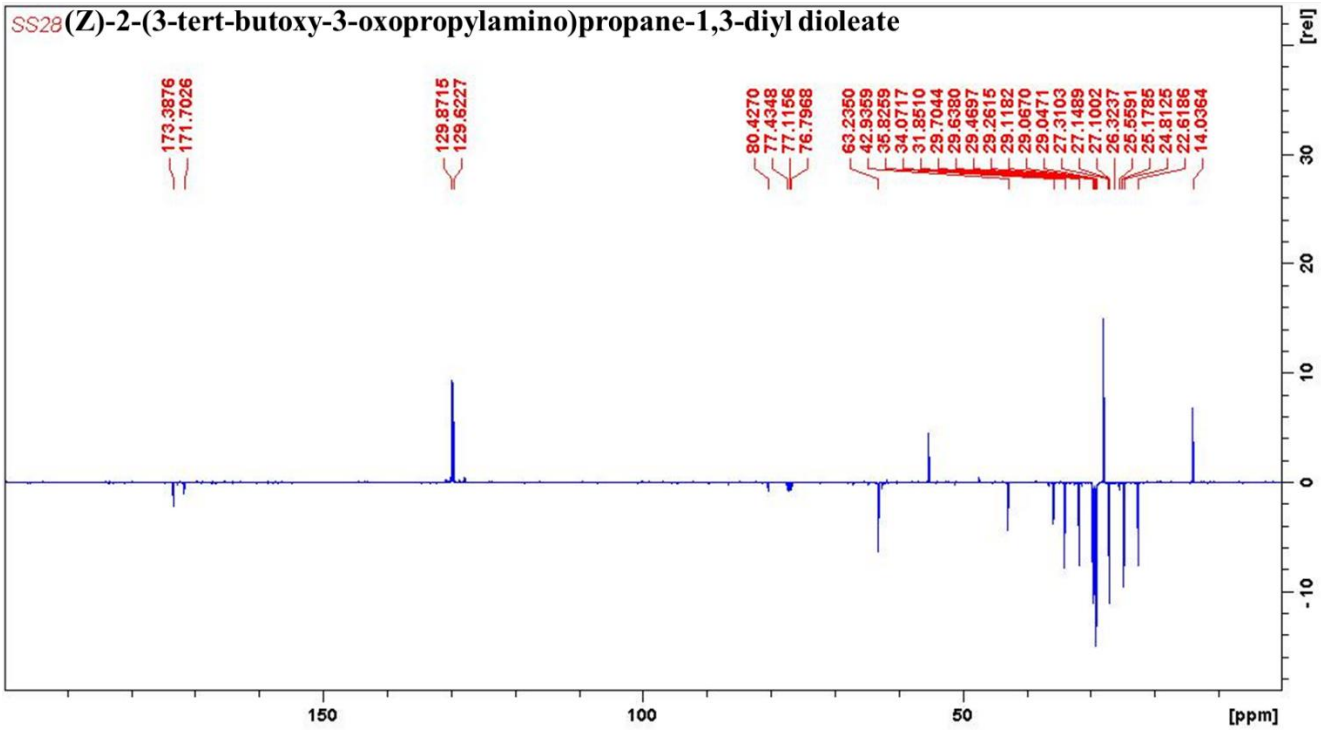

HRMS characterization of compound 5b

Elemental Composition Report **(Z)-2-(3-tert-butoxy-3-oxopropylamino)propane-1,3-diyl dioleate** **Page 1**

Single Mass Analysis
Tolerance = 5.0 PPM / DBE: min = -1.5, max = 100.0
Element prediction: Off
Number of isotope peaks used for i-FIT = 3

Monoisotopic Mass, Even Electron Ions
8 formula(e) evaluated with 1 results within limits (up to 20 closest results for each mass)
Elements Used:
C: 45-50 H: 85-90 N: 0-5 O: 5-10 Na: 1-1
DOAPE 6 (0.169) Cm (1:61)
TOF MS ES+

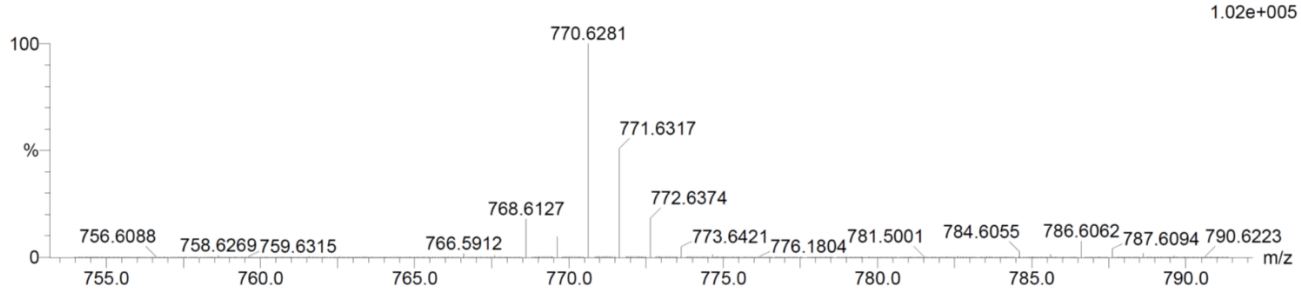

Minimum:				-1.5			
Maximum:		5.0	5.0	100.0			
Mass	Calc. Mass	mDa	PPM	DBE	i-FIT	i-FIT (Norm)	Formula

^{1}H NMR characterization of compound 5c

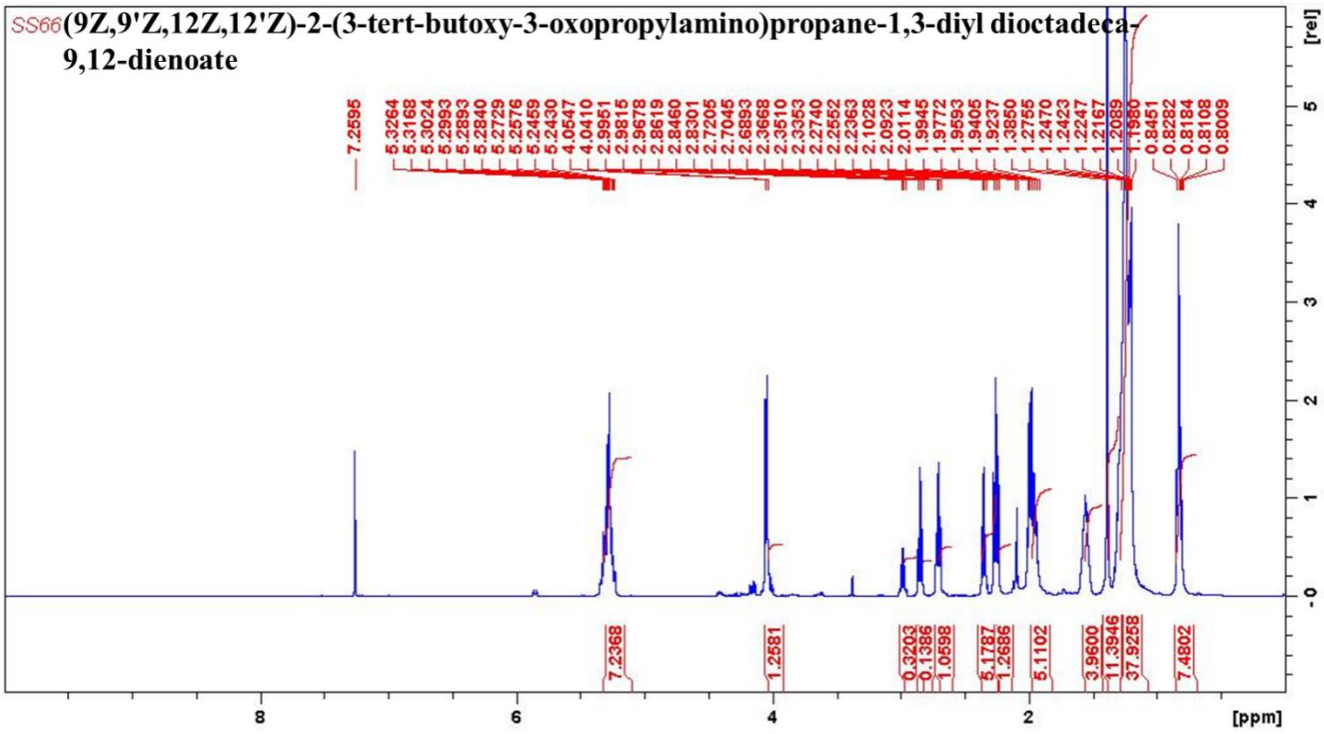

^{13}C NMR characterization of compound 5c

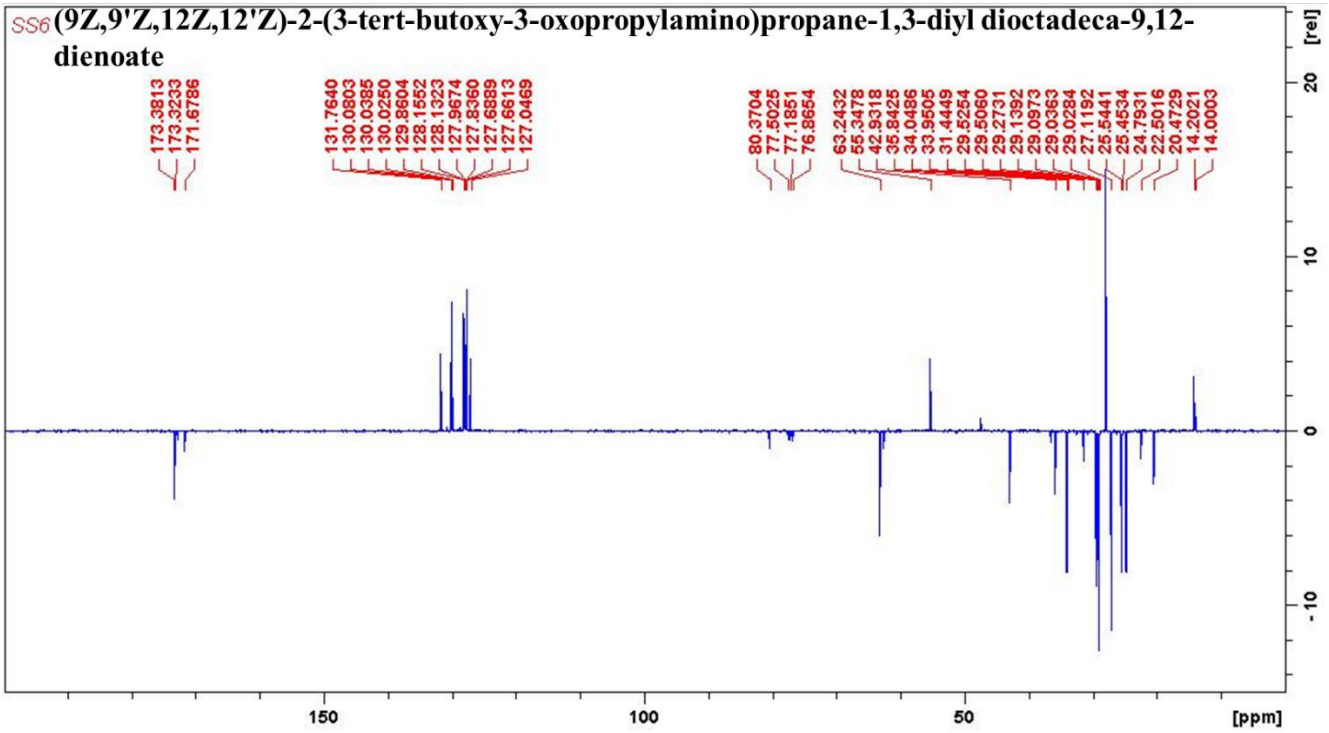

HRMS characterization of compound 5c

Elemental Composition Report **(9Z,9'Z,12Z,12'Z)-2-(3-tert-butoxy-3-oxopropylamino)propane-1,3-diyl dioctadeca-9,12-dienoate** **Page 1**

Single Mass Analysis
Tolerance = 5.0 PPM / DBE: min = -1.5, max = 100.0
Element prediction: Off
Number of isotope peaks used for i-FIT = 3

Monoisotopic Mass, Even Electron Ions
9 formula(e) evaluated with 1 results within limits (up to 20 closest results for each mass)
Elements Used:
C: 45-50 H: 80-90 N: 0-5 O: 5-10 Na: 1-1
DLAPE 3 (0.068) Cm (1:61)
TOF MS ES+

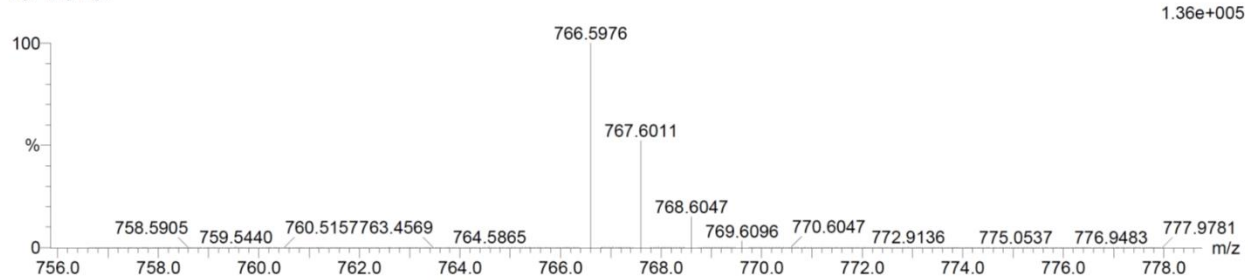

Minimum:				-1.5			
Maximum:		5.0	5.0	100.0			
Mass	Calc. Mass	mDa	PPM	DBE	i-FIT	i-FIT (Norm)	Formula
766.5976	766.5962	1.4	1.8	6.5	412.2	0.0	C46 H81 N O6 Na

^{1}H NMR characterization of compound 5d

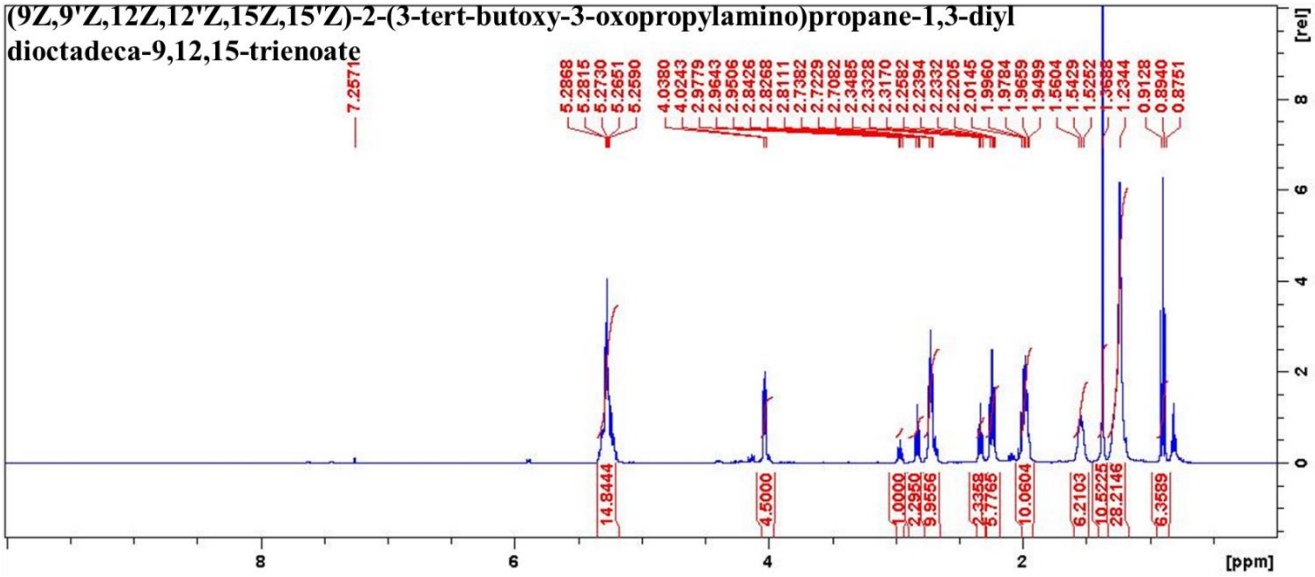

^{13}C NMR characterization of compound 5d

(9Z,9'Z,12Z,12'Z,15Z,15'Z)-2-(3-tert-butoxy-3-oxopropylamino)propane-1,3-diyl dioctadeca-9,12,15-trienoate

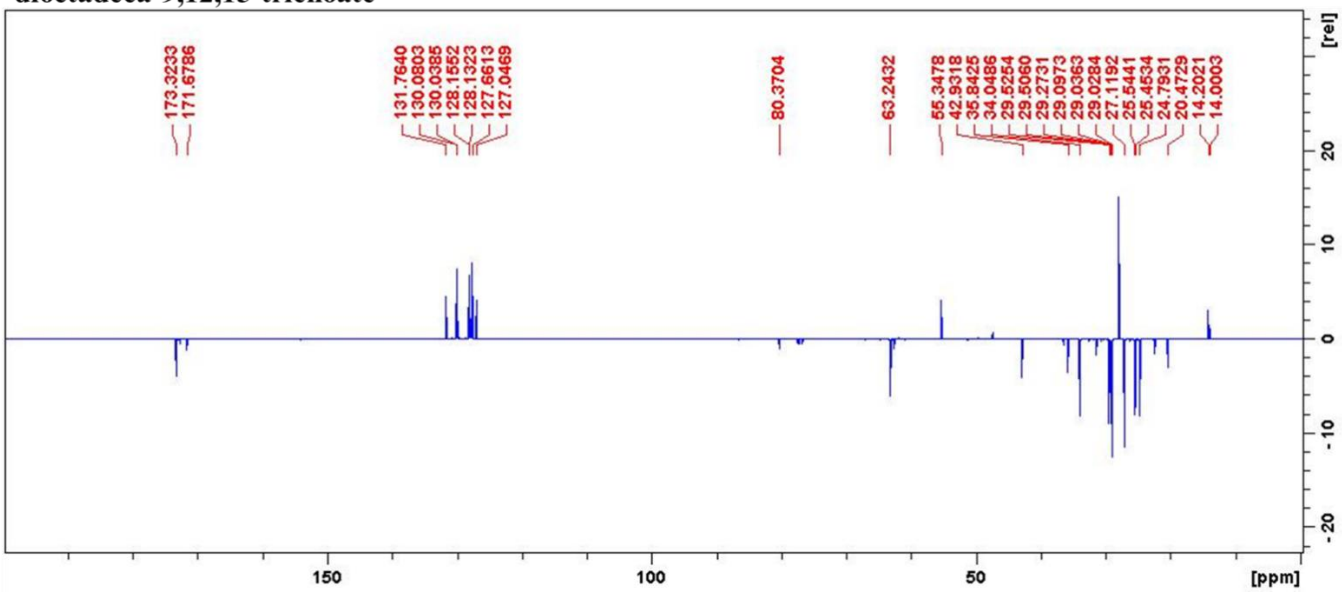

HRMS characterization of compound 5d

Elemental Composition Report **(9Z,9'Z,12Z,12'Z,15Z,15'Z)-2-(3-tert-butoxy-3-oxopropylamino)propane-1,3-diyl dioctadeca-9,12,15-trienoate** **Page 1**

Single Mass Analysis
Tolerance = 5.0 PPM / DBE: min = -1.5, max = 100.0
Element prediction: Off
Number of isotope peaks used for i-FIT = 3

Monoisotopic Mass, Even Electron Ions
13 formula(e) evaluated with 1 results within limits (up to 20 closest results for each mass)
Elements Used:
C: 45-50 H: 75-90 N: 0-5 O: 5-10 Na: 1-1
DLLAPE 46 (1.519) Cm (1:61)
TOF MS ES+

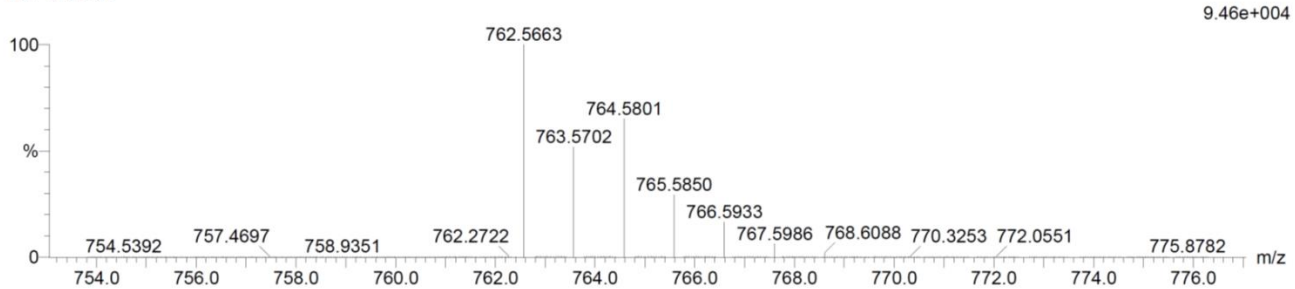

Minimum:				-1.5			
Maximum:		5.0	5.0	100.0			
Mass	Calc. Mass	mDa	PPM	DBE	i-FIT	i-FIT (Norm)	Formula
762.5663	762.5649	1.4	1.8	8.5	408.6	0.0	C46 H77 N O6 Na

FTIR characterization of compound 6a

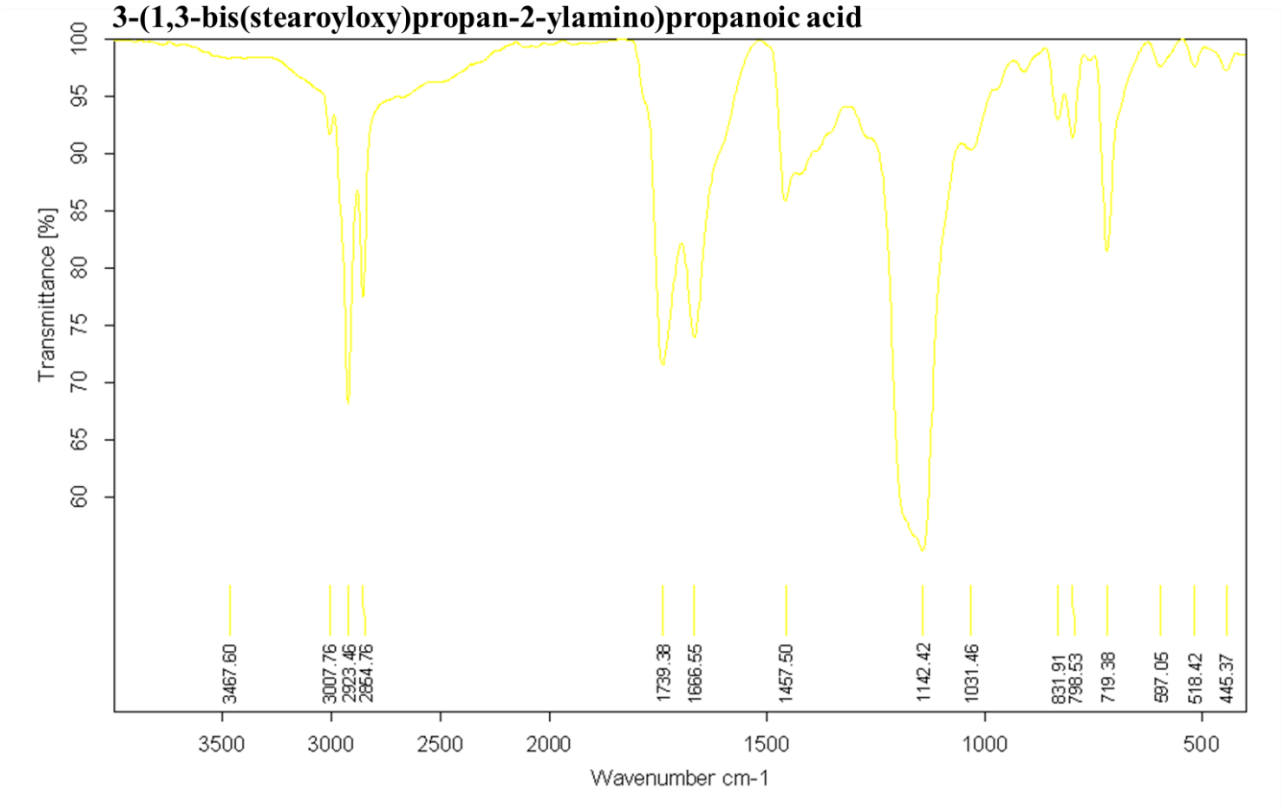

^{1}H NMR characterization of compound 6a

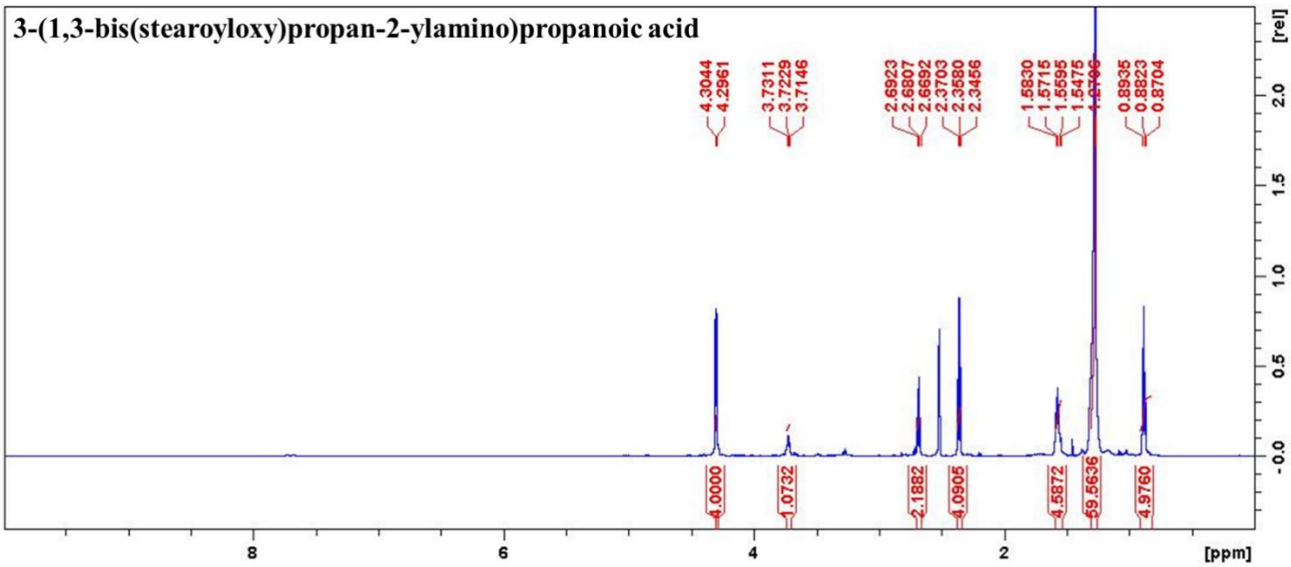

^{13}C NMR characterization of compound 6a

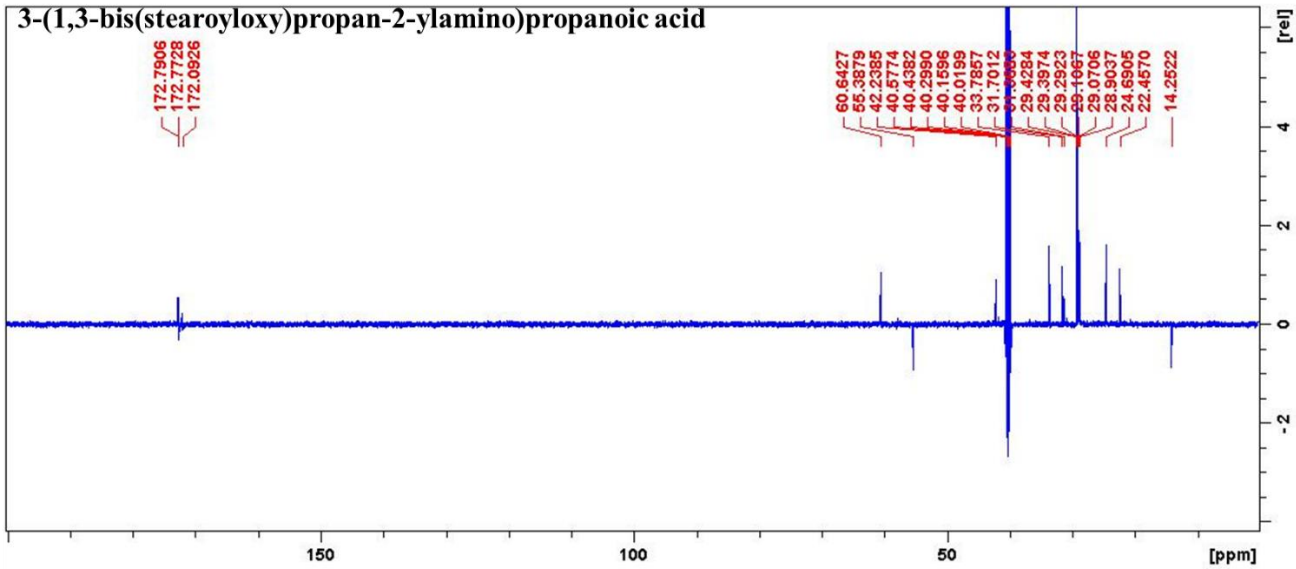

HRMS characterization of Compound 6a

Elemental Composition Report **3-(1,3-bis(stearoyloxy)propan-2-ylamino)propanoic acid** **Page 1**

Single Mass Analysis
Tolerance = 5.0 PPM / DBE: min = -1.5, max = 100.0
Element prediction: Off
Number of isotope peaks used for i-FIT = 2

Monoisotopic Mass, Even Electron Ions
8 formula(e) evaluated with 1 results within limits (up to 20 best isotopic matches for each mass)
Elements Used:
C: 40-45 H: 80-85 N: 0-5 O: 5-10
SAD 58 (1.923) Cm (1:61)
TOF MS ES+

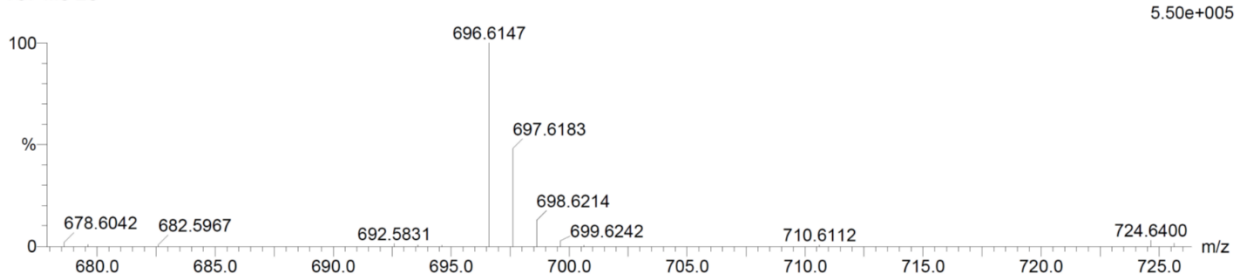

Minimum:				-1.5			
Maximum:		5.0	5.0	100.0			
Mass	Calc. Mass	mDa	PPM	DBE	i-FIT	i-FIT (Norm)	Formula
696.6147	696.6142	0.5	0.7	2.5	13.8	0.0	C42 H82 N O6

FTIR characterization of compound 6b

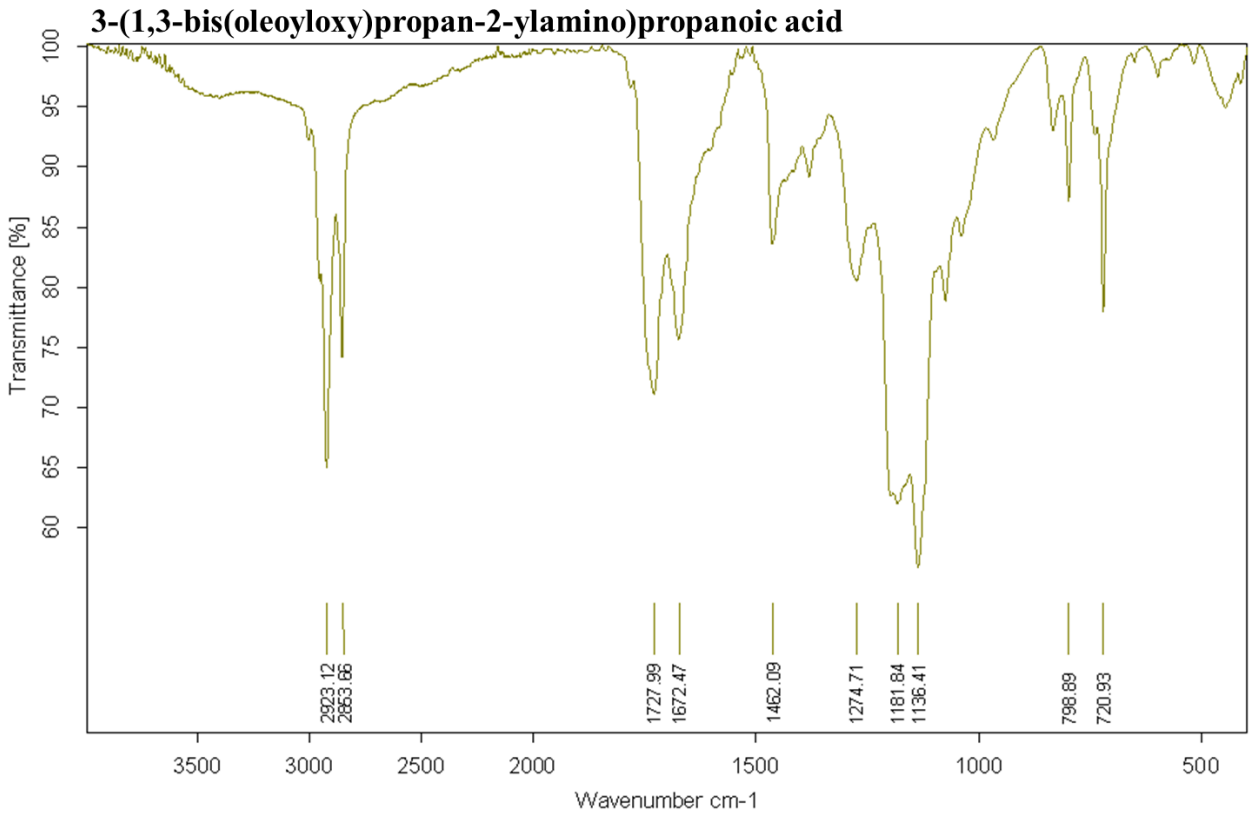

^{1}H NMR characterization of compound 6b

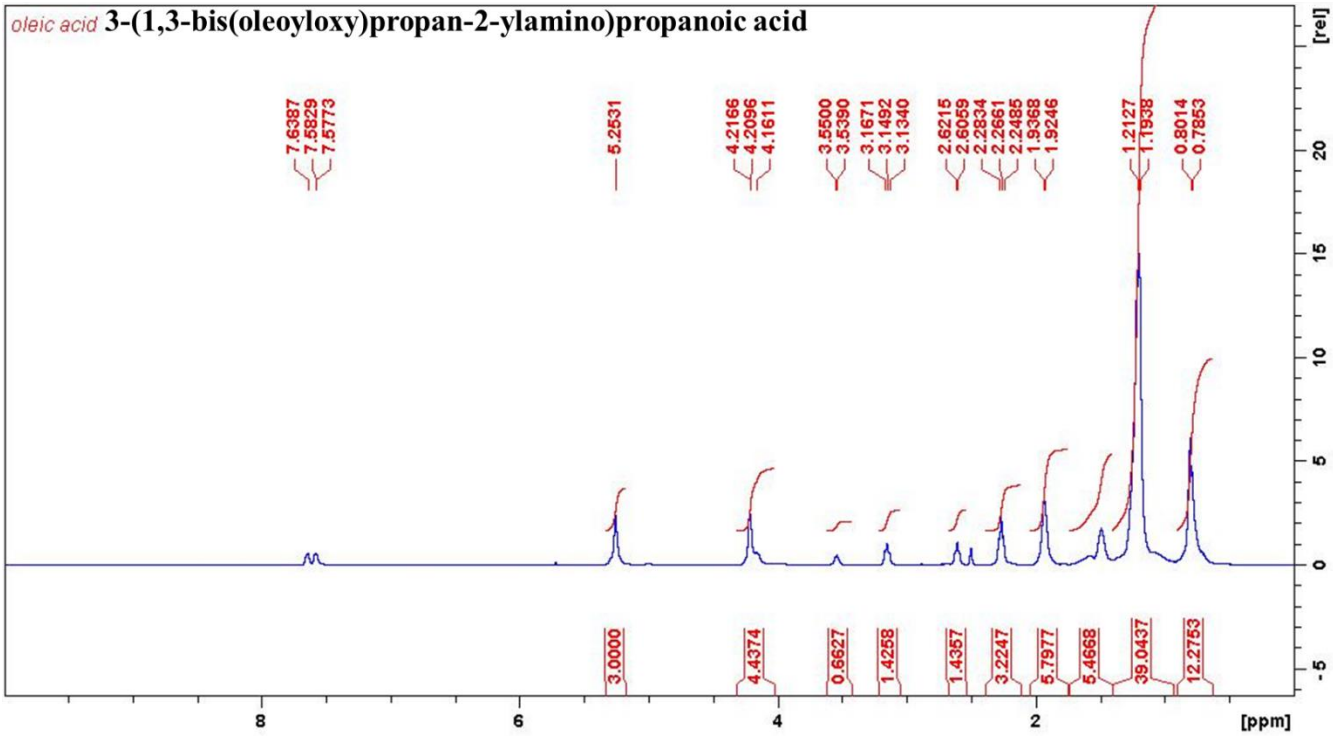

^{13}C NMR characterization of compound 6b

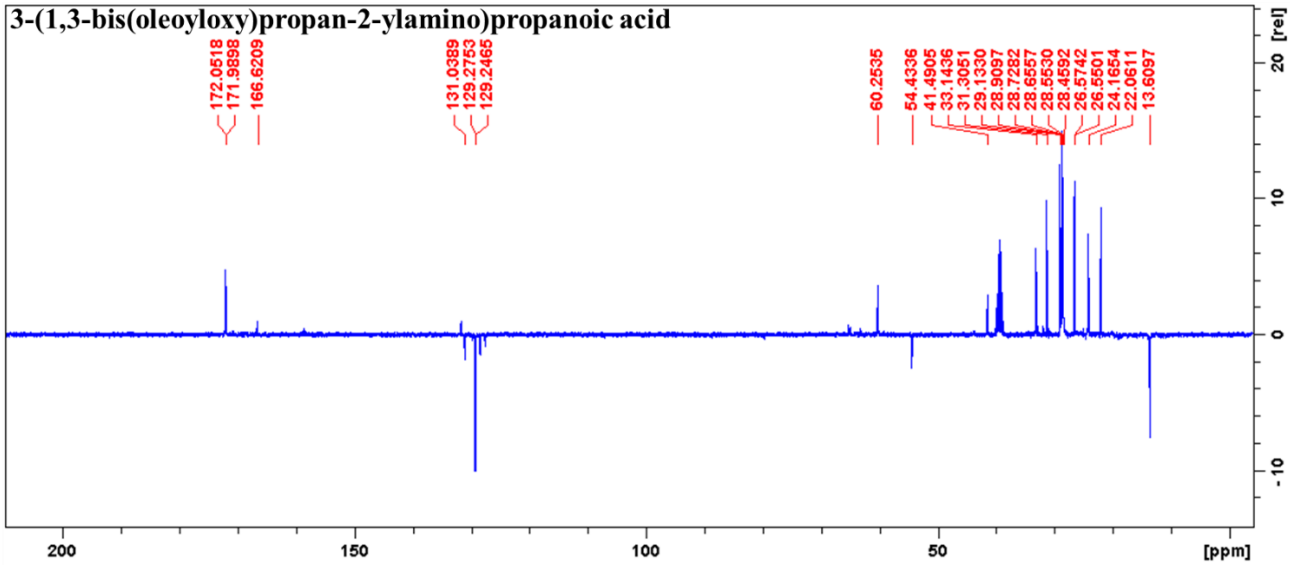

HRMS characterization of Compound 6b

Elemental Composition Report **3-(1,3-bis(oleoyloxy)propan-2-ylamino)propanoic acid** **Page 1**

Single Mass Analysis
Tolerance = 5.0 PPM / DBE: min = -1.5, max = 100.0
Element prediction: Off
Number of isotope peaks used for i-FIT = 2

Monoisotopic Mass, Even Electron Ions
8 formula(e) evaluated with 1 results within limits (up to 20 best isotopic matches for each mass)
Elements Used:
C: 40-45 H: 75-80 N: 0-5 O: 5-10
OAD 47 (1.552) Cm (1:61)
TOF MS ES+

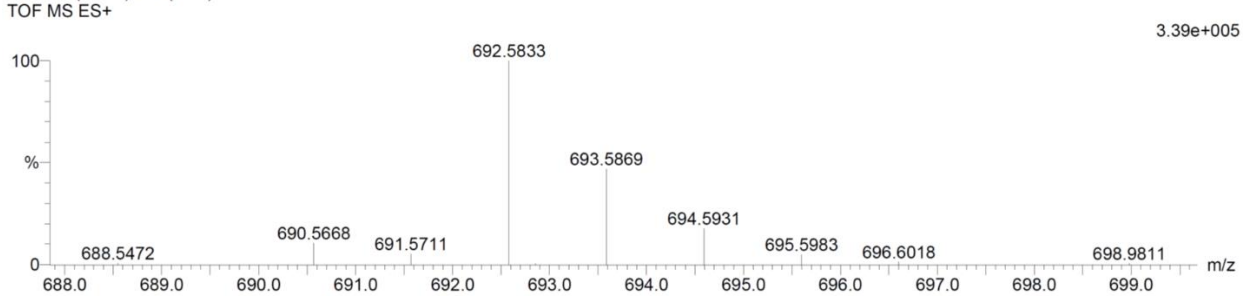

Minimum:				-1.5			
Maximum:		5.0	5.0	100.0			
Mass	Calc. Mass	mDa	PPM	DBE	i-FIT	i-FIT (Norm)	Formula
692.5833	692.5829	0.4	0.6	4.5	29.6	0.0	C42 H78 N O6

FTIR characterization of compound 6c

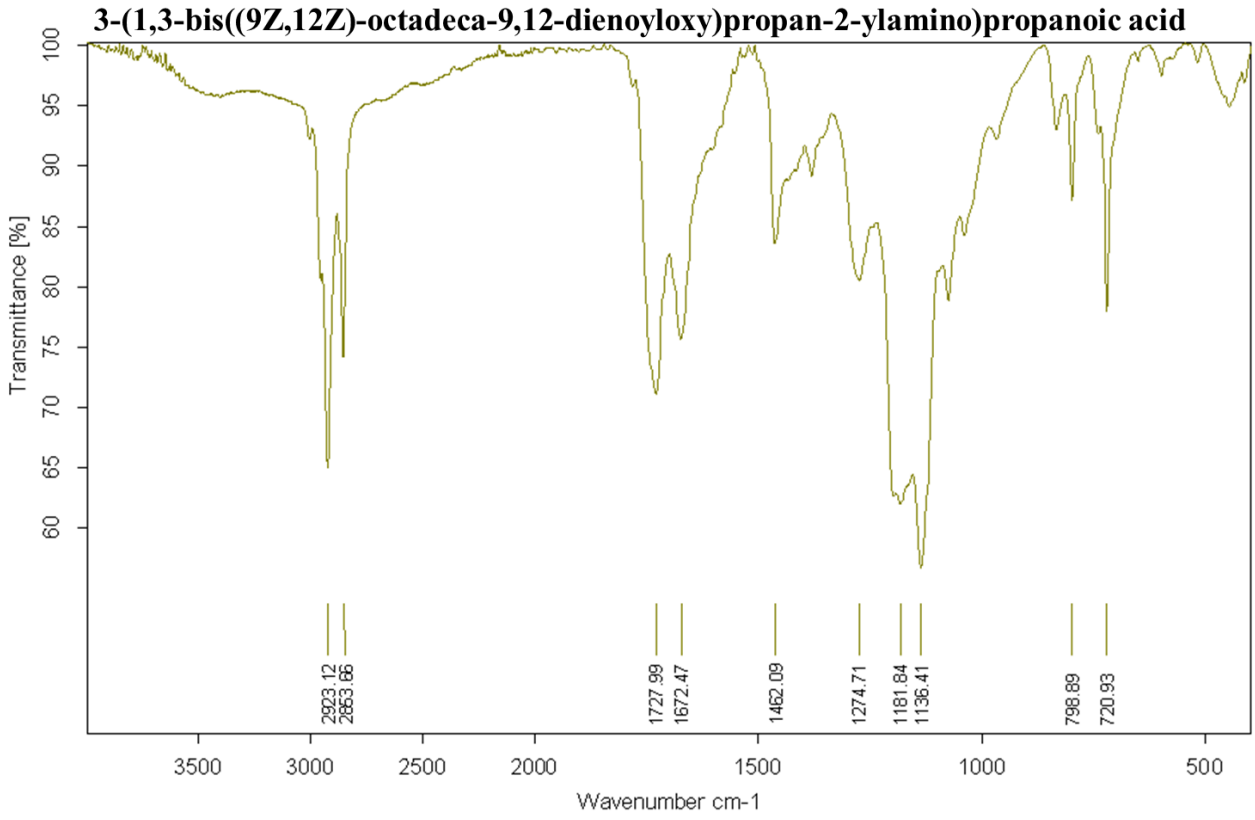

^{1}H NMR characterization of compound 6c

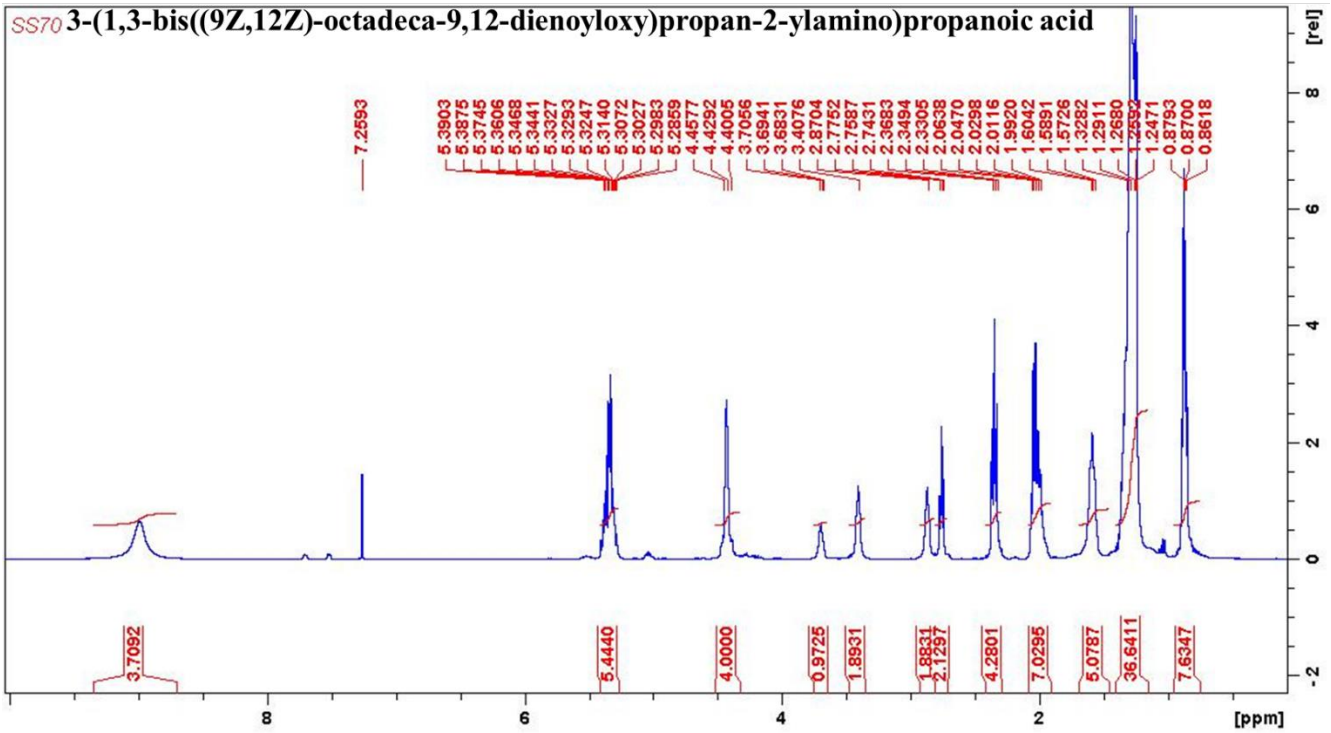

^{13}C NMR characterization of compound 6c

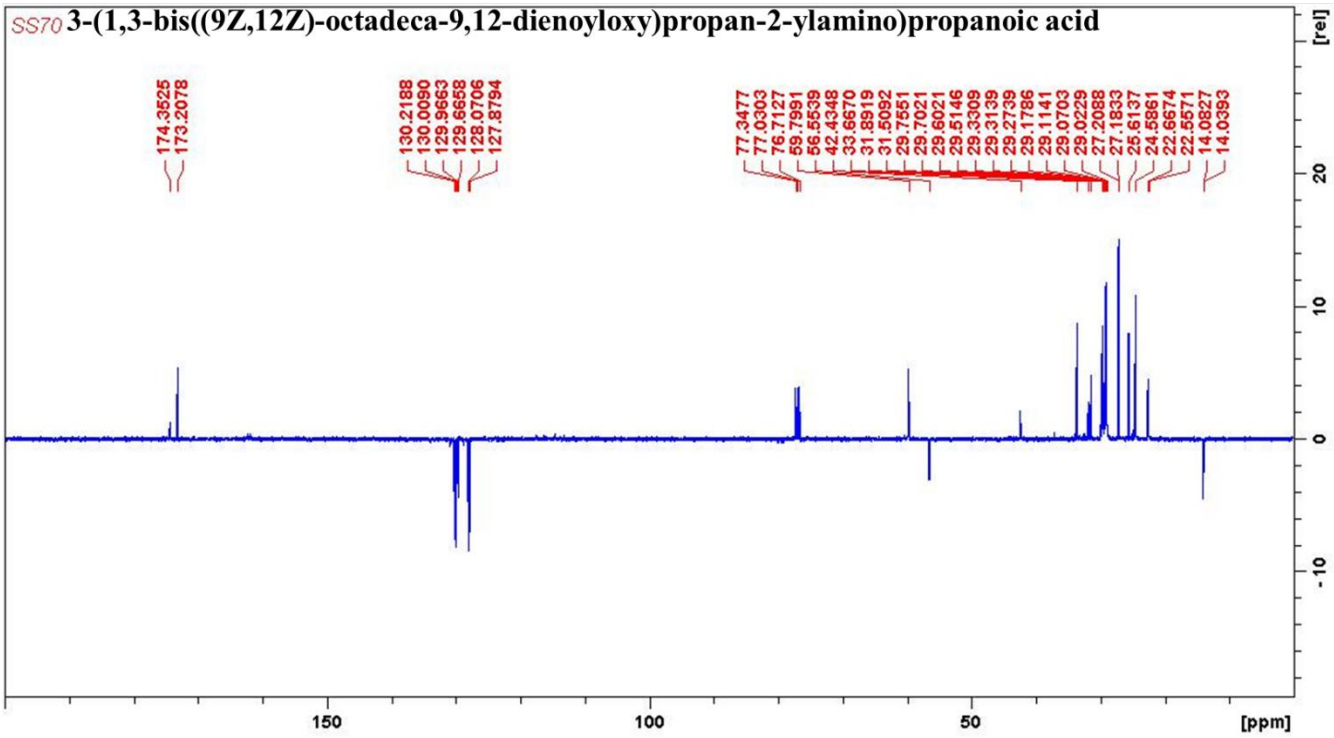

HRMS characterization of Compound 6c

Elemental Composition Report **3-(1,3-bis((9Z,12Z)-octadeca-9,12-dienoyloxy)propan-2-ylamino)propanoic acid** **Page 1**

Single Mass Analysis
Tolerance = 5.0 PPM / DBE: min = -1.5, max = 100.0
Element prediction: Off
Number of isotope peaks used for i-FIT = 2

Monoisotopic Mass, Even Electron Ions
9 formula(e) evaluated with 1 results within limits (up to 20 best isotopic matches for each mass)
Elements Used:
C: 40-45 H: 70-75 N: 0-5 O: 5-10
LAD 20 (0.641) Cm (1:61)
TOF MS ES+

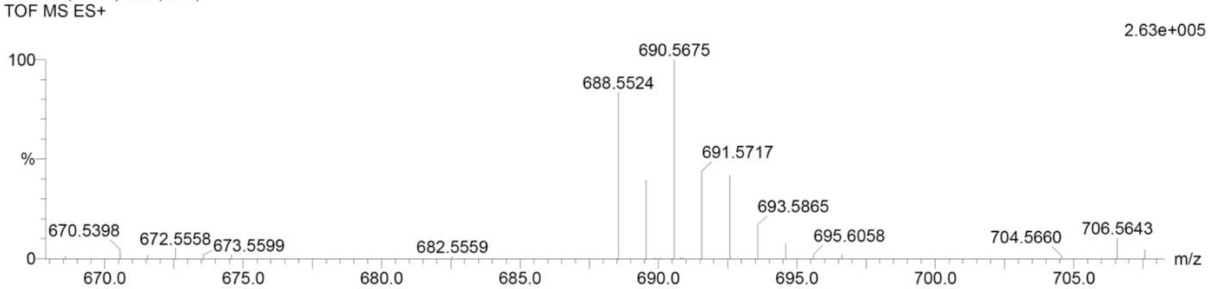

Minimum:				-1.5			
Maximum:		5.0	5.0	100.0			
Mass	Calc. Mass	mDa	PPM	DBE	i-FIT	i-FIT (Norm)	Formula
688.5524	688.5516	0.8	1.2	6.5	27.1	0.0	C42 H74 N O6

FTIR characterization of compound 6d

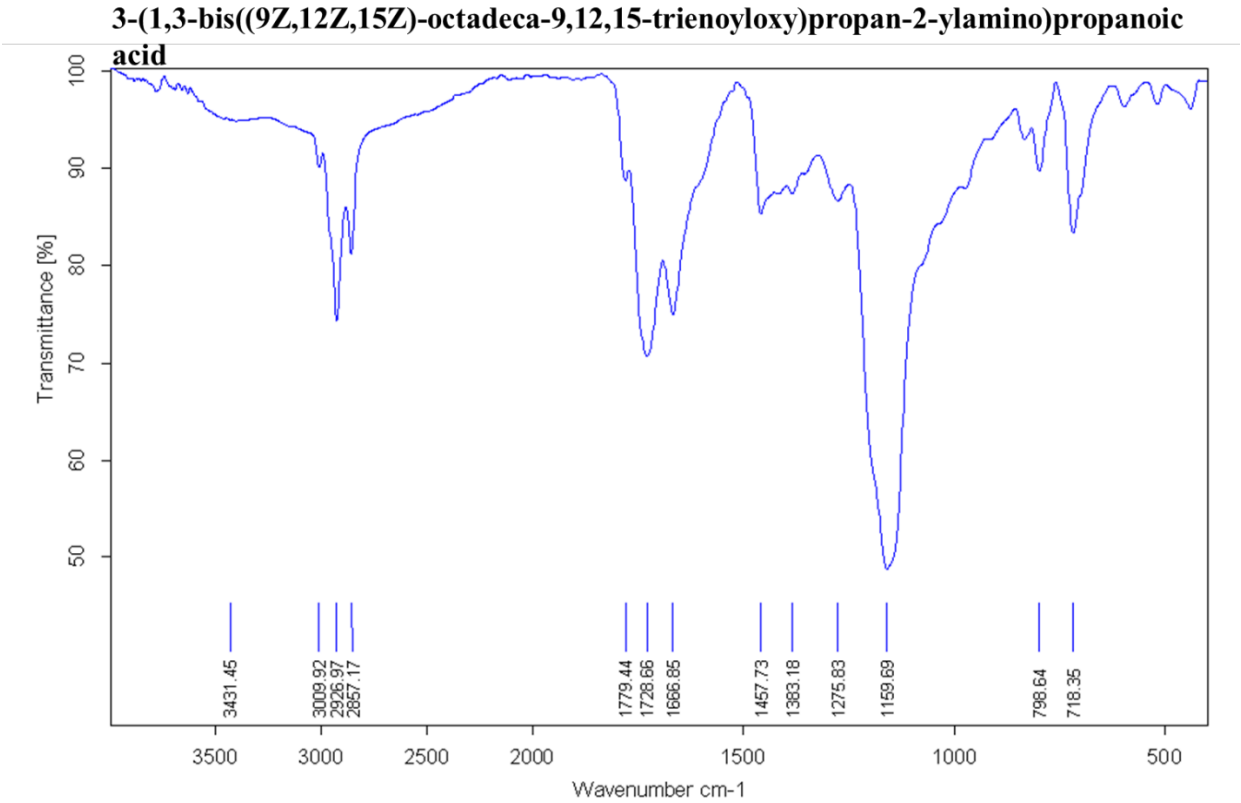

^{1}H NMR characterization of compound 6d

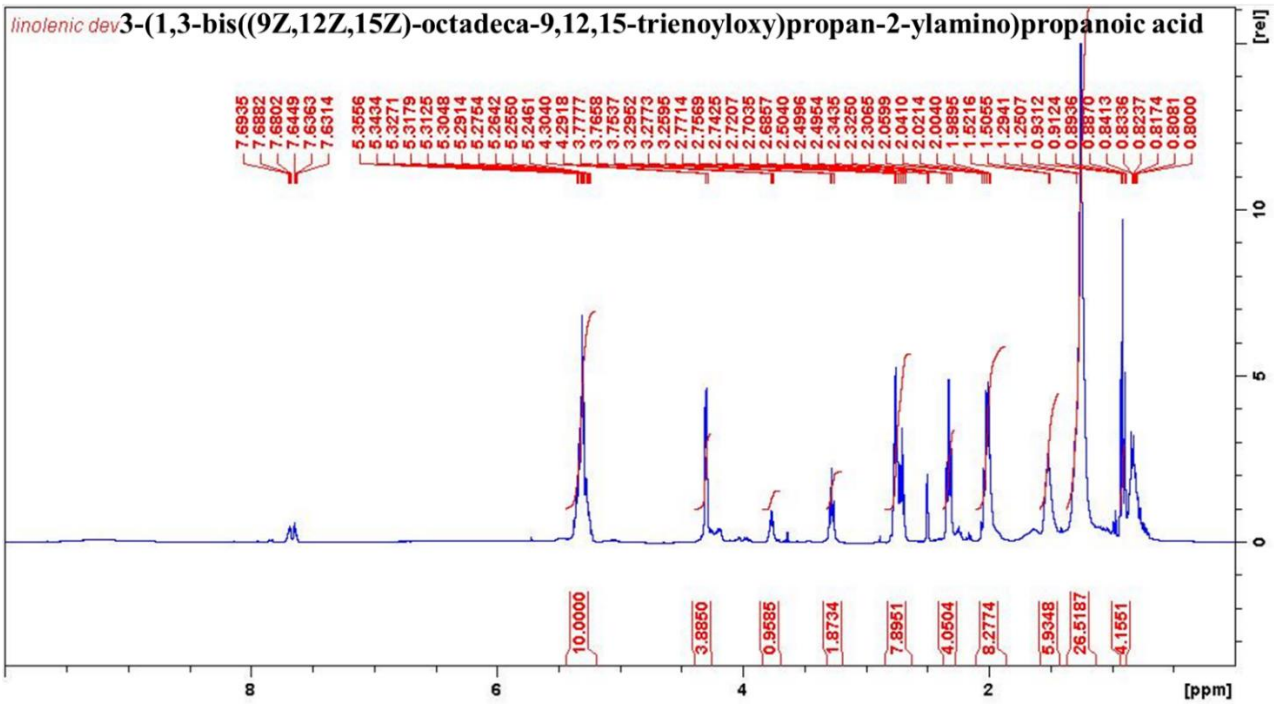

^{13}C NMR characterization of compound 6d

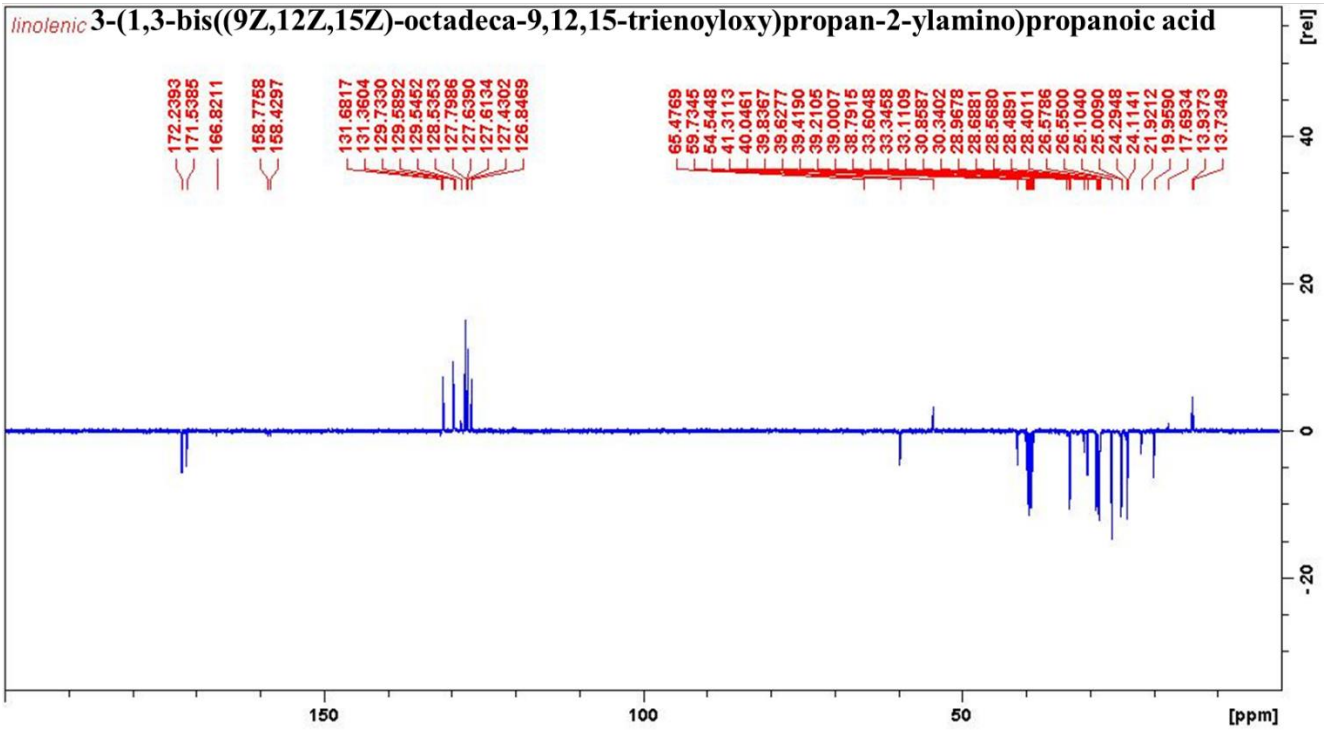

HRMS characterization of Compound 6d

Elemental Composition Report **3-(1,3-bis((9Z,12Z,15Z)-octadeca-9,12,15-trienoyloxy)propan-2-ylamino)propanoic acid** **Page 1**

Single Mass Analysis
Tolerance = 5.0 PPM / DBE: min = -1.5, max = 100.0
Element prediction: Off
Number of isotope peaks used for i-FIT = 2

Monoisotopic Mass, Even Electron Ions
8 formula(e) evaluated with 1 results within limits (up to 20 best isotopic matches for each mass)
Elements Used:
C: 40-45 H: 70-75 N: 0-5 O: 5-10
LLAD 38 (1.248) Cm (1:61)
TOF MS ES+

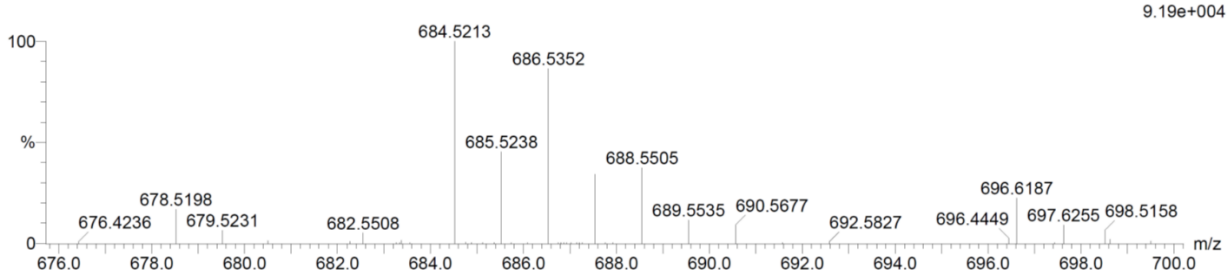

Minimum:				-1.5			
Maximum:		5.0	5.0	100.0			
Mass	Calc. Mass	mDa	PPM	DBE	i-FIT	i-FIT (Norm)	Formula
684.5213	684.5203	1.0	1.5	8.5	74.2	0.0	C42 H70 N O6

Table S1a: Effect of pH on Particle size, PDI and ZP value for different pH-sensitive VCM loaded liposomes.

liposome	**DSAPA-VCM-Lipo**			**DOAPA-VCM-Lipo**		
pH	Size(nm)	PDI	ZP (mV)	Size (nm)	PDI	ZP (mV)
7.4	89.37±0.549	0.184±0.007	-10.4±2.38	96.92±8.732	0.204±0.014	-8.85±3.19
6.0	114.0±2.972	0.629±0.107	-1.20±0.176	162.8±0.012	0.176±0.012	1.54±0.101
5.5	118.8±1.680	0.370±0.016	2.05±0.659	114.5±12.54	0.208±0.023	0.667±0.654

Table S1b: Effect of pH on Particle size, PDI and ZP value for different pH-sensitive VCM loaded liposomes.

Liposome	**DLAPA-VCM-Lipo**			**DLLAPA-VCM-Lipo**		
pH	Size (nm)	PDI	ZP(mV)	Size (nm)	PDI	ZP (mV)
7.4	86.26±11.76	0.203±0.010	-11.3±2.22	88.52±5.078	0.151±0.016	-11.8±2.99
6.0	158±1.908	0.129+0.019	1.02±0.1012	301.2±24.41	0.644±0.230	-1.26±0.427
5.5	97.37±8.928	0.350±0.235	3.10±0.583	282±31.58	0.532±0.170	-0.318±0.746

Table S2a: *In vitro* VCM release data from the different Liposome formulations at pH 7.4

No	Name of release model	DSAPA-VCM-Lipo			DOAPA-VCM-Lipo			DLAPA-VCM-Lipo			DLLAPA-VCM-Lipo		
		R^2	RSME	AIC	R^2	RSME	AIC	R^2	RSME	AIC	R^2	RSME	AIC
1	Zero order	0.4277	17.72	90.54	0.5626	16.05	87.61	0.4188	17.63	90.40	0.6067	17.45	90.07
2	First Order	0.9457	24.29	64.18	0.9609	4.292	57.89	0.9367	5.494	64.16	0.1185	12.88	83.49
3	Higuchi	0.9358	5.919	66.44	0.9634	4.770	61.08	0.9365	5.692	65.43	0.6945	7.610	71.70
4	Korsmeyer-Peppas	1	2	38	0.9836	2.372	38.92	0.9886	1.924	36.06	0.9878	2.231	32.55
5	Weibull	0.9960	1.124	25.57	0.9752	2.926	43.86	0.9882	2.044	38.95	0.9951	0.9455	24.30
6	Hixson-Crowell	0.8921	7.606	71.86	0.9347	5.203	61.66	0.8818	7.593	71.48	0.1052	14.45	85.98

Table S2b: *In vitro* VCM release data from the different Liposome formulations at pH 6.0

No	Name of release model	DSAPA-VCM-Lipo			DOAPA-VCM-Lipo			DLAPA-VCM-Lipo			DLLAPA-VCM-Lipo		
		R^2	RSME	AIC	R^2	RSME	AIC	R^2	RSME	AIC	R^2	RSME	AIC
1	Zero order	0.0033	21.14	94.39	0.0783	22.15	95.33	0.2067	21.71	95.03	0.3804	19.37	92.49
2	First Order	0.8325	8.631	74.74	0.9067	7.041	70.25	0.9322	6.096	66.43	0.9699	4.056	57.22
3	Higuchi	0.8841	7.186	70.60	0.8990	7.280	70.45	0.9160	6.932	69.70	0.9566	5.027	62.53
4	Korsmeyer-Peppas	0.9947	1.407	31.59	0.9969	1.162	27.65	0.9767	3.237	48.07	0.9941	1.568	33.75
5	Weibull	0.9957	1.252	29.70	0.9963	1.226	28.93	0.9818	2.877	46.47	0.9958	1.326	31.07
6	Hixson-Crowell	0.7378	10.78	79.64	0.8510	8.864	75.33	0.8886	7.883	72.29	0.9370	6.032	66.47

Table S3. *In vitro* release best fit values for different formulation at pH 7.4 and 6.0

pH			7.4	6.0
Formulation	Model	Equation	Release Exponent	Release Exponent
DSAPA-VCM-Lipo	KP	$Q = k.t^n$	n = 0.777	n=0.625
	WB	$Q = 1 \exp [-(t)^{a/b}$	n = 0.856	β= 0.792
DOAPA-VCM-Lipo	KP	$Q = k.t^n$	n = 0.629	β= 0.646
	WB	$Q = 1 \exp [-(t)^{a/b}$	n = 0.840	β= 0.842
DLAPA-VCM-Lipo	KP	$Q = k.t^n$	n = 0.777	β= 0.658
	WB	$Q = 1 \exp [-(t)^{a/b}$	n = 0.830	β= 0.825
DLLAPA-VCM-Lipo	KP	$Q = k.t^n$	n =0.536	n= 0.679
	WB	$Q = 1 \exp [-(t)^{a/b}$	n = 0.540	β= 0.667

KP= Korsmeyer-Peppas, WB= Weibull

Table S4a: Effect of storage on physicochemical characteristics of vancomycin loaded liposomes (DSAPA-VCM-Lipo)

Storage condition	Particle size		PDI		ZP	
Time (days)	RT	4 ºC	RT	4 ºC	RT	4 ºC
0	94.44±0.8581	96.94±0.8865	0.225±0.008	0.232±0.007	-11.3±2.65	-7.93±24
30	231.6±71.74	107.4±8.824	0.686±0.264	0.381±0.052	-17.7±8.89	-9.10±3.15
60	681.6±71.74	97.84±6.859	0.686±0.264	0.250±0.046	-22.4±10.5	-15.1±6.94
90	1073±8.741	104.4±9.384	0.534±0.256	0.318±0.077	-25±8.5	-12.2±2.98

Table S4b: Effect of storage on physicochemical characteristics of vancomycin loaded liposomes (DOAPA-VCM-Lipo)

Storage condition	Particle size		PDI		ZP	
Time (days)	RT	4 ºC	RT	4 ºC	RT	4 ºC
0	79.83±1.505	84.17±5.957	0.192±0.009	0.169±0.024	-12.8±3.79	-13.0±3.45
30	84.13±12.59	86.46±1.368	0.248±0.068	0.198±0.025	-15.8±5.45	-12.4±3.82
60	93.30±12.44	80.33±1.566	0.293±0.054	0.191±0.021	-20.2±8.82	-14.4±0.183
90	101.2±9.590	81.58±1.294	0.223±0.040	0.182±0.011	-33.2±7.81	-11.3±3.30

Table S4c: Effect of storage on physicochemical characteristics of vancomycin loaded liposomes (DLAPA-VCM-Lipo)

Storage condition	Particle size		PDI		ZP	
Time (days)	RT	4 ºC	RT	4 ºC	RT	4 ºC
0	82.92±2.615	76.98±0.8767	0.161±0.010	0.170±0.016	-11.8±3.39	-11.2±2.90
30	128.6±5.178	87.13±8.114	0.078±0.010	0.204±0.043	-16.3±3.91	-13.1±5.70
60	157.7±1.754	74.40±1.467	0.207±0.016	0.194±0.020	-18.6±4.4	-14.6±3.51
90	177.6±3.284	81.86±1.249	0.223±0.020	0.182±0.011	-33.2±7.81	-13.2±3.24

Table S4d: Effect of storage on physicochemical characteristics of vancomycin loaded liposomes (DLLAPA-VCM-Lipo)

Storage condition	Particle size		PDI		ZP	
Time (days)	RT	4 ºC	RT	4 ºC	RT	4 ºC
0	91.20±16.42	83.90±6.13	0.217±0.080	0.149±0.017	-10.1±3.06	-11.0±3.27
30	177±7.86	80.51±2.332	0.450±0.376	0.168±0.00	-19.4±13.0	-12.4±3.20
60	257.5±55.86	92.05±4.297	0.296±0.151	0.232±0.052	-11.0±14.5	-13.7±3.94
90	393.9±36.9	104.3±4.949	0.296±0.151	0.240±0.081	-15.8±5.47	-18.8±5.65

CHAPTER 3: EXPERIMENTAL PAPER 2

3.1 Introduction

This chapter addresses Aim 2 and Objectives 1 – 4 and it is a first authored published experimental paper. This chapter highlights the formulation and characterization of pH-responsive micelles from a fatty acid-based lipid Dendritic Amphiphile. The dendritic amphiphile was evaluated for *in vitro* toxicity and used in the formulation of micelles which was also characterized for their physicochemical properties, morphology, bacteria-killing percentage, *in vitro* and *in vivo* antibacterial properties.

The ethical approval is attached in Appendix IV.

3.2 Graphical abstract

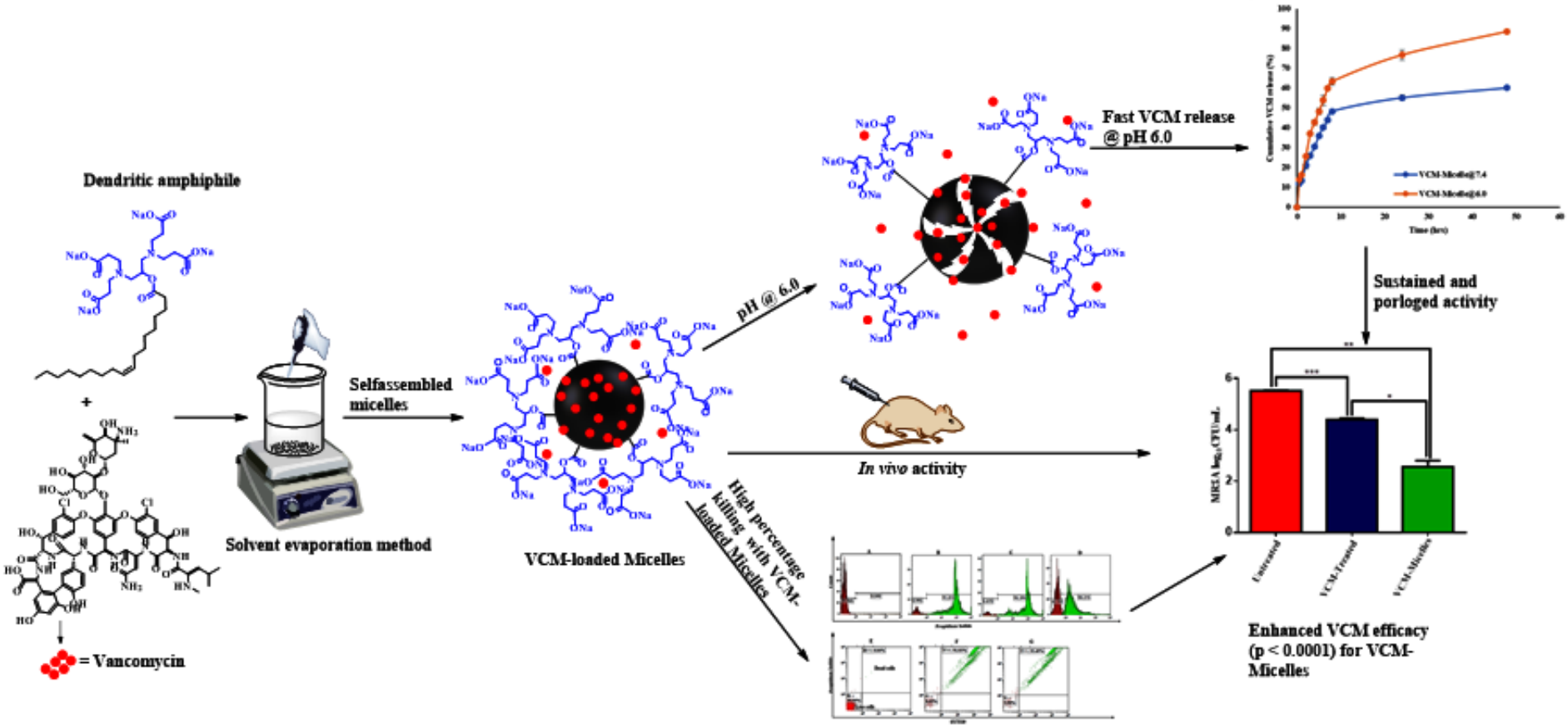

3.3 Published manuscript

pH-Responsive Micelles from an Oleic Acid Tail and Propionic Acid Heads Dendritic Amphiphile for the Delivery of Antibiotics

Sifiso S. Makhathini[1], Calvin A. Omolo[1,2*], Ramesh Gannimani[1], Chunderika Mocktar[1], Thirumala Govender[1]*.

1. Discipline of Pharmaceutical Sciences, College of Health Sciences, University of KwaZulu-Natal, Durban, South Africa.

2. School of Pharmacy and Health Sciences, United States International University of Africa, Nairobi, Kenya

*Corresponding Authors

Email address: govenderth@ukzn.ac.za, comolo@usiu.ac.ke

3.4 Abstract

The aim of this study was to synthesize a novel biocompatible pH-responsive oleic acid-based dendritic lipid amphiphile (OLA-SPDA) which self-assembled into stable micelles (OLA-SPDA -micelles) with a relatively low critical micelle concentration (CMC) of 5.6×10^{-6}M. The formulated micelles had particle size, polydispersity index (PDI) and zeta potential (ZP) of 84.16±0.184 nm, 0.199±0.011 and -42.6±1.98 mV, respectively, at pH 7.4. The vancomycin (VCM) encapsulation efficiency was 78.80±3.26%. The micelles demonstrated pH-responsiveness with an increase in particle size to 141.1±0.0707 nm and a much faster release profile at pH 6.0, as compared to pH 7.4. The minimum inhibitory concentration (MIC) of VCM-OLA-SPDA-micelle against methicillin-resistant *staphylococcus aureus* (MRSA) was 8-fold lower compared to bare VCM, and the formulation had a 4-fold lower MIC at pH 6.0 when compared to the formulation's MIC at pH 7.4. MRSA viability assay showed the micelles had a percentage killing of 93.39% when compared bare-VCM (58.21%) at the same MIC (0.98 µg/ml). *In vivo* mice (BALB/c) skin infection models showed an 8-fold reduction in MRSA burden after treatment with VCM-OLA-SPDA-micelles when compared with bare VCM. The above results suggest that pH-responsive VCM-OLA-SPDA-micelles has the potential to be an effective carrier to enhance therapeutic outcomes against infections characterized by low pH.

Keywords: dendritic amphiphile, pH-responsive micelles, antibacterial, vancomycin, methicillin resistance *S. aureus* targeted drug delivery.

3.5 Introduction

Resistant gram-positive bacteria, such as methicillin-resistant *staphylococcus aureus* (MRSA), have become one of the greatest threats to the global healthcare system [1-3]. The treatment of MRSA infections has been limited within the lipopeptides class of antibiotics, such as vancomycin (VCM); and in recent decades, VCM has remained the last resort in the treatment of serious MRSA infections [3]. However, the emergence of non-susceptible MRSA strains has been associated with the failure of VCM treatment against MRSA, suggesting the need for more effective therapies and therapeutic approaches [1].

Traditional pharmaceutical formulations or dosage forms of antibiotics have been associated with the difficulty in maintaining an effective antibiotic concentration at the site of infection, thus contributing to compromised antibiotic therapeutic outcomes [4, 5]. High antibiotic doses are frequently administered to maintain an effective concentration, which adversely increases the risk of toxic side-effects in the normal cells [6]. These suboptimal concentrations at target sites prevent a complete eradication of infection, resulting in the development of resistant strains [6]. Novel nano-sized, and smart biocompatible, drug carriers have demonstrated the potential to overcome the limitations of conventional dosage forms, showing improved drug pharmacokinetics, safety and drug efficacy through targeting [6, 7]. Most importantly, they can reduce drug-resistance development through high drug dose localisation and high cellular uptake with minimal toxic side-effects [8].

Nanosystems responsive to a specific stimulus (pH, temperature, enzymes, *etc.*) were introduced to achieve the optimum therapeutic effect through targeted and triggered drug release in response to a specific stimulant, thus facilitating drug accumulation at the desired location [9]. pH-responsive drug delivery systems such as micelles have emerged as one of the alternative therapies for diseases characterized by low pH at the disease site, such as inflammation, cancer and bacterial infections [10, 11]. Acidic pH has been found in a wide range of bacterially infected sites, such as soft tissue infections, respiratory tract, urinary tract, skin and intra-abdominal [12, 13]. The pH-responsive micelles can accelerate drug release at the target site, allowing for high drug concentrations for efficient eradication of the bacterial infection [14]. Therefore, developing a pH-responsive delivery system can increase the accumulation of the drug at the infected site and restore the effectiveness of antibiotics such as VCM [15].

Micelles are self-assembled nanostructures of classical amphiphilic molecules characterized by a hydrophobic-hydrophilic segment and offer a wide range of applications in nanomedicine as suitable carriers for poorly soluble drugs [16, 17]. Although pH-responsive micelles are among the most attractive smart drug delivery systems, they still suffer from thermodynamic and kinetic instability after intravenous

injection, which causes the micelles to disintegrate [18]. This results in premature drug release (dose dumping) of the encapsulated drug at unexpected locations when diluted in body fluids [19]. Also, low drug encapsulation efficiency and difficulty in transportation through cell membranes are some of the limitations that hinder the advancement of micelles from bench to clinical trials [20].

Dendritic amphiphiles provide an alternative to the classical amphiphiles in the formulation of structurally stable micelles [21]. These micelles are stable as polymeric assemblies and displays membrane properties like those of the low molecular weight assemblies for better transportation across the cell membrane [21]. They also possess enhanced permeability and retention (EPR) effect. However, most of the reports have demonstrated a lack of active release and targeting of the encapsulated drug in response to a specific stimulus for efficient drug delivery and enhanced therapeutic outcome at the target site [22]. Therefore, designing a stable pH-responsive micelle from pH-responsive dendritic amphiphiles can make micelles a more efficient drug delivery system that can lead to drug accumulation at a lethal dose at disease sites through triggered release. This can ensure sufficient bacterial infection eradication, thus reducing the chances of antibiotic-resistance development [23]

pH-responsive dendritic polymeric micelles are the most commonly studied hyperbranched and multifunctional nanosyatem for efficient delivery of anticancer and antitumor agents [18]. According to our knowledge, no pH-responsive lipid-dendritic micelles for antibiotic delivery have been reported in the literature. The bicephalous dianionic amphiphile is one of the recently reported branched lipid amphiphiles with a similar structural arrangement to dendritic amphiphiles, forming a stable micellar structure with relatively low CMC when compared to convention amphiphiles [21, 24]. The advantage of multivalence of the hydrophilic portion of the branched amphiphiles provides room for surface functionalization for site-specific drug release in response to specific stimuli [25]. The optimum therapeutic outcome of pH-responsive micelles can be achieved through acid-triggered drug release which quickly releases the drug at the target site through a protonation/deprotonation mechanism of the amphiphile. This process induces disassembly of the micelle structure which leads to the drug being released in response to reduced pH, such as the site of infection. Additionally, lipid-based branching amphiphiles can offer high stability, high drug loading capacity for both hydrophilic and lipophilic drugs, longer circulation, and ability to mimic biological membrane components when compared to conventional classical amphiphiles in the formulation of micelles [26, 27]. Thus, these positive attributes of the branched lipid amphiphiles advocate for more research in this area for efficient drug delivery.

The acidic bacterial environment can be exploited using pH-responsive micelles to achieve an optimum antibiotic therapeutic index. Previously, our group has reported on pH-responsive lipid nanosystems, such as liposomes[28], solid lipid nanoparticles[29] and nanostructured lipid carriers [30]. These systems significantly enhanced the activity of VCM through drug localisation, high interaction of the lipid system with the cell membrane, and pH-triggered drug releases. Therefore, in continuation of our search for optimal pH-responsive lipid systems for the efficient delivery of VCM, we herein introduce a pH-responsive lipid-dendritic based nanosystems, formulated from an oleic acid-based dendritic lipid amphiphile that has not been reported before for any class of drug.

In this study, we designed and synthesized a novel oleic acid-derived lipid dendritic amphiphile (OLA-sodium propionate dendritic amphiphile (OLA-SPDA)) to self-assemble into stable micelles containing VCM for targeted delivery at acidic bacterial infection sites for the enhanced eradication of MRSA infection. We envisaged this lipid amphiphile to be biosafe for the formation of stable micelles with properties such as high stability and encapsulation efficiency, pH-responsiveness, and fusion ability with the bacterial cell membrane, for the improvement of antibiotic activity against bacterial infection as a strategy for addressing the current global antimicrobial drug resistance crisis. Furthermore, this pH-responsive lipid-dendritic micellar system can be used for the delivery of other drugs to disease sites characterized by low pH.

3.6 Materials and Methods

3.6.1 Materials

1,3-Diamino-2-propanol was purchased from Sigma-Aldrich (UK). N, N'-dicyclohexyl carbodiimide (DCC) and trifluoroacetic acid (TFA) were procured from Merck (Germany) while tertiary butyl acrylate (TBA) and triisopropylsilane (TIPS) were both purchased from Sigma-Aldrich (Germany). Mueller Hinton agar (MHA) and Nutrient broth were purchased from Biolab Inc. (South Africa). The following reagents; oleic acid (OA), Mueller Hinton broth 2 (MHB), Vancomycin hydrochloride, 4-(dimethylamino) pyridine (DMAP), dialysis tubing cellulose membrane and all other materials were purchased from Sigma-Aldrich (USA). The vancomycin free base (VCM) was obtained from converting vancomycin hydrochloride as described from a previously reported method [21]. An Elix® water purification system Millipore Corp. (USA) was used to obtain milli-Q purified water. Bacterial strains *Staphylococcus aureus* (ATCC 25922) (*S.aureus*) and *Staphylococcus aureus* (Rosenbach) (ATCC®BAA-1683) (MRSA) were used for this project. A Bruker Alpha-p spectrometer with a diamond ATR (Germany) was used to obtain FT-IR spectra for all the compounds synthesized. ^{1}H and ^{13}C NMR spectra were obtained by using a Bruker 400 and 600 Ultra shield™ (United Kingdom) NMR.

3.6.2 Methods

3.6.2.1 Synthesis and characterization of the lipid amphiphile (OLA-SPDA)

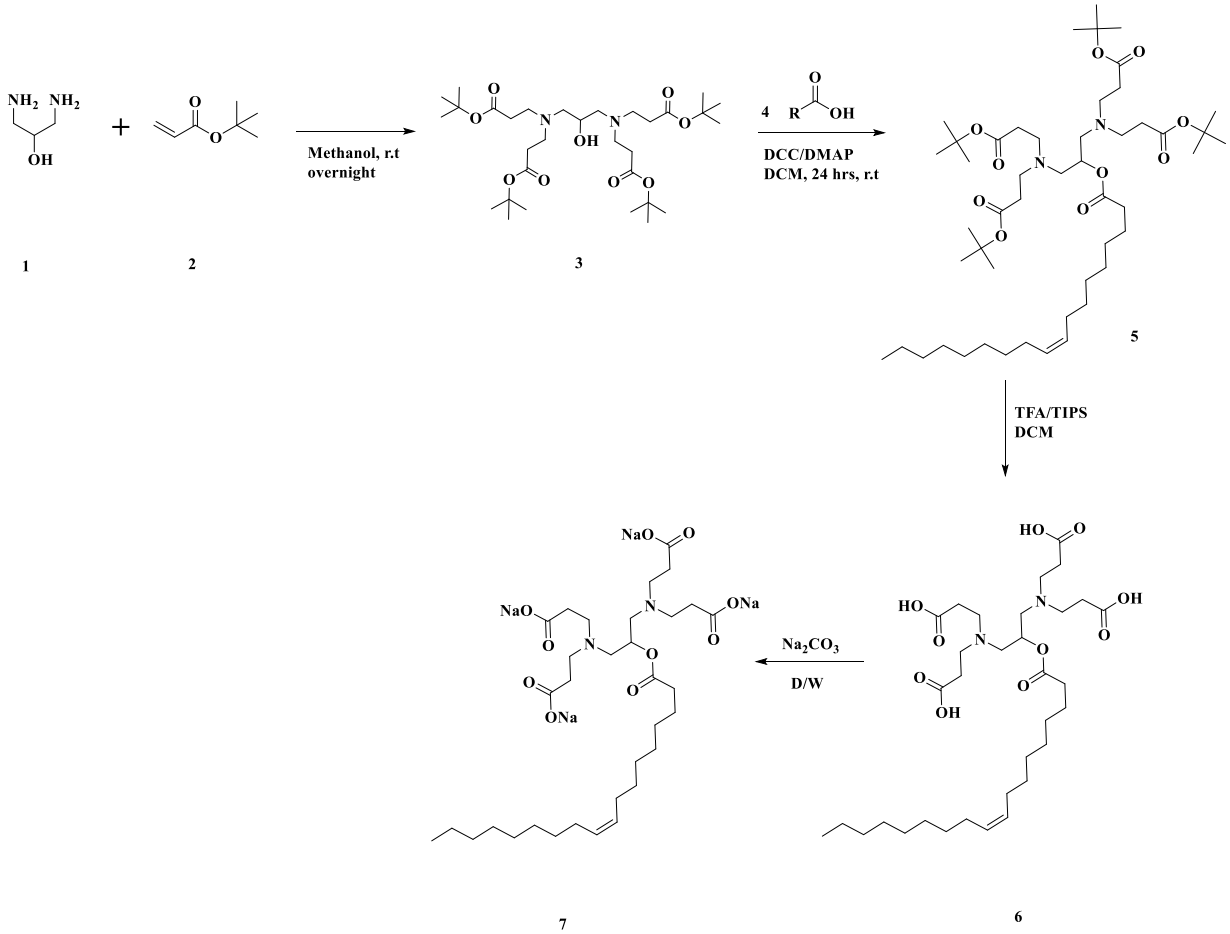

Scheme 1: Synthesis of the oleic acid-sodium propionate dendritic amphiphile (OLA-SPDA) as per the above scheme

3.6.2.2 **Tetra-tert-butyl3,3',3'',3'''- ((2-hydroxypropane-1,3-diyl)bis(azanetriyl)) tetrapropionate** (**3**). In a round-bottom flask kept under inert conditions (purged with nitrogen), 1,3-diamino-2-propanol (2 g, 22.19 mmol) was diluted in methanol (30 ml) and then tert-butyl acrylate (28 g, 221.92 mmol) was added and stirred for 24 h at room temperature while maintaining dark conditions. After reaction completion, the solvent and excess of tert-butyl acrylate were removed under reduced pressure (vacuum) in a rotavapor to give a colourless, oily product with a quantitative yield above 91%. Characterization was as follows: ^{1}H NMR (400 MHz, $CDCl_3$) δ(ppm): 1.33 (s, 36H), 2.28-2.24 (m, 12H), 2.74-2.60 (m, 8H), 3.67-3.64 (m, 1H); ^{13}C NMR (400 MHz, $CDCl_3$) δ(ppm): 28.0, 33.5, 49.8, 58.5, 65.9, 80.2, 171.7.

3.6.2.3 **Tetra-tert-butyl 3,3',3'',3'''- ((2-(oleoyloxy)propane-1,3-diyl)bis(azanetriyl)) tetrapropionate** (**5**). To synthesize compound **5**, oleic acid (2.81g, 9.95 mmol) was added to a stirring mixture of compound

3 (5 g, 8.30), DCC (2.58 g, 13.46 mmol) and DMAP (0.101 g, 0.829 mmol) in dry DCM and further stirred for 24 h under a nitrogen atmosphere at room temperature. Dicyclohexylurea formed was filtered off and the crude product was obtained by removing the solvent (filtrate) under reduced pressure (vacuum). The crude product was then purified by column chromatography on silica gel using ethyl acetate in hexane (10-15% v/v) to give a yield of 95%. Characterization was as follows: ^{1}H NMR (400 MHz, $CDCl_3$) δ(ppm): 0.88 (m, 3H), 1.28-1.25 (m, 20H), 1.42 (s, 36H), 1.61-1.56 (m, 2H), 2.0-1.97 (m, 4H), 2.28-2.24 (m, 2H), 2.39-2.31 (m, 8H), 2.59-2.48 (m, 4H), 2.82-2.73 (m, 8H), 4.98-4.94 (m, 1H), 5.34-5.31 (m,2H); ^{13}C NMR (400 MHz, $CDCl_3$) δ(ppm):14.0, 22.6, 24.8, 27.2, 28.1, 29.0, 29.1, 29.2, 29.3, 29.5, 29.7, 31.8, 33.3, 33.7, 34.5, 49.8, 50.0, 55.4, 58.5, 70.9, 80.5, 171.8, 173.2

3.6.2.4 **3,3',3'',3'''-((2-(oleoyloxy)propane-1,3-diyl)bis(azanetriyl)) tetrapropionic acid** (**6**). Compound **5** (4 g, 4.6 mmol) was treated with 25% trifluoroacetic acid (TFA) in DCM and stirred for 2 h at room temperature. The reaction was monitored by TLC to verify completion. The TFA was removed under reduced pressure to give a viscous oil product. The product was re-dissolved in methanol (10 ml) and evaporated under reduced pressure at least 3 times for a complete TFA removal. The vacuum dried product gave a yield above 89 % and characterization was as follows: ^{1}H NMR (400 MHz, $CDCl_3$) δ(ppm): 0.90 (m, 3H), 1.33-1.29 (m, 20H), 1.62-1.57 (m, 2H), 2.07-2.04, (m, 4H), 2.19-2.16 (m, 1H), 2.60-2.39 (m, 10H), 2.78-2.74 (m, 3), 2.97-2.91 (m, 2H), 3.15-3.04 (m, 5H), 3.29-3.22 (m, 3H), 5.37-5.30 (m, 3H); ^{13}C NMR (400 MHz, $CDCl_3$) δ(ppm): 13.8, 22.5, 25.5, 27.07, 27.2, 27.8, 29.3, 31.4, 31.9, 50.6, 56.3, 62.5, 127.6, 129.5, 160.3, 179.2

3.6.2.5 Sodium 3,3',3'',3'''- ((2-(oleoyloxy)propane-1,3-diyl)bis(azanetriyl)) tetrapropionate (**7**). Compound 7 (1.56 g, 2.43 mmol) was added to an aqueous solution of Na_2CO_3 (0.514 g, 4.85 mmol) under vigorous stirring, in small portions, until the starting material was completely dissolved. This was stirred for 2 h in an open beaker and the resulting solution was freeze-dried for 48 h to give a white hydroscopic product with a yield of 97 %. Characterization was as follows: ^{1}H NMR (400 MHz, $CDCl_3$) δ(ppm): 0.90 (m, 3H), 1.33-1.29 (m, 20H), 1.62-1.57 (m, 2H), 2.07-2.04, (m, 4H), 2.19-2.16 (m, 1H), 2.60-2.39 (m, 10H), 2.78-2.74 (m, 3), 2.97-2.91 (m, 2H), 3.15-3.04 (m, 5H), 3.29-3.22 (m, 3H), 5.37-5.30 (m, 3H); ^{13}C NMR (400 MHz, $CDCl_3$) δ(ppm): 13.8, 22.5, 25.5, 27.07, 27.2, 27.8, 29.3, 31.4, 31.9, 50.6, 56.3, 62.5, 127.6, 129.5, 160.3, 179.2

3.6.3 *In vitro* cytotoxicity (MTT assay) and *In vitro* hemolysis analysis

The MTT assay is a commonly used cell-based study for newly synthesized compounds to assess their cytotoxic effect leading to cell death [31, 32]. After successful synthesis, the biosafety of the OLA-sodium propionate dendric amphiphile (OLA-SPDA) was assessed via MTT assay using three cell lines: human liver hepatocellular carcinoma (HEP G2), human breast adenocarcinoma (MCF7) and adenocarcinoma human alveolar basal epithelial (A549), as described in a previously reported study [33]. Briefly, the cell lines

were grown under humidified conditions (5% CO_2) and 96-well plates were used to seed cells at a density of 2.5×10^3 and incubated for 24 h at 37 °C. After the incubation, the cells were treated with 20, 40, 60, 80, 100 and 120 µg/ml concentrations of the test compound and further incubated for 24 h. After the incubation period, the culture medium was discarded and replaced with the fresh medium, followed by addition of 100 µl of MTT solution (5 mg/ml) in phosphate buffer solutions (PBS) to each well. This was incubated for a further 4 h at 37 °C and the reaction was quenched by lysing the cells with dimethyl sulfoxide (100 µl) in each well. The absorbance for each well was recorded using a microplate spectrophotometer (Mindray MR-96A) set at 540 nm. The culture medium with cells and without cells was used as the positive and negative control respectively. All the experiments were replicated six times. The percentage cell viability of every treated sample was calculated using the following equation:

$$\%\ \text{Cell viability} = \left(\frac{\text{A 540 nm treated cells}}{\text{A 540 nm untreated cells}}\right) \times\ 100 \qquad (1)$$

The hemolysis analysis is a part of the biosafety study within the blood system and was performed on different concentrations of OLA-SPDA against red blood cells (RBCs) according to a previously described method [34]. Briefly, RBCs were harvested from fresh sheep blood by centrifugation at 2800 rpm for 5 min, followed by washing with PBS solution several times and centrifuging to ensure no haemoglobin release. Different concentrations of OLA-SPDA (1.8 ml) ranging from 0.250 to 0.0075 mg/ml were incubated with RBCs suspension (0.2 ml) at 37 ◦C for 60 min. RBCs incubated with PBS and with distilled water were treated as negative and positive controls, respectively. After this, the samples were then centrifuged at 3000 rpm for 10 min. The hemolytic effect from samples can be qualitatively determined through observation of the sample mixtures, indicated by a colour change from clear to red showing release of haemoglobin for samples that are hemolytic. Quantitatively, the percentage of hemolysis can be measured in terms of the amount of haemoglobin released using UV Spectrophotometric (Shimadzu UV- 1650 PC) at 570 nm of the supernatant from each sample at different concentrations. The degree of hemolysis was calculated by the following equation:

$$\%\ \text{hemolysis} = \left(\frac{\text{A(test)} - \text{A(negtive control)}}{\text{A(positive control)} - \text{A(negetive control)}}\right) \times\ 100 \qquad (2)$$

3.6.4 Determining Critical Micelle Concentration (CMC)

A Malvern Zetasizer, NANO ZS90 (Malvern Instruments Limited, U.K.), fitted with a 4 mW He–Ne laser set at a wavelength of 633 nm was used to determine the CMC of the OLA-tetracephelous tetra ionic amphiphile. The detection angle of the scattered light was fixed at an angle of 90° to produce optimal detection of scattered light with a high-quality signal. An aqueous stock solution (0.5 M) of OLA-SPDA

was used in preparing solutions of concentration ranging from 1×10^{-2} to 1×10^{-6} M. A polystyrene cell was used to measure the scattering intensity at 25 °C (n=3) and the output data was processed using a computer attached to the instrument. The CMC value was determined by plotting the changes in intensity (kcps) against the concentration of the corresponding samples [35].

3.7 Preparation and Characterization of VCM-OLA-SPDA-micelles

3.7.1 Preparation

The blank micelles were prepared via a self-assembly approach using the solvent evaporation method reported in the literature [33]. Typically, the OLA-SPDA lipid was completely dissolved in 3 ml THF which was then added dropwise into 10 ml of distilled water under vigorous stirring. The organic solvent was allowed to evaporate by keeping the solution open to air under stirring for 24 h. The solution obtained had a blue tint colour, which was an indication of the successful formation of micelles. The preparation of the drug-loaded formulation followed the same procedure, except that the amphiphilic lipid was added dropwise into 10 ml solution of 0.5 mg/ml VCM in distilled water.

3.7.2 Size, Polydispersity Index (PDI), Zeta Potential (ZP) and Morphology

The physicochemical properties of micelles (size, PDI and ZP) were evaluated using a dynamic light scattering technique. Appropriate dilutions of the formula were made using PBS (pH 7.4 and 6.0) prepared using milli-Q water. Measurements were recorded at room temperature (25º C) using a Zetasizer Nano ZS90 (Malvern Instruments, UK) fitted with a 633 nm laser at 173° detection optics. All parameters were analysed in triplicate from different batches prepared separately to ensure reproducibility of the results. The morphological features of the nanoparticles were characterized by TEM analysis. The prepared samples were negatively stained with 1% uranyl acetate and fixed on a copper grid for drying and images were acquired at 100 kV using JEOL Microscopy (JEM 2010, Japan).

3.7.3 Entrapment Efficiency (EE) and Drug Loading (DL)

The encapsulated VCM amount in micelles was determined using an ultrafiltration method by separating the free drug from the encapsulated drug using centrifugal filter tubes (Amicon® Ultra-4) of 10 KDa molecular weight cut-offs. The drug-loaded formulations (2 ml) were placed in the centrifugal filter tube and centrifuged at 3000 rpm for 30 minutes at 25 °C. To determine the VCM concentration in the filtrate (the unencapsulated VCM), high-performance liquid chromatography (HPLC), Shimadzu Prominence DGU-20A3 at 280 nm was used. The optimized conditions for HPLC were as follows: C18 reversed-phase column (Nucleosil 120-5 C18; 4 × 150 mm, 5µm); acetonitrile: 0.1% TFA in water (15:85 v/v) as a mobile phase; and column temperature, injection volume and flow rate were set at 25 °C, 100µL and 1 mL/min, respectively. The unknown amount of VCM was calculated using the following linear regression equation

y = 24598x−3125.7 with linearity (R^2) of 0.999. The following equations were used to calculate %EE and %DL.

$$\text{EE (\%)} = \left(\frac{\text{Weight of VCM in micelles}}{\text{Weight of VCM added}}\right) \times 100 \qquad (3)$$

$$\text{DL (\%)} = \left(\frac{\text{Weight of VCM in micelles}}{\text{Total weight of micelles}}\right) \times 100 \qquad (4)$$

Where the weight of VCM in micelles, represents the amount of drug entrapped in micelles after separation using centrifugation; weight of VCM added refers to the initial amount of VCM used in the formulation and the total weight of micelles refers to the weighed amount of all the excipients used to formulate micelles in their dry powder form.

3.7.4 Thermal Profiles

Differential scanning calorimetry (Shimadzu DSC-60, Japan) is a widely used thermoanalytical technique to measure the thermal profiles of samples [36]. The thermal profiles of the lipid, freeze-dried drug-loaded formulation, the physical mixture of all the components, and the drug (VCM), were determined by weighing 2 mg of the samples, placing them in aluminium pans and sealing them using a crimper. These (both loaded and empty) pans were heated up to 300 °C at a constant rate of 10 °C/min under a constant nitrogen flow of 20 ml/min.

3.7.5 *In vitro* drug release

The *in vitro* VCM release behavior from VCM-loaded pH-responsive micelles was investigated using diffusion technique using dialysis tubing of cellulose membrane, average flat width 10 mm (MWCO 10,000- 14,000 Da, Sigma-Aldrich, USA) [37]. Briefly, 2 ml of the formulations (blank and drug-loaded) were loaded into dialysis tubes of specified pore size, sealed and dialysed against 40 ml PBS (7.4 and 6.0) at 37 °C in an incubator maintained at 100 rpm. The amount of VCM released was determined with HPLC through following a previously reported procedure, conditions specified in section **2.3.3** [38]. A fresh PBS of the equal amount was added after each sampling to keep sink conditions constant and all experiments were performed in triplicate.

3.8 Antibacterial Studies

3.8.1 *In vitro* antibacterial activity

The minimum inhibitory concentration (MIC) of vancomycin-loaded micelles and bare VCM against *S. aureus* and MRSA at pH 7.4 and pH 6.0 was determined using a broth dilution method [38]. Bacterial cultures of *S. aureus* and MRSA in nutrient broth were grown for 24 h at 37 °C in a Labcon 3081u shaking incubator (USA). The 0.5 McFarland standard (1.5×10^8 CFU)/ml) was achieved by diluting the cell culture with sterile distilled water and measured using a DEN-1B suspension McFarland densitometer (Latvia). This was

further diluted to 1:150 with sterile distilled water giving a concentration of 5×10^5 colony forming units (CFU)/ml necessary for this study. The serially diluted samples (bare VCM, blank micelles, and VCM-OLA-SPDA-micelles) prepared in MHB (pH 7.4 and pH 6) in a 96-well plate, were treated bacterial cell culture (5×10^5 (CFU)/ml). The plates were incubated at in a shaking incubator set at 37 °C, 100 rpm for 24 h. The MIC values were determined by spotting 5 µl of the sample mixture on Mueller-Hinton (MHA) plates at different time intervals (24h, 48h and 72h). The vancomycin-loaded micelles and bare VCM solution were used as positive controls whereas the blank formulation was used as a negative control. All experiments for this study were performed in triplicate.

3.8.2 Bacterial cell viability

Flow cytometry is a commonly used technique to quantify viable MRSA cells [39]. A bacterial cell culture, prepared as described in Section **2.4.1**, was treated with VCM solution (positive control) and VCM-OLA-SPDA-micelles at the concentration equivalent to their respective MICs and were incubated at 37 °C for 6 h. Untreated MRSA cells were utilised as a negative control. In separate flow cytometry tubes containing 350 µl of sheath liquid, 50 µl of the VCM and VCM-OLA-SPDA-micelles solutions were added and vortexed for 5 min. Thereafter, propidium iodide (PI) dye (5 µl) was used to stain the mixture which was incubated for 30 min. As described from a previously reported protocol for assessing the viability of treated cell samples, a BD FACSCANTO II flow cytometer (Becton Dickinson, USA) was used in this study, with a minimum of 10,000 cells being gathered [40].

3.8.3 *In vivo* antibacterial activity

The protocol approved by the Animal Research Ethics Committee of the University of KwaZulu-Natal (approval number: AREC/104/015PD) was followed when conducting this experiment. As per reported procedure, mice skin infection models were used to further evaluate the *in vivo* efficacy of the VCM-OLA-SPDA-micelle formulation in comparison with bare VCM against MRSA [41]. Male BALB/c mice (18-20 g) models were used for this experiment, provided by the Biomedical Research Unit at the University of KwaZulu-Natal. The mice were shaved, disinfected with 70 % ethanol and separated into three groups of four (negative control, positive control and treatment group) before the day of the experiment. The final MRSA concentration of 1.5×10^8 CFU/ml was achieved by diluting 50 µl MRSA with a saline solution which was intradermally administered. After 30 minutes of infection, a positive control group was treated with bare VCM. The treatment group was treated with the formulation whilst the negative control group was treated with saline. After observing for 48 h and keeping the animals under normal conditions, the infected skin from the sacrificed mice was harvested and homogenised in 5 ml of PBS (pH 7.4). The tissue homogenates were serially diluted with PBS and spotted (20 µl) onto on nutrient agar plates. The CFU counts were determined after the incubating for 24 h at 37 °C.

3.9 Physical Stability

The short-term physical stability of OLA-SPDA-micelles formulation kept under different storage conditions (4 °C and room temperature) was evaluated for 90 days. The formulations physical stability was reported at predetermined time intervals (30, 60 and 90 days) by measuring the particle size, PDI, ZP, and assessing their physical appearance. All experiment for this study were performed in triplicate.

3.10 Statistical Analysis

The collected results were analyzed by one-way analysis of variance (ANOVA), followed by Bonferroni's multiple comparison tests using GraphPad Prism® 6 (GraphPad Software Inc., USA), were used for statistically significant difference analysis. The results were expressed as a mean ± standard deviation (SD) and a data point difference between the two groups tested being considered statistically significant when *p*-value < 0.05.

3.11 Results and Discussion

3.11.1 Synthesis of OLA-Sodium Propionate Dendritic Amphiphile (OLA-SPDA)

The synthesis of the oleic acid-derived dendritic amphiphile was done in four steps as shown in **Scheme 1** (above). The first step involved the addition of tertiary butyl acrylate (**2**) to 1,3-diaminopropano-2-ol (**1**) to form compound **3** with four branches, via bis-aza-Michael addition, which was confirmed by both ^{1}H NMR and ^{13}C NMR. A strong singlet peak at chemical shift δ 1.33 ppm, which integrates to 36 protons from the tert-butyl group in ^{1}H NMR, and the presence of carbon peaks at chemical shifts δ 28, 33.5, 49.8, 58.5, 80.2 and 171.7 ppm in ^{13}C NMR, corresponding to C $(CH_3)_3$-COO-, CH_2C=O-, CH_2-N- and C=O functional groups, confirmed the formation of compound **3**. Using the alcoholic functionality from compound **3**, the second step involved esterification of oleic acid using DCC/DMAP coupling chemistry to form compound **5**. The chemical shifts in ^{1}H NMR spectra confirmed the formation of the product through the identification of peaks at δ 0.86 (multiplet), δ 1.26 (multiplet), δ 1.61 (multiplet), δ 2.0 (multiplet), δ 2.28 (multiplet) and δ 5.35 ppm (multiplet), corresponding to the aliphatic chain of oleic acid coupled to compound **3**. The hydrolysis of tertiary butyl ester groups from compound **5** to form compound **6**, with four branches of free carboxyl group using TFA and TIPS (scavengers), was the third step of the synthesis. After the purification procedure, the product structure was elucidated using ^{1}H NMR, which showed the disappearance of isobutane peaks at δ 1.33 ppm and at δ 28 ppm in ^{13}C NMR, confirming a successful hydrolysis reaction. The last step was to convert compound **6** into sodium salt to enhance its solubility in water. This procedure involved the dissolution of compound **6** into an aqueous solution of Na_2CO_3.

3.11.2 *In Vitro* Cytotoxicity and *In Vitro* Hemolysis Study

The cytotoxicity effect of OLA-sodium propionate dendritic amphiphile (OLA-SPDA) was evaluated using an MTT assay over a range of different sample concentrations (20 – 120 µg/ml). This method is based on

the activity of mitochondrion of a living cell, able to convert MTT into formazan crystals. The total activity of the mitochondria is relatable to the number of viable cells in the cell population treated with a potential toxicant. Using human cell lines (A549, Hep G2 and HEK-293), the MTT results demonstrated a high percentage (> 75%) of cell viability after 48 h co-incubation at different sample concentrations studied (**Fig. 1A**). The cell viability of the dendritic lipid amphiphile against different human cell lines A549, Hep G2 and HEK was 98%, 80% and 80%, respectively, with no dose-dependent trend noticed for all concentrations used. Since the cell viability was above 75%, these results suggest that OLA-SPDA has excellent biocompatibility and level of safety and it can be considered as safe for biomedical use [42].

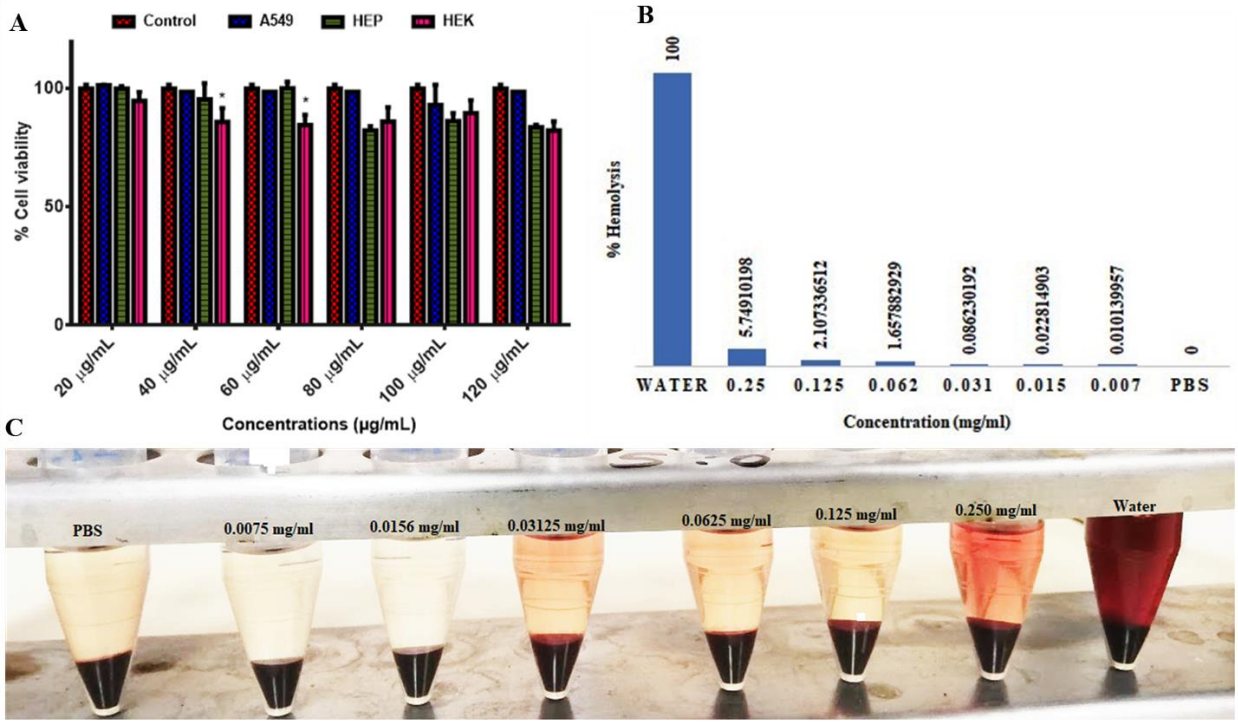

Fig. 1: In vitro cytotoxicity and hemolytic activity of OLA-SPDA. **A**) Percentage cell viability of human cells (A549, HEP G2 and HEK-293) after treatment; **B**) percentage hemolysis; **C**) visual assessment of the tubes containing diluted blood after exposure to OLA-SPDA.

We are proposing an intravenous route of administration for our system, and most biomaterials end up in the bloodstream and come into contact with red blood cells (RBCs) [43]. As an additional biosafety measure, the hemolytic effect of OLA-SPDA was evaluated using sheep's blood. As shown in **Figures 1B** and 1**C**, above, the sample was slightly hemolytic at high concentrations, with low amounts haemoglobin released, as compared to samples treated with water which showed high percentages of hemolysis. The highest and lowest OLA-SPDA concentrations had a hemolytic effect of ~ 5% and ~ 0.01%, respectively, which showed a much lower hemolytic effect than that of water (control). This percentage hemolysis is similar and

significantly lower than the hemolytic effect of other previously reported biomaterials used in formulations [44]. Therefore, after conducting hemolytic analysis and a cell-based study (MTT assay), we conclude that our system may be considered safe for use in the formulation of nanosystems for *in vivo* delivery.

3.11.3 Critical Micelle Concentration (CMC) Determination

The stability of micelles, measured as the lowest concentration of the amphiphile in which they remain assembled, is of importance for *in vivo* application. For this study, the DLS technique was used by recording intensity values and which were plotted against each sample concentration of OLA-SPDA-micelle, as illustrated in **Figure 2**. The point of intersection of the two straight lines drawn corresponds to the lowest concentration in which OLA-SPDA will remain assembled (5.6×10^{-6}M). This was significantly lower than the CMC values of other low-molecular-weight surfactants (1.6×10^{-4}M) reported with the similar structural arrangement, and also falling within the CMC range of polymeric micelles (10^{-6} to 10^{-7} M) [24, 33]. This could be attributed to a balance between the hydrophilic branched head and hydrophobic chain lengths from oleic acid, resulting in the formation of stable micelles. The double-headed sodium salt version of oleic acid-derived amphiphiles, with a single tail, with 2:1 head-to-tail ratio, has been reported to improve the CMC value of the self-assembled micelles when compared to single-headed oleic acid-derived amphiphiles with a 1:1 head-to-tail ratio. In this study, OLA-SPDA with four-head groups and single tail (4:1) demonstrated a remarkably low CMC which can be correlated to the increased hydrophilicity of OLA-SPDA, creating a hydrophobic-hydrophilic balance when compared to single and double-headed amphiphile; steric stabilisation promoting a unique pecking order that allows for the assembly of a stable system; and nanosystems with zeta potential greater than ±25 mV, which have a higher degree of stability. These can significantly contribute towards low the CMC of OLA-SPDA-micelles.

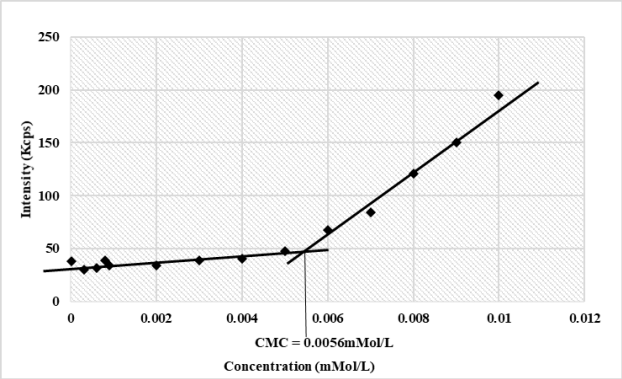

Fig. 2: Concentration (mol/L) plotted against intensity (kcps) for OLA-SPDA-micelles. (n = 3)

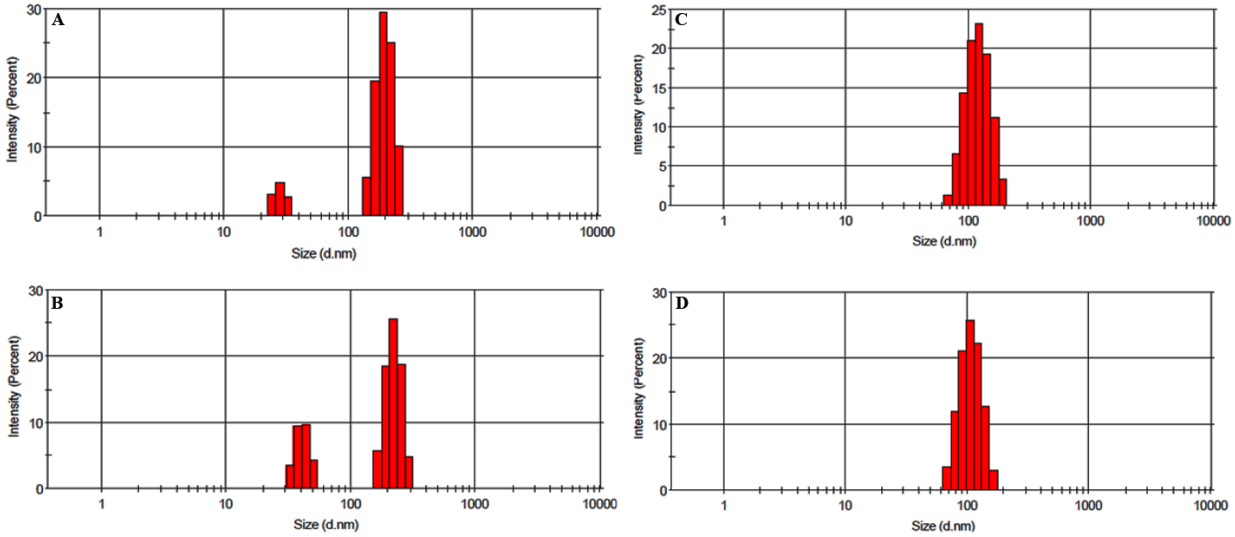

Fig. 3: Particle size distribution of OLA-SPDA-micelles below CMC value: (**A**) 3×10^{-6} mol/L and (**B**) 1×10^{-6} mol/L. PDI; 0.606 and 0.807, respectively. Particle size distribution above CMC value: (**C**) 1×10^{-5} mol/L and (**D**) 7×10^{-6} mol/L. PDI; 0.254 and 0.301, respectively. (n = 3)

The histogram representation of OLA-SPDA-micelles particle size distribution (PDI) in **Figures 3C** and **D** confirmed the stability of micelles, at and above the CMC, with a uniform PDI. Below the CMC there was uneven PDI which confirms the disassembly of micelles (**Figs. 3A** and **B**).

3.11.4 Preparation and Characterization of VCM-Loaded OLA-SPDA-Micelles

3.11.4.1Size, Surface charge, Entrapment efficiency, and Morphology

The optimum conditions for the preparation of pH-responsive OLA-SPDA-micelles were achieved through the screening of water-miscible solvents and an amount of OLA-SPDA to obtain an average particle size ranging from 10 to 200 nm. This is the preferred size distribution necessary to evade phagocytosis and create longer circulation, which can enhance the accumulation of the micelles at the site of infection [45]. Also, the pH-responsiveness of the micelles was assessed by dispersing the formulation in different buffer solutions (pH 7.4, 6.0 and 4.5), and the physicochemical properties (particle size, polydispersity index (PDI) and zeta potential) were measured. In this study, 100 mg of OLA-SPDA in 3 ml of THF was used to formulate both blank and VCM-loaded OLA-SPDA-micelles using a solvent evaporation method. Then the physicochemical properties were measured at different pH values (7.4, 6.0 and 4.5) to evaluate its pH-responsiveness. The optimised micelle formulation was then loaded with VCM to evaluate its encapsulation efficiency. As shown in **Table 1,** the particle size at pH 7.4, 6.0 and 4.5 was 84.16±0.184, 144.3±11.42 and 142.7±3.938 nm, respectively, showing stable micelles at physiological pH (7.4) with a PDI of 0.121±0.063. pH responsiveness was confirmed with the increase in particle size and PDI at different pHs. The average particle size increased from 84.16±0.184 to 144.3±11.42 nm with the change in pH from 7.4

to 6.0, and this change in size can be beneficial for fast drug release at target sites since pH 6 represents an acidic condition at the bacterially-infected site. The increase in size could result from the rearrangement of the amphiphiles in response to changes in pH, causing swelling of micelles. This rearrangement and change in the size of micelles can potentiate a quick release of VCM at the target site at a dose lethal for the efficient eradication of bacterial infection. The change in the physical appearance of samples suspended in different buffer solutions can be correlated with a change in size, with respect to change in pH, as shown in **Figure 4D**. The sample at pH 7.4 is clear, demonstrating no sign of change in particle size or shape; whereas, at pH 6.0 and pH 4.5, the sample becomes more turbid, indicating a disruption of the system, resulting in precipitation or disassembly of micelles in response to reduced pH. The lack of surface charge switch to positive zeta potential at pH 6.0 can be explained using the structural functionalities of OLA-SPDA, consisting of two tertiary amines and four carboxylate ions in a ratio of 2:4. Based on the calculated isoelectric point of OLA-SPDA, it indicates that the overall surface charge will remain negative in pH systems above 3.2, thus giving an overall negative surface charge for our system at pH 6.0. Morphological properties were also analysed using HRTEM as the supporting information for the results obtained using DLS. HRTEM images of OLA-SPDA-micelles, as shown in **Figures 4B and C**, which showed a smooth spherical shape with a particle size similar to the one obtained using DLS (**Fig. 4A**). Micelles had a relatively high VCM encapsulation efficiency of about 78.79±3.26 %. The high entrapment could be a result of two mechanisms of entrapment involved. Firstly, surface groups form electrostatic interactions with the drug through ion pairing, entrapping the drug on the surface of micelles. Secondly, the drug is entrapped within the hydrophobic core matrix of micelles. The high entrapment can help maintain required the concentration whilst reducing the frequency of administration, thus reducing the risk of toxic side-effects. The high entrapment was comparable with other previously reported self-assembly nanosystems showing high entrapment of VCM [35, 38, 46]

Table 1: Size, PDI, ZP, EE % and DL % characterization of VCM-OLA-SPDA-micelles at pH 7.4 and 6.0.

pH	Size	PDI	Zeta	%EE	%DL
7.4	84.16±0.184	0.199±0.011	-42.6±1.98	78.80±3.26	0.392±0.015
6.0	141.1±0.0707	0.278±0.116	-50.4±0.990		
4.5	142.7±3.938	0.179±0.018	-57.8±0.070		

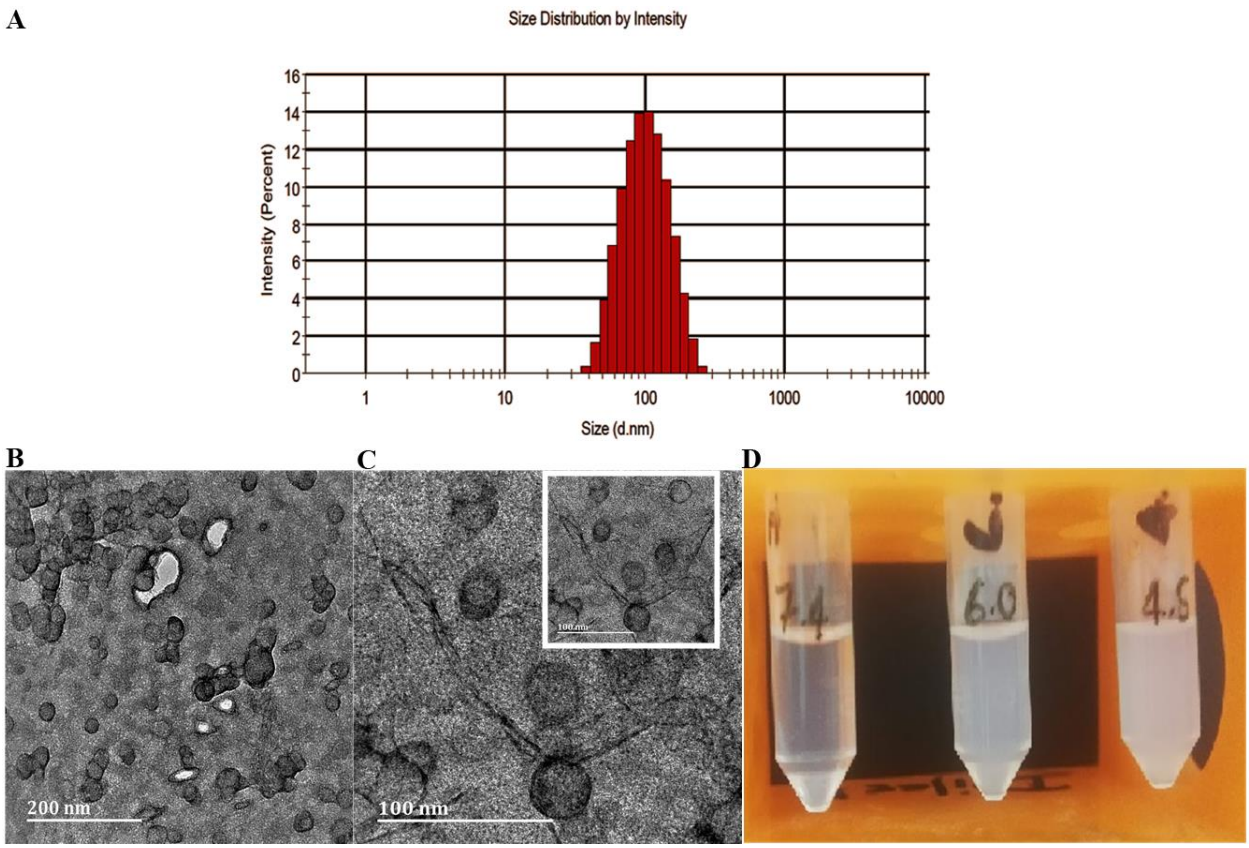

Fig. 4: A: Histogram showing size distribution by intensity; **B** and **C:** TEM images displaying morphology of OLA-SPDA-Micelles; and **D**: Visual assessment of pH-responsiveness in different PBS.

3.11.5 Thermal analysis of VCM-OLA-SPDA-micelles

The DSC is a thermoanalytical technique which can be used to predict drug encapsulation and also the possible interaction between nanocarrier excipients and the drug and it is measured as a function of temperature [47]. If thermal changes are observed, especially for the physical mixture, this would indicate that there is chemical interaction between the drug and the other excipient of the formulation. The thermal behavior of VCM, OLA-SPDA, lyophilized VCM-OLA-SPDA-micelle and the physical mixture of VCM and OLA-SPDA was investigated and compared (**Fig. 5A-D**). As shown in **Figure 5**, below, the thermal peak for VCM was observed at 125.39 ºC, whilst for OLA-SPDA a peak at 113.09 ºC was observed. The physical mixture (OLA-SPDA and VCM) showed almost similar thermal behavior to that observed from their individual thermal profiles, with a slight shift observed at 110.44 and 123.35 ºC, respectively. The minimal change in the thermal behavior of both the drug and the excipients is an indication of no chemical interaction between the drug and the amphiphile, and an indication of no chemical or structural changes in either the drug or the amphiphile. The lyophilised VCM-OLA-SPDA-micelles showed a single peak at 100.83 ºC belonging to OLA-SPDA, and the disappearance the VCM peak can be associated with phase

transition of the drug amphiphile system which can also indicate the encapsulation of VCM within the OLA-SPDA matrix [48].

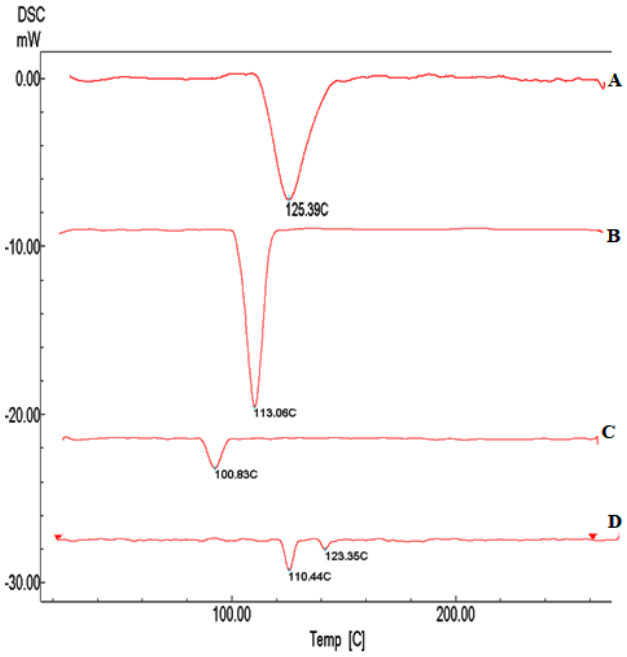

Fig. 5: DSC thermogram of **A**) Bare VCM; **B**) OLA-SPDA; **C**) Lyophilised VCM-OLA-SPDA-micelles; and **D**) Physical mixture of bare VCM and OLA-SPDA

3.11.6 *In vitro* release of optimal VCM-OLA-SPDA-micelles and bare VCM

The *in vitro* VCM release profiles for bare VCM solution and VCM-loaded OLA-micelles were evaluated at physiological conditions (pH 7.4) and at the acidic environment (pH 6.0 bacterial infection site) over a period of 24 h. Also, the VCM release behavior of micelles was compared across both pH conditions to evaluate its pH-responsiveness over 24 h. As shown in **Figure 6A**, below, the percentage cumulative VCM release at pH 7.4 for bare VCM solution was almost 100% at 8 h; whilst the VCM release from VCM-OLA-SPDA-micelles was slow and prolonged, with a cumulative release of about 48% after the same time interval as Bare VCM release profile, demonstrating a sustained release profile. Even though a rapid release from the micelles was observed within the first 8 h, micelles showed a sustained release profile after this time with a cumulative release of about 60% after 48 h when compared to the drug release profile of Bare VCM at pH 7.4. The initial fast release can be explained via the mechanisms of release involved. The VCM which is weakly bound (adsorbed) onto micelles' surface could contribute towards the initial rapid release via dissociation, followed by much slower release of VCM encapsulated within micelle core which is governed by diffusion and other releases mechanism[49]. Additionally, systems made from biomaterials with a high number of surface groups have been reported to have a high entrapment efficiency that is due to the

combined effects of two entrapment mechanisms. The first entrapment mechanism involves surface groups that forms electrostatic interactions with the drug through ion pairing, entrapping the drug on the surface of micelles. The second mechanism involves the drug being entrapped within the hydrophobic core matrix via self-assembly method. Surface group electrostatic entrapment easily dissociates which results in an early quick release and this leads to the first phase of the release profile[50, 51]. Entrapment of the drug within the hydrophobic core matrix is diffusion dependent that needs the drug to partition out of the lipid core matrix, among many other proposed mechanisms which leads to the slower release[53, 54]. The latter encapsulation mechanism forms the second phase of the release profile[52]. There are reports of these kinds of systems with biphasic release profiles that show fast initial release and then a slower release of the loaded drug in the second phase from hours to several days[55-58]. Moreover, the slower release pattern observed at physiological pH suggests that micelles maintain their shape tightly and compactly to reduce the premature release of VCM at an unexpected location, thus reducing the development of toxic side-effects and promoting a possible accumulation of a sufficient amount of the drug at the required site. The slower and prolonged release profile can be helpful for prolonged and sustained antibacterial therapeutic effect. Therefore, our formulation showed superiority over bare VCM solution with a sustained release profile.

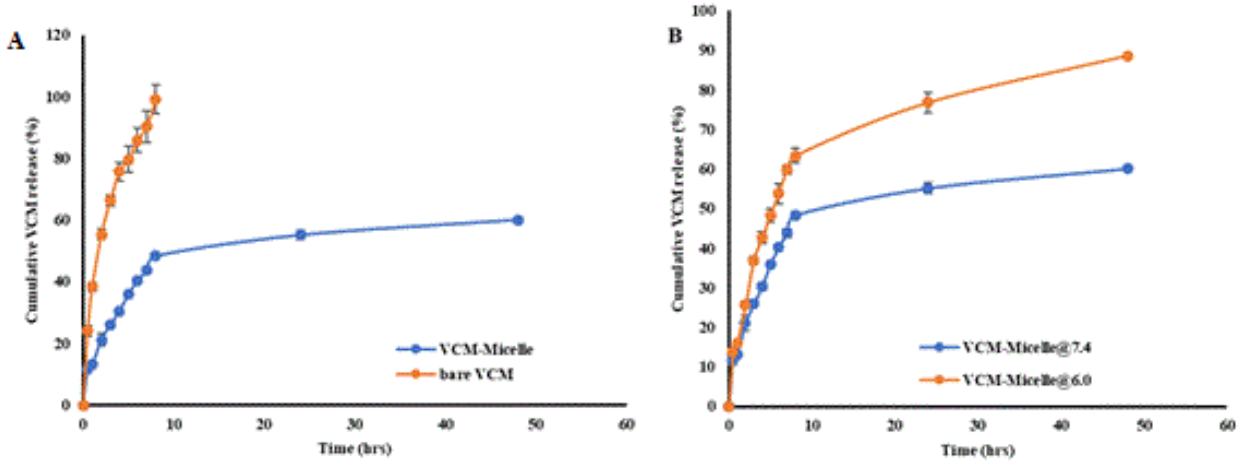

Fig. 6: *In vitro* drug profiles: **A**) between bare VCM and VCM-OLA-SPDA-micelles; and **B**) VCM-OLA-SPDA-micelles at both pH 7.4 and 6.0

Even though the VCM release profile for OLA-SPDA-micelle formulation at both pH 7.4 and 6.0 was slightly similar up to the 5th hour, (**Fig. 6B**), it was observed that the VCM released was pH- and time-dependent with a faster release at pH 6 than at pH 7.4 up to 48 h. As mentioned above, the reduced pH slightly accelerated the release, with more than 88% VCM released at pH 6.0 and only 60% at pH 7.4 after 48 h. The faster release can be attributed to protonation of the tertiary amine of the OLA-SPDA contributing

to both rearranging and swelling, or dissembling, of the micelles, thereby increasing the amount of VCM leaking out of the micellar system due to the large pores created. A similar trend was observed in our previously published work, where we formulated pH-responsive liposome for the targeted delivery of VCM [59]. This suggested that the pH-triggered release can protect and avoid loss of the drug at physiologic pH, whilst improving targeted release, and enhancing drug localisation and bioavailability at the acidic site of infection, which can improve its antibacterial activity.

3.12 *In vitro* antibacterial studies

3.12.1 *In vitro* antibacterial activity

The experiments were conducted to evaluate the efficacy of VCM encapsulated into micelle, in comparison with bare VCM solution; and also, to compare the effectiveness of VCM-OLA-SPDA-micelles against *S.aureus* and MRSA under different pH conditions. Using the broth dilution method, the minimum inhibitory concentration (MIC) for bare VCM, VCM-loaded micelles and the blank-micelles against *S. aureus* and MRSA at pH 7.4 and 6.0 were investigated. As shown in **Table 2**, the MIC values for bare VCM were 3.9 µg/ml and 7.8 µg/ml against *S. aureus* and MRSA under both pH conditions, respectively; whereas VCM-loaded micelles had MIC values of 1.95 µg/ml against *S. aureus* at both pH conditions and 3.9 µg/ml and 0.98 µg/ml against MRSA at pH 7.4 and pH 6.0, respectively. The enhanced activity that was observed over a prolonged time (72 h) for VCM-loaded micelles, whilst the bare drug lost activity after 24 h, could be attributed to the encapsulation of VCM into pH-responsive micelles, providing protection against any form of degradation and reducing the loss of VCM before reaching the site of infection through targeted delivery, thus extending its half-life and restoring its effectiveness against bacterial infection. The nano-sized formulation and lipidic nature of the OLA-SPDA can facilitate long circulation, and enhance cell penetration and cellular uptake by the bacterial cell, thus increasing the bioavailability and interaction of the drug with the bacterial cell for effective bacterial eradication

The antibacterial effect of bare VCM against *S. aureus* and MRSA at both pH conditions was reduced to no activity after the first 24 h, whilst the VCM-loaded micelles demonstrated superior and prolonged activity over a period of 72 h. VCM-loaded micelles enhanced the activity of VCM by 2-fold, against *S. aureus* at both pHs, and against MRSA by a magnitude of 2 and 8-folds when compared to bare VCM at pHs 7.4 and 6.0, respectively. The enhanced and prolonged activity demonstrated by the formulation over bare VCM can be closely correlated to the sustained and prolonged release profile of the formulation over bare VCM. A sustained and prolonged release profile can help to maintain the VCM concentration at a lethal dose at the target site, whilst the bare drug is prone to loss of activity through chemical or enzymatic degradation or through affinity trapping, preventing VCM from crossing the cytoplasmic membrane of MRSA. Also, the loss of VCM activity against MRSA can be correlated to cell-wall thickening from a high

amount of murein monomer produced with a high affinity to VCM, preventing it from penetrating through the bacterial cell. These limitations associated with the bare drug can be addressed by using VCM-loaded micelles with targeting properties. The lipids in formulations are known to facilitate the fusion of formulations with the bacterial cell, thus enhancing the amount of the drug at the target site for a prolonged time, and thus reducing time-dose dependent therapies whilst maintaining the therapeutic effect.

The MIC values for VCM-OLA-SPDA-micelles were compared under different pH conditions to evaluate it pH-responsiveness. The MIC values against *S. aureus* remained at 1.95 µg/ml for both pH conditions, whilst against MRSA, the MICs were 4-folds better at pH 6.0 than at pH 7.4. The enhanced activity at 6.0 can be associated with the fast and prolonged release profile, ensuring that a sufficient amount of the drug is released at the target site in response to reduced pH. This suggests that encapsulation does not only restore the effectiveness of the antibiotic, but the use of the stimuli-responsive delivery system can also elevate its antibiotic effect through triggered release at the required zone. Therefore, this confirms the superior antibacterial activity of VCM-OLA-SPDA-micelles over bare VCM at acidic pH.

Table 2: *In vitro* antibacterial activity of the formulations at pH 7.4 and pH 6.

***In vitro* antibacterial activity at pH 7.4**						
Time (h)	**24**	**48**	**72**	**24**	**48**	**72**
	SA (MIC µg/ml)			**MRSA (MIC µg/ml)**		
Bare VCM	3.9	NA	NA	7.8	NA	NA
VCM-OLA-SPDA -Micelle	1.95	1.95	7.81	3.9	3.9	7.81
Blank- OLA-SPDA-Micelle	NA	NA	NA	NA	NA	NA
***In vitro* antibacterial activity at pH 6**						
Time (h)	**24**	**48**	**72**	**24**	**48**	**72**
	SA (MIC µg/ml)			**MRSA (MIC µg/ml)**		
Bare VCM	3.9	NA	NA	7.8	NA	NA
VCM-OLA-SPDA -Micelle	1.95	1.95	3.9	0.98	0.98	1.95
Blank-OLA-SPDA-Micelle	NA	NA	NA	NA	NA	NA

NA = No activity. The values are expressed as mean ± SD (n = 3).

3.12.2 Bacterial cell viability

The quantitative cell viability analysis was done using the flow cytometry method. Specialised fluorescence dyes, propidium iodide (PI) and SYTO9, were used to differentiate dead cells from live cells after treatment. As shown in **Figure 7**, red and green represent live and dead cells after treatment, respectively. PI can passively transverse into a dead cell and bind to the DNA due to loss of plasma membrane integrity, irrespective of the mechanism of death; whilst SYTO9 can penetrate both alive and dead cell populations [60]. The PI uptake corresponds to the number of dead cells, as represented in a histogram plot of cell count (*y-axis*) vs PI fluorescence (*x-axis*) (**Fig. 7A-D**). The VCM inhibition mechanism against MRSA involves disruption of the bacterial cell synthesis, therefore PI uptake is expected after treating bacteria with VCM and the fluorescence intensity/count corresponds to the number of dead cells. The MRSA cells were treated with bare VCM and with VCM-OLA-SPDA-micelles. A fluorescence shift was observed, and gates were set to differentiate the viable cells from non-viable cells in the MRSA population. As shown in **Figure 7**, the fluorescence shift of PI after treating bacterial cells with bare VCM and VCM-OLA-SPDA-micelles at their respective MICs (7.8 μg/ml and 0.98 μg/ml, respectively) was observed. As shown in **Figure 7**, **A** represents MRSA cells without treatment; **B** shows VCM-treated MRSA with a 91.01% killing; **C** shows VCM-OLA-SPDA-micelles treated MRSA with a 93.39% killing at their respective MICs. For comparison purposes, VCM treatment was done at the formulation MIC (0.98 μg/ml), which gave a killing percentage of only 54.21% (**7D**). A similar cell-viability pattern was observed from the dot plot of PI vs SYTO9 (**Fig. 7F** to **G**). These results indicate that the formulation has a higher killing percentage at low concentrations when compared to bare VCM, which shows a similar killing percentage at a higher concentration (7.8 μg/ml). This suggests that encapsulation maintains the same therapeutic effect exhibited by bare VCM, but at a low concentration. This holds potential for becoming an alternative mode of a treatment since it may

reduce issues related to toxic side-effects due to high doses administered to achieve therapeutic effects.

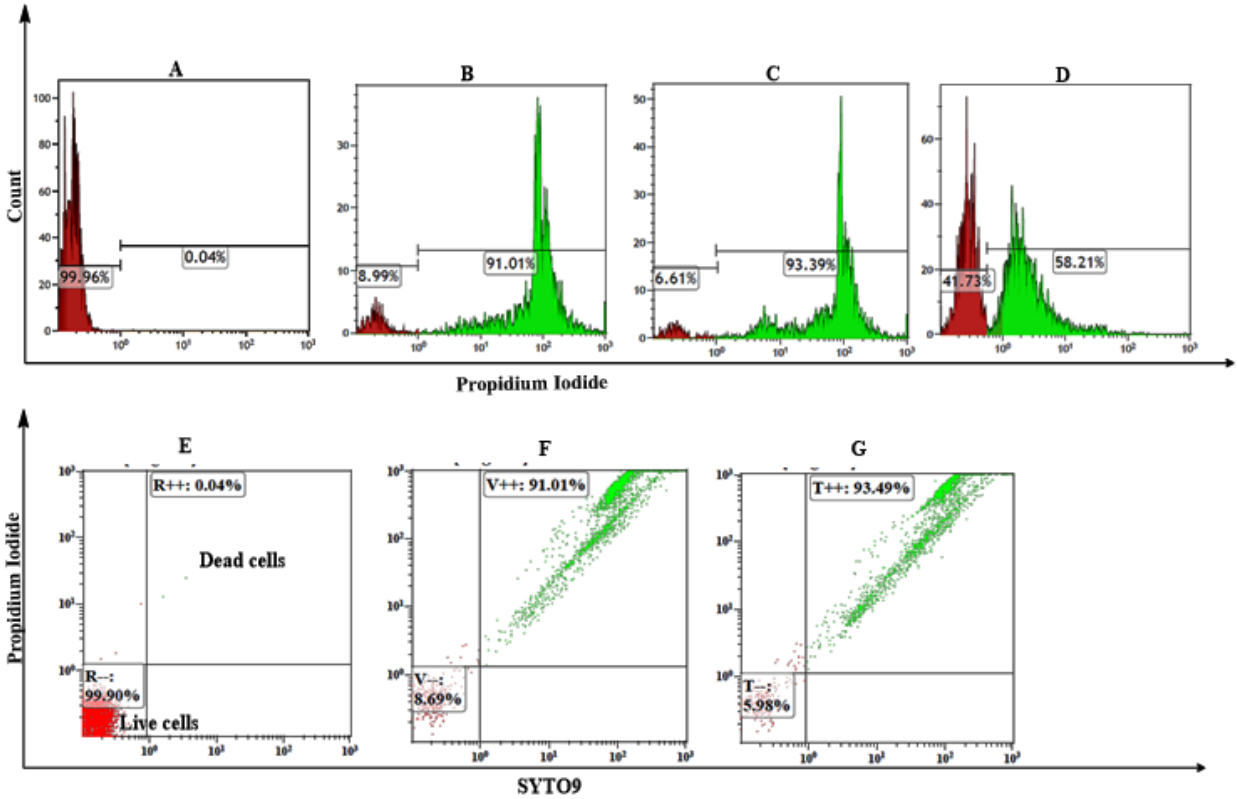

Fig. 7: Histogram plot from the flow cytometry analysis: **A**) untreated MRSA cells; **B**) MRSA cells treated with bare VCM at 7.81 µg/ml; **C)** and **D**) MRSA cells treated with VCM-OLA-SPDA-micelles and bare VCM at 0.98 µg/ml; scatter plot of **E**), untreated MRSA cells; **F**) MRSA cells treated with bare VCM at 7.81 µg/ml; and **G**) VCM-OLA-SPDA-micelles at 0.98 µg/ml showing a shift in SYTO9 and PI fluorescence after treatment.

3.12.3 *In vivo* antibacterial activity

Staphylococcus aureus and its resistant strain (MRSA) account for the majority of skin infections. A mice skin infection model study is a widely used preclinical model mimicking the infections observed in humans to assess the efficacy of any form of antimicrobial therapies against such pathogens [61]. The BALB/c mice skin infection models were used for this study to further assess the efficacy of VCM-OLA-SPDA-micelles against MRSA in comparison with bare VCM. A short-term localisation of bacteria (MRSA) was performed via intradermal injection and the CFU counts were quantified for treated and untreated groups. There was a significant reduction in the bacterial count of the skin samples treated with both VCM-OLA-SPDA-micelles and VCM when compared to the untreated group.

Application of the one-way ANOVA test showed a statistically significant ($p < 0.0001$) reduction in the bacterial (MRSA) load recovered from the group treated with bare VCM and VCM-OLA-SPDA-micelles when compared to the untreated group. The mean bacterial counts ($\log_{10}$ CFU) recovered from the mice skin treated with VCM and VCM-OLA-SPDA-micelles were 3.40 ± 0.053(2533 CFU/ml) and 2.50 ± 0.17(300 CFU/ml), which were 133 ($p = 0.0002$) and 1126 ($p < 0.0001$) times better than the untreated group, respectively. Furthermore, the bacterial count from the sample treated with VCM-micelles showed a significant 8-fold reduction ($p < 0.0001$) when compared to skin samples treated with bare VCM (**Fig. 8**).

VCM-OLA-SPDA-micelles demonstrated a high bacterial load reduction from the skin samples when compared to other groups. These results are in line with results discussed in previous sections (**2.5.1** and **2.5.2**) demonstrating the superiority of VCM-micelles in enhancing the efficacy of VCM. The enhanced activity can be associated with the nano-size range of the formulation which allows for better penetration and enhanced cellular uptake and longer circulation within the system when compared to big molecules such as VCM. The targeting, pH triggered, and sustained release profile helps in maintaining high VCM doses at the site of infection over a prolonged time. Therefore, pH-responsive VCM-micelles could potentially, be an alternative therapy for VCM and other antibiotics in the fight against antibiotic-resistant MRSA.

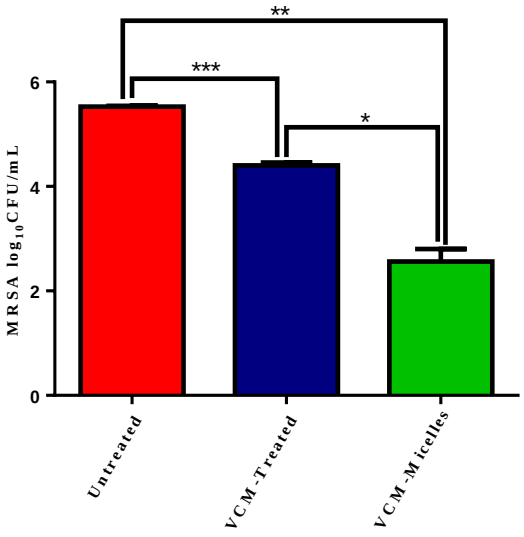

Fig. 8: MRSA count after 48 h of treatment. Data represent the mean ± SD (n = 3). *denotes statistical significance for VCM-OLA-SPDA-micelles versus the bare VCM. **denotes significant difference between untreated versus VCM-OLA-SPDA-micelles. ***denotes the significant difference between the untreated and bare VCM.

3.12.4 Stability During Storage

A short-term physical stability study of OLA-SPDA-micelle samples stored under different conditions (room temperature and at 4ºC) for three months was evaluated using DLS. The physical appearance, particle size, PDI and zeta potential were measured at predetermined times (0, 30, 60 and 90 days). The results showed that samples stored at 4ºC were more stable over a period of three months (**Table 3**). There was insignificant change ($p > 0.05$) in particle size for the sample stored at 4 ºC between day 0 (75.54±0.566 nm) and day 90 (81.6±0.95); whereas for samples stored at room temperature, size changed significantly ($p < 0.05$) from 75.54±0.566 nm to 143.9±0.35 between day 0 and day 90. Additionally, the samples stored at both temperatures showed no sign of deterioration, with no colour change observed or precipitation occurring. This suggests that the OLA-SPDA-micelle, in aqueous solution and stored 4 ºC, was stable over a period of three months, whereas samples kept at room temperature showed a moderate change in size after the first month. This suggests that 4 ºC is preferable for storage for our system.

Table 3. Stability studies of OLA-SPDA-micelle formulation

Storage condition	**RT**			**4 °C**		
Days	**Size (nm)**	**PDI**	**ZP (mV)**	**Size (nm)**	**PDI**	**ZP (mV)**
0	75.54±0.566	0.239±0.003	-53.5±2.19	75.54±0.566	0.239±0.003	-53.5±2.19
30	119.3±0.964	0.271±0.002	-80.3±0.424	75.6±0.848	0.312±0.010	-80.3±0.141
60	121.3±2.317	0.264±0.009	-82.2±1.82	80.9±2.33	0.340±0.057	-80.8±0.53
90	143.9±0.35	0.207±0.007	-71.1±0.07	81.6±0.95	0.296±0.007	-64.0±1.15

3.13 Conclusion

The challenges associated with conventional antibiotic dosage forms that lead to the development of bacterial resistance requires an alternative delivery system and biocompatible materials to improve the efficacy of existing antibiotics. To address these problems, in this study, pH-responsive VCM-OLA-SPDA-micelles was successfully formulated from OLA-SPDA which self-assembles into stable micelles for targeted delivery of VCM against MRSA infections. The pH-responsiveness of micelles was demonstrated by the change in size and PDI with respect to change in pH from 7.4 to 6.0. The formulation displayed an encapsulation efficiency above 70% for VCM. The system also showed a sustained and prolonged VCM release profile which correlated to its prolonged *in vitro* antibacterial effect when compared to bare VCM. The cell viability and *in vivo* studies also confirmed the superiority of the formulation, showing a significant bacterial cell (MRSA) count reduction after treatment, when compared to bare VCM. The prolonged and enhanced antimicrobial activity can help reduce the frequency of administration of the antibiotic and can thus prevent the possible development of drug resistance. Therefore, this material demonstrates a possible

alternative for the delivery of other antibiotics to improve their effectiveness against bacterial infections characterized by low pH.

Conflict of interest

The authors declare that there is no conflict of interest.

Acknowledgement

The authors acknowledge the University of KwaZulu-Natal (UKZN), UKZN Nanotechnology Platform and the National Research Foundation (NRF) of South Africa for financial support (Grant No. 87790 and 88453). We also thank Biomedical Resource Unit (BRU), Microscopy and Microanalysis Unit (MMU), Flow Cytometry Research Laboratory and Department of Human Physiology at UKZN for technical assistance.

3.14 References

1. Choo, E. J.; Chambers, H. F., Treatment of methicillin-resistant Staphylococcus aureus bacteremia. Infection & chemotherapy. 2016, 48 (4), 267-273.

2. Culos, K. A.; Cannon, J. P.; Grim, S. A., Alternative agents to vancomycin for the treatment of methicillin-resistant Staphylococcus aureus infections. American Journal of therapeutics. 2013, 20 (2), 200-212.

3. Rose, W. E.; Fallon, M.; Moran, J. J.; Vanderloo, J. P., Vancomycin tolerance in methicillin-resistant Staphylococcus aureus: influence of vancomycin, daptomycin, and telavancin on differential resistance gene expression. Antimicrobial Agents and Chemotherapy. 2012, 56 (8), 4422-4427.

4. Singh, S.; Hussain, A.; Shakeel, F.; Ahsan, M. J.; Alshehri, S.; Webster, T. J.; Lal, U. R., Recent insights on nanomedicine for augmented infection control. International Journal of Nanomedicine. 2019, 14, 2301-2325.

5. Kalhapure, R. S.; Suleman, N.; Mocktar, C.; Seedat, N.; Govender, T., Nanoengineered drug delivery systems for enhancing antibiotic therapy. Journal of Pharmaceutical Sciences. 2015, 104 (3), 872-905.

6. Begg, E. J.; Barclay, M. L.; Kirkpatrick, C. J., The therapeutic monitoring of antimicrobial agents. British journal of clinical pharmacology. 1999, 47 (1), 23-30.

7. Anselmo, A. C.; Mitragotri, S., Nanoparticles in the clinic. Bioengineering & translational medicine. 2016, 1 (1), 10-29.

8. Sharma, A.; Kumar Arya, D.; Dua, M.; Chhatwal, G. S.; Johri, A. K., Nano-technology for targeted drug delivery to combat antibiotic resistance. Expert Opinion on Drug Delivery. 2012, 9 (11), 1325-1332.

9. Goyal, A. K.; Rath, G.; Faujdar, C.; Malik, B., Application and Perspective of pH-Responsive Nano Drug Delivery Systems. In Applications of Targeted Nano Drugs and Delivery Systems, Elsevier. 2019, 15-33.

10. Canaparo, R.; Foglietta, F.; Giuntini, F.; Della Pepa, C.; Dosio, F.; Serpe, L., Recent Developments in Antibacterial Therapy: Focus on Stimuli-Responsive Drug-Delivery Systems and Therapeutic Nanoparticles. Molecules. 2019, 24 (10), 1991.

11. Zhou, Q.; Zhang, L.; Yang, T.; Wu, H., Stimuli-responsive polymeric micelles for drug delivery and cancer therapy. International journal of nanomedicine. 2018, 13 (2018), 2921.

12. Stubbings, W.; Leow, P.; Yong, G. C.; Goh, F.; Körber-Irrgang, B.; Kresken, M.; Endermann, R.; Labischinski, H., In vitro spectrum of activity of finafloxacin, a novel, pH-activated fluoroquinolone, under standard and acidic conditions. Antimicrobial Agents and Chemotherapy. 2011, 55 (9), 4394-4397.

13. Lemaire, S.; Tulkens, P. M.; Van Bambeke, F., Contrasting effects of acidic pH on the extracellular and intracellular activities of the anti-gram-positive fluoroquinolones moxifloxacin and delafloxacin against Staphylococcus aureus. Antimicrobial Agents and Chemotherapy. 2011, 55 (2), 649-658.

14. Liao, Z.-S.; Huang, S.-Y.; Huang, J.-J.; Chen, J.-K.; Lee, A.-W.; Lai, J.-Y.; Lee, D.-J.; Cheng, C.-C., Self-Assembled pH-Responsive Polymeric Micelles for Highly Efficient, Noncytotoxic Delivery of Doxorubicin Chemotherapy To Inhibit Macrophage Activation: In Vitro Investigation. Biomacromolecules. 2018, 19 (7), 2772-2781.

15. Lemaire, S.; Van Bambeke, F.; Mingeot-Leclercq, M.-P.; Glupczynski, Y.; Tulkens, P. M., Role of acidic pH in the susceptibility of intraphagocytic methicillin-resistant Staphylococcus aureus strains to meropenem and cloxacillin. Antimicrobial Agents and Chemotherapy. 2007, 51 (5), 1627-1632.

16. Le Garrec, D.; Ranger, M.; Leroux, J.-C., Micelles in anticancer drug delivery. American Journal of Drug Delivery. 2004, 2 (1), 15-42.

17. Feng, S., Studies on drug solubilization mechanism in simple micelle systems. 2009.

18. Krämer, M.; Stumbé, J. F.; Türk, H.; Krause, S.; Komp, A.; Delineau, L.; Prokhorova, S.; Kautz, H.; Haag, R., pH-responsive molecular nanocarriers based on dendritic core-shell architectures. Angewandte Chemie International Edition. 2002, 41 (22), 4252-4256.

19. Ahmad, Z.; Shah, A.; Siddiq, M.; Kraatz, H.-B., Polymeric micelles as drug delivery vehicles. Royal Society of Chemistry Advances. 2014, 4 (33), 17028-17038.

20. Lu, Y.; Park, K., Polymeric micelles and alternative nanonized delivery vehicles for poorly soluble drugs. International Journal of Pharmaceutics. 2013, 453 (1), 198-214.

21. Thota, B. N.; Urner, L. H.; Haag, R., Supramolecular architectures of dendritic amphiphiles in water. Chemical reviews. 2015, 116 (4), 2079-2102.

22. Stylianopoulos, T., EPR-effect: utilizing size-dependent nanoparticle delivery to solid tumors. Therapeutic delivery. 2013, 4 (4), 421-423.

23. Nair, H. A.; Singh Rajawat, G.; Nagarsenker, M. S., Chapter 8 - Stimuli-responsive micelles: A nanoplatform for therapeutic and diagnostic applications. In Drug Targeting and Stimuli Sensitive Drug Delivery Systems, William Andrew Publishing. 2018, 303-342.

24. Kalhapure, R. S.; Akamanchi, K. G., A novel biocompatible bicephalous dianionic surfactant from oleic acid for solid lipid nanoparticles. Colloids Surface B Biointerfaces. 2013, 105 (2013), 215-22.

25. Branco, M. C.; Schneider, J. P., Self-assembling materials for therapeutic delivery. Acta Biomaterialia. 2009, 5 (3), 817-831.

26. Trappmann, B.; Ludwig, K.; Radowski, M. R.; Shukla, A.; Mohr, A.; Rehage, H.; Böttcher, C.; Haag, R., A new family of nonionic dendritic amphiphiles displaying unexpected packing parameters in micellar assemblies. Journal of the American Chemical Society. 2010, 132 (32), 11119-11124.

27. Berlepsch, H. v.; Thota, B.; Wyszogrodzka, M.; de Carlo, S.; Haag, R.; Böttcher, C., Controlled self-assembly of stomatosomes by use of single-component fluorinated dendritic amphiphiles. Soft matter. 2018, 14 (25), 5256-5269.

28. Makhathini, S. S.; Kalhapure, R. S.; Jadhav, M.; Waddad, A. Y.; Gannimani, R.; Omolo, C. A.; Rambharose, S.; Mocktar, C.; Govender, T., Novel two-chain fatty acid-based lipids for development of vancomycin pH-responsive liposomes against Staphylococcus aureus and methicillin-resistant Staphylococcus aureus (MRSA). Journal of drug targeting. 2019, 27 (10), 1094-1107

29. Mhule, D.; Kalhapure, R. S.; Jadhav, M.; Omolo, C. A.; Rambharose, S.; Mocktar, C.; Singh, S.; Waddad, A. Y.; Ndesendo, V. M.; Govender, T., Synthesis of an oleic acid based pH-responsive lipid and its application in nanodelivery of vancomycin. International journal of pharmaceutics. 2018, 550 (1-2), 149-159.

30. Osman, N.; Omolo, C. A.; Gannimani, R.; Waddad, A. Y.; Rambharose, S.; Mocktar, C.; Singh, S.; Parboosing, R.; Govender, T., Novel fatty acid-based pH-responsive nanostructured lipid carriers for enhancing antibacterial delivery. Journal of Drug Delivery Science and Technology. 2019, 101125.

31. Riss, T. L.; Moravec, R. A.; Niles, A. L.; Duellman, S.; Benink, H. A.; Worzella, T. J.; Minor, L., Cell viability assays. In Assay Guidance Manual [Internet], Eli Lilly & Company and the National Center for Advancing Translational Sciences: 2016.

32. Aslantürk, Ö. S., In Vitro Cytotoxicity and Cell Viability Assays: Principles, Advantages, and Disadvantages. InTechopen: 2018; Vol. 2.

33. Omolo, C. A.; Kalhapure, R. S.; Jadhav, M.; Rambharose, S.; Mocktar, C.; Ndesendo, V. M.; Govender, T., Pegylated oleic acid: A promising amphiphilic polymer for nano-antibiotic delivery. European Journal of Pharmaceutics and Biopharmaceutics. 2017, 112, 96-108.

34. Chen, M.; Wei, J.; Xie, S.; Tao, X.; Zhang, Z.; Ran, P.; Li, X., Bacterial biofilm destruction by size/surface charge-adaptive micelles. Nanoscale. 2019, 11 (3), 1410-1422.

35. Omolo, C. A.; Kalhapure, R. S.; Jadhav, M.; Rambharose, S.; Mocktar, C.; Ndesendo, V. M.; Govender, T., Pegylated oleic acid: A promising amphiphilic polymer for nano-antibiotic delivery. European Journal of Pharmaceutics and Biopharmaceutics. 2017, 112 (2017), 96-108.

36. Montenegro, L.; Castelli, F.; Sarpietro, M., Differential scanning calorimetry analyses of idebenone-loaded solid lipid nanoparticles interactions with a model of bio-membrane: A comparison with in vitro skin permeation data. Pharmaceuticals. 2018, 11 (4), 138.

37. Cheng, X.; Yan, H.; Jia, X.; Zhang, Z., Preparation and in vivo/in vitro evaluation of formononetin phospholipid/vitamin E TPGS micelles. Journal of drug targeting. 2016, 24 (2), 161-168.

38. Walvekar, P.; Gannimani, R.; Rambharose, S.; Mocktar, C.; Govender, T., Fatty acid conjugated pyridinium cationic amphiphiles as antibacterial agents and self-assembling nano carriers. Chemistry and physics of lipids. 2018, 214 (2018), 1-10.

39. O'Brien-Simpson, N. M.; Pantarat, N.; Attard, T. J.; Walsh, K. A.; Reynolds, E. C., A rapid and quantitative flow cytometry method for the analysis of membrane disruptive antimicrobial activity. PloS one. 2016, 11 (3), e0151694.

40. Duarte, A. R. C.; Costa, M. S.; Simplício, A. L.; Cardoso, M. M.; Duarte, C. M., Preparation of controlled release microspheres using supercritical fluid technology for delivery of anti-inflammatory drugs. International Journal of Pharmaceutics. 2006, 308 (1-2), 168-174.

41. Huang, C.-M.; Chen, C.-H.; Pornpattananangkul, D.; Zhang, L.; Chan, M.; Hsieh, M.-F.; Zhang, L., Eradication of drug resistant Staphylococcus aureus by liposomal oleic acids. Biomaterials. 2011, 32 (1), 214-221.

42. Liu, Z.; Deng, X.; Wang, M.; Chen, J.; Zhang, A.; Gu, Z.; Zhao, C., BSA-modified polyethersulfone membrane: preparation, characterization and biocompatibility. Journal of Biomaterials Science, Polymer Edition. 2009, 20 (3), 377-397.

43. Neun, B. W.; Dobrovolskaia, M. A., Method for analysis of nanoparticle hemolytic properties in vitro. Methods in Molecular Biology. 2011, 697, 215-24.

44. Song, Z.; Zhu, W.; Liu, N.; Yang, F.; Feng, R., Linolenic acid-modified PEG-PCL micelles for curcumin delivery. International Journal of Pharmaceutics. 2014, 471 (1), 312-321.

45. Ree, B. J.; Satoh, Y.; Sik Jin, K.; Isono, T.; Jong Kim, W.; Kakuchi, T.; Satoh, T.; Ree, M., Well-defined and stable nanomicelles self-assembled from brush cyclic and tadpole copolymer amphiphiles: a versatile smart carrier platform. Nature Publishing Group Asia Materials. 2017, 9 (12), e453-e453.

46. Walvekar, P.; Gannimani, R.; Salih, M.; Makhathini, S.; Mocktar, C.; Govender, T., Self-assembled oleylamine grafted hyaluronic acid polymersomes for delivery of vancomycin against methicillin resistant Staphylococcus aureus (MRSA). Colloids and Surfaces B: Biointerfaces. 2019, 182 (2019), 110388.

47. Chiu, M. H.; Prenner, E. J., Differential scanning calorimetry: An invaluable tool for a detailed thermodynamic characterization of macromolecules and their interactions. Journal of Pharmacy and Bioallied Sciences. 2011, 3 (1), 39-59.

48. Pupe, C. G.; Villardi, M.; Rodrigues, C. R.; Rocha, H. V. A.; Maia, L. C.; de Sousa, V. P.; Cabral, L. M., Preparation and evaluation of antimicrobial activity of nanosystems for the control of oral pathogens Streptococcus mutans and Candida albicans. International journal of nanomedicine. 2011, 6, 2581-2590.

49. Zhu, D.; Wu, S.; Hu, C.; Chen, Z.; Wang, H.; Fan, F.; Qin, Y.; Wang, C.; Sun, H.; Leng, X., Folate-targeted polymersomes loaded with both paclitaxel and doxorubicin for the combination chemotherapy of hepatocellular carcinoma. Acta Biomaterialia. 2017, 58, 399-412.

50. D'Emanuele, A.; Attwood, D., Dendrimer–drug interactions. Advanced drug delivery reviews. 2005, 57 (15), 2147-2162.

51. Li, Y.-M.; Jiang, T.; Lv, Y.; Wu, Y.; He, F.; Zhuo, R.-X., Amphiphilic copolymers with pendent carboxyl groups for high-efficiency loading and controlled release of doxorubicin. Colloids and Surfaces B: Biointerfaces. 2015, 132, 54-61.

52. Khopade, A. J.; Caruso, F.; Tripathi, P.; Nagaich, S.; Jain, N. K., Effect of dendrimer on entrapment and release of bioactive from liposomes. International journal of pharmaceutics. 2002, 232 (1-2), 157-162.

53. Gibaldi, M.; Feldman, S., Establishment of sink conditions in dissolution rate determinations. Theoretical considerations and application to nondisintegrating dosage forms. Journal of pharmaceutical sciences. 1967, 56 (10), 1238-1242.

54. Wurster, D. E.; Polli, G. P., Investigation of drug release from solids IV. Influence of adsorption on the dissolution rate. Journal of pharmaceutical sciences. 1961, 50 (5), 403-406.

55. Li, B.; Brown, K. V.; Wenke, J. C.; Guelcher, S. A., Sustained release of vancomycin from polyurethane scaffolds inhibits infection of bone wounds in a rat femoral segmental defect model. Journal of Controlled Release. 2010, 145 (3), 221-230.

56. She, W.; Li, N.; Luo, K.; Guo, C.; Wang, G.; Geng, Y.; Gu, Z., Dendronized heparin−doxorubicin conjugate based nanoparticle as pH-responsive drug delivery system for cancer therapy. Biomaterials. 2013, 34 (9), 2252-2264.

57. Vivek, R.; Babu, V. N.; Thangam, R.; Subramanian, K.; Kannan, S., pH-responsive drug delivery of chitosan nanoparticles as Tamoxifen carriers for effective anti-tumor activity in breast cancer cells. Colloids and Surfaces B: Biointerfaces. 2013, 111, 117-123.

58. Ping, Y.; Guo, J.; Ejima, H.; Chen, X.; Richardson, J. J.; Sun, H.; Caruso, F., pH-Responsive Capsules Engineered from Metal–Phenolic Networks for Anticancer Drug Delivery. Small. 2015, 11 (17), 2032-2036.

59. Makhathini, S. S.; Kalhapure, R. S.; Jadhav, M.; Waddad, A. Y.; Gannimani, R.; Omolo, C. A.; Rambharose, S.; Mocktar, C.; Govender, T., Novel two-chain fatty acid-based lipids for development of vancomycin pH-responsive liposomes against Staphylococcus aureus and methicillin-resistant Staphylococcus aureus (MRSA). Journal of drug targeting. 2019, 27 (10), 1094-1107.

60. Stiefel, P.; Schmidt-Emrich, S.; Maniura-Weber, K.; Ren, Q., Critical aspects of using bacterial cell viability assays with the fluorophores SYTO9 and propidium iodide. BioMed Central microbiology. 2015, 15 (1), 36.

61. Siddiqui, A. H.; Koirala, J., Methicillin Resistant Staphylococcus Aureus (MRSA). In StatPearls, StatPearls Publishing: 2018.

Paper 2 Supporting Information

Paper tittle

pH-Responsive Micelles from an Oleic Acid Tail and Propionic Acid Heads Dendrons Amphiphile for the Delivery of Antibiotics

^{1}HNMR Tetra-tert-butyl3,3',3'',3'''- ((2-hydroxypropane-1,3-diyl)bis(azanetriyl)) tetra propionate

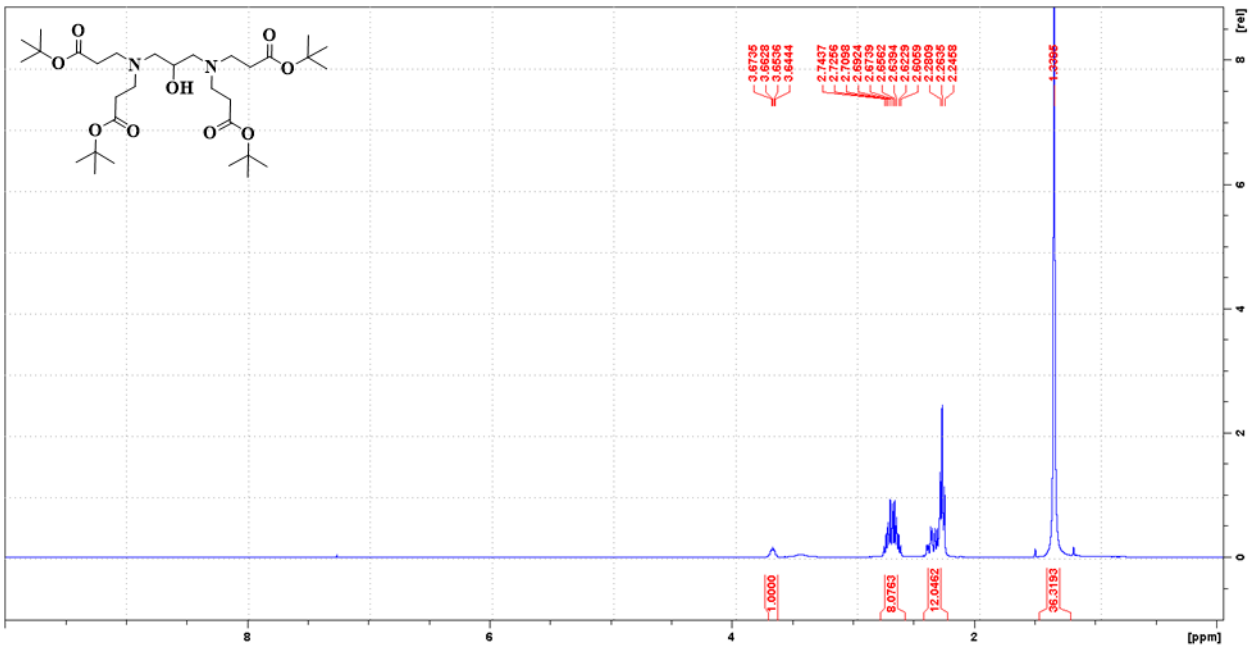

^{13}CNMR Tetra-tert-butyl3,3',3'',3'''- ((2-hydroxypropane-1,3-diyl)bis(azanetriyl)) tetrapropionate

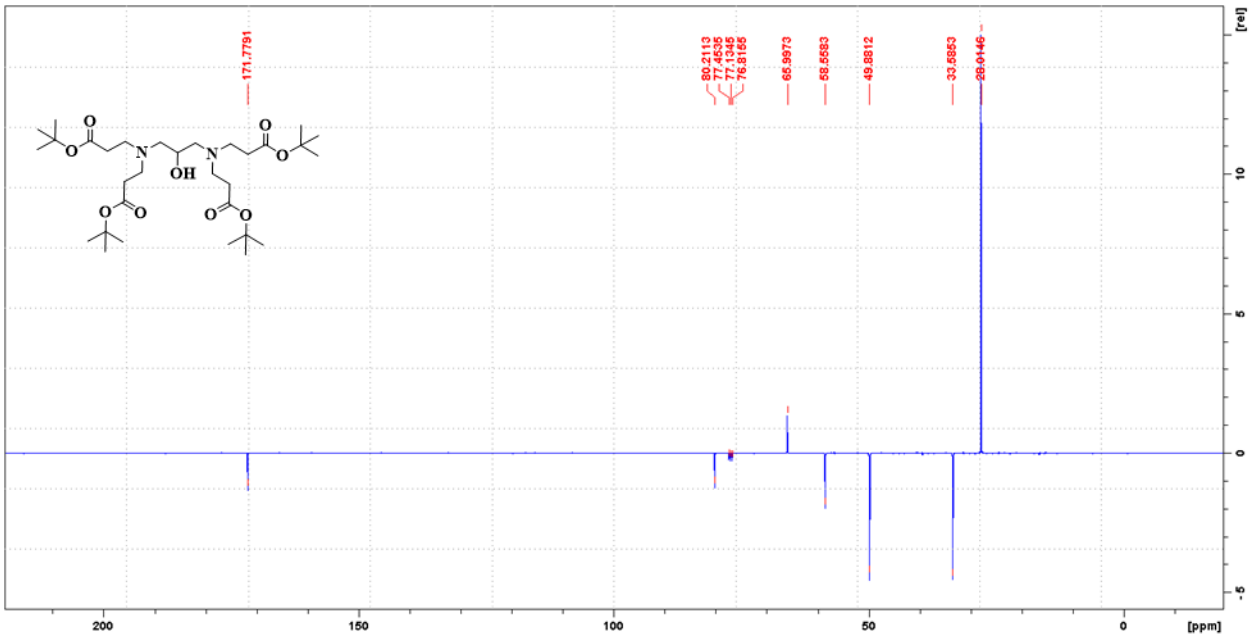

[1]HNM Tetra-tert-butyl 3,3',3'',3'''- ((2-(oleoyloxy) propane-1,3-diyl)bis(azanetriyl)) tetrapropionate

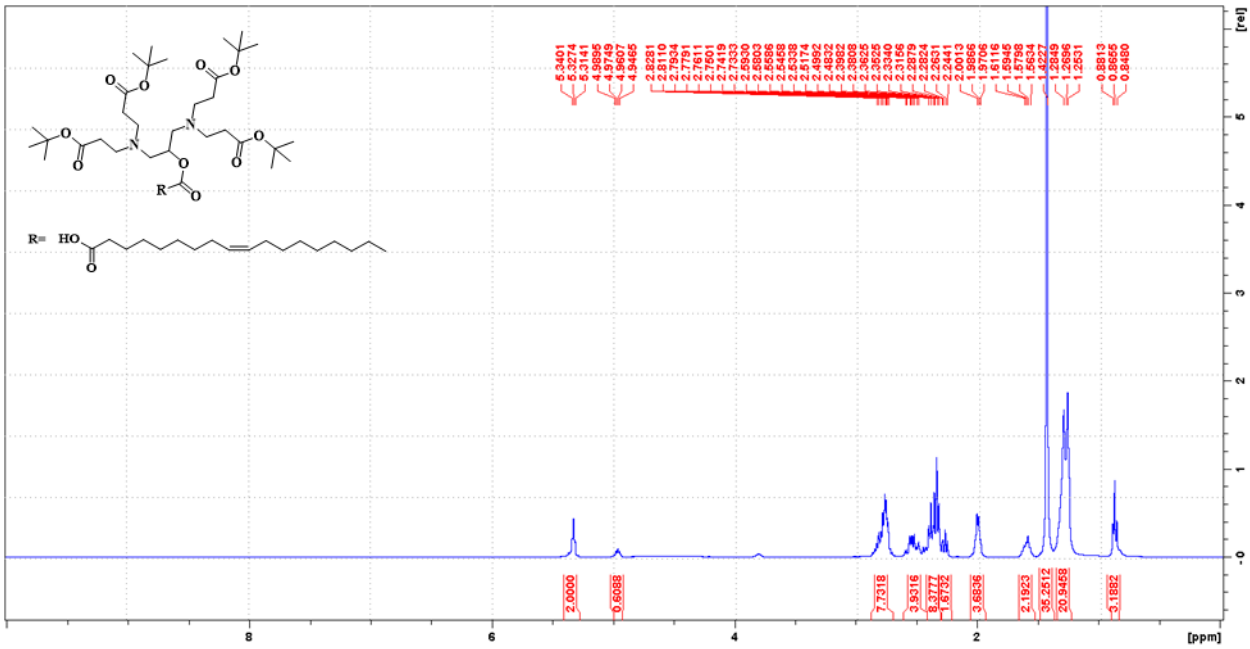

^{13}CNMR Tetra-tert-butyl 3,3',3'',3'''- ((2-(oleoyloxy) propane-1,3-diyl) bis (azanetriyl)) tetra propionate

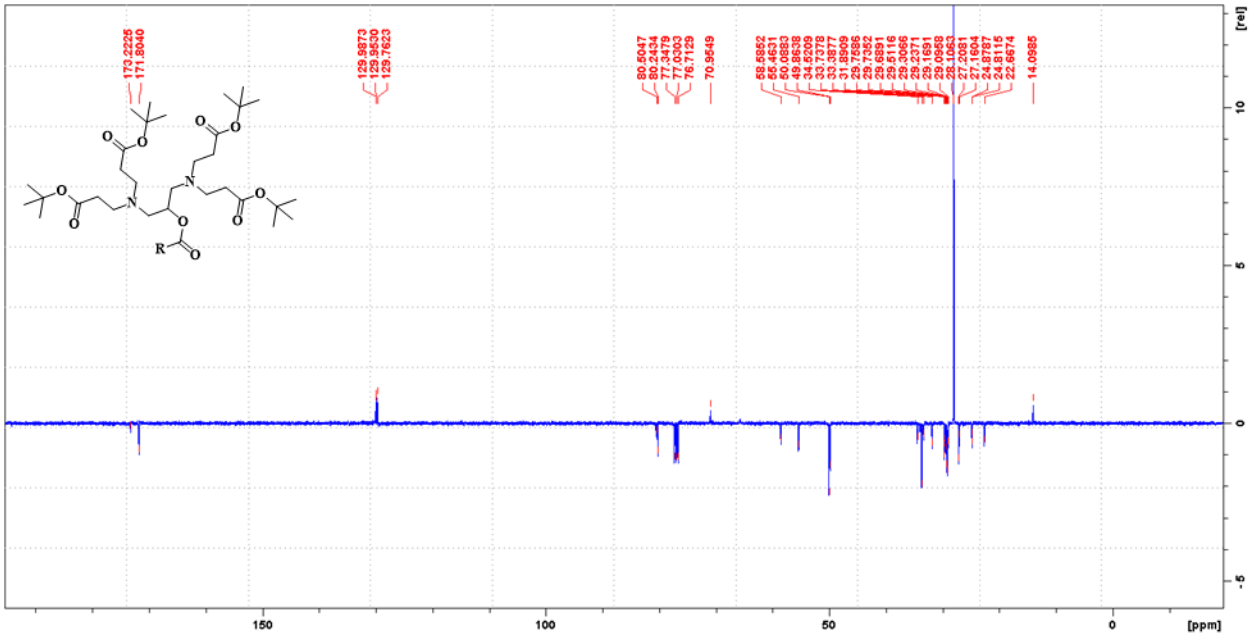

^{1}HNMR 3,3',3'',3'''-((2-(oleoyloxy)propane-1,3-diyl)bis(azanetriyl)) tetrapropionic acid

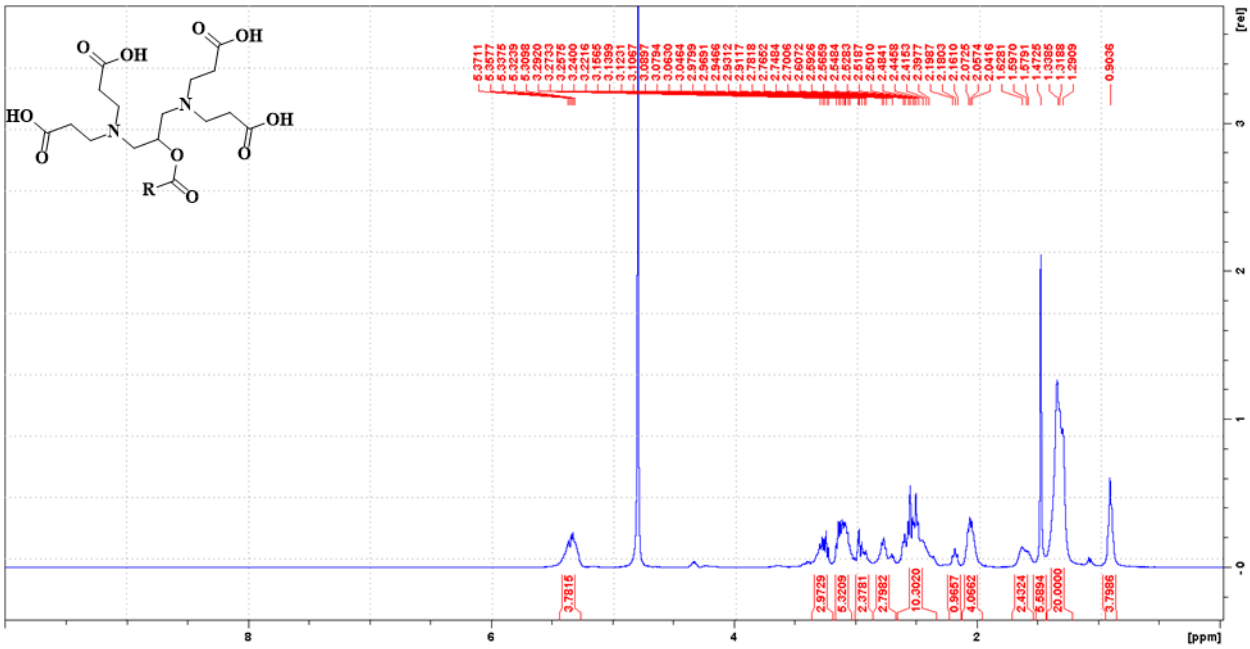

^{13}CNMR 3,3',3'',3'''-((2-(oleoyloxy)propane-1,3-diyl)bis(azanetriyl)) tetrapropionic acid

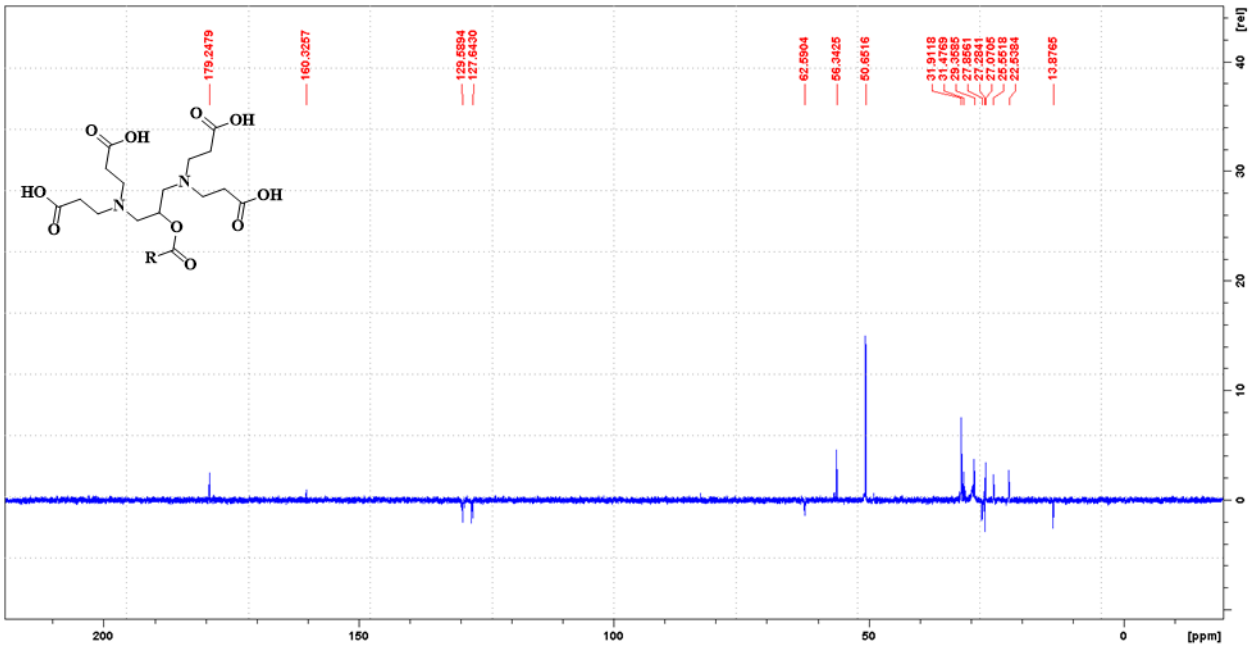

FTIR 3,3',3'',3'''-((2-(oleoyloxy)propane-1,3-diyl)bis(azanetriyl)) tetrapropionic acid

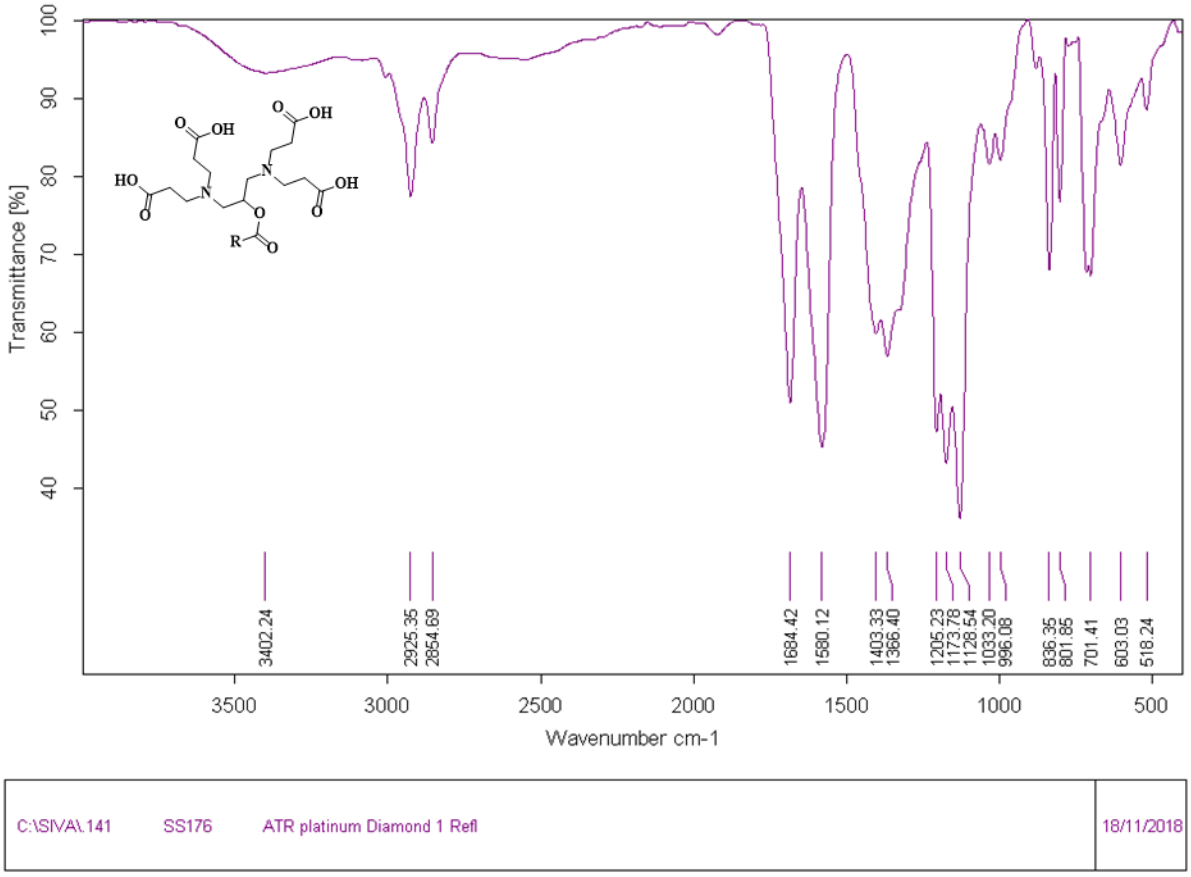

Page 1/1

CHAPTER 4: EXPERIMENTAL PAPER 3

4.1 Introduction

This chapter addresses Aim 3, Objectives 1–3 and is a first-authored experimental article in preparation for submission. This article highlights the synthesis of a novel fatty acid-based bi-tailed pH-responsive zwitterionic DMGSAD-lipid, the *in vitro* toxicity evaluation, formulation development of VCM loaded LPHNPs, characterization of its physical properties, *in vitro* and *in vivo* antibacterial properties.

4.2 Manuscript in preparation

Development of pH-responsive Dimethylglycine Zwitterionic Surface-modified Branched Lipids for Targeted Delivery of Antibiotics.

Sifiso S. Makhathini[1,] Calvin A. Omolo[1,2], Pavan Walvekar[1], Nikita Devnarain[1], Chunderika Mocktar[1], Thirumala Govender[1]*

1. Discipline of Pharmaceutical Sciences, College of Health Sciences, University of KwaZulu-Natal, Durban, South Africa.

2. School of Pharmacy and Health Sciences, United States International University of Africa, Nairobi, Kenya

*Corresponding Authors

Email address: govenderth@ukzn.ac.za, comolo@usiu.ac.ke

4.3 Abstract

The rampant antimicrobial resistance crisis calls for efficient and targeted drug delivery of antibiotics at the infectious site. Hence, in this study, we aimed to synthesize a zwitterionic pH-responsive dimethylglycine surface-modified branched lipid (DMGSAD-lipid). The synthesized lipid was in conjunction with polymeric surfactants (HS15 or RH40), which was explored for their potential to formulate pH-responsive lipid-polymer hybrid nanoparticles (LPHNPs) to deliver vancomycin (VCM) against MRSA infections. The structure of the synthesized lipid was confirmed using ^{1}H NMR and ^{13}C NMR. The biocompatibility of the DMGSAD-lipid was evaluated on HEK 293, A549 and MCF-7 cell lines using the *in vitro* cytotoxicity assay. The LPHNPs were formulated using the solvent evaporation method and were characterized for their physicochemical properties, morphology, *in vitro* drug release and *in vitro* antibacterial efficacy. The resulting two LPHNPs (VCM_HS15_LPHNPs and VCM_RH40_LPHNPs) were optimized after the screening, yielding a formulation with the desired size, polydispersity index (PDI) and zeta potential (ZP). Both formulations demonstrated pH-responsiveness through a change in size, PDI and ZP with respect to change in pH from 7.4 to 6.0. The ZP of RH40_VCM_LPHNPs changed from 0.55±0.14 to 9.44±0.33 mV, whereas for SH15_VCM_LPHNPs, ZP changed from -1.55±0.184 Vm to 9.83±0.52 Vm at pH 7.4 and 6.0, respectively. Both formulations exhibited a surface charge switch from negative to positive at reduced pH. The efficiency of encapsulation of VCM_HS15_LPHNPs and VCM_RH40_LPHNPs was 47.78±0.68 % and 43.31±1.85 %, respectively. The VCM release profile, together with release kinetic study on LPHNPs, demonstrated the influence of pH on the high rate of VCM release at pH 6.0 as compared to pH 7.4. LPHNPs had better antibacterial activity against *Staphylococcus*

aureus (*S. aureus*) and methicillin-resistance *S. aureus* (MRSA) at both pH conditions when compared to bare VCM. Furthermore, the antibacterial activity of LPHNPs against MRSA showed 8-fold better MICs at pH 6.0 than at 7.4. bare VCM-treated specimens. Thus, this study confirms that pH-responsive LPHNPs have the potential for enhancing the treatment of bacterial infections and other diseases characterized by acidic conditions at the target site.

Keywords: Lipid-polymer hybrid nanoparticle, pH-responsive zwitterionic lipid, antibacterial, vancomycin, MRSA targeted drug delivery.

4.4 Introduction

Staphylococcus aureus (*S. aureus*) is one of the bacteria that form the normal flora of our bodies. However, it is a common source of respiratory, skin, and bone infections. During the 1950s, penicillin G was one of the β-lactam antibiotics used to treat *S. aureus* infections. Unfortunately, the use of different antibiotics to treat *S. aureus* infections over the years led to the emergence of the invasive form of *S. aureus*, multi-resistant Methicillin-resistant *S. aureus* strain (MRSA). Among gram-positive bacteria, MRSA infections have been the leading cause of high morbidity and mortality rates globally. Limited therapeutic options have made it difficult to treat MRSA infections, thus posing a serious threat to public healthcare worldwide. Increasing antimicrobial resistance is narrowing the available armamentarium to treat infections from superbugs; thus, vancomycin has remained as one of the last resorts against MRSA infections. However, there is an ever-growing concern over the prevalence of vancomycin-resistant strains. Current reports have demonstrated that, if poorly treated, MRSA infections can escalate to a potentially life-threatening condition known as sepsis[1, 2]. Unfortunately, the lack of new antibiotics to treat MRSA infections represents a serious public health problem causing a major setback and undermining the efforts in containing the spread and severity of the MRSA infections[3, 4]. Therefore, according to the World Health Organization, there is an urgent need for a new effective approach to combat antibiotic resistance that arises from treating MRSA infection using conventional therapeutic ways[5].

The discovery and introduction of new antibiotic agents to the commercial market is a big challenge[6]. Moreover, the science is not straight forward; the research and development process is time-consuming (10-15 years) and discovered candidates often fail clinical trials[7]. Furthermore, bacteria have always become resistant once the newly introduced antibiotics enter the market[8]. Therefore, to mitigate resistance and to protect the existing and new antibiotics, novel drug delivery approaches are being employed as one of the approaches to combat resistance. The nano-drug delivery approach has shown to be a potential

alternative to improve the therapeutic benefits of the existing antibiotics in treating an array of microbial infections[9-11]. This therapeutic approach restores the efficiency of antibiotics by protecting the drug against bio/chemical degradation, minimize drug exposure to healthy tissues while maximizing concentration at infection site[9, 12]. Additionally, it improves the solubility of antibiotics, prolongs their systemic-circulation time, enhances targeted delivery, and provides sustained antibiotic release which will allow lower drug doses to administered and subsequently reduces systemic side effects and development of antibiotics resistance[9, 12]. Several nanocarriers have reached different stages of clinical trials in the fight against infectious diseases[13, 14].

Lipid-polymer hybrid nanoparticles (LPHNPs) are one of the nano-drug delivery systems that are promising for efficient drug delivery to overcome the shortcomings of conventional dosage forms[15]. The integration of their respective unique properties has proven to yield nanosystems with a sustained release profile, enhanced cell membrane permeability, long circulation time, improved serum stability, differential targeting and excellent biocompatibility[15, 16]. The LPHNPs are nanostructures with a lipid core surrounded by a polymer shell and stabilized by surfactants. Polymers have been employed in formulating hybrid systems with lipids because polymers have demonstrated better drug release properties[17, 18]. In contrast, the lipid increases drug loading efficiency and membrane permeability[19, 20]. The reported LPHNPs in the literature contain lipid, polymer and stabilizing surfactants. However, replacing the polymer with amphiphilic polymers could result in better systems with less excipients as there will be no need for the surfactants. Polymeric surfactants that are amphiphilic in nature are attractive biomaterials because they often offer long circulation, better stability, high loading capacity, enhanced solubilization of drugs, biodegradability and could allow surface modification via covalent bonds or complexation[21]. Moreover, the surface of the lipid layer of the LPHNPs can be functionalized to suit the desired application. The surface functionalization includes the use of biomaterials that have a unique response to different stimuli conditions at the disease site[22]. Several surface-functionalized “smart” nanocarriers that respond to endogenous stimuli such a pH, enzyme redox, temperature, etc., have been developed[12, 23]. These “smart” nanocarriers contribute to high drug localization through targeting and stimuli-triggered drug release at the site of infection and have been reported to enhance the efficacy of the drug and could potentially reduce the risk of drug resistance[24]. There has been extensive progressive research in developing “smart” biomaterials to formulate nanocarriers to tackle antibiotic resistance effectively, indicating the success in this strategy in fighting antibacterial resistance[25, 26]

In order to formulate nano-drug delivery systems that have desirable properties, such as disease targeting and long circulation, there is a need for the design and synthesis of advanced materials to prepare superior

novel nano-drug delivery systems with enhanced antibacterial activity[12]. With the advancements in synthetic and analytical chemistry ,scientists can tailor biomaterials by altering chemical and physical parameters during the synthetic process[27]. In recent years, there has been a significant demand for the development of stimuli-responsive materials for targeted delivery of bioactive molecules[12]. Thus, continuous efforts to develop such biomaterials ought to be undertaken in this field.

One of the stimuli-responsive biomaterials are those that are responsive to pH. Due to differences in pH conditions of healthy and disease tissue sites, pH is among the endogenous stimuli that have been widely exploited for tumor, bacteria and cancer-targeted drug delivery[28]. Nanoantibiotics delivery has been widely explored using different pH-responsive lipid and polymer-based nanoparticles. However, the scope of application of LPHNPs to treat bacterial infections is not known. Hence, there is limited data in the literature reported on pH-responsive LPHNPs for delivery of antibiotics[26, 29, 30]. Developing a novel pH-responsive biomaterial for the formulation of LPHNPs for antibiotic delivery could potentially address both limitations of conventional as well as the limitation of the above mentioned clinically approved nanoantibiotic medicine. Herein, we report a detailed synthesis of a pH-responsive lipid composed of fatty acid-based bi-tailed zwitterionic lipid.

The smart lipid and polymeric surfactants in the market were then employed to formulate novel LPHNPs for delivery of antibiotics. pH-responsive and surface charge switching zwitterionic lipids are known to greatly enhance drug release from the delivery system in response to change in pH while minimizing toxicity encountered when using cationic and anionic lipids. We envisage that ionization of headgroups (amine groups) of the fatty acid-based bi-tailed zwitterionic lipid will be responsible for the pH-responsive behavior. Under acidic conditions, the lipid surface monolayer gets protonated, creating a repulsive force within the lipid layer. The repulsion may lead to the rearrangement or destabilization or swelling of the lipid layer, which may contribute to the leakage or burst release of the drug at the site of infection. Also, the protonation mechanism will induce surface charge switching to positive, which is beneficial for surface electrostatic binding with the negatively charged bacterial cell wall, thus enhancing cellular uptake and drug localization. The formulation of most reported have incorporated a lipid system, a polymer and a surfactant or several surfactants[31, 32]. We, therefore, also report a novel hybrid polymer lipid system that will use the FDA approved polymeric surfactants in the market and the synthesized novel smart lipid. This approach will reduce the number of excipients in the formulation, thus enhancing the safety profile of the smart system. Our system is composed of a newly synthesized fatty acid-based bi-tailed zwitterionic lipid and lipid-PEG (Cremophor® RH 40/ Solutol® HS 15) used as a surfactant. The amphiphilic zwitterionic lipid was synthesized by conjugating fatty acid chains with dimethylglycine. The lipid tail from both

zwitterionic lipid and lipid-PEG form a hydrophobic core to encapsulate the drug through hydrophobic interactions. At the same time, the dimethylglycine head groups and PEG form the outer surface of the system. The dimethylglycine head groups will be responsible for surface charge switching in response to reduced pH to potentiate drug release, whereas PEG mainly contributed to stability and long circulation. Thus, this system could potentially enhance the binding affinity of the positively charged LPHNPs with the negatively charged bacterial surface for high drug localization, while minimizing exposure to healthy host cells.

4.5 Materials and Methods

4.5.1 Materials

2-aminopropane-1,3-diol was purchased from Sigma-Aldrich (UK). 1-Ethyl-3- (3-dimethylaminopropyl) carbodiimide hydrochloride and trifluoroacetic acid (TFA) were procured from Merck (Germany) while Di-tert-butyl decarbonate was purchased from Sigma-Aldrich (Germany). MTT (3-(4, 5-dimethylthiazol-2-yl)-2, 5-diphenyltetrazolium bromide) was purchased from Alfa Aesar (UK), Mueller Hinton Agar (MHA), Nutrient Agar and Nutrient Broth were obtained from Biolab (South Africa). The following reagents: 4-(dimethylamino) pyridine (DMAP), Stearic Acid (SA), Mueller Hinton broth 2 (MHB), Vancomycin hydrochloride, dialysis tubing cellulose membrane (MWCO 14,000 Da) and all other materials were purchased from Sigma-Aldrich (USA). The vancomycin free base (VCM) was obtained from converting vancomycin hydrochloride as described from a previously reported method [21]. An Elix® water purification system Millipore Corp. (USA) was used to obtain milli-Q purified water. Bacterial strains *S. aureus* (ATCC 25922) and *S. aureus* (Rosenbach) (ATCC®BAA-1683) (MRSA) were used for this project. A Bruker Alpha-P spectrometer with a diamond ATR (Germany) was used to obtain FT-IR spectra for all the compounds synthesized. ^{1}H and ^{13}C NMR spectra were obtained by using a Bruker 400 and 600 Ultra shield™ (United Kingdom) NMR.

4.5.2 Methods

4.5.2.1 Synthesis and characterization of zwitterionic DMGSAD-lipid

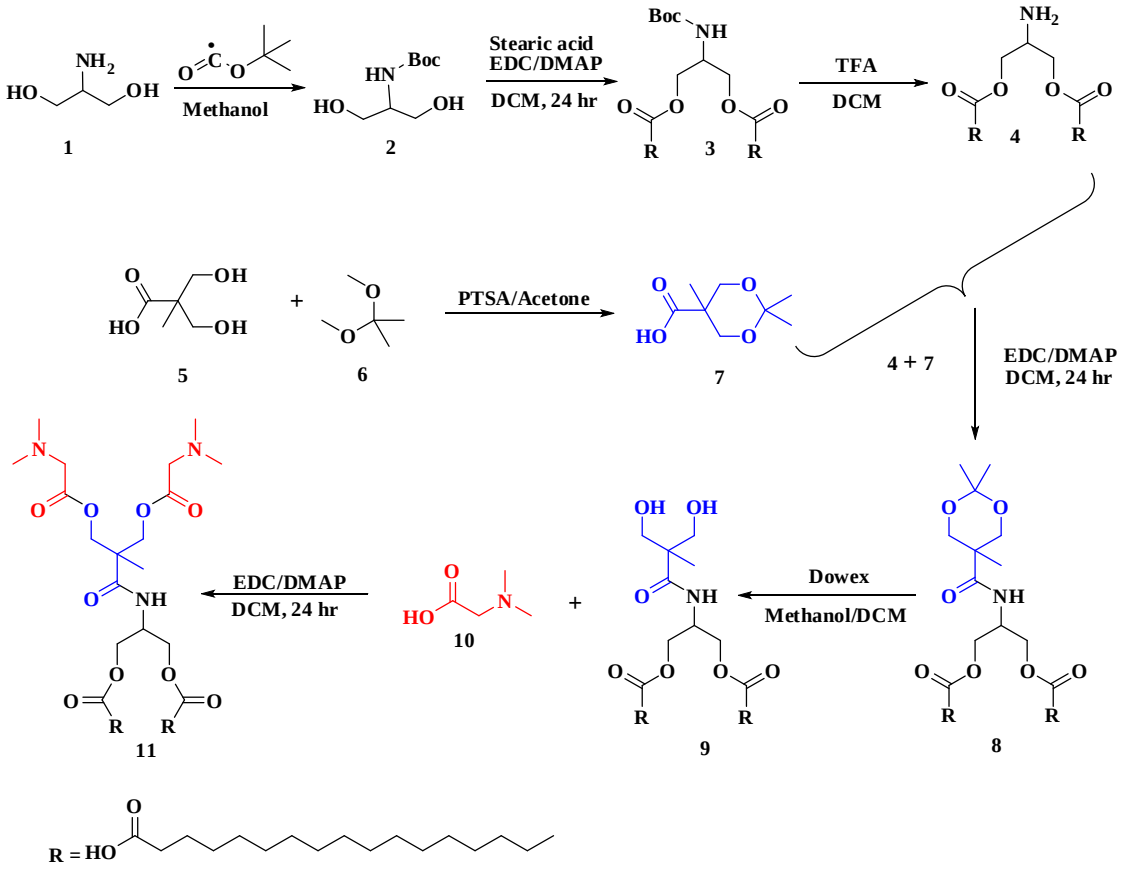

Scheme1: Synthesis of 2,2-(3-((dimethylglycyl)oxy) methyl)-2-methylpropanamido) propane-1,3-diyldistearate (zwitterionic DMGSAD-lipid) as per the above scheme.

4.5.2.2 **tert-butyl (1,3-dihydroxypropan-2-yl) carbamate** (**2**). tert-butyl dicarbonate (7.90 g, 36.2 mmol) was added to a solution of serinol (**1**) (3 g, 32.9 mmol) in MeOH (300 ml). The reaction mixture was then stirred at room temperature for 14 h. After this time, the solvent was evaporated to complete dryness to give a white crude product which was purified by flash chromatography (5 % MeOH/CH_2Cl_2) to yield a crystal white solid (5.76 g, 92%): Characterization was as follows: ^{1}H NMR (400 MHz, $CDCl_3$) δ(ppm): 1.38 (s, 9H), 3.75 (m, 4H), 3.76 (m, 1H); ^{13}C NMR (400 MHz, $CDCl_3$) δ(ppm): 28.5, 54.0, 60.1, 79.4, 156.2

4.5.2.3 **2-((tert-butoxycarbonyl) amino) propane-1,3-diyl distearate** (**3**). Compound **3** was synthesized by the addition of stearic acid (5.96 g, 20.9 mmol) to a stirring reaction mixture of compound **2** (2 g, 10.5 mmol), EDC.HCl (3.25 g, 20.9 mmol) and DMAP (0.64 g, 5.23 mmol) in dry DCM. The reaction mixture was stirred under inert conditions ($N_{2(g)}$) at room temperature for 24 h. The dicyclohexylurea was filtered off and the solvent was removed under reduced pressure (vacuum) to obtain a crude product which was

further purified by column chromatography on silica gel using ethyl acetate in hexane (10-15 % v/v) to give a yield of 95%. Characterization was as follows: ^{1}H NMR (400 MHz, $CDCl_3$) δ(ppm): 0.88 (m, 6H), 1.30-1.26 (m, 56H), 1.42 (s, 9H), 1.64-1.51 (m, 4H), 2.32-2.0 (m, 4H), 4.30-4.27 (m, 4H), 4.78 – 4.67 (m, 1H); ^{13}C NMR (400 MHz, $CDCl_3$) δ(ppm): 14.1, 22.7, 25.0, 28.4, 29.0, 29.3, 29.6, 31.8, 33.9, 47.9, 63.9, 79.5, 155.6, 173.1.

4.5.2.4 **2-aminopropane-1,3-diyl distearate** (**4**). To synthesized compound **4**, To a solution of Compound **3** (4.79 g, 5.5 mmol) in DCM was 25 % TFA was added dropwise and stirred for 2 h at room temperature. After this time, TFA was removed under reduced pressure to give a viscous oil product. The traces amount of TFA remaining was removed by re-dissolving the crude product in ethyl acetate and washed with a saturated solution of Na_2CO_3 and followed by washing with brine solution separately. The organic layer was dried over anhydrous $MgSO_4$ to remove traces amount of water and filtered off. The solvent was vacuum dried to give the final product at yield above 95 % and characterization was as follows: ^{1}H NMR (400 MHz, $CDCl_3$) δ(ppm): 0.88 (t, 6H, *J*=7.0 Hz), 1.2 - 1.18 (m, 56H),1.38 (s, 9H),1.64-1.61(m, 4H), 2.23 (t, 4H, *J* =7.33 Hz), 3.8-3.3(m, 1H), 4.33 (d, 4H, *J* =4.52 Hz); ^{13}C NMR (400 MHz, $CDCl_3$) δ(ppm): 14.1, 22.7, 25.0, 28.4, 29.0, 29.3, 29.6, 31.8, 33.9, 47.9, 63.9, 79.5, 155.6, 173.1.

4.5.2.5 **2,2,5-trimethyl-1,3-dioxane-5-carboxylic acid** (**7**). A mixture of bis-MPA (**5**) (10 g, 74.55 mmol), *p*-toluenesulfonic acid monohydrate (0.71 g, 3.73 mmol) and 2,2-dimethoxypropane (**6**) (13.8 ml, 111.83 mmol) in 50 ml acetone. The reaction mixture was stirred at room temperature for 2 h. The catalyst was neutralized with 1 ml of NH_3/MeOH solution and the solvent was vacuum evaporated at room temperature. The crude product was re-dissolved in 200 ml CH_2Cl_2 and extracted three times with 20 ml water. The organic layer was dried over $MgSO_4$ and vacuum dried to give a white crystal product (**7**) at a yield above 97 %. The product was used in the following reaction step without any further structural elucidation.

4.5.2.6 2-(2,2,5-trimethyl-1,3-dioxane-5-carboxamido) propane-1,3-diyl distearate (8). To a solution of Compound **4** (2 g, 3.2 mmol) in dry DCM, compound **7** (0.67 g, 3.8 mmol) was added followed by addition of EDC.HCl (1.2 g, 6.4 mmol) and DMAP (0.195 g, 1.6 mmol). The reaction mixture was stirred overnight under inert conditions ($N_{2(g)}$) at room temperature. The EDC urea formed was removed by extracting with two portions of water followed by DMAP neutralization using 1N HCl. The solution was dried over anhydrous $MgSO_4$ and filtered off. The organic solvent (filtrate) was evaporated under vacuum and the crude product was purified by column chromatography on silica gel using ethyl acetate in hexane (10-15 % v/v) to give a yield above 86%. Characterization was as follows: ^{1}H NMR (400 MHz, $CDCl_3$) δ(ppm) : 0.83 (m, 6H), 1.31-1.26 (m, 56H), 1.32 – 1.31 (m, 6H), 1.39 1.36, (m, 3H), 1.62-1.59 (m, 4H), 2.60-2.32 (m, 4H), 3.88 – 3.56 (m, 2H), 4.13 (d, 2H), 4.27 (d, 4H), 4.76 – 4.73 (m, 1H); ^{13}C NMR (400 MHz, $CDCl_3$) δ(ppm): 14.2, 16.0, 22.7, 25.3, 26.1, 30.0, 30.1, 30.5, 31.9, 46.4, 47.0, 64.0, 70.3, 98.2, 174.3, 178.8.

4.5.2.7 2-(3-hydroxy-2-(hydroxymethyl)-2-methylpropanamido) propane-1,3-diyl distearate (9). Compound (**8**), 2.00 g (2.56 mmol), was dissolved in 30 ml of methanol and a scoop of a Dowex, H^+ resin was added, and the reaction mixture was stirred for 3 h at room temperature. After this time, the Dowex, H^+ resin was filtered off and carefully washed with methanol. The methanol was evaporated to give compound **9** as white crystals at yield above 3.35 g, (97 %) and characterization was as follows: ^{1}H NMR (400 MHz, $CDCl_3$) δ(ppm): 0.88 (m, 6H), 1.31 – 1.24 (m, 56H), 1.35(s, 3H), 1.66 – 1.52(m, 4H), 2.33 – 2.0(m, 4H), 3.70(s, 4H), 4.27(d, 4H), 4.80(m, 1H); ^{13}C NMR (400 MHz, $CDCl_3$) δ(ppm): 14.1, 15.9, 22.7, 24.9, 29.0, 29.4, 29.8, 32.2, 34.0, 47.1, 48.5, 65.1, 66.3, 174.3, 1778.5

4.5.2.8 2-(3-((dimethylglycyl)oxy)-2-(((dimethylglycyl)oxy)methyl)-2-methylpropanamido)propane-1,3-diyl distearate (11). To a solution of Compound **9** (1.6 g, 2.26 mmol), EDC.HCl (1.3 g, 6.8 mmol) and DMAP (0.14 g, 1.1 mmol) in dry DCM, compound **10** (0.466 g, 4.5 mmol) was added. The reaction mixture was stirred overnight under inert conditions ($N_{2(g)}$) at room temperature. The EDC urea formed was removed by extracting with two portions of water followed by DMAP neutralization using 1N HCl. The solution was dried over anhydrous $MgSO_4$ and filtered off. The organic solvent (filtrate) was evaporated under vacuum and the crude product was purified by column chromatography on silica gel using ethyl acetate in hexane (10-15 % v/v) to give a yield above 80%. Characterization was as follows: ^{1}H NMR (400 MHz, $CDCl_3$) δ(ppm); 0.88 (m, 6H), 1.31 - .24(m, 56H), 1.38(s, 3H), 1.65 – 1.53(m, 4H), 2.30 – 2.15(m, 4H), 2.65 (s, 4H), 2.77(s, 12H), 3.52(s, 4H), 4.30 – 4.25(m, 4H), 4.75 – 4.70(m, 1H). ^{13}C NMR (400 MHz, $CDCl_3$) δ(ppm): 14.1, 22.6, 22.7, 25.0, 29.0, 29.3, 29.8, 30.1, 32.0, 33.9, 46.2, 48.0, 49.2, 64.0, 66.6, 174.3, 177.6, 204.0.

4.5.3 *In vitro* cytotoxicity (MTT assay)

The evaluation of the non-toxic nature of any novel material to be used in pharmaceutical and biomedical applications is of paramount importance[33]. The relative cytotoxicity associated with zwitterionic DMGSAD-lipid was evaluated using the MTT assay. Briefly, three cell lines, human embryonic kidney cells (HEK 293), human cervix adenocarcinoma (HeLa) cells and human breast adenocarcinoma cells (MCF-7) were used to assess the biosafety of the lipid as described in a previously reported study[34]. Grown cell lines were seeded in 96-well plate at a density of 2.5×10^3 and incubated for 24 h at 37 °C. After this time, seeded cells were treated with 20, 40, 60, 80, 100 µg/ml concentrations of the tested compound and further incubated for 24 h. Culture medium and the tested material were replaced with 100 µl fresh medium and 100 µl of MTT solution (5 mg/ml) in phosphate buffer solutions (PBS) per well and further incubated for 4 h at 37 °C. After that, dimethyl sulfoxide (100 µl) was added in each well to solubilize the MTT formazan crystal. Using 96-well microplate reader (Mindray MR-96A), the amount of formazan was measured by reading the absorbance set at 540 nm wavelength. The culture medium with cells and without

cells was used as the positive and negative control, respectively. All the experiments were done in a replica of six times. The percentage cell viability of every treated sample was calculated using the following equation:

$$\% \text{ Cell viability} = \left(\frac{\text{A 540 nm treated cells}}{\text{A 540 nm untreated cells}}\right) \times 100 \qquad (1)$$

4.5.4 Preparation and Characterization of VCM-LPHNPs

4.5.4.1 Preparation

LPHNPs were formulated using a slightly modified solvent evaporation method as previously reported in the literature[35]. The preliminary studies were performed to obtain an optimal formulation with desired physicochemical properties. The optimal blank formulation consisted of pH-responsive zwitterionic lipid and surfactant in specified ratios. Whereas for VCM-loaded LPHNPs, 1 mg/ml of VCM was added. Briefly, DMGSAD-lipid was dissolved in 3 ml THF and added dropwise into 10 ml of distilled water containing 200 mg of the surfactant under vigorous sonication at 30 % amplitude. After complete addition, the solution was sonicated for further 10 min and the organic solvent was allowed to evaporate under stirring 24 h in the open air. The solution obtained had a blue tint colour, which was an indication of the successful formation of LPHNPs. The drug-loaded formulations were prepared using the same procedure, except that the drug is dissolved in the same solution as the surfactant.

4.5.4.2 Size, Polydispersity Index (PDI), Zeta Potential (ZP) and Morphology

The formulated LPHNPs were characterized for their size, PDI and ZP using dynamic light scattering technique. Measurements were recorded using Zetasizer Nano ZS90 (Malvern Instruments, UK) fitted with a 633 nm laser at 173° detection optics at room temperature (25º C). The formulated LPHNPs were appropriately diluted using PBS (pH 7.4 and 6.0) and measured in triplicate from separate prepared batches to ensure reproducibility. The morphological features of the nanoparticles were characterized by TEM analysis. The prepared samples were negatively stained with 1 % uranyl acetate and fixed on a copper grid for drying and images were acquired at 100 kV using JEOL Microscopy (JEM 2010, Japan).

4.5.4.3 Entrapment Efficiency (EE) and Drug Loading (DL)

The efficiency of entrapment (%EE) of VCM encapsulated into LPHNPs was determined using an ultrafiltration method. This method works by separating the free drug from the encapsulated drug using centrifugal filter tubes (Amicon® Ultra-4) of 10 Da molecular weight cut-off. Briefly, 2 ml of the drug-loaded formulation was placed in the centrifugal filter tube and centrifuged at 3000 rpm for 30 min at 25 °C. The filtrate was used to measure the amount of free (the unencapsulated VCM) using high-performance

liquid chromatography (HPLC), Shimadzu Prominence DGU-20A3 set at 280 nm wavelength. The optimized conditions for HPLC were as follows: C18 reversed-phase column (Nucleosil 120-5 C18; 4 × 150 mm, 5µm); acetonitrile: 0.1 % TFA in water (15:85 v/v) as a mobile phase; and column temperature, injection volume and the flow rate was set at 25 °C, 100 µl and 1 ml/min, respectively. Using the following linear regression equation y = 24598x−3125.7 with linearity (R^2) of 0.999, the unknown amount of VCM entrapped was calculated. The following equations were used to calculate %EE and %DL.

$$\text{EE (\%)} = \left(\frac{\text{Weight of VCM in micelles}}{\text{Weight of VCM added}}\right) \times 100 \qquad (3)$$

$$\text{DL (\%)} = \left(\frac{\text{Weight of VCM in micelles}}{\text{Total weight of micelles}}\right) \times 100 \qquad (4)$$

4.5.5 *In vitro* drug release

The diffusion technique using a dialysis tube (MWCO 14,000 Da) was used to investigate the *in vitro* VCM release behavior from VCM-loaded pH-responsive LPHNPs was investigated using [36]. Briefly, dialysis tubes of specified pore size were loaded with 2 ml of the formulations (blank and drug-loaded), sealed and dialyzed against 40 ml of PBS at pH 7.4 and 6.0 at 37 °C in an incubator and maintained set at 100 rpm. The released amount of VCM at different predetermined time intervals was determined with HPLC through following a previously reported procedure, conditions specified in section **2.3.3** [37]. The sink conditions were maintained by adding an equivalent amount of fresh PBS after each sampling. All experiments were performed in triplicate.

4.5.6 Antibacterial Studies

4.5.6.1 *In vitro* antibacterial activity

VCM-loaded pH-responsive LPHNPs were evaluated for their antibacterial efficacy against *S. aureus* and MRSA at pH 7.4 and pH 6.0 using a broth dilution method[38]. The cell culturing and broth dilution method was done following a previously described procedure[39]. The bacterial cell culture (*S. aureus* and MRSA) were grown in Mueller-Hilton Broth (MHB) for 24 h at 37 °C in a Labcon 3081 (USA) shaking incubator set at 100 rpm. Using appropriate dilutions, 0.5 McFarland standard (1.5×10^8 CFU)/ml) was achieved by diluting the cell culture with sterile distilled water and measured using a DEN-1B suspension McFarland densitometer (Latvia). This concentration (1.5×10^8 CFU)/ml) was further diluted to a concentration of 5×10^5 colony forming units (CFU)/ml necessary for this study. Serial dilutions using bare VCM and VCM-loaded LPHNPs formulations (VCM_HS15_LPHNPs and VCM_RH40_LPHNPs) were prepared in HMB broth adjusted to 7.4 and 6.0 pH levels and incubated with bacterial culture a shaking incubator set at 37 °C, 100 rpm for 24 h. After that, at predetermined time intervals (24, 48, 72 h), 5 µl of the sample mixture

was spotted on Mueller-Hinton (MHA) plates and the minimum sample concentration at which no bacterial growth was observed and recorded as the minimum inhibitory concentration (MIC). All experiments for this study, including VCM-free LPHNPs (negative control), VCM-loaded LPHNPs and bare VCM (positive control), were performed in triplicate.

4.6 Results and Discussion

4.6.1 Synthesis of fatty acid-based zwitterionic DMGSAD Lipid

Seven synthetic steps were followed to successfully synthesise the zwitterionic DMGSAD Lipid, as shown in **Scheme 1** (above). The first step is the boc protection reaction of serinol to obtain compound **2**, which was confirmed by both ^{1}H NMR and ^{13}C NMR. A singlet peak that integrates to 9 protons at chemical shift δ 1.33 ppm using proton NMR was identified as protons belonging to the tert-butyl group confirming the formation of compound **2**. Using EDC/DMAP coupling chemistry, compound **3** was synthesized from compound **2** via an esterification reaction. The proton peaks at chemical shifts δ 0.83 (multiplet), δ 1.26 (multiplet), δ 1.64 (multiplet), δ 2.23 (multiplet) were identified as corresponding to the aliphatic chain of stearic acid coupled to compound **2**. Boc deprotection reaction using 25 % TFA was used to obtain compound **4** from compound **3**. The obtained compound after purification was elucidated using ^{1}H NMR, which showed the disappearance of isobutane peaks at δ 1.38 ppm and at δ 28.4 ppm in 13C NMR, confirming a successful deprotection reaction.

4.6.2 *In Vitro* Cytotoxicity

The cytotoxicity effect associated with DMGSAD Lipid was evaluated using an MTT assay as described in literature[40]. Briefly, different sample (DMGSAD Lipid) concentrations ranging from 20 – 100 µg/ml were tested against three different cell lines (MCF-7, HeLa and HEK 293) and the results are represented in **Fig 1**. The cell viability is measured in terms of the total activity of mitochondrion of a living cell population in converting MTT into formazan crystals after being treated with a potential toxicant. After incubation for 24 h, DMGSAD Lipid displayed a cell viability between 93.65 - 81.28%, 99.75 - 75.51 % and 82.53 – 75.14 % for HEK 293, MCF-7 and HeLa cells, respectively. Even though cell viability was reduced to about 75 % at the concentration of the lipid higher than 80 µg/ml. According to literature reports, materials with cell viability greater than 75 % can be considered as less toxic and biosafe for biological application[41, 42]. Therefore, these results of the MTT test proved that the cell viability was not compromised with cell viability >75 % with respect to an increase in the concentration of the tested potential toxicant at different concentrations tested. Therefore, the non-toxic nature of our material indicates its suitability for biomedical applications.

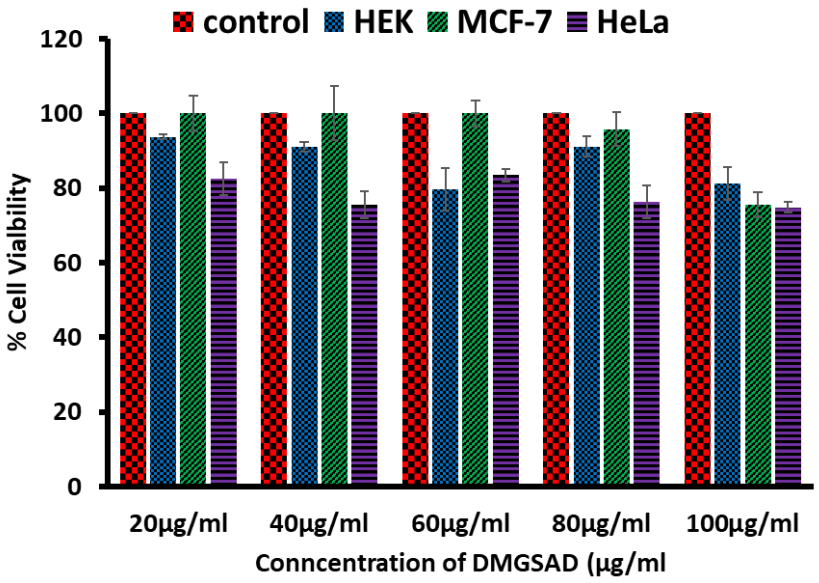

Fig. 1: Percentage cell viability of human cells (HeLa, MCF-7 and HEK 293) after treatment with DMGSAD.

4.6.3 Preparation and Characterization of VCM-Loaded LPHNPs

4.6.3.1 Size, Surface charge, Entrapment efficiency and Morphology

The LPHNPs were formulated via a slightly modified solvent evaporation method[39, 43]. Preliminary studies were performed to obtain an optimal formulation. Different types of surfactants were screened at a fixed concentration to identify the most stable formulation of LPHNPs with desirable physicochemical characteristics. The polymeric surfactants used were Cremophor RH 40, Lutrol® F 68, Solutol HS 15 and Poloxamer 407 as shown in **Table 1**. The prepared LPHNPs were characterized for pH-responsiveness and other physicochemical characteristics by dispersion in different buffer solutions (pH 7.4 and 6.0). Among the surfactants screened, Cremophor RH 40 and Solutol HS 15 stabilized formulations displayed the best results in terms of particle size, PDI and ZP. The optimized formulations were given code names based on the surfactant used, Cremophor RH 40 as RH40_VCM_LPHNPs and Solutol HS 15 as SH15_VCM_LPHNPs. Both formulations demonstrated pH-responsiveness through a change in size, PDI and ZP with respect to change in pH from 7.4 to 6.0. The size and ZP of RH40_VCM_LPHNPs changed from 64.05 ± 0.64 to 113.6 ± 0.20 nm and from 0.55 ± 0.14 to 9.44 ± 0.33 Vm at pH 7.4 and 6.0, respectively. Whereas for SH15_VCM_LPHNPs, only change in ZP from -1.55 ± 0.184 Vm to 9.83 ± 0.52 Vm was observed at pH 7.4 and 6.0, respectively. A change in particle size in response to acidic conditions is an indication of rearrangement or swelling of the particles, which is necessary for leakage and high localization of the drug at the site of infection. A change in surface charge can be associated with the presence of tertiary amines from dimethylglycine head groups of the lipids. The tertiary amines will remain

neutral at physiological pH and undergo protonation at acidic pH contributing towards the overall positive surface charge of the particle.

Additionally, surface charge switching is also vital in making the system more hydrophilic to potentiate fusion with the lipid-based membrane of the bacterial. It also facilitates the release of higher quantities of the drug through repulsion force within the lipid membrane of the delivery system at the infection sites (Mura et al., 2013). Lastly, it enables the carrier to bind easily to the negatively charged bacterial cells, allowing for high drug localization for better therapeutic outcomes. Morphological analysis using TEM showed that LPHNPs were discrete and had an almost spherical shape as shown in **Fig 2 C and D**. Both formulations had a relatively high VCM encapsulation efficiency as reported in **Table 2.**

Table 1: Screening of surfactants to identify a stable pH-responsive formulation.

Surfactants	**pH 7.4**			**pH 6.0**		
	Size (nm)	**PDI**	**ZP (mV)**	**Size (nm)**	**PDI**	**ZP (mV)**
Kolliphor® RH 40	141.9± 0.64	0.257±0.024	-2.76±0.064	60.56±0.15	0.473±0.003	7.61±0.25
Solutol SH15	35.83±0.098	0.128±0.005	-11.9±0.85	34.46±0.24	0.119±0.003	6.82±1.13
Kolliphor® P188	183.9±3.18	0.322±0.010	5.64±0.49	134.4±0.14	0.307±0.38	22.0±1.20
Poloxamer 407	270.5±0.35	0.400±0.014	1.67±0.064	161.9±0.64	0.373±0.006	17.0±0.071

Table 2: Effect of pH on size, PDI, ZP and %EE of VCM-LPHNPs

Surfactants	**pH 7.4**			**pH 6.0**			
	Size (nm)	**PDI**	**ZP (mV)**	**Size (nm)**	**PDI**	**ZP (mV)**	**%EE**
Kolliphor® RH 40	64.05± 2.64	0.277±0.057	0.55±0.14	113.6±0.20	0.384±0.033	9.44±0.33	43.31±1.85
Solutol SH15	73.41±0.468	0.487±0.001	-1.50±0.184	70.86±0.89	0.476±0.010	9.83±0.52	47.78±0.69

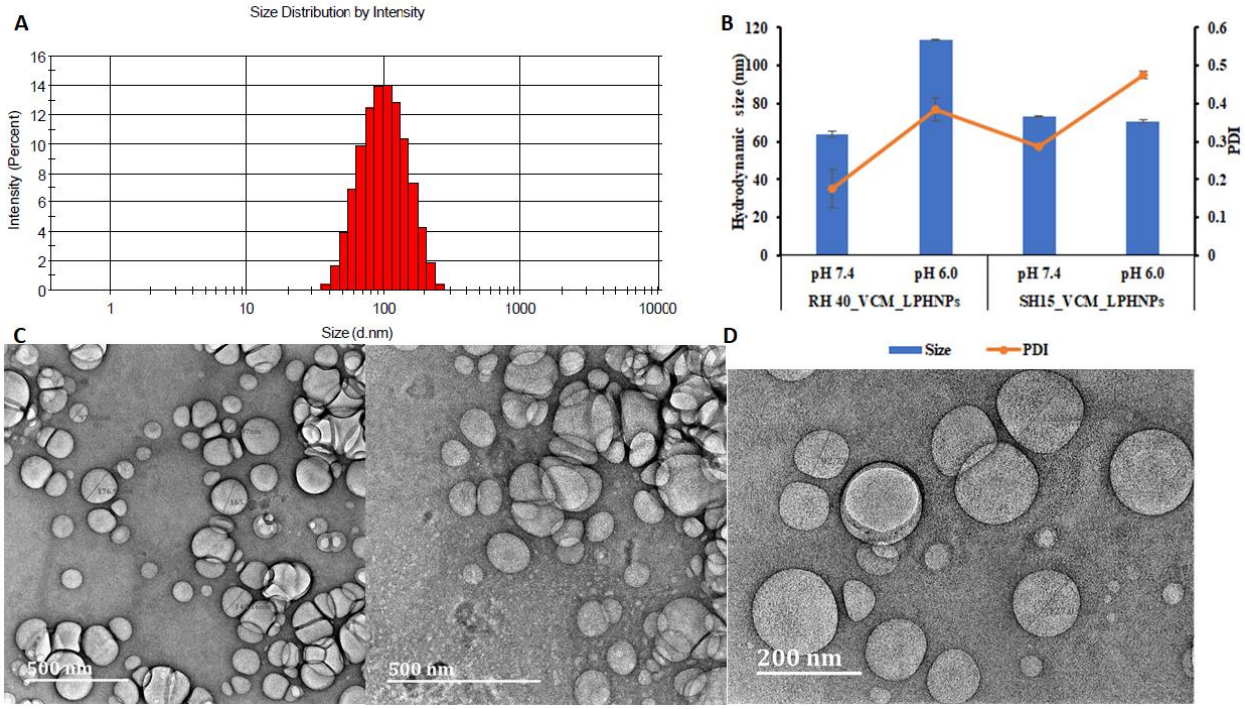

Fig. 2: A: Histogram showing size distribution by intensity; **B**; Optimized formulation at pH 7.4 and 6.0, **C;** LPHNPs population and **D** Magnified TEM images displaying morphology of LPHNPs.

4.6.4 *In vitro* drug release profiles and drug release kinetics

The efficiency of stimuli (pH)-responsive delivery systems stems from their ability to improve targeted drug release while avoiding premature drug release and promoting high localization of the drug at the targeted site. The system undergoes conformational changes that promote drug release at high concentrations at the targeted site in response to specific stimuli and thus, improving the therapeutic drug efficacy over traditional therapies. Therefore, for this study, VCM-loaded pH-responsive LPHNPs (RH40_VCM_LPHNPs and SH15_VCM_LPHNPs) were prepared and their pH-responsiveness was investigated using different PBS solutions (pH 7.4 and 6.0), and was compared with bare VCM solution in the same release conditions throughout 48 h as shown in **Fig 3**. The phosphate buffer pH 7.4 and 6.0 were used to simulate the normal physiological and the acidic bacterial infected environment, respectively. As shown in **Fig 3 A** and **B,** the drug release ratio at both pH conditions (7.4 and 6.0) for bare VCM solution was almost complete (~90%) within the first 8 h.

In contrast, both formulations (RH40_VCM_LPHNPs and SH15_VCM_LPHNPs) at both pH levels demonstrated a slow and prolonged VCM release with the cumulative percentage release of about 50 % within the first 8 h. As shown in **Fig 3 C**, both formulations demonstrated a similar drug release profile at pH 7.4 and 6.0 within the first 8 h. After 8 h, there was a increase in VCM release ~85 % at pH 6.0 as

compared to ~60 % at pH 7.4 for both formulations in 24 h. The initial release profile within the first 8 h at both pH levels could be attributed to VCM localized on the surface of the LPHNPs due to the presence of dimethylglycine head groups causing surface electrostatic attachment of the drug. After this hour, the increased drug release at pH 6.0 could be due to the pH triggered VCM release via ionization of tertiary amines from dimethylglycine head groups. At pH 7.4, the tertiary amine remains unionized, exhibiting a minimum swelling and retaining most of its entrapped drug. Whereas, at pH 6, due to ionization, a maximal swelling is expected due to the electrostatic repulsion causing deformation or destabilization of LPHNPs. Thus, more drug is released at pH 6.0 than at 7.4. The minimal swelling of LPHNPs at 7.4 can help reduce premature release or loss of the drug to the nonspecific site. In contrast, the maximum swelling of LPHNPs at acid pH (infection site) may contribute to a high concentration of the drug release at the targeted site for better therapeutic outcomes. Also, the ionization of the dimethylglycine head groups induces an overall positive charge on the surface of the LPHNPs. This positive charge enhances its binding affinity to the negatively charged bacterial cell wall via electrostatic binding, promoting high drug localization at the target site at a lethal dose.

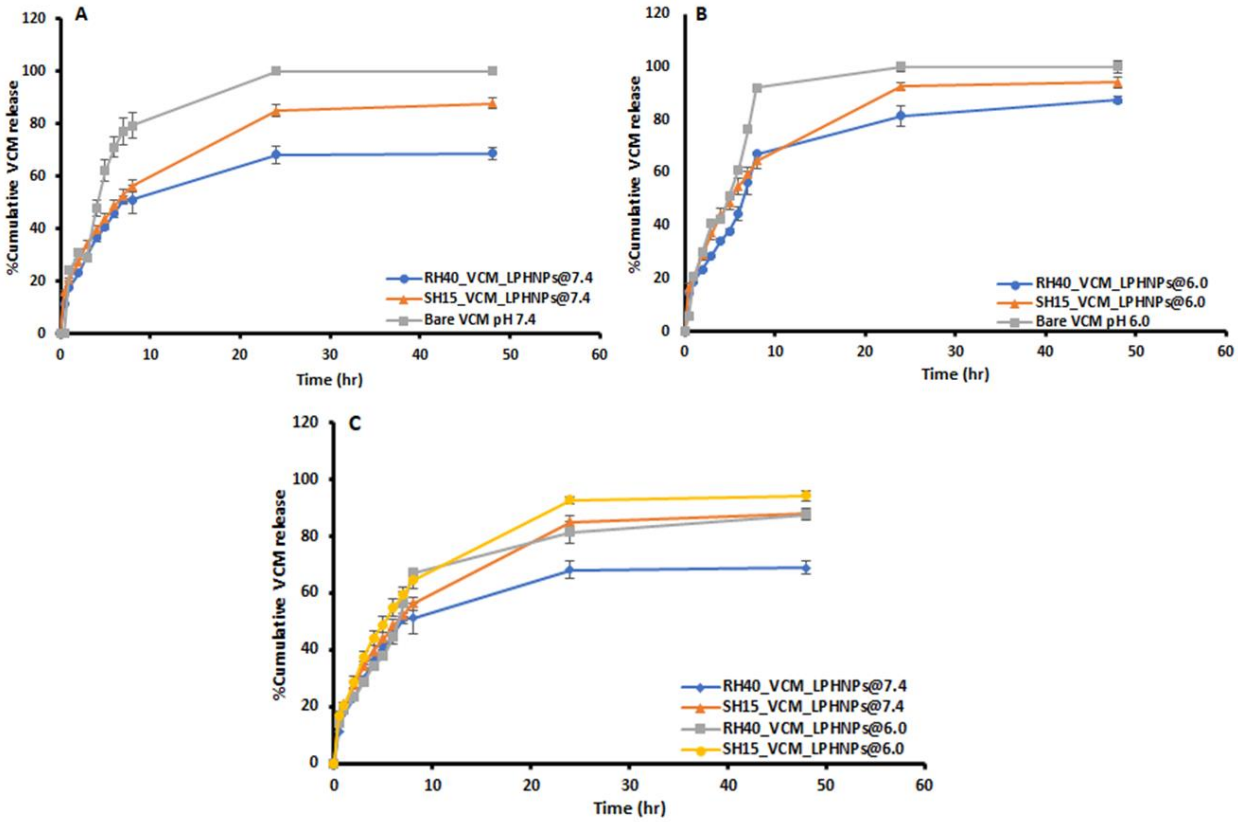

Fig. 3: Effect of pH on drug release profiles of (A and B) bare VCM, RH40_VCM_LPHNPs and SH15_VCM_LPHNPs at pH 7.4 and (C) RH40_VCM_LPHNPs and SH15_VCM_LPHNPs at pH 7.4 and 6.0 respectively (n=3).

Table 3: Release Kinetics Data of SH15_VCM_LPHNPs from different models.

	pH 7.4			**pH 6.0**		
Model	**R^2**	**RMSE**	**β/n- value**	**R^2**	**RMSE**	**β/n- value**
Zero order	-1.2246	29.7315		-0.2475	32.0605	
First order	0.4334	15.0099		0.9705	4.9016	
Higuchi	0.4646	14.5662		0.8218	12.0861	
Korsmeyer-Peppas	0.9967	0.9755	n = 0.488	0.9964	1.1701	n = 0.529
Hixson-Crowell	0.2086	17.7366		0.8544	10.8837	
Weibull	0.9908	1.6871	β = 0.614	0.9902	1.9292	β = 0.676

Table 4: Release Kinetics Data of RH40_VCM_LPHNPs from Different Models

	pH 7.4			**pH 6.0**		
Model	**R^2**	**RMSE**	**β/n- value**	**R^2**	**RMSE**	**β/n- value**
Zero order	-0.5449	26.8112		-0.3610	24.6736	
First order	0.6790	12.0755		0.7130	11.3267	
Higuchi	0.7123	11.5503		0.7955	9.5545	
Korsmeyer-Peppas	0.9576	4.1306	n = 0.398	0.9848	2.3475	n = 0.9848
Hixson-Crowell	0.5487	14.3842		0.6052	13.2868	
Weibull	0.9811	2.7567	β = 0.541	0.9909	1.8089	β = 0.583

The release kinetics study using various mathematical models to further understand the release mechanism of the formulation at both pH 7.4 and 6.0 was performed (**Table 3 and 4**). The mathematical models of interest used include Zero order, First order, Higuchi, Korsmeyer-Peppas, Hixon-Crowell, and Weibull. The best fit model to describe the release mechanism was selected based on the model with the highest correlation coefficient (R^2) closer to 1 and the lowest root mean-square error (RMSE). The VCM release behavior from SH15_VCM_LPHNPs was found to follow the Korsmeyer-Peppas model with an "*n*" exponent value of 0.488 and 0.529 at pH 7.4 and 6.0, respectively. The "*n*" value below 0.5 at pH 7.4 indicates that the Fickian mechanism governed the drug release pattern of the formulation, which is mainly the diffusion mechanism. At pH 6.0, the release behavior was found to be non-Fickian with an "*n*" value above 0.5. This was an indication that at pH 6.0, there was more than one release mechanism involved apart from diffusion.

The VCM release behavior from RH40_VCM_LPHNPs was also investigated and the Weibull model was found to be the best fit as it had the highest R^2 value closer to 1 and the lowest RMSE. The VCM release mechanism can be further understood using the β value, which describes the shape of the dissolution curve

progression. The calculated β value for our formulation was within the range of $0.75 < \beta < 1$, indicating that more than one release mechanism was involved. Apart from diffusion-controlled release, a pH-controlled release contributed to the release mechanism (combined release mechanism) and the shape of the dissolution profile of the formulation. This suggested that the incorporation of pH-responsive zwitterionic lipids does influence a high rate of drug release and release patterns in response to reduced pH.

4.6.5 *In vitro* antibacterial studies

4.6.5.1 *In vitro* antibacterial activity

Table 5 summarizes the *in vitro* antibacterial activity of bare VCM, VCM-loaded LPHNPs and blank LPHNPs. The efficacy of the formulations, in comparison with the bare drug, was tested using the broth dilution method to determine the MIC of the formulation at pH 7.4 and 6.0. In this study, pH 7.4 represent physiological conditions, whereas pH 6.0 (slightly acidic) represents the bacterially infected site. LPHNPs showed enhanced antibacterial activity against both *S. aureus* and MRSA at pH 7.4 and 6.0 when compared with bare VCM. According to the literature, there is high interaction of the nanosized delivery system with the bacteria due to their large surface area, thus enhancing the activity of LPHNPs when compared to bare VCM. The nanosized delivery systems can also accumulate inter- and intracellularly through binding onto or penetrating the bacterial cell membrane. Therefore, it allows for high localization of the drug at the infection site, enhancing and restoring the therapeutic outcome of the drug delivered.

The MIC values of bare VCM at pH 6.0 against both *S. aureus* and MRSA were 2-folds higher when compared to pH 7.4. The loss of activity at acidic pH could be due to the chemical degradation of VCM by the acidic environment, reducing the effective drug concentration to treat the bacteria. The formulations (VCM_RH40_LPHNPs and VCM_SH15_LPHNPs) showed a prolonged activity throughout 72 h and this can be correlated to a prolonged and sustained VCM release profile from the formulations. Effective concentration over a prolonged time can be achieved through a sustained release mechanism, thus inducing an enhanced therapeutic effect over a long period, which, therefore, can help reduce the frequency of administration and subsequent toxic side effects. The formulations demonstrated an enhanced antibacterial activity for 72 h when compared to bare VCM, which was significantly losing activity over time.

Furthermore, the efficacy of the formulations was tested at pH 7.4 and 6.0 to evaluate their pH-responsiveness against *S. aureus* and MRSA. The MIC of the formulation at both pH levels against *S. aureus* was similar, whereas, against MRSA, the MIC for both formulations was eight folds better at pH 6.0 when compared to pH 7.4. Under acidic conditions (pH 6.0), the LPHNPs undergo surface charge switching to positive as a result of protonation of the dimethylglycine head group. According to literature,

the cationic surface charged nanoparticles interact or selectively bind to the negatively charged bacterial membrane. This could lead to an enhanced antibacterial activity through target drug delivery and high localization of the drug at the infection site. Therefore, targeting the bacterial infection site by pH-responsive nanosystems could be a promising alternative treatment for enhancing antimicrobial outcome and reducing the development of bacterial resistance. Whilst the VCM-Loaded LPHNPs can improve activity of VCM, there was no pH-responsive improvement against *S. aureus*. This is contrary to MRSA, which showed enhanced antibacterial activity with respect to change in pH. According to the literature, the MIC for VCM against *S. aureus* is considered as susceptible if it is ≤ 2 µg/ml and resistant if it is > 8 µg/ml[44]. Due to high sensitivity of S. aureus to VCM under normal conditions, the slight change in VCM concentration due to pH responsive system may not show difference in MIC values. On the other hand, the low sensitivity of MRSA to VCM due to the modified cell wall may lead to a measurable change in MIC values as a result of change in the levels of VCM due to pH responsive system. Hence against MRSA there was enhanced activity with respect to change in pH.

Table 5: MIC Values of Bare VCM, Blank LPHNPs, and VCM-Loaded LPHNPs at pH 7.4 and 6.0 at different time intervals against *S. aureus* and MRSA

***In vitro* antibacterial activity at pH 7.4**						
Time (h)	**24**	**48**	**72**	**24**	**48**	**72**
	***S. aureus* (MIC µg/ml)**			**MRSA (MIC µg/ml)**		
Bare VCM	1.95	3.9	3.9	3.9	7.8	15
VCM_RH40_LPHNPs	0.97	1.95	1.95	3.9	3.9	7.8
VCM_SH15_LPHNPs	1.95	1.95	1.95	3.9	3.9	3.9
Blank_RH40_LPHNPs	NA	NA	NA	NA	NA	NA
Blank_SH15_LPHNPs	NA	NA	NA	NA	NA	NA
***In vitro* antibacterial activity at pH 6.0**						
Time (h)	**24**	**48**	**72**	**24**	**48**	**72**
	***S. aureus* (MIC µg/ml)**			**MRSA (MIC µg/ml)**		
Bare VCM	3.9	3.9	7.8	7.8	15	15
VCM_RH40_LPHNPs	0.97	1.95	1.95	0.48	0.97	0.97
VCM_SH15_LPHNPs	1.95	1.95	1.95	0.48	0.97	1.95
Blank_RH40_LPHNPs	NA	NA	NA	NA	NA	NA
Blank_SH15_LPHNPs	NA	NA	NA	NA	NA	NA

NA = No Activity

4.7 Conclusion

In addressing the global challenge of antibiotic resistance, novel biomaterials have been used in the formulation of stimuli-responsive delivery systems to improve the efficacy of the existing antibiotics. In this regard, a novel fatty acid-based zwitterionic lipid was successfully synthesized and its potential to prepare VCM-loaded pH-responsive lipid polymer hybrid nanoparticles was explored. The biocompatibility studies showed that zwitterionic DMGSAD-lipid is non-toxic for pharmaceutical and biomedical applications. Stable LPHNPs were formulated with desired size, PDI, ZP and %EE. The pH-responsiveness of LPHNPs was demonstrated by the change in surface charge and with higher VCM release at pH 6.0 when compared to pH 7.4. The *in vitro* antibacterial activity of the VCM_LPHNPs against MRSA at pH 6.0 was better than the antibacterial activity of VCM_LPHNPs and bare VCM at pH 7.4. Our findings suggest that VCM_LPHNPs formulations provide a promising and rational strategy for stable and efficient delivery of VCM to the site of infection characterized by low pH. This can potentially overcome the current public health issues of antimicrobial drug resistance

Conflict of interest

The authors declare that there is no conflict of interest.

Acknowledgment

The authors acknowledge the University of KwaZulu-Natal (UKZN), UKZN Nanotechnology Platform and the National Research Foundation (NRF) of South Africa for financial support. We also thank Biomedical Resource Unit (BRU), Microscopy and Microanalysis Unit (MMU), Flow Cytometry Research Laboratory and Department of Human Physiology at UKZN for technical assistance.

4.8 References

1. Ortwine, J. K.; Bhavan, K., Morbidity, mortality, and management of methicillin-resistant S. aureus bacteremia in the USA: update on antibacterial choices and understanding. Hospital Practice. 2018, 46 (2), 64-72.

2. Kulkarni, A. P.; Nagvekar, V. C.; Veeraraghavan, B.; Warrier, A. R.; TS, D.; Ahdal, J.; Jain, R., Current Perspectives on Treatment of Gram-Positive Infections in India: What Is the Way Forward? Interdisciplinary perspectives on infectious diseases. 2019, 2019.

3. Varaldo, P. E.; Facinelli, B.; Bagnarelli, P.; Menzo, S.; Mingoia, M.; Brenciani, A.; Giacometti, A.; Barchiesi, F.; Brescini, L.; Cirioni, O., Antimicrobial Resistance: A Challenge

for the Future. In The First Outstanding 50 Years of "Università Politecnica delle Marche", Springer. 2020, 13-29.

4. Ferri, M.; Ranucci, E.; Romagnoli, P.; Giaccone, V., Antimicrobial resistance: a global emerging threat to public health systems. Critical reviews in food science and nutrition. 2017, 57 (13), 2857-2876.

5. Sharma, A.; Kumar Arya, D.; Dua, M.; Chhatwal, G. S.; Johri, A. K., Nano-technology for targeted drug delivery to combat antibiotic resistance. Expert Opinion on Drug Delivery, 2012, 9 (11), 1325-1332.

6. Lewis, K., New approaches to antimicrobial discovery. Biochemical Pharmacology. 2017, 134, 87-98.

7. Parvathaneni, V.; Kulkarni, N. S.; Muth, A.; Gupta, V., Drug repurposing: a promising tool to accelerate the drug discovery process. Drug Discovery Today. 2019, 24 (10), 2076-2085.

8. Morel, C. M.; Lindahl, O.; Harbarth, S.; de Kraker, M. E.; Edwards, S.; Hollis, A., Industry incentives and antibiotic resistance: an introduction to the antibiotic susceptibility bonus. The Journal of Antibiotics. 2020, 73, 421–428.

9. Eleraky, N. E.; Allam, A.; Hassan, S. B.; Omar, M. M., Nanomedicine Fight against Antibacterial Resistance: An Overview of the Recent Pharmaceutical Innovations. Pharmaceutics. 2020, 12 (2), 142.

10. Singh, S.; Hussain, A.; Shakeel, F.; Ahsan, M. J.; Alshehri, S.; Webster, T. J.; Lal, U. R., Recent insights on nanomedicine for augmented infection control. International journal of nanomedicine. 2019, 14, 2301.

11. Baptista, P. V.; McCusker, M. P.; Carvalho, A.; Ferreira, D. A.; Mohan, N. M.; Martins, M.; Fernandes, A. R., Nano-strategies to fight multidrug resistant bacteria—"A Battle of the Titans". Frontiers in microbiology. 2018, 9, 1441.

12. Canaparo, R.; Foglietta, F.; Giuntini, F.; Della Pepa, C.; Dosio, F.; Serpe, L., Recent developments in antibacterial therapy: focus on stimuli-responsive drug-delivery systems and therapeutic nanoparticles. Molecules. 2019, 24 (10), 1991.

13. Caster, J. M.; Patel, A. N.; Zhang, T.; Wang, A., Investigational nanomedicines in 2016: a review of nanotherapeutics currently undergoing clinical trials. Wiley Interdisciplinary Reviews: Nanomedicine and Nanobiotechnology. 2017, 9 (1), e1416.

14. Ventola, C. L., Progress in nanomedicine: approved and investigational nanodrugs. Pharmacy and Therapeutics. 2017, 42 (12), 742.

15. Hallan, S. S.; Kaur, P.; Kaur, V.; Mishra, N.; Vaidya, B., Lipid polymer hybrid as emerging tool in nanocarriers for oral drug delivery. Artificial cells, nanomedicine, and biotechnology. 2016, 44 (1), 334-349.

16. Zhang, L.; Chan, J. M.; Gu, F. X.; Rhee, J.-W.; Wang, A. Z.; Radovic-Moreno, A. F.; Alexis, F.; Langer, R.; Farokhzad, O. C., Self-assembled lipid− polymer hybrid nanoparticles: a robust drug delivery platform. American Chemical Society nano. 2008, 2 (8), 1696-1702.

17. Kumari, A.; Yadav, S. K.; Yadav, S. C., Biodegradable polymeric nanoparticles based drug delivery systems. Colloids and Surfaces B: Biointerfaces. 2010, 75, 1-18.

18. Makadia, H. K.; Siegel, S. J., Poly lactic-co-glycolic acid (PLGA) as biodegradable controlled drug delivery carrier. Polymers. 2011, 3, 1377-1397.

19. Dos Santos, N.; Cox, K. A.; McKenzie, C. A.; van Baarda, F.; Gallagher, R. C.; Karlsson, G.; Edwards, K.; Mayer, L. D.; Allen, C.; Bally, M. B., pH gradient loading of anthracyclines into cholesterol-free liposomes: Enhancing drug loading rates through use of ethanol. Biochimica et Biophysica Acta - Biomembranes. 2004, 1661, 47-60.

20. Chaize, B.; Colletier, J. P.; Winterhalter, M.; Fournier, D., Encapsulation of enzymes in liposomes: High encapsulation efficiency and control of substrate permeability. Artificial Cells Blood Substitutes and Biotechnology. 2004, 32, 67-75.

21. Ahirwar, C. S.; Pathak, A., Insights into the Self assembled Lipid-Polymer hybrid Nanoparticles as Drug Delivery system. International Journal of Scientific Research and Management. 2017, 5 (6).

22. Karimi, M.; Ghasemi, A.; Zangabad, P. S.; Rahighi, R.; Basri, S. M. M.; Mirshekari, H.; Amiri, M.; Pishabad, Z. S.; Aslani, A.; Bozorgomid, M., Smart micro/nanoparticles in stimulus-responsive drug/gene delivery systems. Chemical Society Reviews. 2016, 45 (5), 1457-1501.

23. Mane, S. R.; Dinda, H.; Sathyan, A.; Das Sarma, J.; Shunmugam, R., Increased bioavailability of rifampicin from stimuli-responsive smart nano carrier. ACS applied materials & interfaces. 2014, 6 (19), 16895-16902.

24. Lombardo, D.; Kiselev, M. A.; Caccamo, M. T., Smart nanoparticles for drug delivery application: development of versatile nanocarrier platforms in biotechnology and nanomedicine. Journal of Nanomaterials. 2019, 2019, 26.

25. Anirudhan, T. S.; Mohan, A. M., Novel pH sensitive dual drug loaded-gelatin methacrylate/methacrylic acid hydrogel for the controlled release of antibiotics. International journal of biological macromolecules. 2018, 110, 167-178.

26. Kalhapure, R. S.; Sikwal, D. R.; Rambharose, S.; Mocktar, C.; Singh, S.; Bester, L.; Oh, J. K.; Renukuntla, J.; Govender, T., Enhancing targeted antibiotic therapy via pH responsive solid lipid nanoparticles from an acid cleavable lipid. Nanomedicine: Nanotechnology, Biology and Medicine. 2017, 13 (6), 2067-2077.

27. Yi, G.; Son, J.; Yoo, J.; Park, C.; Koo, H., Application of click chemistry in nanoparticle modification and its targeted delivery. Biomaterials research. 2018, 22 (1), 1-8.

28. Wu, W.; Luo, L.; Wang, Y.; Wu, Q.; Dai, H.-B.; Li, J.-S.; Durkan, C.; Wang, N.; Wang, G.-X., Endogenous pH-responsive nanoparticles with programmable size changes for targeted tumor therapy and imaging applications. Theranostics. 2018, 8 (11), 3038.

29. Mhule, D.; Kalhapure, R. S.; Jadhav, M.; Omolo, C. A.; Rambharose, S.; Mocktar, C.; Singh, S.; Waddad, A. Y.; Ndesendo, V. M.; Govender, T., Synthesis of an oleic acid based pH-responsive lipid and its application in nanodelivery of vancomycin. International journal of pharmaceutics. 2018, 550 (1-2), 149-159.

30. Kalhapure, R. S.; Jadhav, M.; Rambharose, S.; Mocktar, C.; Singh, S.; Renukuntla, J.; Govender, T., pH-responsive chitosan nanoparticles from a novel twin-chain anionic amphiphile for controlled and targeted delivery of vancomycin. Colloids and Surfaces B: Biointerfaces. 2017, 158, 650-657.

31. Maji, R.; Omolo, C. A.; Agrawal, N.; Maduray, K.; Hassan, D.; Mokhtar, C.; Mackhraj, I.; Govender, T., pH-Responsive Lipid–Dendrimer Hybrid Nanoparticles: An Approach To Target and Eliminate Intracellular Pathogens. Molecular pharmaceutics. 2019, 16 (11), 4594-4609.

32. Hassan, D.; Omolo, C. A.; Fasiku, V. O.; Mocktar, C.; Govender, T., Novel chitosan-based pH-responsive lipid-polymer hybrid nanovesicles (OLA-LPHVs) for delivery of vancomycin against methicillin-resistant Staphylococcus aureus infections. International Journal of Biological Macromolecules. 2020, 147, 385-398.

33. Lee, K. Y.; Mooney, D. J., Alginate: properties and biomedical applications. Progress in polymer science. 2012, 37 (1), 106-126.

34. Makhathini, S. S.; Kalhapure, R. S.; Jadhav, M.; Waddad, A. Y.; Gannimani, R.; Omolo, C. A.; Rambharose, S.; Mocktar, C.; Govender, T., Novel two-chain fatty acid-based lipids for development of vancomycin pH-responsive liposomes against Staphylococcus aureus and methicillin-resistant Staphylococcus aureus (MRSA). Journal of drug targeting. 2019, 27 (10), 1094-1107.

35. Omolo, C. A.; Kalhapure, R. S.; Jadhav, M.; Rambharose, S.; Mocktar, C.; Ndesendo, V. M.; Govender, T., Pegylated oleic acid: A promising amphiphilic polymer for nano-antibiotic delivery. European Journal of Pharmaceutics and Biopharmaceutics. 2017, 112, 96-108.

36. Cheng, X.; Yan, H.; Jia, X.; Zhang, Z., Preparation and in vivo/in vitro evaluation of formononetin phospholipid/vitamin E TPGS micelles. Journal of drug targeting. 2016, 24 (2), 161-168.

37. Walvekar, P.; Gannimani, R.; Rambharose, S.; Mocktar, C.; Govender, T., Fatty acid conjugated pyridinium cationic amphiphiles as antibacterial agents and self-assembling nano carriers. Chemistry and physics of lipids. 2018, 214 (2018), 1-10.

38. Jorgensen, J. H.; Turnidge, J. D., Susceptibility test methods: dilution and disk diffusion methods. In Manual of Clinical Microbiology, Eleventh Edition, American Society of Microbiology. 2015,1253-1273.

39. Makhathini, S. S.; Omolo, C. A.; Gannimani, R.; Mocktar, C.; Govender, T., pH-Responsive Micelles from an Oleic Acid Tail and Propionic Acid Heads Dendritic Amphiphile for the Delivery of Antibiotics. Journal of Pharmaceutical Sciences. 2020, 109 (8), 2594-2606.

40. Curcio, M.; Mauro, L.; Naimo, G. D.; Amantea, D.; Cirillo, G.; Tavano, L.; Casaburi, I.; Nicoletta, F. P.; Alvarez-Lorenzo, C.; Iemma, F., Facile synthesis of pH-responsive polymersomes based on lipidized PEG for intracellular co-delivery of curcumin and methotrexate. Colloids and Surfaces B: Biointerfaces. 2018, 167, 568-576.

41. Hamid, R.; Rotshteyn, Y.; Rabadi, L.; Parikh, R.; Bullock, P., Comparison of alamar blue and MTT assays for high through-put screening. Toxicology in vitro. 2004, 18 (5), 703-710.

42. Mosmann, T., Rapid colorimetric assay for cellular growth and survival: application to proliferation and cytotoxicity assays. Journal of immunological methods. 1983, 65 (1-2), 55-63.

CHAPTER 5,

CO-AUTHORED PAPERS

5.1 Introduction

In addition to the first authored experimental papers in Chapters, 2, 3 and 4 focusing on aims 1, 2 and 3, I have also been involved in other papers within our group as a Ph.D. student. As these papers also focused on the broad aim of this PhD project to improve treatment of bacterial infections, these papers have been included in the thesis. This chapter therefore includes one published experimental paper and one review article in an ISI International Journals: Colloids and Surfaces B: Biointerfaces (Impact Factor = 3.973) and WIREs Nanomedicine & Nanobiotechnology (Impact Factor = 7.689).

5.2 Co-authored paper 1

Self-assembled oleylamine grafted hyaluronic acid polymersomes for delivery of vancomycin against methicillin resistant *Staphylococcus aureus* (MRSA)

Walvekar, Pavan, Ramesh Gannimani, Mohammed Salih, Sifiso Makhathini, Chunderika Mocktar, and Thirumala Govender. Colloids and Surfaces B: Biointerfaces. 2019 Oct 1;182:110388. (Appendix II)

5.2.1 Abstract

MRSA infections are a major global healthcare problem associated with high morbidity and mortality. The application of novel materials in antibiotic delivery has efficiently contributed to the treatment of MRSA infections. The study aimed to develop novel hyaluronic acid oleyl amine (HA-OLA) conjugates with 25-50% degrees of conjugation, for application as a nano-drug carrier with inherent antibacterial activity. The biosafety of synthesized novel HA-OLA conjugates was confirmed by *in vitro* cytotoxicity assay. The drug loading ability of HA-OLA conjugates was confirmed by 26.1-43.12% of vancomycin (VCM) encapsulation in self-assembled polymersomes. These polymersomes were dispersed in nano-sized range (196.1-360.9 nm) with a negative zeta potential. Vancomycin loaded polymersomes were to found have spherical and bilayered morphology. The VCM loaded polymersomes displayed sustained drug release for 72 h. *In vitro* studies showed moderate antibacterial activity for HA-OLA conjugates against both *S. aureus* and MRSA with minimum inhibitory concentration (MIC) of 500 μg/mL. The VCM loaded HA-OLA polymersomes displayed four-fold lower MIC (1.9 μg/mL) than free VCM (7.8 μg/mL) against MRSA. Furthermore, synergism was observed for VCM and HA-OLA against MRSA. Flow cytometry showed 1.8-fold higher MRSA cell death in the population for VCM loaded polymersomes relative to free drug, at concentration of 1.95 μg/mL. Bacterial cell morphology showed that the drug loaded polymersomes had stronger impact on MRSA membrane, compared to free VCM. These findings suggest that, HA-OLA conjugates are promising nano-carriers to function as antibiotic delivery vehicles for the treatment of bacterial/MRSA infections.

5.3 Co-authored paper 2

Intrinsic Stimuli-Responsive Nanocarriers for Smart Drug Delivery of Antibacterial Agents – An In-Depth Review of the Last Two Decades

Nikita Devnarain, Nawras Osman, Victoria Fasiku, Sifiso Makathini, Mohammed Salih, Usri Ibrahim and Thirumala Govender. (2020). WIREs Nanomedicine & Nanobiotechnology. Manuscript ID: NANOMED-651 (In Press).

5.3.1 Abstract

Antibiotic resistance due to suboptimal targeting and inconsistent antibiotic release at bacterial infection sites has driven the formulation of stimuli-responsive nanocarriers for antibacterial therapy. Unlike conventional nanocarriers, stimuli-responsive nanocarriers have the ability to specifically enhance targeting and drug release profiles. There has been a significant escalation in the design and development of novel nanomaterials worldwide; in particular, intrinsic stimuli-responsive antibiotic nanocarriers, due to their enhanced activity, improved targeted delivery and superior potential for bacterial penetration and eradication. Herein, we provide an extensive and critical review of pH-, enzyme-, redox- and ionic microenvironment-responsive nanocarriers that have been reported in literature to date, with an emphasis on the mechanisms of drug release, the nanomaterials used, the nanosystems constructed and the antibacterial efficacy of the nanocarriers. The review also highlights further avenues of research for optimising their potential and commercialisation. This review confirms the potential of intrinsic stimuli-responsive nanocarriers for enhanced drug delivery and antibacterial killing.

CHAPTER 6.

CONCLUSION:

6.1 General conclusions

One of the greatest challenges facing modern medicine is the common occurrence of antibiotic-resistant bacterial pathogens, which have reached an alarming level throughout the world, with available treatment options gradually becoming ineffective to treat multi-drug resistant bacteria. The nano-drug delivery approach has been recognized as one of the most promising strategy to improve clinical failures of conventional antibiotic therapies by demonstrating considerable potential in restoring the effectiveness of existing antibiotics against bacterial infections. Hence, there is a high demand for advanced biomaterials to design novel drug delivery systems that can improve pharmacokinetic properties of drugs, contribute to enhance their antibacterial efficacy and to counteract AMR development. Therefore, the broad aim of this study was to design and synthesize pH-responsive fatty acid-based lipid materials, as well as explore their potential for the preparation of novel lipid-based pH-responsive delivery systems to treat *S. aureus* and MRSA infections. The specific research aims of this study were therefore, to: (1) synthesize four novel two chain fatty acid-based lipids (FAL) and employ them to deliver VCM via pH-responsive liposomes against *S. aureus* and MRSA infections; (2) synthesize novel biocompatible pH-responsive oleic acid-based dendritic lipid amphiphile and explore their potential to deliver VCM via pH-responsive micelles against *S. aureus* and MRSA infections, and (3) to synthesise novel fatty acid-based bi-tailed pH-responsive zwitterionic DMGSAD-lipid and explore their potential to deliver VCM via pH-responsive LPHNPs against *S. aureus* and MRSA infections.

The main conclusions generated from the research data are summarised below:

Aim 1

- Four novel pH-sensitive two chain fatty acid-based lipid derivatives (stearic, oleic, linoleic, and linolenic acid derivatives) were successfully synthesized, and their structures were confirmed using FT-IR, ^{1}H and ^{13}C NMR and HRMS.
    - Di -Stearoyl Amino Propionic acid tert-butyl Ester (DSAPE)
    - Di - Oleoyl Amino Propionic acid tert-butyl Ester (DOAPE)
    - Di- Linoleoyl Amino Propionic acid tert-butyl Ester (DLAPE)
    - Di- LinoLenoyl Amino Propionic acid tert-butyl Ester (DLLAPE)

- The cytotoxicity study using MTT assay on three different mammalian cell lines i.e., adenocarcinoma alveolar basal epithelial cells (A549), liver hepatocellular carcinoma (HepG2) cell lines and human breast adenocarcinoma (MCF7), showed that the synthesized lipids were biosafe.
- The synthesized four lipids were used in the formulation of VCM-loaded pH-responsive liposomes. The formulated liposomes were stable with mean vesicle diameters and PDI of between 86.28 ± 11.76 to 282 ± 31.58 nm and 0.161 ± 0.003 to 0.151 ± 0.016 to 0.204 ± 0.014 at different pHs, respectively. The ZP values were negative at physiological pH (7.4) and shifted towards positivity with a decrease in pH. The %EE and loading capacity were in the range of 29.86 ± 4.5% and 44.27 ± 9.2%, respectively. The VCM release increased and was more sustained at acidic pH than at the physiological pH.
- Enhanced antibacterial activity at pH 6.0 was observed for the DOAPA-VAN-Lipo and DLAPA-VAN-Lipo formulations. Flow cytometry studies indicated a high killing rate of MRSA cells using DOAPA-VAN-Lipo (71.98%) and DLAPA-VAN-Lipo (73.32%) at the MIC of 1.59 µg/ml. *In vivo* studies showed reduced MRSA recovered from mice treated with formulations by 4- and 2-folds lower than bare VAN-treated mice, respectively.

Aim 2

- Novel pH-responsive oleic acid-based dendritic lipid amphiphile (OLA-SPDA) was successfully synthesized and structurally confirmed using FT-IR and ^{1}H and ^{13}C NMR.
- Cytotoxicity studies performed using an MTT assay on three mammalian cell lines, HEK-293, human liver hepatocellular carcinoma (HEP G2) and adenocarcinoma human alveolar basal epithelial (A549) revealed that the synthesized OLA-SPDA lipid is biosafe.
- pH-responsive oleic acid-based dendritic lipid amphiphile self-assembled into stable micelles with particle size, PDI, ZP and %EE of 84.16 ± 0.184 nm, 0.199 ± 0.011 and -42.6 ± 1.98 and 78.80 ± 3.26%, respectively. The micelles demonstrated pH-responsiveness with an increase in particle size to 141.1 ± 0.070 nm and a much faster release profile at pH 6.0, as compared to pH 7.4 (84.16 ± 0.18 nm). The *in vitro* VCM release from micelles was sustained compared to free VCM.
- The MIC of VCM-OLA-SPDA-micelle against MRSA was 8-fold lower compared to bare VCM, and the formulation had a 4-fold lower MIC at pH 6.0 when compared to the

formulation's MIC at pH 7.4. MRSA viability assay showed the micelles had a percentage killing of 93.39% when compared bare VCM (58.21%) at the same MIC (0.98 µg/ml). *In vivo* mice (BALB/c) skin infection models showed an 8-fold reduction in MRSA burden after treatment with VCM-OLA-SPDA-micelles when compared with bare VCM.

Aim 3

- The successful synthesis of novel fatty acid-based bi-tailed pH-responsive zwitterionic DMGSAD-lipid was confirmed using FT-IR and ^{1}H and ^{13}C NMR.
- The cytotoxicity studies performed using an MTT assay on three mammalian cell lines, cervical cancer cell lines (HeLa), human breast adenocarcinoma (MCF-7) and human embryonic kidney cells 293 (HEK 293) confirmed the synthesized DMGSAD-lipid to be biosafe for *in vivo* application.
- Screening of surfactant revealed that using RH40 and HS15 gave the optimal formulation of LPHNPs.
- The optimize formulations RH40_VCM_LPHNPs and SH15_VCM_LPHNPs showed pH-responsiveness through a significant change in surface charge from 0.55 ± 0.14Vm to 9.44 ± 0.33 Vm and from -1.55 ± 0.184 to 9.83 ± 0.52 Vm at 7.4 and 6.0, respectively.
- The *in vitro* VCM release from LPHNPs was sustained compared to free VCM.
- The antibacterial efficacy of VCM loaded LPHNPs was 8 fold better at pH 6.0 when compared to pH 7.4.

The findings of this study, therefore, confirmed that the synthesized novel lipids were biosafe for biomedical applications. These lipids displayed great potential in the formulation of lipid-based nano-carriers to encapsulate antibiotics (VCM) and treat *S. aureus* and MRSA infections more efficiently than the free drug under acidic conditions. In addition to their ability to encapsulate therapeutic agents, these novel materials also hold great potential in delivering any drug class for the treatment of a variety of infections characterized by acidic conditions. The additional experimental paper presented in Chapter 5 as a co-author, confirmed the potential of a novel self-assembled polymeric conjugate (HA-OLA) for the treatment of bacterial infections. Also, the review article in Chapter 5 elucidates the potential of different intrinsic stimuli-responsive nanocarriers for the treatment of bacterial infections.

6.2 Significance of the findings in the study

The newly synthesized materials and designed nano-formulations, VCM-loaded pH-responsive liposome, micelles and LPHNPs were successfully employed to address the limitations associated with conventional dosage forms of antibiotics and antibacterial resistance. The significance of the findings in this study include the following:

New pharmaceutical products*:* This study has generated new pharmaceutical materials, i.e., two chain fatty acid-based lipid derivatives (DSAPE, DOAPE, DLAPE and DLLAPE), OLA-SPDA and fatty acid-based bi-tailed DMGSAD-lipid. This will expand the range of the available pharmaceutical excipients for preparing new medicines, which can stimulate local pharmaceutical industries to manufacture superior cost-effective medicines

Improved patient therapy and disease treatment*:* The newly designed VCM-loaded pH-responsive liposome, micelles and LPHNPs nanosystems were formulated successfully with improved antibacterial efficacy against *S. aureus* and MRSA infections. These novel nano-systems lowered the MIC of the loaded drugs significantly and can effectively control the infection with reduced dosing frequency without affecting therapeutic outcomes at low pH conditions. These findings, therefore, prove the potential of these novel lipid nano-systems in improving patient therapy and treatment of bacterial infections, and thereby ultimately improving the quality of patients' lives as well as save lives.

Creation of new knowledge to the scientific community*:* The various studies and their findings have contributed to the pharmaceutical sciences knowledge database in several ways. These include the following:

- New synthetic pathways, characterization and determination of the toxicity profiles of novel two chain fatty acid-based lipid derivatives (DSAPE, DOAPE, DLAPE and DLLAPE), OLA-SPDA and DMGSAD-lipid were developed. The *in vitro* and *in vivo* evaluation of drug-loaded nano-systems can add to the conception of new knowledge.
- Formulation and process parameters of VCM-loaded pH-responsive liposomes, VCM-OLA-SPDA-micelles and VCM-LPHNPs were identified using various experimental techniques.

- By combining novel materials having intrinsic antibacterial activity and an antibiotic, a strategy for achieving synergistic antibacterial activity in nano-vesicular form was described.
- For all the pH-responsive formulations, VCM-loaded liposome, VCM-OLA-SPDA-micelles and VCM-LPHNPs, there was a correlation of results generated from the antimicrobial activity study through *in vitro* MIC determination and *in vivo* antibacterial mice infection models of the developed novel nano-drug delivery system.

***Stimulation of new research**:* The research findings of the various studies and the successful development of VCM-loaded pH-responsive liposomes, micelles and LPHNPs can stimulate new research areas, including the following:

- The newly synthesized novel two chain fatty acid-based lipid derivatives (DSAPE, DOAPE, DLAPE and DLLAPE), OLA-SPDA lipid and DMGSAD-lipid can be utilized for delivering other classes of drugs to treat various disease conditions, such as cancer, HIV/AIDS, fungal infections, gene therapy-related diseases and metabolic diseases.
- Besides bacterial infections, pH-responsive liposomes, OLA-SPDA-micelles and LPHNPs can also assist to treat other diseases that are associated with low pH conditions, such as tumors
- Delivery of antibiotics using an antibacterial nano-carrier can contribute to combination therapy in combating bacterial infections more effectively.

6.3 Recommendations for future studies

Although VCM-loaded pH-responsive liposomes, VCM-OLA-SPDA-micelles, VCM-LPHNPs displayed great prospects as novel nano-drug delivery systems to eradicate the problem of bacterial resistance, additional studies are necessary to further explore and improve their potential to ensure eventual regulatory approval for patient use. The following studies are proposed:

- In the case of VCM-loaded pH-responsive liposomes, molecular dynamic (MD) simulations could be performed to show the binding affinity of the positively charged liposome surface to a negatively charged bacterial membranes.

- The successfully developed liposome, micelles and LPHNPs for VCM delivery can be loaded with different classes of antibiotics and tested against various bacterial strains to evaluate their synergism and advantages over different antibiotics.
- Simultaneous delivery of multiple antibiotics from these nano-systems can be explored to achieve enhanced and synergistic activities.
- Encapsulation of multiple hydrophilic as well as hydrophobic drugs in these vesicular nano-systems can be explored.
- Application of these lipids as surfactants to stabilize other nanoparticulated systems such as SLNs, PLNs etc., can be studied.
- Further studies including cytotoxicity studies using macrophages and other cell lines is recommended
- *In vivo* intravenous infection model, bioavailability and pharmacokinetic studies followed by clinical trials on both the developed nano-systems could be performed to achieve approval for market introduction.
- *In vivo* acute, intermediate and long-term toxicity study models can be performed to determine the full toxicological profile of the material and the formulations reported in this study.
- Antibacterial testing using VRSA could be performed to evaluate the enhanced efficacy of our novel nanomaterials.
- A method for the bulk production of the nano-systems presented in this study could be developed to enable their applications for pharmaceutical industries.

6.4 Conclusion

The findings of this study therefore specifically demonstrate the potential of the newly developed pH-responsive liposomes, OLA-SPDA-micelles and LPHNPs as nano-carriers having inherent antibacterial activity as well as their drug delivery potential, for improving the treatment of *S. aureus* and MRSA infections. This current research has therefore made significant contributions to nano-based approaches to overcome limitations of current/conventional dosage forms. The study further directed a way towards the synthesis of novel pH-responsive lipid materials to develop multifunctional nano-systems to treat bacterial infections characterized by low pH

conditions. The understanding of novel antibacterial materials and nanotechnology to address the current global antibiotic drug therapy crisis will be dependent on future intensive and multidisciplinary research. This strategic approach will play a vital role in improving the treatment of bacterial infections as well as other diseases that are associated with bacterial infections, thereby saving lives and improving the quality of lives of communities.

Appendix I

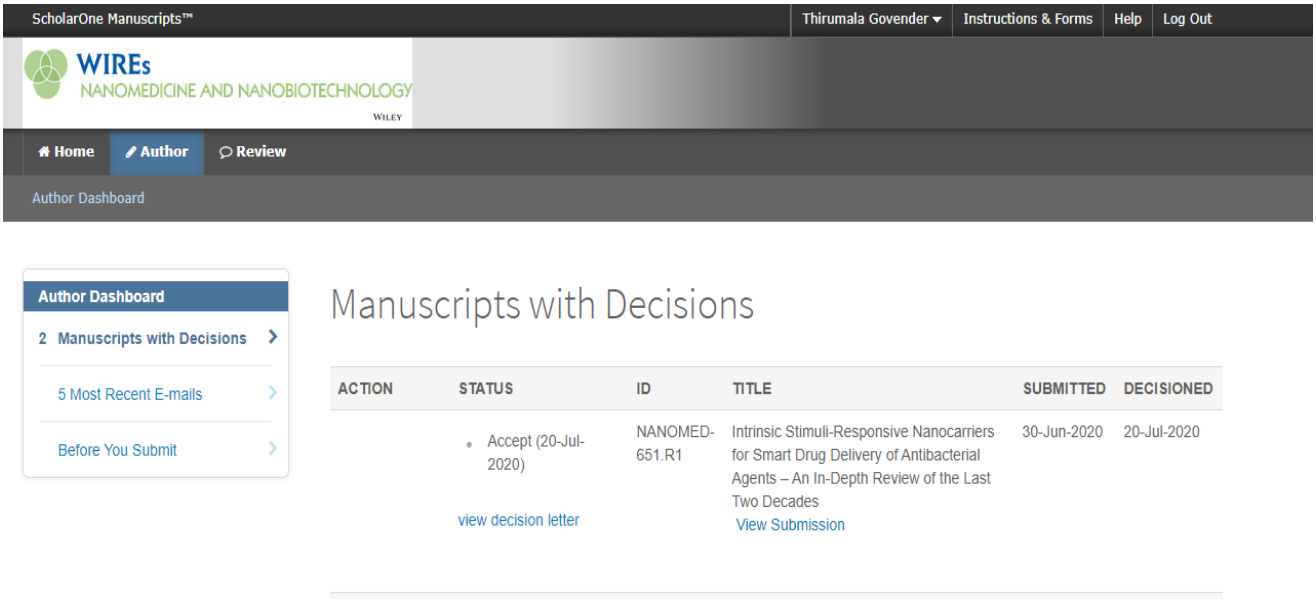
ScholarOne Manuscripts™
Thirumala Govender
Instructions & Forms
Help
Log Out
WIREs
NANOMEDICINE AND NANOBIOTECHNOLOGY
WILEY
Home
Author
Review
Author Dashboard
Author Dashboard
2 Manuscripts with Decisions
5 Most Recent E-mails
Before You Submit
Manuscripts with Decisions
ACTION
STATUS
ID
TITLE
SUBMITTED
DECISIONED
Accept (20-Jul-2020)
view decision letter
NANOMED-651.R1
Intrinsic Stimuli-Responsive Nanocarriers for Smart Drug Delivery of Antibacterial Agents – An In-Depth Review of the Last Two Decades
View Submission
30-Jun-2020
20-Jul-2020

1759

Appendix II

Colloids and Surfaces B: Biointerfaces 182 (2019) 110388

Contents lists available at ScienceDirect

Colloids and Surfaces B: Biointerfaces

journal homepage: www.elsevier.com/locate/colsurfb

Self-assembled oleylamine grafted hyaluronic acid polymersomes for delivery of vancomycin against methicillin resistant *Staphylococcus aureus* (MRSA)

Pavan Walvekar, Ramesh Gannimani, Mohammed Salih, Sifiso Makhathini, Chunderika Mocktar, Thirumala Govender*

Discipline of Pharmaceutical Sciences, School of Health Sciences, University of KwaZulu-Natal, Private Bag X54001 Durban, 4000, South Africa

ARTICLE INFO

Keywords:
Hyaluronic acid-oleylamine conjugates
Inherent antibacterial activity
Self-assembly
Vancomycin delivery
Enhanced antibacterial activity

ABSTRACT

MRSA infections are a major global healthcare problem associated with high morbidity and mortality. The application of novel materials in antibiotic delivery has efficiently contributed to the treatment of MRSA infections. The aim of the study was to develop novel hyaluronic acid-oleylamine (HA-OLA) conjugates with 25–50% degrees of conjugation, for application as a nano-drug carrier with inherent antibacterial activity. The biosafety of synthesized novel HA-OLA conjugates was confirmed by *in vitro* cytotoxicity assay. Drug carrying ability of HA-OLA conjugates was confirmed by 26.1–43.12% of vancomycin (VCM) encapsulation in self-assembled polymersomes. These polymersomes were dispersed in nano-sized range (196.1–360.9 nm) with a negative zeta potential. Vancomycin loaded polymersomes were found to have spherical and bilayered morphology. The VCM loaded polymersomes displayed sustained drug release for 72 h. *In vitro* studies showed moderate antibacterial activity for HA-OLA conjugates against both *S. aureus* and MRSA with minimum inhibitory concentration (MIC) of 500 μg/mL. The VCM loaded HA-OLA polymersomes displayed four-fold lower MIC (1.9 μg/mL) than free VCM (7.8 μg/mL) against MRSA. Furthermore, synergism was observed for VCM and HA-OLA against MRSA. Flow cytometry showed 1.8-fold higher MRSA cell death in the population for VCM loaded polymersomes relative to free drug, at concentration of 1.95 μg/mL. Bacterial cell morphology showed that the drug loaded polymersomes had stronger impact on MRSA membrane, compared to free VCM. These findings suggest that, HA-OLA conjugates are promising nano-carriers to function as antibiotic delivery vehicles for the treatment of bacterial/MRSA infections.

1. Introduction

Resistant strains of *Staphylococcus* bacteria are currently a significant factor contributing to deterioration of the health status in infected individuals, thus causing premature mortality [1]. Predominantly, MRSA has acquired resistance to virtually all potent antibiotics, making it extremely difficult to eliminate from the host, thus challenging current drug therapy [2]. Vancomycin (VCM) being the drug of choice to treat MRSA infections, has also capitulated to resistance to some of the isolates, known as vancomycin resistant *Staphylococcus aureus* [3]. Therefore, there is a need for novel and innovative approaches to treat MRSA infections effectively. In recent years, nano drug delivery systems have attracted large interest in the treatment of bacterial infections, because of their ability to target specific infection sites, thus increasing localized drug concentration; to provide sustained drug release, thus lowering the frequency of administration; and to improve physico-chemical properties of drugs *etc.* This can lead to improved therapeutic outcomes and patient compliance and can overcome drug resistance mechanisms [4]. Numerous antibiotic-loaded nano-systems are being reported for combating bacterial infections [5–7]. Therefore, antibiotic loaded nano-systems may efficiently overcome MRSA infections.

Among the various nano drug delivery systems, polymeric nano-systems have gained considerable interest to deliver therapeutic agents and treat many diseases. Polymeric nano-systems are considered to be more stable and reliable than other organic nano-platforms such as lipidic systems [8,9]. For example, liposomes tend to lose their structural configuration upon storage thus resulting in leakage of encapsulated payloads. However, polymeric nano-systems are comparatively more robust and stable, and do not lose their integrity during long term

* Corresponding author at: Private Bag X54001 Durban, 4000, KwaZulu-Natal, South Africa.
E-mail address: govenderth@ukzn.ac.za (T. Govender).

https://doi.org/10.1016/j.colsurfb.2019.110388
Received 9 May 2019; Received in revised form 15 July 2019; Accepted 23 July 2019
Available online 25 July 2019
0927-7765/

1760

storage. Furthermore, polymeric nano-systems can facilitate sustained/controlled, targeted and intracellular drug delivery to improve the therapeutic efficacy of encapsulated payloads [7,10]. In addition to these advantages, polymers with surface functionalities can be easily structurally modified with other compounds to make graft or block copolymers that can suit various drug delivery applications. For example, hyaluronic acid was grafted with poly(L-histidine) for the preparation of pH responsive and tumor-targeted amphiphilic copolymer for use as a carrier for anticancer drugs [11].

Various naturally occurring, synthetic and semi-synthetic polymers such as chitosan, dextran, polylactic acid, polyglycolic acid, poly(lactic-co-glycolic acid), polyacrylic acid, methyl cellulose *etc*, have been used to construct nano-drug delivery systems to deliver therapeutic agents. These nano-systems have shown promising outcomes thus far in treating many diseases including bacterial infections [6]. Recently, hyaluronic acid (HA), a naturally occurring biodegradable hydrophilic polymer has captured considerable attention in designing various drug delivery nanotherapeutics. Many reports on HA-based nano-systems can be found in the literature to deliver anticancer drugs [12]. The application of HA to construct antibiotic loaded nano-systems may display improved and synergistic antibacterial activity because of its inherent bacteriostatic and antibiofilm effects against certain strains [13,14]. Some evidences have also been documented where, polycarboxylic acids such as HA are shown to lower the pH of infection, thus creating an environment where pathogens find it difficult to survive [15]. Furthermore, HA is also known to possess wound healing, tissue regeneration and anti-inflammatory properties, which may help to cure dermal infections and facilitate quick recovery [16]. Recently, Zhu et al. reported HA-based nanogel loaded with chlorhexidine diacetate (an antibacterial agent) to demonstrate prolonged antimicrobial activity against *S. aureus* and *E. coli* followed by accelerated hemostasis and wound healing [16]. Therefore, there is a need for novel HA-based polymeric nano-systems to be used as antibiotic carriers to combat bacterial infections.

Self-assembling amphiphiles are considered as one of the most prominent and promising candidates for drug delivery applications [17]. HA is a completely hydrophilic polymer, and cannot self-organise to form nano-assemblies on its own. Therefore, an additional support is needed from a hydrophobic moiety to make it an amphiphile. Biodegradable hydrophobic long fatty chains are one class of compounds that have been frequently used to make amphiphiles [18]. Furthermore, long fatty chains have also been reported to enhance the activity of other antibacterial agents [19,20]. The grafting of these hydrophobic long fatty chains with hydrophilic HA can make ideal amphiphilic drug cargoes. HA can be grafted with oleylamine (a long fatty chain) at certain degrees of conjugation to synthesize hyaluronic acid-grafted-oleylamine amphiphiles. To date, no HA-fatty amine conjugates have been used to deliver antibiotics.

Our research group has primarily been focussing on developing various novel nano-systems to deliver VCM for combating MRSA infections. Amongst, various other nano-systems, we have developed polyacrylic acid, chitosan and dextran sulphate based polymeric nano-systems to deliver VCM, and fight MRSA infections [21–23]. In these findings, we have achieved decent entrapments for VCM with sustained and improved antibacterial activities against MRSA. In addition, these nano-formulations also enabled ease of preparation with good physical stability, which may enable the future commercialization of these VCM nano-systems. In continuation of our efforts to develop novel polymers, in this study, hydrophilic HA was grafted with hydrophobic oleylamine (OLA) to promote self-assembly and simultaneous encapsulation of VCM to combat MRSA infections. To the best of our knowledge, VCM has not been delivered using HA based polymeric nano-system to fight MRSA infections. Therefore, this research undertaken aimed to synthesize a novel amphiphile comprising of hydrophilic HA and hydrophobic oleylamine (fatty chain) for the formulation of self-assembled nano-carriers to deliver VCM and treat MRSA infections.

2. Materials and methods

Hydrochloride form of vancomycin was purchased from Sinobright Import & Export Co. Ltd. (China). 1-Ethyl-3- (3-dimethylaminopropyl) carbodiimide hydrochloride (EDC.HCl) was acquired from Carbosynth (UK). Oleylamine (≥ 98%) and Mueller Hinton Broth-2 (MHB) was procured from Sigma Aldrich (USA). N-Hydroxysuccinimide (NHS) was purchased from Sigma-Aldrich (Japan) Sodium hyaluronate (9.47 KDa) was purchased from Spec-Chem IND. INC. MTT (3-(4, 5-dimethylthiazol-2-yl)-2, 5-diphenyltetrazolium bromide) was purchased from Alfa Aesar (UK), Mueller Hinton Agar (MHA), Nutrient Agar and Nutrient Broth were obtained from Biolab (South Africa). The dialysis tube (MWCO 14,000 Da) was purchased from Sigma-Aldrich (USA) for drug release studies. Double distilled water obtained from a Direct-Pure EDI water system was used throughout the experiment. Gram positive bacteria, *Staphylococcus aureus* (*S. aureus*, ATCC 25923) & methicillin resistant *Staphylococcus aureus* (MRSA, ATCC 700699) were used to study the antibacterial activity.

2.1. Synthesis and characterization of HA-OLA conjugates

As sodium hyaluronate was not freely soluble in formamide, sodium salt of HA was converted to HA, to facilitate the reaction. Briefly, 2 g of sodium hyaluronate was dissolved in water, and 48 mL of 1 M HCl was added slowly to the solution, followed by stirring for two hours. The obtained solution was freeze dried to obtain HA. Synthesis of HA-OLA with various degrees of conjugation (50%, 33% and 25%) was planned to evaluate the self-assembling behaviour of HA after conjugation with OLA. Synthesis of HA-OLA conjugates were performed in one pot reaction as indicated in Scheme 1. EDC/NHS coupling chemistry was used to graft OLA to carboxylic acid groups of HA. Considering the molecular

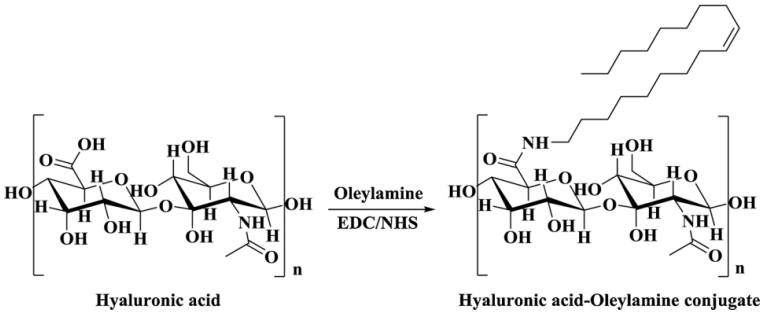

Scheme 1. Synthesis of HA-OLA conjugates.

weight of HA, ~24 carboxylic acids were calculated per molecule. As OLA conjugated to 50% of carboxylic acids of HA became too hydrophobic, and did not self-assemble, it was not considered suitable for the present study. To synthesize 33% of conjugation, briefly, 500 mg of HA was allowed to completely dissolve in formamide, followed by sequential addition of 113 mg (8 equivalents) of OLA, 48.6 mg (8 equivalents) of NHS and 162 mg (16 equivalents) of EDC, and allowed to react for 48 h. The resulting reaction mixture was dialysed (MWCO = 3500 Da) against water for two days to purify the polymer. Further, the polymer solution was freeze dried to obtain HA-OLA conjugates. To yield 25% of conjugation, the same procedure was followed, where OLA, NHS and EDC used were 84.8 mg (6 equivalents), 36.4 mg (6 equivalents) and 121.7 (12 equivalents) respectively. As twelve, eight and six carboxylic acids were targeted for conjugation, HA-OLA conjugates with 50%, 33% and 25% of conjugation were termed as HA-OLA12, HA-OLA8 and HA-OLA6 respectively. The HA-OLA conjugates were characterized by FTIR and ^{1}H NMR spectroscopy (D_2O).

2.2. MTT assay

To evaluate the biosafety of the synthesized novel HA-OLA conjugates, MTT assay was performed on human embryonic kidney cells (HEK-293), human cervix adenocarcinoma (HeLa) cells and human breast adenocarcinoma cells (MCF-7) according to previously published method [24]. Briefly, cell lines grown at 37 °C under humidified atmosphere of 5% CO_2 were seeded at a density of 3.0×10^3 cells in 96-well plates and incubated for 24 h. Thereafter, cells were treated with test compounds (HA-OLA6 and HA-OLA8) at various concentrations (20–100 μg/mL) and allowed to incubate for 48 h. Thereafter, the spent culture medium was replaced with 100 μL of fresh medium and 20 μL of MTT (5 mg/mL in PBS) in each well and incubated for 4 h, followed by the removal of the used medium and addition of 100 μL of DMSO to dissolve the MTT formazan crystals. The absorbance was recorded at 570 nm using a microplate spectrophotometer (Spectrostar nano, Germany). Untreated cells in the culture medium was used as negative control. The study was performed in pentaplicates, and the percentage cell viability was calculated as follows.

$$\%\,\text{Cell viability} = \left(\frac{\text{A570 nm treated cells}}{\text{A570 nm untreated cells}}\right) \text{X } 100\%$$

2.3. Preparation of VCM loaded HA-OLA polymersomes

The VCM loaded polymersomes were prepared using a probe ultrasonication technique [25]. Since, HA-OLA12 became highly hydrophobic, and did not self-assemble, it was therefore not included in the optimization process of polymersomes. Briefly, specified amounts of HA-OLA6 or HA-OLA8 conjugates were dispersed in 10 mL of water containing VCM (5/10 mg). The resulting mixture was ultrasonicated at 30% amplitude for 10 min under, cold water bath to obtain VCM loaded polymersomes of nano-sized range. Empty polymersomes were prepared using the same procedure by excluding VCM. All formulations in optimization process were prepared in triplicate.

2.4. Size, polydispersity index (PDI), zeta potential (ZP), morphology and stability

The determination of size, PDI and ZP of polymersomes was achieved through a zeta sizer (Nano ZS90, Malvern Instruments Ltd., UK) at 25 °C, without further dilution. Prior measurement, the polymersomes suspension were filtered through a 0.45 μm membrane filter to obtain a dust-free nano-system. Morphological characterisation of drug loaded polymersomes was investigated using a transmission electron microscopy (TEM - Jeol, JEM-1010, Japan). The samples were prepared and captured as previously reported [26].

A previously reported protocol was followed to assess the stability of polymersomes [25]. The stability of HA-OLA6 polymersomes in the presence of 10% FBS was measured by dynamic light scattering (DLS) technique at 37 °C. HA-OLA6 polymersomes were dissolved in DMEM containing 10% FBS, and incubated in a shaking incubator at 100 rpm and 37 °C. The mean particle diameter (n = 3) of polymersomes were obtained every 24 h for three consecutive days.

2.5. Entrapment efficiency (%EE) and drug loading capacity (DLC)

An ultrafiltration method was employed for the determination of % EE of VCM loaded polymersomes. Briefly, 2 mL of drug loaded polymersomes was placed in Amicon® Ultra-4 centrifugal filter tubes (MWCO, 10 kDa), and centrifuged at 3000 rpm at 25 °C for 30 min. The un-entrapped drug in the filtrate was assayed using reversed-phase high performance liquid chromatography (HPLC), Shimadzu Prominence DGU-20A3 with UV detection at 280 nm. A Nucleosil 120-5 C18 column (4 × 150 mm, 5 μm) was used, and the mobile phase consisted of acetonitrile:0.1% TFA in water (15:85 v/v). The flow rate and injection volume were 1 mL/min and 100 μL, respectively. The %EE and DLC were determined using the following equations [26].

$$\%\text{EE} = \left(\frac{\text{Amount of VCM in polymersomes}}{\text{Amount of VCM added}}\right) \text{X } 100$$

$$\%\text{DLC} = \left(\frac{\text{Amount of VCM in polymersomes}}{\text{Total weight of polymersomes}}\right) \text{X } 100$$

2.6. Differential scanning calorimetry (DSC)

DSC (Shimadzu DSC-60, Japan) was employed to study the thermal behaviours of free VCM, HA-OLA6, physical mixture (drug and the polymer) and lyophilized drug loaded polymersomes. Approximately, two mg of samples were transferred and sealed in an aluminium pan, which was further heated to 300 °C at a constant rate (10 °C/min) under a constant nitrogen flow (20 mL/min) using an empty pan as reference.

2.7. In vitro drug release

The release profiles of free VCM and VCM loaded polymersomes were studied using the dialysis bag method in PBS (pH 7.4) at 37 °C [27]. Both free VCM and VCM loaded polymersomes, each of 1 mL were loaded separately into dialysis bags (MWCO 14,000 Da). The loaded tubings were tightly sealed and dialyzed against 40 mL of PBS at 37 ± 0.5 °C in a shaking incubator at 100 rpm. At defined time intervals, 3 mL samples were withdrawn from the dissolution media and replaced with an equal amount of fresh PBS to maintain a uniform volume and sink condition. The amount of VCM present in the samples was measured spectrophotometrically at 280 nm using HPLC (as specified in Section 2.5). The study was performed in triplicate. *In vitro* drug release kinetics and analysis were determined using DD Solver. Zero order, first order, Higuchi, Hixon-Crowell, Korsmeyer-Peppas and Weibull models. The parameters such as correlation coefficient (R^2), root mean square error (RMSE) and mean dissolution time (MDT) were calculated to determine the release kinetics and best fit model.

2.8. Antibacterial activity

2.8.1. In vitro antibacterial activity

The *in vitro* antibacterial effects of free VCM, free HA, HA-OLA6, HA-OLA8, and VCM loaded polymersomes (made up of HA-OLA6 and HA-OLA8) were studied against *S. aureus* and MRSA by determining MIC using broth dilution technique [28]. *S. aureus* and MRSA cultures were grown overnight in Nutrient Broth at 37 °C in a shaking incubator at 100 rpm. The overnight grown cultures were diluted with sterile distilled water to achieve a concentration equivalent to 0.5 MacFarland

standard using a DEN-1B densitometer (Latvia). MHB (135 µL) was added to 96 well plates. Further, 135 µL of test samples were added in the first well and were serially diluted. The 0.5 MacFarland bacterial suspension were further diluted to 1:150 with sterile distilled water to achieve a final concentration equivalent to 5×10^5 colony forming units (CFU)/mL. The diluted bacterial culture (15 µL) was added to 96 well plates containing the mixture of MHB and the test samples. The plates were placed in a shaking incubator (100 rpm) at 37 °C for 24 h. MIC was determined as the lowest concentration that inhibited bacterial growth. The MIC was determined by spotting 10 µL of each broth on MHA plates followed by incubation for 24 h at 37 °C. The spotting was repeated for the next two days, *i.e.*, at 48 h and 72 h. The study was performed in triplicate.

Σ Fractional Inhibitory Concentration (FIC) was used to study the combined effect of novel HA-OLA6 and VCM in VCM loaded polymersomes against both *S. aureus* and MRSA. ΣFIC was calculated on the basis of MIC data that was generated by *in vitro* antibacterial study. A previously reported method was followed to calculate the FIC [26]. The ΣFIC was calculated using the following equations and Table S1 (Supplementary material).

FIC (VCM) = MIC of VCM in combination with HA-OLA6/MIC of HA-OLA6

FIC (HA-OLA6) = MIC of HA-OLA6 in combination with VCM/MIC of VCM

ΣFIC = FIC (VCM) + FIC (HA-OLA6)

2.8.2. Flow cytometry bacterial cell viability

A flow cytometry assay was employed to study the cell viability of MRSA cells after treatment with free VCM and VCM-loaded polymersomes for 18 h [29]. The bacterial cultures were prepared as previously described in Section. 2.8.1. Sterile distilled water (135 µL) was added to the 96 well plate. Further, 135 µL of free VCM (positive control) and VCM-loaded polymersomes were added to the plate, and were serially diluted. Thereafter, bacterial suspension (15 µL) containing 5×10^5 CFU/mL was added at respective MICs of test samples, and incubated at 37 °C in a shaking incubator (100 rpm). To flowcytometry tubes containing 350 µL of the sheath fluid, free VCM and VCM loaded polymersomes treated broths were added and vortexed for five minutes. The tubes containing sheath fluid and test samples were further incubated for 30 min with 5 µL of propidium iodide (PI) and Syto9, which served as cell wall impermeable and permeable dyes, respectively. The fluorescence of PI was excited at 455 nm and collected through a 636 nm bandpass filter (red wavelength), whereas Syto9 excited at 485 nm, and collected at 498 nm (green wave length). Pure untreated MRSA cells were used as a negative control. A flow cytometer (BD FACSCanto II, Becton Dickinson, USA) was used for the experiment. Sheath fluid and sample flow rate were set at 16 mL/min and 0.1 mL/min, respectively. BD FACSDiva v8.0.1 (a flow cytometer software) was used to collect the data for fixed cells [30]. To analyse fluorescence-activated cell sorting, the voltage settings were, 731, 538, 444 and 451 for forward scatter, side scatter, PI and Syto9, respectively. The MRSA cells were initially gated using forward scatter, further, cells of appropriate size were gated and at least 10,000 cells were collected. The study for each sample was performed in triplicate, and position of the 'live' and 'dead' cells gates were determined. The detection threshold was set to 1000 in side scatter analysis to avoid any background signal from particles smaller than bacteria [31].

2.8.3. Bacterial killing kinetics

Free VCM and VCM-PS6 were added at concentrations equivalent to five times the MIC to the MRSA culture (5×10^5 CFU/mL). Sterile water was added to MRSA broth, which served as a control. Bacterial killing kinetics was monitored from 0 h to 24 h. At defined time periods (0, 1, 2, 4, 6, 8, 12 and 24 h), the samples were collected in sterile eppendorf tubes and serially diluted three times (1 : 10) with sterile water. The diluted broths were plated in triplicate on Mueller Hinton Agar plates, and incubated for 48 h at 37 °C. Thereafter, the total number of colonies were counted and converted to $\log_{10}$ values, followed by plotting a graph [32].

2.8.4. Bacterial cell morphology

VCM acts on the cell-wall of bacteria therefore, a membrane disruption study was undertaken using high resolution transmission electron microscopy (HRTEM). The study was performed for free VCM, VCM-PS6 and untreated MRSA, where, the former and latter served as positive and negative controls, respectively. Briefly, MRSA suspension (5×10^5 CFU/mL) was incubated with free VCM (500 µg/mL) and VCM-PS6 containing 500 µg/mL of VCM, at 1:1 ratio separately for 4 h. The test samples were fixed onto the surface of copper grids followed by drying. The images were captured using JEOL HRTEM 2100 (bright-field, darkfield, STEM diffraction).

2.9. Statistical analysis

The results obtained were reported as mean ± standard deviation (SD) and the data analysis was performed using GraphPad Prism®5 (Graphpad Software Inc., USA). Bonferroni's Multiple Comparison Test and One-way ANOVA were used to analyse the data and the difference was considered significant when $p < 0.05$.

3. Results and discussion

3.1. Synthesis

The conjugation of OLA to the carboxylic groups of HA was confirmed by FTIR and ^{1}H NMR studies. The spectra included in the supplementary material shows the comparative FTIR and ^{1}H NMR spectra of free HA and HA-OLA conjugates. The changes that appeared in the infrared vibrational frequencies of HA chemical bonds, provided a preliminary confirmation of the grafting of OLA to HA. The parent HA was characterised by the presence of peaks at 1725 cm^{-}1 and 1648 cm^{-}1 in the FTIR spectra, which corresponded to the carbonyl groups of carboxylic acids and acetamide bonds, respectively. After the grafting of HA with OLA, the peak at 1648 cm^{-}1 was shifted to 1643 cm^{-}1. In addition, the intensity of the peak was increased, which was due to the increase in the number of amide bonds after the conjugation of OLA to HA. Both HA and HA-OLA conjugates contained broad peaks at ~3298 and sharp peaks at ~2923 cm^{-}1, which corresponded to OH and NH groups of amides respectively. These small shifts in bands were observed after the conjugation of OLA to HA. The results observed in FTIR were further verified by ^{1}H NMR studies. The appearance of new peaks at δ 0.903 and δ 1.30 in the ^{1}H NMR spectra of HA-OLA6 was attributed to the aliphatic protons of OLA, thus confirming the successful conjugation of OLA to HA.

3.2. MTT assay

Determining bio-safe dosages of novel materials is critical for any biomedical applications [33]. The *in vitro* cytotoxicity study demonstrated that both HA-OLA6 and HA-OLA8 displayed cell viability over 78% on HEK-293, HeLa and MCF-7, at all tested concentrations (Fig. 1A and B). The percentage cell viability of HA-OLA6 and HA-OLA8 ranged between 79.96–96.66%, 78.08–100.95% and 78.01–88.50% for HEK-293, HeLa and MCF-7, respectively, with no dose dependent toxicity observed at the tested concentrations. The percentage cell viability displayed on all tested cell-lines was above 75%, thus HA-OLA6 and HA-OLA8 can be considered as biologically safe and non-toxic to human cells [34].

3.3. Preparation cf VCM loaded HA-OLA polymersomes

Self-assembled VCM loaded HA-OLA polymersomes were prepared

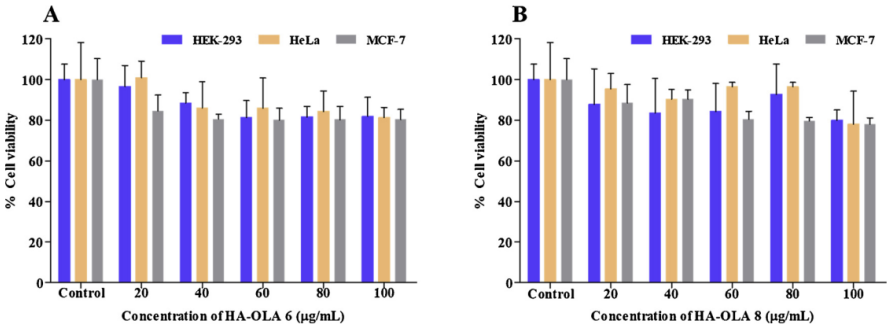

Fig. 1. *In vitro* cytotoxicity of A) HA-OLA6 and B) HA-OLA8 on HEK-293, HeLa and MCF-7 (n = 5).

using a simple probe ultrasonication technique without the use of any organic solvent, surfactant, stabilizer or emulsifier. HA and oleylamine serving as the hydrophilic backbone and grafted hydrophobic chains, respectively, could have influenced the self-assembly of amphiphilic HA-OLA, under aqueous conditions to form polymeric vesicles (polymersomes), thereby encapsulating VCM in hydrophilic cores. This green approach to formulate polymersomes may circumvent the toxic effects of surfactants and residual organic solvents [35].

Several VCM loaded polymersomes were prepared using both HA-OLA6 and HA-OLA8 by varying the amounts of polymer and drug to optimize in terms of size, PDI, ZP and %EE. A combination of 5 mg and 20 mg of VCM and HA-OLA 6, respectively, showed satisfactory results with respect to size, PDI, ZP and %EE (Table 1). The results obtained from DLS revealed that, VCM (5 mg) loaded HA-OLA6 (20 mg) polymersomes (VCM-PS6) had a mean particle diameter of 248.7 ± 3.08 nm with a narrow size distribution of 0.189 ± 0.01 and a negative ZP of -17.6 ± 0.6 mV. The %EE and DLC of VCM-PS6 were found be 43.12 ± 2.18% and 8.62 ± 0.91% respectively, which were comparable with the reports for other VCM encapsulated vesicles [36,37]. The polymersomes made up of HA-OLA8 were of smaller size compared to HA-OLA6 at all respective concentrations of polymer and drug. A similar trend was observed by Qui et.al, where, the diameter of micelles decreased with the increase in grafting of octadecylamine on HA [25]. Furthermore, polymersomes made up of HA-OLA8 displayed lower %EE compared to VCM-PS6 at all respective concentrations of polymer and drug (Supplementary material, Table S2). We assume that, smaller particle size and increased hydrophobicity in HA-OLA8, due to the presence of greater number of oleylamines might have reduced the encapsulation of hydrophilic VCM. Since, VCM-PS6 exhibited good results in terms of size and %EE compared to other formulations, it was therefore considered as the optimized formulation to perform other studies.

The surface morphology of VCM-PS6 was studied using TEM imaging. The images revealed a bilayered vesicular morphology with particles being spherical, and dispersed discretely and homogeneously (Fig. 2A). The polymersomes were found to be in the size range obtained with DLS (Fig. 2B).

The stability of nanoparticles in serum environment is important, as serum proteins can interact with them and may adversely affect *in vivo* efficacy [11]. The stability of polymersomes was investigated by measuring the change in their particle size as a function of time in the presence of a complete medium with FBS at 37 °C. As shown in Fig. 2C, the polymersomes were found to be stable after incubation in FBS for 72 h, with average diameter remaining almost the same on all three days with no significant difference ($p > 0.05$). The results indicate that the hydrophilic anionic shell present in HA-OLA6 polymersomes might have prevented the adsorption of serum proteins on polymersomes [25].

3.4. Differential scanning calorimetry (DSC)

DSC studies were performed to confirm the loading of VCM into HA-OLA6 polymersomes. The thermal behaviour of VCM, HA-OLA6, physical mixture of VCM and HA-OLA6 and lyophilised drug loaded formulation were studied (Fig. 3). As many chemical and physical transitions are associated with consumption or generation of heat, an abrupt change in the thermal behaviour may indicate a possible interaction between the excipients [38,39]. A broad endothermic peak was observed for free VCM at 129.96 °C, which displayed its thermal decomposition, while for HA-OLA6, a similar peak was noticed at 203.93 °C. Two separate endothermic peaks with slightly upward shifts were observed for VCM and HA-OLA6 mixture at 137.25 °C and 208.68 °C respectively, whereas, the thermogram of VCM loaded HA-OLA6 polymersomes (VCM-PS6) did not display any thermal peaks for neither VCM nor HA-OLA6. This disappearance of VCM suggested that the drug was encapsulated into the polymersomes in non-crystalline form [40].

3.5. In vitro drug release

The drug release behaviour of free VCM and VCM-PS6 were studied in PBS 7.4, and are represented in Fig. 4. The cumulative percentage release for free VCM and VCM from polymersomes at 12 h was 75% and 57%, respectively, displaying ~22% of difference in the release pattern between free VCM and VCM in polymersomes, respectively. After 24 h, almost 90% of free VCM was released, whereas, it took 72 h for the

Table 1
Effect of various concentrations of VCM and HA-OLA6 on formulation optimization (n = 3).

VCM	HA-OLA6	Size (nm)	PDI	ZP	%EE
5	10	201.4 ± 3.25	0.196 ± 0.01	−20.4 ± 1.84	33.12 ± 2.11
5	20	248.7 ± 3.08	0.189 ± 0.01	−17.6 ± 0.61	43.12 ± 2.18
5	40	339.5 ± 3.37	0.222 ± 0.01	−18.8 ± 1.42	41.04 ± 1.85
10	10	203.7 ± 3.81	0.181 ± 0.01	−19.2 ± 0.89	27.68 ± 2.41
10	20	251.3 ± 1.21	0.202 ± 0.01	−18.4 ± 1.26	36.48 ± 2.06
10	40	360.9 ± 5.84	0.225 ± 0.01	−18.5 ± 1.11	38.34 ± 4.74

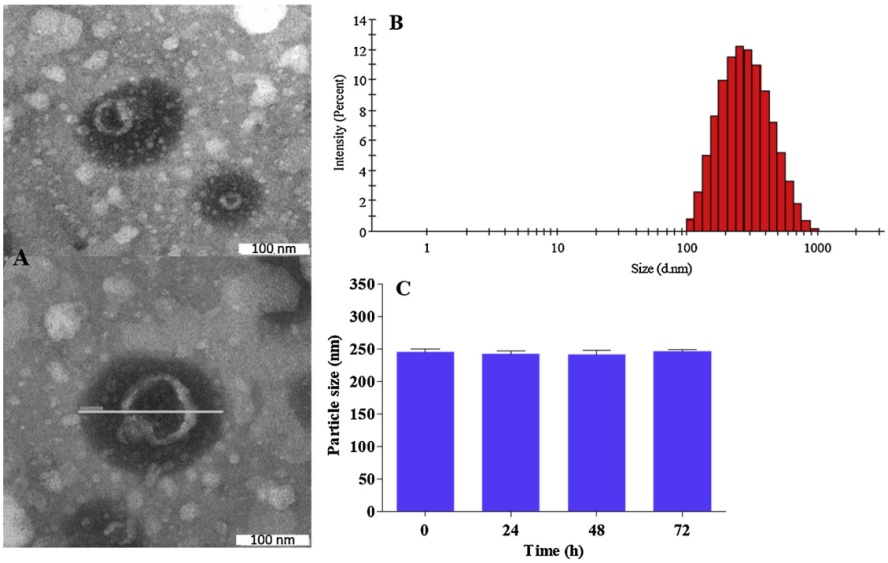

Fig. 2. A) TEM images of VCM-PS6 showing bilayered morphology. B) Size distribution of VCM-PS6 determined by DLS. C) Stability of HA-OLA6 polymersomes in 10% FBS (n = 3).

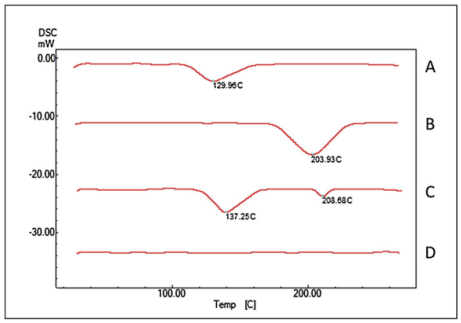

Fig. 3. Thermograms of (A) Free VCM; (B) HA-OLA6; (C) physical mixture of VCM and HA-OLA6 and (D) Lyophilized VCM-PS6.

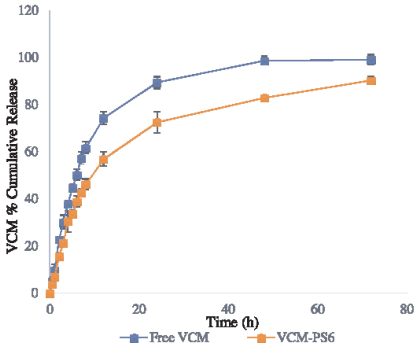

Fig. 4. *In vitro* drug release profiles of free VCM and VCM-PS6.

polymersomes to release same amount of drug. Although, the release profiles of free VCM and VCM from polymersomes were comparable at initial hours, a sustained drug release was observed with nano-formulation after 6 h. The initial quick release could have been governed by diffusion and greater concentration gradient of drug, whereas, sustained drug release might have been due to polymer erosion and degradation [41]. From these observations, it was evident that, polymersomes made from HA-OLA6 were able to release the encapsulated VCM in a sustained manner, compared to free drug. Considering, the ability of polymersomes to release VCM in a slow manner, this formulation could provide required lethal doses of encapsulated antibiotic in bacterial microenvironment for a prolonged period of time to facilitate improved and sustained antibacterial activity. Furthermore, this sustained release of VCM may also overcome the development of resistance.

Various mathematical models were used to understand the release kinetics of VCM from HA-OLA6 polymersomes (Table 2). Among the studied mathematical models, the release of VCM from polymersomes was found to fit in Weibull model with a higher co-relation coefficient of 0.994 and a lower root mean square error of 2.433. The '*n*' exponent (0.488), that was obtained from Korsmeyer-Peppas equation indicated that the release mechanism was anomalous or non-fickian transpot [42]. Apart from drug diffusion, polymer erosion and degradation may have significant roles in releasing VCM slowly from polymersomes. The MDT values calculated for the release of free VCM and VCM polymersomes were 9.76 and 15.06, respectively, indicating slower release of

Table 2
Various mathematical models for drug release from VCM-PS6.

Model	Equation	R^2	RMSE	Release exponent (*n*)
Zero order	$Q = k.\ t + Q_0$	0.2724	24.581	–
First order	$Q = Q_0.\ e^{kt}$	0.9579	5.9115	–
Higuchi	$Q = k.\ t^{½}$	0.9100	8.6468	–
Hixon-Crowell	$Q^{⅓} = kt + Q_0^{⅓}$	0.9045	8.9037	–
Korsmeyer-Peppas	$Q = k.\ t^n$	0.9460	6.2425	0.488
Weibull	$Q = 1\ \exp - (t)^{a/b}]$	0.9940	2.4334	–

Table 3
MIC values of free VCM, free HA, HA-OLA6, HA-OLA8, VCM-PS6 and VCM-PS8.

Time (h)	24	48	72	24	48	72
	S. aureus (μg/mL)			MRSA (μg/mL)		
Free VCM	1.95	250	NA	7.8	NA	NA
Free HA	NA	NA	NA	NA	NA	NA
HA-OLA6	500	500	500	500	500	500
HA-OLA8	500	500	500	500	500	500
VCM-PS6	1.95	1.95	1.95	1.95	1.95	1.95
VCM-PS8	1.95	1.95	1.95	1.95	1.95	1.95

NA = No activity, n = 3.

VCM from polymersomes.

3.6. Antibacterial activity

3.6.1. In vitro antibacterial activity

The *in vitro* antibacterial studies were performed for free VCM, free HA, HA-OLA6 and optimized drug loaded formulation, *i.e.*, VCM-PS6 against *S. aureus* and MRSA (Table 3). Since OLA is an antibacterial enhancer, MIC values were determined for HA-OLA8 and VCM (5 mg) loaded HA-OLA8 (20 mg) polymersomes (VCM-PS8) as well. There was no antibacterial activity observed for free HA against the tested strains of *S. aureus* and MRSA. Interestingly, the novel amphiphilic polymers synthesized in this study, HA-OLA6 and HA-OLA8 displayed moderate antibacterial activities against both *S. aureus* and MRSA with MIC values of 500 μg/mL, over the studied period of 72 h. The MIC values for free VCM against *S. aureus* and MRSA were 1.95 and 7.8 μg/mL, respectively at 24 h. Although, the MIC values for VCM-PS6 and VCM-PS8 remained same as free VCM against *S. aureus*, enhanced activities were observed against MRSA with MIC values of 1.95 μg/mL, displaying 4-fold improvement. At 48 h, free VCM started to lose its potential antibacterial activity, displaying an increased MIC value (250 μg/mL) against *S. aureus* and complete bacterial growth against MRSA. At the end of day three, free VCM had no activity against both *S. aureus* and MRSA. In contrast, VCM-PS6 and VCM-PS8 retained the activity of VCM at 48 h and 72 h against both bacterial strains with MIC values (1.95 μg/mL), remaining same as day one. From these results, both VCM-PS6 and VCM-PS8 showed better activity than free VCM against the tested bacterial strains. The nano-formulations preserved the antibacterial potency of VCM for three days against both strains, while free VCM lost its activity after 24 h. The improved and sustained antibacterial activity of VCM loaded polymersomes can be attributed to slow and controlled release of VCM in bacterial environment over a prolonged period of time. This sustained antibacterial potential of VCM-PS6 and VCM-PS8 can efficiently control infection with reduced frequency of dose and adverse effects. Although, HA-OLA6 and HA-OLA8 were not as potent as VCM, they were able to improve the antibacterial activity of VCM against both *S. aureus* and MRSA. Therefore, the grafted polymers synthesized in this study can make promising nano-carriers to deliver antibiotics and treat MRSA infections.

To understand the combined effect of HA-OLA6 and VCM in VCM loaded HA-OLA6 polymersomes (VCM-PS6) against *S. aureus* and MRSA, FIC values were calculated. As free VCM had lost its potential activity at the end of 24 h, FIC values for both free VCM and free HA-OLA6 were determined at 24 h. The calculated FIC values for VCM-PS6 were found to be 1.01 and 0.25 against *S. aureus* and MRSA, indicating that there was indifference and synergistic antibacterial activity

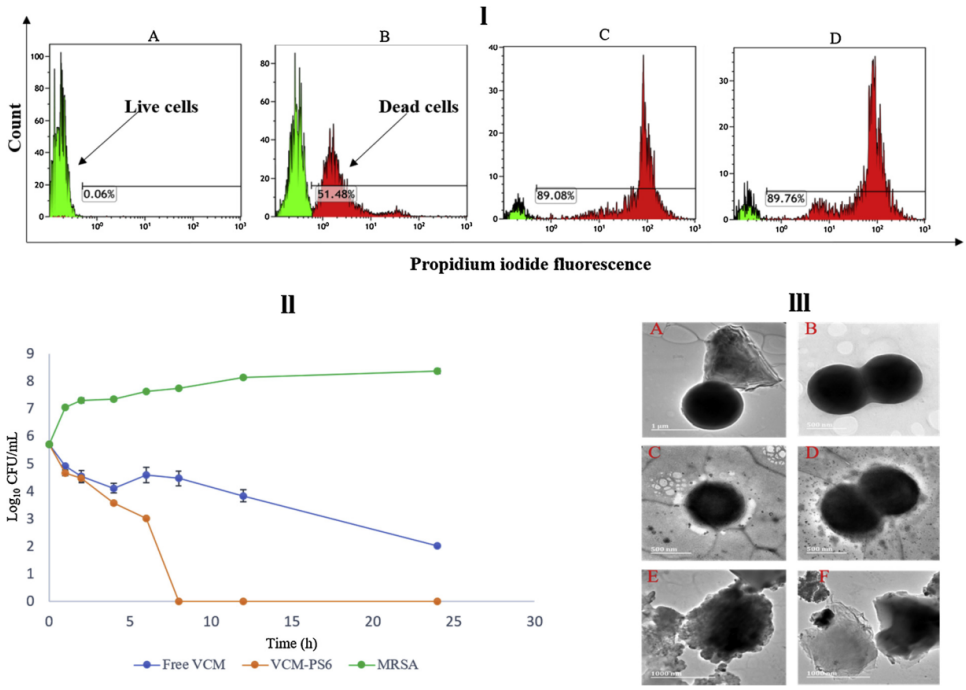

Fig. 5. (I) MRSA cell counts *vs* PI uptake histogram where, A represents untreated MRSA (live cells); B, C and D represents percentage of dead cells in the population after incubation with free VCM at MIC of 1.95 μg/mL, free VCM at its MIC (7.8 μg/mL) and VCM-PS6 at its MIC (1.95 μg/mL) respectively; (II) Bacterial killing kinetics of MRSA exposed to 5 x MIC of free VCM, VCM-PS6 and sterile water; (III) HRTEM images showing morphological differences of untreated MRSA (A and B); VCM treated MRSA (C and D) and VCM-PS6 treated MRSA (E and F).

respectively (Table S3, supplementary material).

3.6.2. Flow cytometry bacterial cell viability

The rapid cell viability of MRSA cells was analysed using a Flow cytometry technique [29]. The MRSA cells were incubated with free VCM and VCM-PS6. The bacterial cells, upon incubation with antibiotics, change their morphology and cell-division cycle, which can be measured using special dyes. PI, a cell-wall non-permeant dye and Syto9, a non-selective cell wall permeant dye were used to detect dead and live cells, respectively [43]. Kaluza-2.1 (Beckman Coulter USA) flow cytometer software was used to analyse the data. Two gates were created to differentiate viable cells (green) and dead cells (red). VCM acts by interfering with the cell wall integrity, which enables the uptake of PI in bacterial cells. The PI inside the cell, intercalate the DNA showing a shift in PI fluorescence, indicating bacterial cell death. Whilst, untreated MRSA showed ˜100% viable cells, the bacteria treated with free VCM and VCM-PS6 showed a shift in PI fluorescence, where two distinct populations of live and dead bacteria were observed (Fig. 51). The free VCM (Fig. 51 C) and VCM-PS6 (Fig. 51 D) showed 88.7 ± 1.21% and 89.2 ± 0.60% dead MRSA cells in the population, after treating at their MICs of 7.8 and 1.95 µg/mL respectively. However, the MRSA treated with free VCM at a concentration same as of MIC of VCM-PS6 (1.95 µg/mL), had reduced killing percentage of bacterial cells, *i.e.*, 51.22 ± 1.21% ($p < 0.05$) (Fig. 51 B). VCM-PS6 proved to be more efficient than free VCM at concentration of 1.95 µg/mL, showing 1.8-fold more dead cells. These results further supported the antibacterial superiority of VCM-PS6.

3.6.3. Bacterial killing kinetics

Time-kill curve for free VCM and VCM-PS6 at 5 x MIC against MRSA is presented in Fig. 5ll. Rapid bactericidal activity was observed for VCM-PS6 after eight hours of exposure, displaying 3-log reduction (99.9% clearance). In contrast, free VCM displayed slow killing rate (2-log reduction) after 24 h treatment. A complete bacterial inhibition was not observed for free VCM over the studied period of 24 h. It was worth noting that, VCM-PS6 at four times lower concentration than free VCM, achieved bactericidal activity within eight hours of treatment. This may lead to rapid elimination of bacteria, thus reducing the dose and course of treatment.

3.6.4. Bacterial cell morphology

The ability of free VCM and VCM-PS6 to disrupt bacterial cell membrane was determined by assessing the morphological changes/differences induced in MRSA cells after four hours of treatment. The HRTEM images showed that, untreated MRSA, which was used as negative control exhibited smooth and integrated cell membrane with intact cocci (Fig. 5lll A and lll B). The MRSA cells that were treated with VCM alone displayed a deformed and impaired cell membrane after four hours (Fig. 5lll C and lll D). In contrast, after same incubation period, the MRSA cells treated with VCM-PS6 were damaged and ruptured intensely (Fig. 5lll E and lll F). The closer view of VCM-PS6 treated cells revealed that, the drug loaded formulation had a strong impact on the integrity of MRSA cell membrane. Furthermore, the membrane and shape of cocci was completely altered with distinguished perforations and leakage of cytosol (Fig. 5lll E and lll F). VCM-PS6 were found to be more potent than free VCM in disrupting MRSA membrane. These results corroborate well with *in vitro* antibacterial activity, flow cytometry analysis and bacterial killing kinetics.

4. Conclusions

Recently, there has been a surge of interest to develop novel drug carrier systems for antibiotic delivery. In this study, conjugates of HA and OLA were synthesized depending on various percentage of conjugation. The novel HA-OLA conjugates were proven to be bio-safe on the cell lines tested and exhibited moderate antibacterial activity against *S. aureus* and MRSA. VCM loaded HA-OLA6 polymersomes (VCM-PS6) were dispersed in nano-sized range with particle sizes < 250 nm and entrapment efficiency of 43.12 ± 2.18%. The polymersomes exhibited slow and sustained release for VCM throughout the studied period of 72 h. The *in vitro* antibacterial activity against MRSA revealed that, VCM-PS6 had 4-fold enhanced activity, compared to free VCM. Furthermore, synergism was observed for VCM and HA-OLA6 against MRSA. The antibacterial studies using flow cytometry revealed that, VCM-PS6 showed 1.8-fold more dead cells of MRSA, compared to free VCM, when samples were treated at MIC of 1.95 µg/mL. Bacterial cell morphology showed that, VCM loaded polymersomes had a stronger impact on MRSA membrane disruption compared to free VCM. These results indicate that, VCM-PS6 was more potent than free VCM against MRSA in all performed antibacterial studies. In summary, these findings suggest that, HA-OLA conjugates can make promising antibiotic nano-carriers to combat multi-drug resistant bacterial strains. In addition, these novel conjugates can be further explored to encapsulate other classes of pharmacologically active agents to manage various disease conditions effectively.

Declaration of Competing Interest

The authors declare no conflict of interest.

Acknowledgments

The authors acknowledge the College of Health Sciences, University of KwaZulu-Natal (UKZN) and UKZN Nanotechnology Platform, National Research Foundation of South Africa (Grant No. 106040) and Medical Research Council of South Africa for financial support. We acknowledge Microscopy and Microanalysis Unit and Department of Human Physiology at UKZN for use of facilities and Ms. Charlotte Ramadhin for proof reading.

Appendix A. Supplementary data

Supplementary material related to this article can be found, in the online version, at doi:https://doi.org/10.1016/j.colsurfb.2019.110388.

References

[1] T. Foster, Staphylococcus, in: S. Baron (Ed.), Medical Microbiology, 1996.
[2] D.C. Kaur, S.S. Chate, Study of antibiotic resistance pattern in methicillin resistant Staphylococcus aureus with special reference to newer antibiotic, J. Glob. Infect. Dis. 7 (2015) 78.
[3] A. Gupta, S. Mumtaz, C.-H. Li, I. Hussain, V.M. Rotello, Combatting antibiotic-resistant bacteria using nanomaterials, Chem. Soc. Rev. 48 (2019) 415–427.
[4] L. Zhang, F. Gu, J. Chan, A. Wang, R. Langer, O. Farokhzad, Nanoparticles in medicine: therapeutic applications and developments, Clin. Pharmacol. Ther. 83 (2008) 761–769.
[5] M.-H. Xiong, Y. Bao, X.-Z. Yang, Y.-H. Zhu, J. Wang, Delivery of antibiotics with polymeric particles, Adv. Drug Deliv. Rev. 78 (2014) 63–76.
[6] A.J. Huh, Y.J. Kwon, "Nanoantibiotics": a new paradigm for treating infectious diseases using nanomaterials in the antibiotics resistant era, J. Control. Release 156 (2011) 128–145.
[7] W. Gao, S. Thamphiwatana, P. Angsantikul, L. Zhang, Nanoparticle approaches against bacterial infections, Wiley Interdiscip. Rev. Nanomed. Nanobiotechnol. 6 (2014) 532–547.
[8] H. Pinto-Alphandary, A. Andremont, P. Couvreur, Targeted delivery of antibiotics using liposomes and nanoparticles: research and applications, Int. J. Antimicrob. Agents 13 (2000) 155–168.
[9] W.S. Cheow, K. Hadinoto, Factors affecting drug encapsulation and stability of lipid–polymer hybrid nanoparticles, Colloids Surf. B Biointerfaces 85 (2011) 214–220.
[10] U.S. Toti, B.R. Guru, M. Hali, C.M. McPharlin, S.M. Wykes, J. Panyam, J.A. Whittum-Hudson, Targeted delivery of antibiotics to intracellular chlamydial infections using PLGA nanoparticles, Biomaterials 32 (2011) 6606–6613.
[11] L. Qiu, Z. Li, M. Qiao, M. Long, M. Wang, X. Zhang, C. Tian, D. Chen, Self-assembled pH-responsive hyaluronic acid–g-poly (l-histidine) copolymer micelles for targeted intracellular delivery of doxorubicin, Acta Biomater. 10 (2014) 2024–2035.
[12] J.M. Wickens, H.O. Alsaab, P. Kesharwani, K. Bhise, M.C.I.M. Amin, R.K. Tekade, U. Gupta, A.K. Iyer, Recent advances in hyaluronic acid-decorated nanocarriers for targeted cancer therapy, Drug Discov. Today 22 (2017) 665–680.

[13] P. Pirnazar, L. Wolinsky, S. Nachnani, S. Haake, A. Pilloni, G.W. Bernard, Bacteriostatic effects of hyaluronic acid, J. Periodontol. 70 (1999) 370–374.
[14] L. Drago, L. Cappelletti, E. De Vecchi, L. Pignataro, S. Torretta, R. Mattina, Antiadhesive and antibiofilm activity of hyaluronic acid against bacteria responsible for respiratory tract infections, APMIS 122 (2014) 1013–1019.
[15] B.S. Nagoba, N.M. Suryawanshi, B. Wadher, S. Selkar, Acidic environment and wound healing: a review, Wounds 27 (2015) 5–11.
[16] J. Zhu, F. Li, X. Wang, J. Yu, D. Wu, Hyaluronic acid and polyethylene glycol hybrid hydrogel encapsulating nanogel with hemostasis and sustainable antibacterial property for wound healing, ACS Appl. Mater. Interfaces 10 (2018) 13304–13316.
[17] A. Rösler, G.W. Vandermeulen, H.-A. Klok, Advanced drug delivery devices via self-assembly of amphiphilic block copolymers, Adv. Drug Deliv. Rev. 64 (2012) 270–279.
[18] J.-P. Douliez, C. Gaillard, Self-assembly of fatty acids: from foams to protocell vesicles, New J. Chem. 38 (2014) 5142–5148.
[19] A. Desbois, K. Lawlor, Antibacterial activity of long-chain polyunsaturated fatty acids against Propionibacterium acnes and Staphylococcus aureus, Mar. Drugs 11 (2013) 4544–4557.
[20] T. Kitahara, N. Koyama, J. Matsuda, Y. Aoyama, Y. Hirakata, S. Kamihira, S. Kohno, M. Nakashima, H. Sasaki, Antimicrobial activity of saturated fatty acids and fatty amines against methicillin-resistant Staphylococcus aureus, Biol. Pharm. Bull. 27 (2004) 1321–1326.
[21] D.R. Sikwal, R.S. Kalhapure, S. Rambharose, S. Vepuri, M. Soliman, C. Mocktar, T. Govender, Polyelectrolyte complex of vancomycin as a nanoantibiotic: preparation, in vitro and in silico studies, Mater. Sci. Eng. C 63 (2016) 489–498.
[22] R.S. Kalhapure, M. Jadhav, S. Rambharose, C. Mocktar, S. Singh, J. Renukuntla, T. Govender, pH-responsive chitosan nanoparticles from a novel twin-chain anionic amphiphile for controlled and targeted delivery of vancomycin, Colloids Surf. B Biointerfaces 158 (2017) 650–657.
[23] D. Hassan, C.A. Omolo, R. Gannimani, A.Y. Waddad, C. Mocktar, S. Rambharose, N. Agrawal, T. Govender, Delivery of novel vancomycin nanoplexes for combating methicillin resistant staphylococcus aureus (MRSA) infections, Int. J. Pharm. (2019).
[24] C.A. Omolo, R.S. Kalhapure, N. Agrawal, S. Rambharose, C. Mocktar, T. Govender, Formulation and molecular dynamics simulations of a fusidic acid nanosuspension for simultaneously enhancing solubility and antibacterial activity, Mol. Pharm. 15 (2018) 3512–3526.
[25] L. Qiu, M. Zhu, Y. Huang, K. Gong, J. Chen, Mechanisms of cellular uptake with hyaluronic acid—octadecylamine micelles as drug delivery nanocarriers, RSC Adv. 6 (2016) 39896–39902.
[26] P. Walvekar, R. Gannimani, S. Rambharose, C. Mocktar, T. Govender, Fatty acid conjugated pyridinium cationic amphiphiles as antibacterial agents and self-assembling nano carriers, Chem. Phys. Lipids 214 (2018) 1–10.
[27] S.J. Sonawane, R.S. Kalhapure, S. Rambharose, C. Mocktar, S.B. Vepuri, M. Soliman, T. Govender, Ultra-small lipid-dendrimer hybrid nanoparticles as a promising strategy for antibiotic delivery: in vitro and in silico studies, Int. J. Pharm. 504 (2016) 1–10.
[28] M. Balouiri, M. Sadiki, S.K. Ibnsouda, Methods for in vitro evaluating antimicrobial activity: a review, J. Pharm. Anal. 6 (2016) 71–79.
[29] N.M. O'Brien-Simpson, N. Pantarat, T.J. Attard, K.A. Walsh, E.C. Reynolds, A Rapid and Quantitative flow cytometry method for the analysis of membrane disruptive antimicrobial activity, PLoS One 11 (2016) e0151694.
[30] A.R.C. Duarte, M.S. Costa, A.L. Simplício, M.M. Cardoso, C.M. Duarte, Preparation of controlled release microspheres using supercritical fluid technology for delivery of anti-inflammatory drugs, Int. J. Pharm. 308 (2006) 168–174.
[31] S. Renggli, W. Keck, U. Jenal, D. Ritz, Role of autofluorescence in flow cytometric analysis of Escherichia coli treated with bactericidal antibiotics, J. Bacteriol. 195 (2013) 4067–4073.
[32] P. Vaudaux, A. Gjinovci, M. Bento, D. Li, J. Schrenzel, D.P. Lew, Intensive therapy with ceftobiprole medocaril of experimental foreign-body infection by methicillin-resistant Staphylococcus aureus, Antimicrob. Agents Chemother. 49 (2005) 3789–3793.
[33] S. Choksakulnimitr, S. Masuda, H. Tokuda, Y. Takakura, M. Hashida, In vitro cytotoxicity of macromolecules in different cell culture systems, J. Control. Release 34 (1995) 233–241.
[34] X. Cao, C. Cheng, Y. Ma, C. Zhao, Preparation of silver nanoparticles with antimicrobial activities and the researches of their biocompatibilities, J. Mater. Sci. Mater. Med. 21 (2010) 2861–2868.
[35] I. Hussain, N. Singh, A. Singh, H. Singh, S. Singh, Green synthesis of nanoparticles and its potential application, Biotechnol. Lett. 38 (2016) 545–560.
[36] J. Liu, Z. Wang, F. Li, J. Gao, L. Wang, G. Huang, Liposomes for systematic delivery of vancomycin hydrochloride to decrease nephrotoxicity: characterization and evaluation, Asian J. Pharm 10 (2015) 212–222.
[37] M. Jadhav, R.S. Kalhapure, S. Rambharose, C. Mocktar, S. Singh, T. Kodama, T. Govender, Novel lipids with three C18-fatty acid chains and an amino acid head group for pH-responsive and sustained antibiotic delivery, Chem. Phys. Lipids 212 (2018) 12–25.
[38] G. Höhne, W.F. Hemminger, H.-J. Flammersheim, Differential Scanning Calorimetry, Springer Science & Business Media, 2013.
[39] G. Ceschel, R. Badiello, C. Ronchi, P. Maffei, Degradation of components in drug formulations: a comparison between HPLC and DSC methods, J. Pharm. Biomed. Anal. 32 (2003) 1067–1072.
[40] C.G. Pupe, M. Villardi, C.R. Rodrigues, H.V.A. Rocha, L.C. Maia, V.P. de Sousa, L.M. Cabral, Preparation and evaluation of antimicrobial activity of nanosystems for the control of oral pathogens Streptococcus mutans and Candida albicans, Int. J. Nanomedicine 6 (2011) 2581.
[41] J. Ritsema, E. Herschberg, S. Borgos, C. Løvmo, R. Schmid, Y. Te Welscher, G. Storm, C.F. van Nostrum, Relationship between polarities of antibiotic and polymer matrix on nanoparticle formulations based on aliphatic polyesters, Int. J. Pharm. 548 (2018) 730–739.
[42] P.L. Ritger, N.A. Peppas, A simple equation for description of solute release I. Fickian and non-fickian release from non-swellable devices in the form of slabs, spheres, cylinders or discs, J. Control. Release 5 (1987) 23–36.
[43] M. Fittipaldi, A. Nocker, F. Codony, Progress in understanding preferential detection of live cells using viability dyes in combination with DNA amplification, J. Microbiol. Methods 91 (2012) 276–289.

1777

Appendix III

DESIGN AND DEVELOPMENT OF pH-RESPONSIVE LIPOSOMES FOR TARGETED DELIVERY OF VANCOMYCIN AGAINST *STAPHYLOCOCCUS AUREUS* AND METHICILLIN-RESISTANT *STAPHYLOCOCCUS AUREUS*

UNIVERSITY OF KWAZULU-NATAL
INYUVESI YAKWAZULU-NATALI

Sifiso S. Makhathini, Rahul Kalhapure, Mahantesh Jadhav, Ayman Y. Waddad, Chunderika Mocktar, Thirumala Govender*

*Discipline of Pharmaceutical Sciences, School of Health Sciences, University of KwaZulu-Natal, Private Bag X54001, Durban, South Africa.

INTRODUCTIONN AD AIMS

- The development of bacterial resistance against antibiotics has become a challenge posing a threat to public health worldwide.[1]
- The increase in resistance against vancomycin which is considered as the last-line antibiotic for the treatment of Gram-positive bacterial infections, can be linked with most deaths reported.[2]
- Targeted therapy with nano delivery systems has become a promising strategy to enhance efficacy of antibiotics, reducing resistance and toxicity.[3]
- pH-Responsive nano drug delivery systems can maximize targeting and drug release at infection sites which are acidic as compared to non-infection site. [4]
- The identification of novel pH-responsive lipids for liposomes can improve their performance.[4]
- The aim of this study was to synthesize novel pH-responsive lipids for the development of vancomycin hydrochloride encapsulated liposomes (VANH-Lips) for activity against *Staphylococcus aureus* (*SA*) and methicillin-resistant *Staphylococcus aureus* (*MRSA*).

METHODS

Synthesis of pH responsive lipids

- Novel pH-sensitive mono-substituted two chain lipids derived from Stearic (SA), Oleic (OA), Linoleic (LA) and Linolenic acid (LLA) were synthesized and characterized using FTIR, ^{1}H and ^{13}C NMR.

Preparation of Liposomes (VANH-Lips)

- VANH-Lips were prepared from phosphatidylcholine (PC), cholesterol and each pH-sensitive lipid using the thin-film hydration method.
- The film was hydrated with 10 mL aqueous solution containing VANH (1 mg/mL) at room temperature.
  The liposomes were sonicated for 15 min (30% amplitude) using a probe sonicator.

Characterization

size, polydispersity index (PDI) and zeta potential (ZP)

- The formulation was characterized for particle using a Zetasizer Nano ZS90 (Malvern Instruments Ltd., UK).

Encapsulation efficiency (%EE)

- Encapsulation efficiency was calculated using UV spectrophotometry at 280.4 nm

In vitro drug release

- Drug release was performed in PBS at both pH 7.4 and pH 6.0 at 37 ºC using dialysis bag and UV spectrophotometry at 280.4nm wavelength.

In vitro antibacterial activity

- The minimum inhibitory concentration (MIC) values for VANH-Lips were determined against *S. aureus* and *MRSA* at pH 7.4 and 6.0 using a broth dilution method.

RESULTS AND DISCUSSION

Table 1. Particle size, PDI, ZP and entrapment efficiency (EE) characterization of VANH-Lips (n = 3).

pH		SA Derivative	OA Derivative	LA Derivative	LLA Derivative
7.4	Size (mn)	89.37±0.549	96.92±8.732	**88.52±5.078**	86.26±11.76
	PDI	0.184±0.007	0.204±0.014	**0.151±0.016**	0.203±0.010
	Zeta (mV)	-10.4±2.38	-8.85±3.19	**-11.8±2.99**	-11.3±2.22
6.0	Size(mn)	114.0±2.972	162.8±4.350	**158±1.98**	301.2±24.41
	PDI	0.629±0.107	0.176±0.012	**0.129±0.019**	0.644±0.230
	Zeta (mV)	1.20±0.714	1.54±0.101	**1.023±0.1012**	1.26±0.427
	EE (%)	36.43%	44.27%	**38.68%**	29.86%

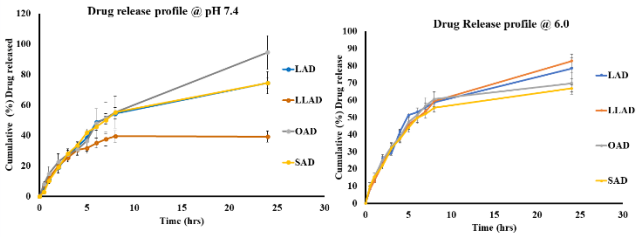

Figure 1. In vitro release profile of VANH-Lips from pH-responsive liposome. (n = 3)

Table 2. In vitro antibacterial activity from Linoleic Acid derivative formulated liposomes at pH 7.4.

	S. aureus (MIC µg/mL)			*MRSA* (MIC µg/mL)		
Time (hours)	24	48	72	24	48	72
Bare VANH	1.95	NA	NA	7.8	NA	NA
Conv-Lips	1.95	7.8	250	3.9	3.9	NA
VANH-Lips	0.97	1.9	3.9	>0.488	>0.488	>0.488
Blank	NA	NA	NA	NA	NA	NA

N.A = No Activity **Conv-Lips = Conventional liposome**

Table 3. In vitro antibacterial activity from Linoleic Acid derivative formulated liposomes at pH 6.0.

	SA (MIC µg/mL)			MRSA (MIC µg/mL)		
Tim (hours)	24	48	72	24	48	72
Bare VANH	3.9	NA	NA	7.8	NA	NA
Conv-Lips	1.95	7.8	NA	3.9	3.9	NA
VANH-Lips	>0.488	>0.488	3.9	>0.488	7.8	7.8
Blank	NA	NA	NA	62.5	NA	NA

N.A = No Activity **Conv-Lips = Conventional liposome**

- Liposomes from all derivatives demonstrated a desired size, PDI, zeta potential, good encapsulation of the drug and sustained drug release profile.
- There was notable change in size and zeta potential with respect to change in pH from 7.4 to 6.0 demonstrating the responsiveness of the system.
- Percentage drug release with all pH-responsive derivative at pH 6 was high than the drug released at pH 7.4 after 24 hours.
- The study also revealed that among four derivatives and non-responsive liposomes, LAD VANH-Lips had a prolonged activity at pH 6 against *SA* with no growth of bacteria observed as compared to bare vancomycin after 48 hours.

CONCLUSION

- pH-Sensitive liposomes from novel pH-responsive lipids were successfully formulated and characterized.
- These results suggest that the novel pH-sensitive liposomes hold great potential for becoming an alternative targeted intracellular delivery system for antibiotics to avoid drug resistance and these results can be further supported with *in vivo* studies.

REFERENCES & ACKNOWLEDGMENT

References

1. Abed, Nadia, and Patrick., *International journal of antimicrobial agents.* 2014, pp 485-496.
2. Ventola, Lee., *Pharmacy and Therapeutics.* 2015, pp 277
3. Xiong, Meng-Hua, et al., *Advanced drug delivery reviews.* 2014 pp63-76.
4. Zhu, Ying-Jie, and Feng Chen., *Chemistry–An Asian Journal.* 2015 pp 284-305.

Acknowledgment

College of Health Sciences, UKZN Nanotechnology Platform and National Research Foundation of South Africa.

Appendix IV

UNIVERSITY OF KWAZULU-NATAL
INYUVESI YAKWAZULU-NATALI

15 April 2019

Dr Ayman Waddad (60072)
School of Health Sciences
Westville Campus

Dear Dr Waddad,

Protocol reference number: AREC/104/015PD
Project title: *In vivo* antibacterial activity of antimicrobial based nanoantibiotic formulations in BALB/c mice

Full Approval – Renewal Application

With regards to your renewal application received on 05 November 2018 and your response on 20 March 2019 to our letter of 05 November 2019. The documents submitted have been accepted by the Animal Research Ethics Committee and **FULL APPROVAL** for the protocol has been granted with the following conditions:

Please note: Any Veterinary and Para-Veterinary procedures must be conducted by a SAVC registered VET or SAVC authorized person.

Any alteration/s to the approved research protocol, i.e Title of Project, Location of the Study, Research Approach and Methods must be reviewed and approved through the amendment/modification prior to its implementation. In case you have further queries, please quote the above reference number.

Please note: Research data should be securely stored in the discipline/department for a period of 5 years.

The ethical clearance certificate is only valid for a period of one year from the date of issue. Renewal for the study must be applied for before 15 April 2020.

Attached to the Approval letter is a template of the Progress Report that is required at the end of the study, or when applying for Renewal (whichever comes first). An Adverse Event Reporting form has also been attached in the event of any unanticipated event involving the animals' health / wellbeing.

I take this opportunity of wishing you everything of the best with your study.

Yours faithfully

.....
Dr Sanil D Singh, PhD
Acting Chair: Animal Research Ethics Committee

/ms

cc Supervisor: Professor Thirumala Govender
Cc Academic Leader Research: Dr Brenda de Gama
Cc Registrar: Mr Simon Mokoena
Cc BRU – Dr Linda Bester

Animal Research Ethics Committee (AREC)
Ms Mariette Snyman (Administrator)
Westville Campus, Govan Mbeki Building
Postal Address: Private Bag X54001, Durban 4000
Telephone: +27 (0) 31 260 8350 **Facsimile:** +27 (0) 31 260 4609 **Email:** animalethics@ukzn.ac.za
Website: http://research.ukzn.ac.za/Research-Ethics/Animal-Ethics.aspx